NextGen Agriculture: Novel Concepts and Innovative Strategies

Series Editor, Chittaranjan Kole

SMART AGRICULTURE

CONCEPTS, STRATEGIES, AND CASE STUDIES

Edited by Verónica Saiz-Rubio,
Francisco Rovira-Más, and Chittaranjan Kole

Smart Agriculture

Smart Agriculture: Concepts, Strategies, and Case Studies showcases improvements in agricultural technology, bringing together work from leading experts in the field. It explores techniques and disciplines essential for the widespread adoption of precision agriculture, including artificial intelligence (AI), machine learning, the Internet of Things (IoT), Agriculture 5.0, smart spraying systems, and decision support tools that are transforming modern farming practices.

Designed to introduce readers to the vast potential of data-driven agriculture, this book presents information on smart agriculture through practical, real-world applications. It features a diverse range of case studies across various crops and agricultural operations, offering actionable insights into innovative solutions. Highlights include variable-rate orchard spraying for high-density canopies like olives and oranges, image analysis for evaluating apple and grape properties, digital tools for optimizing irrigation, geostatistical modeling of *Xylella fastidiosa*, UAV-assisted fertilization of olive trees, automated wheat growth monitoring, smart agriculture techniques for peach production, greenhouse data management, digital twins for strawberry cultivation, deep learning for obstacle detection in robotic rice harvesters, and IoT middleware solutions for arable crops and livestock.

A book in the *NextGen Agriculture: Novel Concepts and Innovative Strategies* series, this comprehensive resource is ideal for professional engineers, researchers in agricultural engineering, computer science, machine vision, and remote sensing, as well as technology developers. Graduate students specializing in digital agriculture and precision farming will also find this book invaluable for understanding the transformative power of modern agricultural technologies.

NextGen Agriculture: Novel Concepts and Innovative Strategies
Chittaranjan Kole
Series Editor

Allele Mining for Genomic Designing of Fruit Crops
Chittaranjan Kole, Kenta Shirasawa, and Anil Kumar Singh

Allele Mining for Genomic Designing of Cereal Crops
Chittaranjan Kole, Sharat Kumar Pradhan, and Vijay K Tiwari

Allele Mining for Genomic Designing of Vegetable Crops
Chittaranjan Kole, Tusar Kanti Behera, and Prashant Kaushik

Allele Mining for Genomic Designing of Oilseed Crops
Chittaranjan Kole, Manish Kumar Pandey, and Naveen Puppala

Sustainable Urban Agriculture: New Frontiers
Kheir Al-Kodmany, Madhav Govind, Sharmin Khan, and Chittaranjan Kole

Allele Mining for Genomic Designing of Grain Legume Crops
Chittaranjan Kole, C. Bharadwaj, and Abhimanyu Sarkar

The Vertical Farm: Scientific Advances and Technological Developments
Kheir Al-Kodmany, Andrew Keong Ng, Abel Tablada, and Chittaranjan Kole

Next Generation Food Crops for Human Health
Edited by Sangam Dwivedi, Rodomiro Ortiz, and Chittaranjan Kole

Smart Agriculture: Concepts, Strategies, and Case Studies
Edited by Verónica Saiz-Rubio, Francisco Rovira-Más, and Chittaranjan Kole

For more information, please visit our website: https://www.routledge.com/Nextgen-Agriculture/book-series/NGA

Smart Agriculture

Concepts, Strategies, and Case Studies

Edited by
Verónica Saiz-Rubio, Francisco Rovira-Más,
and Chittaranjan Kole

CRC Press
Taylor & Francis Group
Boca Raton London New York

CRC Press is an imprint of the
Taylor & Francis Group, an **informa** business

Designed cover image: Shutterstock

First edition published 2026
by CRC Press
2385 NW Executive Center Drive, Suite 320, Boca Raton FL 33431

and by CRC Press
4 Park Square, Milton Park, Abingdon, Oxon, OX14 4RN

CRC Press is an imprint of Taylor & Francis Group, LLC

ISBN: 9781032823386 (hbk)
ISBN: 9781032839714 (pbk)
ISBN: 9781003510598 (ebk)

DOI: 10.1201/9781003510598

Typeset in Times
by KnowledgeWorks Global Ltd.

Dedicated to

Dr. Norman Ernest Borlaug

The Father of Green Revolution, Nobel Peace Prize winner
and the Founder of the World Food Prize

Who inspired my research and academic works with
his generous appreciations and advice

Contents

Preface

The book *Smart Agriculture: Concepts, Strategies, and Case Studies* is a volume from the series *NextGen Agriculture: Novel Concepts and Innovative Strategies*. This text comes from the necessity of collecting advanced work from representative groups working on cutting-edge techniques in agriculture and farming. Terms like AI, machine or deep learning, Internet of Things, Agriculture 5.0, smart spraying, decision support systems, or digital twins are already related to agricultural solutions that need to be accepted and adopted, as the ultimate turn of the screw of precision agriculture. This way of farming is optimized via digital tools that produce high amounts of data to help producers make better decisions and thus reach the highest quality and production in their fields.

The editors aim at introducing readers to the wide scope of possibilities enabled by a modern and data-driven agriculture known as smart agriculture. In this book, the reader will learn about many digital agriculture tools explained through use cases covering various agricultural operations and multiple crops. There are 11 chapters showing diverse techniques to deal with specific agricultural production challenges relevant today. Chapter 1 explains variable-rate systems applied to the sensitive task of orchard spraying in high-density canopies such as olives and oranges. Image analysis techniques for the assessment of fruit properties are described in Chapter 2, with use cases focused on apples and grapes. Chapter 3 explains digital solutions to optimize irrigation. The bacterium *Xylella fastidiosa*, devastating for olive groves, is monitored in Chapter 4 through geostatistical modeling. Unmanned aerial vehicles are introduced in Chapter 5 for assisting in the fertilization of olive trees, and in Chapter 9 for the automatic monitoring of crop growth in wheat. Chapter 6 applies smart agriculture for the production of peaches. Chapter 7 enhances the importance of making informed decisions in the management of greenhouses. Chapter 8 explains the concept of digital twins and applies this technology to the production of strawberries. Chapter 10 explains how to implement deep learning algorithms for object detection as a safety mechanism in robotic rice harvesters. Finally, Chapter 11 addresses IoT middleware solutions for arable crops and livestock farming.

Smart Agriculture: Concepts, Strategies, and Case Studies will be interesting to professional engineers and researchers in agricultural engineering, computer science, machine vision, remote sensing, and technology developers, as well as to graduate students specializing in digital agriculture and precision farming.

Preface to the Series

Agriculture is going through a phase of transformation now. It has both challenges and opportunities. One of the major challenges it is facing is obviously food security. A population of about 9.3 billion projected by 2050 necessitates an increase of crop production by 60%–70%. Another 10%–15% increase would be needed to counter the reduction of crop production due to global warming and climate change. Nutrition security is another challenge with more than 800 million people suffering from malnutrition. Depletion of fossil fuel and increasing dependence on biofuel from crop residues is another challenge. Loss of biodiversity and land degradation also add to the list of challenges. The cultivable area is also decreasing fast due to housing, transport, and industrialization. Above all, climate change and global warming have a huge impact on agriculture, health, and environment.

Several novel concepts and strategies are emerging to address the above challenges. For example, practice of precision farming will lead to precise and timely use of inputs resulting in higher yield and better quality of produce on the one hand and reduction of loss of inputs on the other. Similarly, urban agriculture and vertical agriculture will add a lot of cultivable areas in future. Protected farming will facilitate growing crops under controlled conditions leading to reduction in biotic and abiotic stresses and precise utilization of inputs.

Agriculture requires maintenance of the philosophy farmers have been following since inception over thousands of years which are being sold today in new packages with sophisticatedly coined labels such as traditional agriculture, natural agriculture, sustainable agriculture, conservation agriculture, integrated agriculture, regenerative agriculture, and organic agriculture.

In the changing scenarios, next generation agriculture will need designed crop varieties and breeds produced through designed practices. This book series aims at deliberations on several novel concepts and innovative strategies developed for next generation agriculture and will hopefully benefit agricultural education, research, and outreach.

Chittaranjan Kole

Special Acknowledgment

Phullara Kole

For her outstanding assistance in editing this book series.

About the Editors

Verónica Saiz-Rubio studied agricultural engineering and holds a PhD in automation, robotics, and industrial informatics from the Universitat Politècnica de València (UPV, Valencia, Spain) and a degree in mechanical engineering from Linnéuniversitetet (Växjö, Sweden). She completed a postdoctoral fellowship at the Field Robotics Laboratory (FiRO) in Kyoto, Japan. As a member of the Agricultural Robotics Laboratory (ARL) at the UPV, she is responsible for data and image processing and the development of high-resolution plot maps. She also collaborates in the design, construction, and automation of ground robots developed within the European projects VineRobot, VineScout, and Cerberus, serving as part of the coordinating team for the latter two. Dr. Saiz-Rubio has received seven research awards, including an award for the quality of scientific articles from the American Society of Agricultural and Biological Engineers (ASABE), an award for outstanding young researcher articles (Armand Blanc Prize) from the International Commission of Agricultural and Biosystems Engineering (CIGR), and an award for innovative young researcher projects (Farming by Satellite Prize) from the European Navigation Satellite Systems Agency (GSA). Regarding her teaching activities, she has collaborated on courses on precision agriculture and digital technologies for the agri-food sector. She currently teaches at the university level in the areas of agricultural robotics and digital agriculture.

Francisco Rovira-Más earned a degree in agricultural engineering in 1996 from the Universitat Politècnica de València (UPV, Valencia, Spain), where he was Assistant Professor from 1997 to 2000. He earned his PhD in 2003 from the University of Illinois at Urbana-Champaign (Urbana, IL, USA). He has been a member of the Intelligent Vehicle Systems group at the John Deere Technology Center in Moline, IL, USA. He has also been Research Associate with the Department of Agricultural and Biological Engineering at the University of Illinois, conducting research at the John Deere Intelligent Vehicle Systems unit (formerly Agricultural Management Solutions—AMS) in Urbandale, IA, USA. Currently, Dr. Rovira-Más is Professor at the Universitat Politècnica de València in Spain and Director of the Agricultural Robotics Laboratory. His research interests include autonomous vehicles, machine vision, controls, off-road equipment automation, robotics, and artificial intelligence. Dr. Rovira-Más has been the technical manager of the European project VineRobot and the coordinator of the EU H2020 FTI project VineScout. At present, he is the coordinator of project Cerberus, funded with 4.8 M€ and involving 13 institutions from Slovenia, Italy, Cyprus, and Spain.

Chittaranjan Kole is an internationally reputed scientist with an illustrious professional career spanning over 38 years and original contributions in the fields of plant genomics, biotechnology, and molecular breeding leading to the publication of more than 160 quality research articles and reviews. He has edited over 170 books for the leading publishers of the world. Prof. Kole's scientific contributions and editing acumen have been appreciated by seven Nobel Laureates, including Profs. Norman Borlaug, Arthur Kornberg, Werner Arber, Phillip Sharp, Günter Blobel, Lee Hartwell, and Roger Kornberg. He has been honored with a number of fellowships, honorary fellowships, and national and international awards, including the Outstanding Crop Scientist award conferred by the International Crop Science Society. He has served at all prestigious positions in academia, including as Vice-Chancellor BC Agricultural University, Project Coordinator of Indo-Russian Center of Biotechnology in India, and Director of Research of Institute of Nutraceutical Research of Clemson University, in USA. He worked also in the Pennsylvania State University and Clemson University as Visiting Professor in USA. He was awarded with the Raja Ramanna Fellow by the Department of Energy, Government of India. Prof. Kole is also heading the International Climate-Resilient Crop Genomics Consortium and International consortium for Phytomedomics and Nutriomics as their founding Principal Coordinator and presently as President.

Contributors

Tommaso Adamo
University of Salento
Lecce, Italy

Orly Enrique Apolo-Apolo
Universidad de Sevilla
Sevilla, Spain

Simon Appeltans
Hasselt University
Hasselt, Belgium

Konstantinos G. Arvanitis
Agricultural University of Athens
Athens, Greece

Valentina de la Barrera
INIA
Chile

Stanley Best
INIA
Chile

Irene Borra-Serrano
ICA-CSIC
Madrid, Spain

Ana de Castro
INIA CSIC
Madrid, Spain

Pietro Catania
University of Palermo
Palermo, Italy

Daeun Choi
University of Florida
Wimauma, FL, USA

Lucio Colizzi
University of Bari Aldo Moro
Bari, Italy

Gregorio Egea
Universidad de Sevilla
Sevilla, Spain

Spyros Fountas
Agricultural University of Athens
Athens, Greece

Emanuela Guerriero
University of Salento
Lecce, Italy

Michihisa Iida
Graduate School of Agriculture
Kyoto, Japan

Yang Li
Chinese Academy of Agricultural Sciences
Hangzhou, Zheijiang, China

Nunzia Lomonte
University of Bari Aldo Moro
Bari, Italy

Dimitrios Loukatos
Agricultural University of Athens
Athens, Greece

Joe Mari Maja
South Carolina State University
Orangeburg, SC, USA

José Maldonado
Instituto de Investigaciones Agropecuarias (INIA)
Chile, South America

Chrysanthos Maraveas
Agricultural University of Athens
Athens, Greece

Juan Carlos Melgar
Clemson University
Clemson, SC, USA

Omeed Mirbod
University of Florida
Wimauma, FL, USA

Kelly Nascimento-Silva
University of São Paulo
Piracicaba, Brazil

Melany Navarro
Instituto de Investigaciones Agropecuarias (INIA)
Chile, South America

José Manuel Peña
ICA CSIC
Madrid, Spain

Manuel Perez-Ruiz
Universidad de Sevilla
Sevilla, Spain

Eliseo Roma
University of Palermo
Palermo, Italy

Carla Román
IRTA
Lleida, Spain

Francisco Rovira-Más
Universitat Politècnica de València (UPV)
Valencia, Spain

Verónica Saiz-Rubio
Universitat Politècnica de València (UPV)
Valencia, Spain

Luis Sánchez-Fernández
Universidad de Sevilla
Sevilla, Spain

Eleni Symeonaki
University of West Attica
Egaleo, Greece

Julie Tang
UNSW
Sydney, Australia

Annie Xu Wang
UNSW
Sydney, Australia

Xu Wang
University of Florida
Wimauma, FL, USA

Mark Whitty
UNSW
Sydney, Australia

Jiajun Zhu
Lovol Japan Co., Ltd.
Osaka, Japan

Abbreviations

2D	two dimensions
3D	three dimensions
AGB	aboveground biomass
AI	artificial intelligence
ANN	artificial neural networks
API	application programming interface
Ca	calcium
CCD	charge-coupled device
CMOS	complementary metal oxide semiconductor
CNN	convolutional neural networks
CO_2	carbon dioxide
CPP	crop protection product
CSM	crop surface models
CWSI	crop water stress index
DAPPM	deep aggregation pyramid pooling module
DBMS	database management system
DC	duty cycle
DDRNets	deep dual-resolution networks
DEM	digital elevation model
DL	deep learning
DSLR	digital single-lens reflex
DSR	digital surface model
DSS	decision support systems
DTM	Digital Terrain Model
EC	electrical conductivity. Also, European Commission
ELC	empirical linear calibration
EM	electromagnetic radiation
EPPO	European and Mediterranean plant protection organization
ER	relational model or entity-relationship model
ET	evapotranspiration
ETo	reference evapotranspiration
EVOO	extra virgin olive oil
EXIF	exchangeable image file format
FAO	Food and Agriculture Organization (of the United Nations)
FCN	fully convolutional network
FDR	frequency domain reflectance
GCP	ground control points
GIS	geographic information system
GMO	genetically modified organisms
GNDVI	Green Normalized Difference Vegetation Index
GNSS	Global Navigation Satellite System
GPRS	General Packet Radio Service
GPS	Global Positioning System
GPU	graphics processing unit
GRVI	Green-Red Vegetation Index
GSD	ground surface distance
HLB	Huanglongbing

HMI	human-machine-interface
HSI	hue, saturation, intensity
HSV	hue, saturation, value
HTPPS	Hypertext Transfer Protocol Secure
IaaS	Infrastructure as a Service
ID	identification
IMU	inertial measurement unit
IoT	Internet of Things
IoU	intersection over union
IPM	integrated pest management
ISO	International Organization for Standardization
JSON	JavaScript Object Notation
K	potassium
KPI	key performance indicator
LAI	leaf area index
LCA	life cycle analysis
LIDAR	Light Detection and Ranging
LoRaWAN	Long-range, low-power wireless communication technology
LPWAN	Low-Power Wide-Area Network
LTP	local tangent plane
M3CI	Modified Canopy Chlorophyll Content Index
MED	minimum effective dose
Mg	magnesium
ML	machine learning
MQTT	Message Queuing Telemetry Transport
MSAVI	Modified Soil Adjusted Vegetation Index
MZ	management zones
N	nitrogen
NB-IoT	narrowband IoT
NDRE	Normalized Difference Red Edge
NDVI	Normalized Difference Vegetation Index
NIR	near infrared
$\mathbf{O_2}$	oxygen
OBIA	Object-based image analysis
OQDS	Olive Rapid Decline Syndrome
OWL	web ontology language
P	phosphorous
PaaS	Platform as a Service
PCD	plant cell density
PCR	polymerase chain reaction
PFRB	Peach Flat-headed Root Borer
pH	hydrogen potential
PMU	power management unit
PRI	photochemical reflectance index
PWM	pulse width modulation
QoS	Quality of Service
QR	quick response
RER	Red Edge Ratio
RGB	red, green, blue (color sensor)
RGB-D	red, green, blue (color sensor) plus depth sensor
ROS	Robot Operating System

RTK	real-time kinematic
RVI	Ratio Vegetation Index
S	sulfur
SaaS	Software as a Service
SD	secure digital
SDG	Sustainable Development Goals
SfM	structure from motion
SH	segmentation head
Si	silicon
SOAP	Simple Object Access Protocol
SOC	soil organic carbon
SPLA	Services Provider License Agreement
SQL	Structured Query Language
SSL	Secure Sockets Layer
SWIR	Shortwave infrared
TCP/IP	Transmission Control Protocol/Internet Protocol
TDR	Time Domain Reflectance
TIR	thermal infrared
TLS	Transport Layer Security
UAV	Unmanned Aerial Vehicles
USDA	United States Department of Agriculture
VI	vegetation indices
VLOS	visual line of sight
VRA	variable rate application
Wi-Fi	wireless fidelity
WSAN	Wireless Sensors and Actuators Networks
Xf	*Xylella fastidiosa*
XML	Extensible Markup Language

Glossary

Agriculture 4.0 Precision Agriculture where operations have improved accuracy due to telematics and data management

Agriculture 5.0 This kind of agriculture is based on precision agriculture and implies the use of robots and some forms of artificial intelligence

API A set of rules and specifications that allows different software applications to communicate and interact with each other. It is an intermediary that facilitates the exchange of data and functionality between different systems, without the systems needing to know the internal details of each other

API REST A type of web API that follows a set of architectural principles for building lightweight and efficient web services

Artificial Intelligence (AI) The ability of machines to mimic human intelligence processes like learning, problem-solving, and decision-making

Big data Extremely large and complex data sets that are difficult to process with traditional tools

Cloud computing On-demand computing resources (such as storage and infrastructure) as services over the Internet

Compaction Mechanical compression of soil particles and their aggregates

Consumer grade camera They focus on general photography and video recording, emphasizing image quality and ease of use

Deep learning It is a branch of machine learning that focuses on the use of multi-layered artificial neural networks to analyze data and learn complex patterns, similar to how the human brain works

Differentiated harvesting Practice of harvesting at different times or locations based on specific characteristics or needs

Digital twin Virtual representation of a physical object, process, or system that is updated with real-time data

Downsample The process of reducing the spatial resolution of an image, often by averaging or skipping pixel values. It is used, in this context, to simulate lower quality or match the resolution expected during model deployment

Drift Wasted spray fraction released into the air

DSLR camera Camera that works with a fixed digital sensor. It can autofocus and store a high number of photos on its internal memory card

Epoch A complete pass of the entire training dataset through the learning algorithm

FCNs-Edge (Fully Convolutional Networks—Edge) A deep learning model that was proposed for precise semantic segmentation in agricultural imagery

Gateway A device or software that acts as an intermediary to connect networks or systems that use different protocols. It translates and transfers data between those environments, enabling communication between them

Ground truth In the context of artificial intelligence and machine learning, it refers to accurate and verified data that is used as a reference for training, validating, and testing models

Holistic planning It considers all aspects of planning including data management, data collection, data processing and visualization

Hyperspectral imaging (HSI) Technique that captures and processes information across a wide range of electromagnetic spectrum wavelengths, providing detailed spectral information for each pixel in an image. HSI systems acquire hundreds of narrow spectral bands, allowing for the identification of materials and objects based on their unique spectral signature

Internet of Things (IoT) Systems Networks of interconnected devices, sensors, and actuators that collect, exchange, and analyze data through the internet

IoT Node Physical device within an Internet of Things (IoT) system that collects data from sensors, processes it, and communicates the information to other parts of the network, often via a gateway

LoRaWAN Open-source communication protocol that adopts LoRa (Long Range) low power wide area network technology

Machine learning A branch of artificial intelligence (AI) that focuses on the development of systems that can learn from data and improve their performance with experience, without being explicitly programmed for each task

Machine vision camera It provides visual feedback to vision-guided robotic systems. They are designed for automation tasks, prioritizing precision, robustness, and consistent performance

Middleware Software that acts as a bridge or intermediary between different applications or software components, enabling their communication and data management

Minimum Effective Dose The lowest amount of product that is necessary for effective pest control

MQTT Lightweight, publish-subscribe, machine-to-machine (M2M) messaging protocol that is ideal for IoT applications

Nadir Point on the celestial sphere directly below the observer, opposite the zenith

NB-IoT Narrowband IoT, wireless communication technology designed for connecting IoT devices to mobile networks

NoSQL Non-relational database that stores data in a non-tabular format, allowing for working with unstructured or semi-structured data, such as documents, key-value pairs, or graphs

Overlay In mapping and photogrammetry, image overlap refers to the amount of shared area between consecutive images captured by a camera

Perennial crop A plant that lives for more than two years, often producing harvests for multiple years without needing to be replanted each year

Phenology In the context of agriculture, science that examines the timing of life cycle events in plants

Raster In the context of geographic information systems (GIS), type of data that represents a surface divided into a regular grid of cells or pixels

ROS bag files Short for Robot Operating System bag files, these are file formats used in the ROS framework to record and store message data published over topics during a robotics session. They are commonly used for offline playback, analysis, and debugging of sensor data such as images, LiDAR, or GPS

Server Program or device that provides services to other programs or devices, called clients. These services may include data storage and management, web page hosting, sending and receiving email, etc.

SigFox It is a global, low-power, long-range communications network specifically designed for the Internet of Things (IoT)

SQL Programming language used to manage relational databases

Synergistic agriculture Farming technique that involves increasing the number of species per square meter in order to trigger positive interactions between them, increasing biodiversity in the soil and, consequently, strengthening the resilience of the cropping system

Test pit Excavation of ground for studying or sampling the composition and structure of the subsurface

Timestamp A digital record of the date and time when an event occurred

Training dataset Collection of labeled data used to train machine learning models

Trellis structure Framework (typically metal, but also wood, or bamboo) used to guide and support the vertical growth of plants, especially vines and climbing crops. Trellises offer numerous benefits, including increased sunlight exposure, improved air circulation, easier harvesting, and better disease management

Upsample The process of increasing the spatial resolution of an image, typically using interpolation techniques. However, in agricultural imagery, upsampling is often limited in effectiveness, as it cannot restore lost detail or improve the quality of low-resolution source data

Variable rate In the context of smart spraying, agricultural technique that adjusts the application rate of chemicals to optimize results and resources

VGG-16 (Visual Geometry Group—16-layer model) A convolutional neural network architecture introduced by Simonyan and Zisserman, characterized by its uniform use of small (3×3) convolution filters and a deep structure with 16 weight layers. Designed for large-scale image classification tasks, VGG-16 became known for its simplicity and effectiveness, especially in competitions like ImageNet (Simonyan & Zisserman, 2014)

Wavelength In the context of the book, range of the electromagnetic spectrum used to measure plant or soil radiation

Waypoint In the context of UAVs or drones, a geographic point defined on a route that a drone automatically follows during its flight

ZigBee Wireless communication protocol designed for personal area networks (PAN) of low consumption and low data velocity

1 Variable-Rate Spraying for Sustainable Citrus and Grape Production

Verónica Saiz-Rubio, Francisco Rovira-Más, and Carla Román-Rochina

1.1 INTRODUCTION

Agriculture faces increasing pressure to meet stringent market standards while minimizing food waste and adhering to sustainable practices. Pests and diseases, if not effectively managed, contribute significantly to food losses, threatening global food security and causing substantial economic losses. This challenge is particularly acute in high-value specialty crops, such as fresh-market fruits, where the precise application of crop protection products (CPP) is critical. Ineffective pest management can lead to crop losses of 55%–100% in specialty crops (Knutson & Smith, 1999), as demonstrated by recent outbreaks such as huanglongbing (HLB) in citrus and *Xylella fastidiosa* in olives (Barbieri et al., 2023; Morelli et al., 2021). However, the regular use of pesticides carries inherent risks to human health and the environment, making balanced and efficient crop protection strategies necessary. To address environmental and regulatory challenges, new European Union legislation introduced in 2009 significantly reshaped pesticide regulations by incorporating the sustainability principles outlined in the Sixth Environmental Action Program. In particular, Regulation 1107/2009, which governs the authorization and marketing of plant protection products (European Commission (EC), 2009a), as well as Directives 2009/127/EC and 2009/128/EC, which address pesticide application equipment and the sustainable use of pesticides (EC, 2009b, 2009c). In 2019, the European Commission launched the *European Green Deal* (EC, 2019), followed by the 2020 *Farm to Fork Strategy*, which proposed a 50% reduction in pesticide use by 2030 (EC, 2020). Despite ongoing debates surrounding its implementation, there is a broad recognition of the need for safer and more environmentally responsible pesticide use. A key strategy to achieve this reduction is dose adjustment—defined by EPPO (2021) as adapting pesticide doses to specific circumstances—ensuring that real applications remain as close as possible to the minimum effective dose (MED). The MED is the lowest amount of product that is necessary for effective pest control (EPPO, 2012), taking into account factors such as canopy structure (shape, volume, and leaf density), sprayer technology, specific pest properties, biotic pressure, or the specific CPP to be applied.

Traditional blast sprayers, widely used in specialty crops, can result in approximately 50% of the spray being deposited on the target canopy, with about 30% lost to drift (wasted spray fraction released into the air) and 20% lost to ground (Garcerá et al., 2017; Jensen & Olesen, 2014). Although these losses can be reduced by proper dose adjustment and careful sprayer calibration, conventional application techniques still apply a constant rate across the entire field, ignoring in-field variability in canopy size or density. This typically leads to overapplication in areas of smaller vegetation and under-application in denser canopies. In fact, spatial variability in vegetation—caused by factors such as soil composition, slope, or localized pest and disease pressures—creates opportunities for variable rate (VR) application (VRA) technologies. VRA enables the adaptation of spray doses to specific canopy characteristics, allowing differentiated management of CPP inputs. Three fundamental aspects underpin VRA: Accurate canopy characterization, precise positioning in the field,

DOI: 10.1201/9781003510598-1

and stable control of spray flow. Proximal- and remote-sensing technologies are therefore crucial, as they provide detailed information on crop conditions that help determine the relevant variables for dose adjustment. These crop sensors can be mounted on ground-based agricultural machinery (*proximal sensors*) or on aerial platforms such as drones, airplanes, and satellites (*remote sensors*).

Among the primary sensor types used for canopy characterization for VRA of CPPs are ultrasonic sensors, which use sound waves to measure the distance between the sensor and the vegetation, providing an estimate of canopy volume at different heights; LiDAR (Light Detection and Ranging), which emits laser pulses and measures their return time to construct three-dimensional (3D) images of the crop canopy, enabling precise spray-volume adjustments; RGB-D sensors, which combine depth sensors with color (RGB) imaging to capture 3D images with simultaneous color and distance data for detailed canopy density analysis; and multispectral cameras, which capture images in multiple electromagnetic bands and thus allow the calculation of key vegetation indices such as NDVI and PCD (plant cell density), indicators of plant vigor. By dynamically adjusting pesticide flow rates according to canopy characteristics, VRA systems can reduce pesticide use by 20%–80% (Campos et al., 2020; Román et al., 2021, 2023; Wei et al., 2022), yielding substantial cost savings for growers while maintaining or even improving pest control efficacy. VRA also contributes to more sustainable and environment-friendly farming practices by minimizing drift into the atmosphere and reducing soil and water contamination. These improvements protect surrounding ecosystems, ensure safer working conditions for farmers, and promote healthier environments for nearby communities. Additionally, the advantages of VRA technology are well aligned with multiple United Nations Sustainable Development Goals (SDGs). In particular, by enhancing sustainable food production, it aligns with SDG 2 (Zero Hunger) and the associated KPI 2.4.1 on sustainable agricultural practices. By reducing pesticide exposure and environmental contamination, VRA also contributes to SDG 3 (Good Health and Well-Being), specifically KPIs 3.9.1 and 3.9.2, which aim to lower deaths and illnesses linked to pollution.

Specialty crops, such as orchard-grown fruits, pose unique challenges for crop protection due to their dense canopies. Achieving uniform droplet size and maintaining consistent spray pressure can be problematic when using high flow rates and changing application volumes. A fluctuating pressure often reduces deposition efficiency and coverage, thereby compromising pest control outcomes (Ortiz et al., 2023; Rovira-Más et al., 2024). This can result in unknown droplet size distributions and uncontrolled pesticide dispersion, exacerbating contamination and inefficiency. In light of these factors, this chapter shows the critical importance of adopting effective crop protection strategies by underlining the relevance of VRA technologies as a solution to face the challenges of sustainable spraying, offering significant benefits for meeting the stringent fresh-market standards of specialty crops.

1.2 SMART GROUND-BASED SPRAYING PLATFORMS: SYSTEM ARCHITECTURE

The management cycle of Figure 1.1 relies on the systematic availability of field information, where multiple types of data are regularly collected for supporting decision-making. Based on this cycle, the second stage between the growing crop and its related data is represented by data-collecting platforms. It generally refers to any potential platform, including Earth observation satellites, unmanned aerial vehicles (UAV or drones), and ground vehicles, where non-invasive sensors are carried to retrieve data from the crop (Saiz-Rubio & Rovira-Más, 2020). When this procedure is applied to the current case of sustainable spraying, several platforms must be considered. First, the smart sprayer, a ground or aerial vehicle (not legal yet in many countries) enabled to vary spray rate in real time to optimally adjust the volume of applied products to the canopy needs. Second, if the sprayer is reading a prescription map, a spray map generator, which can be derived from a vegetation map obtained from aerial images captured by satellites or UAVs, or alternatively by scouting ground platforms such as smart tractors or robots, either human-operated or autonomous (Unmanned Ground Vehicles or UGV). The practical cases described in this chapter feature a smart

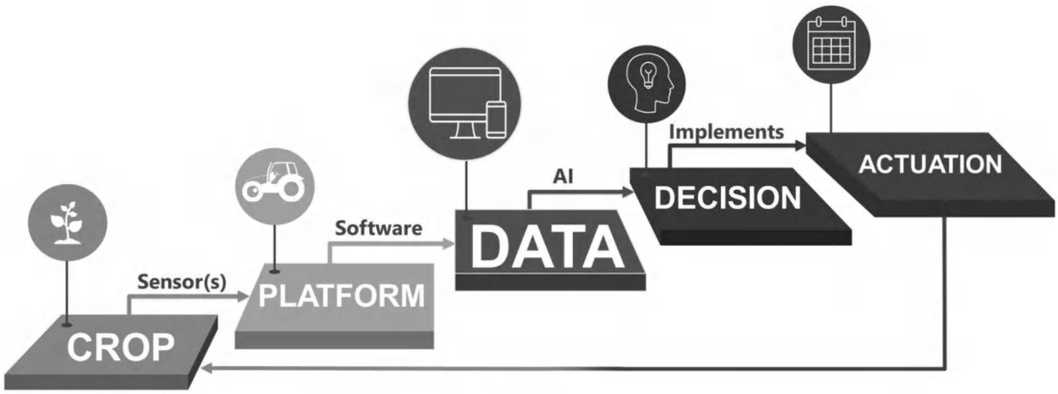

FIGURE 1.1 Data-based management cycle for advanced agriculture. (From Saiz-Rubio & Rovira-Más, 2020.)

ground sprayer enabled to read prescription maps obtained from NDVI (normalized difference vegetation index) images downloaded from the Sentinel-2 satellites of the Earth Observation European Program Copernicus.

A smart sprayer, as any other intelligent vehicle, is an agricultural vehicle that uses artificial intelligence to automate any of its key functions. In the case of sprayers, this automation can be applied to two critical functionalities:

1. Autonomous navigation
2. Real-time adjustment of spray rate to site-specific canopy properties.

Figure 1.2 depicts a conceptual architecture of a vehicle featuring both functionalities, what can be considered as *full autonomy.* As shown in the schematic, different systems for sensing, actuation, and interfacing need to be optimally and mutually connected. Full autonomy will require at least one computing unit for processing sensor data, calculating control parameters and sending actuation commands. When both functionalities are implemented in the same vehicle, at least one processing unit should be in charge of each functionality for safety purposes, as the calculation of navigation commands should never be compromised in resources by the estimation or calculation

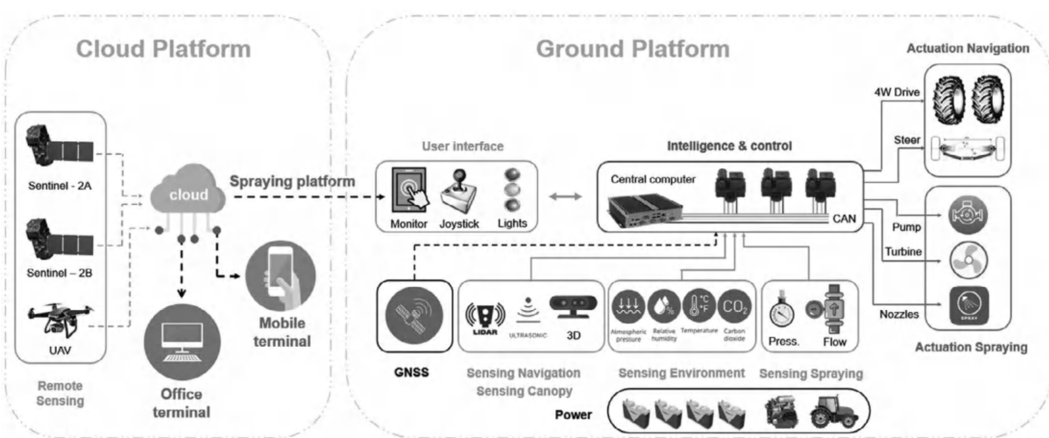

FIGURE 1.2 Generic system architecture for smart sprayers.

of spray parameters. Autonomous navigation requires the calculation and execution of navigation commands, which can follow diverse approaches according to the way the vehicle is guided: If positioning is accurately determined by one (or more) GNSS receiver, reliable devices and an advantageous location of the antennas are crucial; however, if local perception is in charge of supplying steering cues, sensors capable of perceiving the vehicle surroundings, such as 3D cameras (stereo vision or time of flight), LiDAR, or ultrasonics, are typical components to consider. Likewise, steering actuation can be achieved differently by automatically turning the steering wheel with an electric motor, or alternatively by mechanically actuating on the steering linkage with either fluid power or electric motors. In addition to steering control, autonomous navigation also requires speed control, which always has to be overrun by the safety system (or layer as described in Rovira-Más, 2010), in particular for obstacle detection. In this sense, navigation approaches based on local perception bring an advantage over GNSS-based systems, as any sudden obstacle interfering with the vehicle trajectory will be immediately detected.

The second functionality that automatically adjusts spray rate to canopy volume and density hits the core of spraying actuation and therefore is probably the most important advancement to meet current sustainability goals of reducing pesticide use, atmosphere pollution by spray drift, and soil contamination by runoff. In this case, the key parameter to calculate in real time is the site-specific spray rate (L/ha), which depending on row spacing (m) and vehicle speed (m/s) is instantly transformed to flow rate (L/min) as the basic control command. Although not common in practice, a highly automated spray system might also automatically control the rotation of the pump (rpm) and the air flow (m^3/s) by varying the speed of a turbine in blast sprayers, as indicated in Figure 1.2. For the calculation of the site-specific spray rate, the principal parameter, two approaches leading to different architectures can also be followed. If the rates are calculated before the field treatment and coded into a prescription map, the sprayer needs a reliable GNSS receiver that accurately locates the vehicle in the field, such that map-coded rates are precisely transferred to the vehicle in real time. The maps have to be uploaded to the smart sprayer before the beginning of the spraying task, and it can be done manually from a memory drive or wirelessly from the cloud if the proper cloud-based interfacing platform has been set. The major disadvantage for farmers of this approach is the need to generate a prescription map of their field. This used to be a barrier for vehicle operators not familiar with digital technologies, as composing a prescription map is typically dependent on controller design and thus requires learning proprietary software that changes for each machine. To circumvent these obstacles to a wide implementation, Rovira-Más et al. (2024) developed a format-free coding method for building prescription maps in simple text files containing only geodetic coordinates and desired spray rates. The alternative approach to generate spray rates on the fly requires proximal sensors that characterize the canopy in real time. The perception sensors of Figure 1.2 used for navigation can also be used for rendering the profile of the canopy as a measurement of volume, which can be further refined with other environmental sensors to better adjust canopy needs to spray volume. Once the spray rate has been determined by either approach, the final stage is common to both of them and consists of executing the spray action and deliver the calculated amount of product. This is not a trivial matter, given the complexities of a highly dynamic hydraulic system. As explained in Section 1.3, there are alternative ways to actuate over the nozzles to reach the desired target rate at every instant. Section 1.4 explains in greater detail how a pressure-based control system can keep the pressure in an acceptable range regardless of the automatic opening and closing of the valves. Finally, the architecture of Figure 1.2 also includes sensors for the two key hydraulic parameters of spraying systems: Flow rate and pressure. In addition to provide feedback measurements for the automatic control of pressure (Section 1.4), the real-time registry of flow and pressure in the onboard computer provides a systematic way for certifying good sustainability practices, as flow measurements will prove pesticide reduction in real applications, whereas pressure series can prove that droplet size has been kept in the optimum range for the majority of the treatment.

The system architecture depicted in Figure 1.2 represents the most demanding case of full autonomy, which implies the automation of both navigation and spraying. However, from the operator perspective, driving a tractor is much easier than changing the spray rate while in motion according to the canopies being sprayed. In addition, autonomous navigation of machines that typically include water tanks between 1000 L and 3000 L entails serious risks when unmanned. The sprayer of Figure 1.3a features the system architecture of Figure 1.3b, which is a customization of the architecture of Figure 1.2 by which spray rate is automatically determined by a prescription map uploaded before the treatment.

The goals of the sprayer of Figure 1.3 are the reduction of pesticide use and the prevention of drift; therefore, automation was focused on the accurate determination and delivery of rates. The flow chart of Figure 1.4 indicates how map information is translated to instantaneous rates linked to a geographical location, and how these rates are applied by actuating pulse width modulation (PWM) solenoid valves, whose working principles are explained in Section 1.3. As shown in the diagram, the sprayer needs a GNSS receiver and a reliable estimation of ground speed to convert spray rates (L/ha) to flow rates (L/min), as the ultimate executing commands that actuate the solenoid valves (duty cycle %). Even though ground speed can be retrieved from the GNSS VTG NMEA strings, this speed tends to be too noisy and often leads to the wrong calculation of flow rates. An advantage of prescription maps versus reactive systems that estimate canopy properties with proximal sensors in real time is the possibility of using external information, historical data, and calibrating functions using maximum and minimum values of canopy parameters. Case Study 2 describes the results and performance of the sprayer of Figure 1.3 for orchards of different canopy structures (intensive and traditional), and Case Study 1 describes the results of a prototype adapted for vineyards, which was endowed with the same architecture of Figure 1.3b.

1.3 APPROACHES TO VARIABLE RATE APPLICATIONS IN SPECIALTY CROPS

VR technology enables the dynamic adjustment of pesticide application in response to spatial and temporal variability in the field. The two key components of VR strategies are the following:

1. how the optimal rate is determined
2. how the sprayer flow is controlled to deliver that rate accurately.

This section describes the main approaches for determining pesticide rates – either directly from onboard sensing or from prescription maps – and for controlling spray flow by adjusting circuit pressure or using PWM nozzles.

1.3.1 Rates Determination

1.3.1.1 Real-Time Rate Calculation from Perception Sensors

Real-time VR sprayers rely on sensors that measure canopy characteristics and compute the appropriate application rate on-the-go. Ultrasonic transducers estimate canopy structure by emitting sound waves and measuring their return time, which provides the distance from the sensor to the nearest foliage surface (line of sight). To approximate canopy volume, these measurements are combined with the known row spacing (depth) and the sensor's mounting height, allowing the system to compute a cross-sectional area (Llorens et al., 2010). Sprayers equipped with ultrasonic sensors have limited resolution, but this can be improved by increasing the number of sensors placed at different heights. However, they remain susceptible to environmental factors such as wind-induced leaf movement or water on the sensor, and multiple sensors may interfere with each other's signals (Jeon et al., 2011). In contrast, LiDAR also measures distances but uses laser pulses to generate high-resolution three-dimensional point clouds of the canopy, capturing detailed information on shape

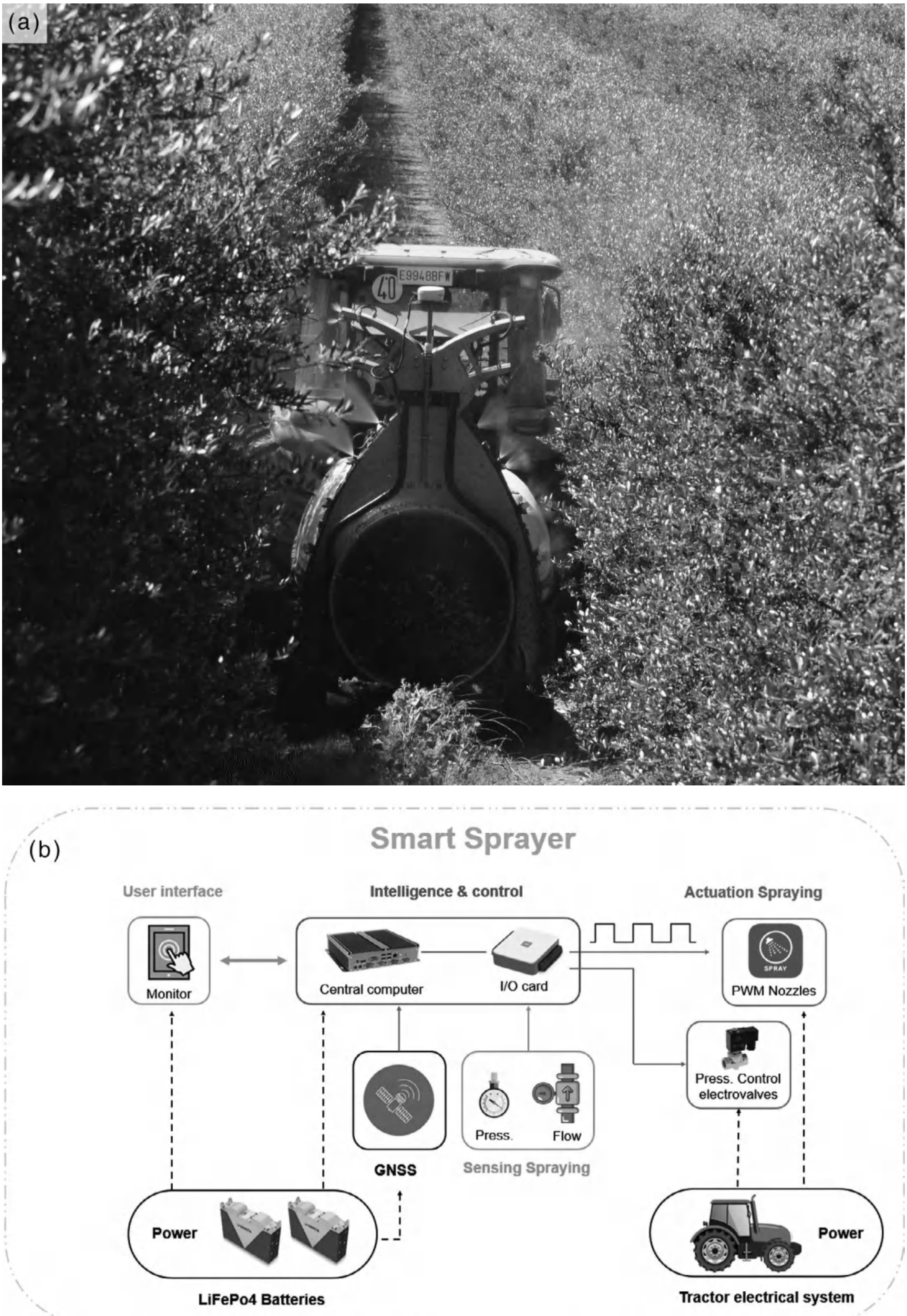

FIGURE 1.3 Smart sprayer prototype for orchards: (a) sprayer; (b) system architecture.

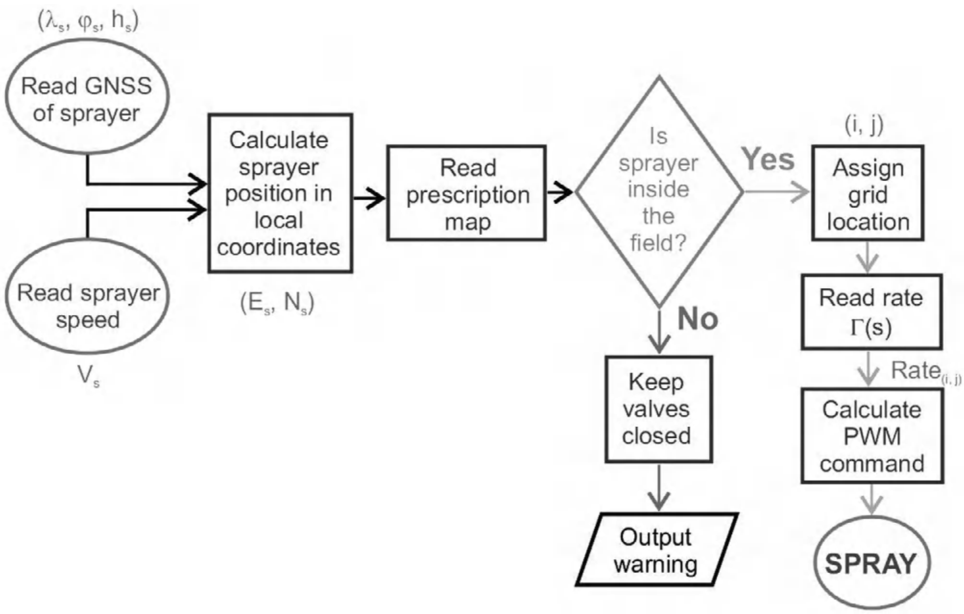

FIGURE 1.4 Automated spraying with prescription maps and PWM-actuated nozzles.

and density along the canopy height. Unlike ultrasonic sensors, a single LiDAR unit can scan both rows (left and right of the sprayer) simultaneously, capturing the complete canopy profile (Llorens et al., 2011; Shen et al., 2017). This level of precision makes LiDAR particularly valuable for complex canopies, but it can be expensive and requires significant processing power.

RGB-D cameras, which combine color imaging with depth sensing, have been proven capable of measuring complex canopy volume using stereo vision (Jeon & Zhu, 2023). This technique estimates depth by analyzing disparities between images captured from slightly different viewpoints, allowing the system to determine the distance from detected objects to the sensor. Compared to ultrasonic sensors, RGB-D cameras offer higher resolution but require at least one camera per row side. Although they are not as accurate as LiDAR, they provide a cost-effective alternative for canopy profiling (Román et al., 2023). Moreover, these sensors can capture color and infrared data at the pixel level, enabling more complex analyses of leaf density, plant health, or even the presence of diseases. By analyzing spectral variations, algorithms can detect stress indicators (discolorations) or anomalies such as disease spots, which can be used for targeted (spot) spraying applications (Zhang et al., 2022). At present, even though RGB-D cameras typically have a shorter range and are slightly sensitive to bright outdoor light, they remain a more affordable option than LiDAR for canopy assessment and integrate well with vision-based workflows.

Once sensor data is collected, canopy volume is usually estimated from sensor-measured distances, which are subtracted from the distance between the sensor and the center of the tree row to determine the vegetation depth to be treated, along with the cross-sectional area, ensuring that application rates are proportional to canopy volume. For example, if a sensor identifies 1 m^3 of canopy and the recommended rate is 0.08 L/m^3, then 0.08 L of product would be applied by the sprayer nozzles to that segment, ensuring that the canopy receives the proportional volume rate. However, these calculations must account for several factors. The distance between sensors and nozzles in the traveling direction must be considered, as it introduces a time delay between measurement and application. As a result, processing speed is crucial in interpreting sensor data quickly enough to prevent exceeding this delay. Additionally, the sprayer travel speed affects the available time for adjustments, with higher speeds reducing the window for data processing. To compensate for these challenges, the width considered in the cross-sectional area calculation can be increased, allowing for smoother adjustments and maintaining an acceptable application accuracy (Jeon & Zhu, 2022).

Regardless of the sensing technology used to model canopy volume, a seamless integration with the sprayer flow-control hardware is essential. Rapid nozzle adjustments—whether through pressure modulation or PWM solenoid valves—are necessary to maintain the intended dose at the intended crop location. The most notable advantages of sensor-based VR systems is their ability to adapt in real time to changing canopy conditions. By applying product only where needed and in proportion to canopy size or density, growers can reduce input costs and minimize environmental impact. Additionally, when integrated with sprayer controllers, these systems enable automated operations, reducing operator's workload significantly. Ongoing research has focused on the development of VR prototypes that use different sensors and control strategies to improve the efficiency of pesticide application. Some systems rely on ultrasonic sensors at multiple heights to adapt spraying according to individual canopy strata (Jeon & Zhu, 2012; Llorens et al., 2010; Salas et al., 2025), whereas other approaches combine LiDAR scanning with PWM actuation to achieve precise volume measurements and rapid flow changes (Salcedo et al., 2020; Shen et al., 2017). RGB-D cameras have also been explored for volume-based applications, offering additional color data to estimate leaf density at a lower cost than LiDARs (Román et al., 2023; Xue et al., 2023). On the commercial side, the USDA (United States Department of Agriculture) has developed a LiDAR-based VR kit, marketed as **Smart Apply®**, which combines LiDAR, PWM, and VR for retrofitting conventional sprayers. This system has shown promising results in vineyards to effectively control fungal diseases and the Japanese beetle, reducing spray volume by 29%–83% (Wodzicki et al., 2023). Laboratory prototypes using hyperspectral imaging have also been tested for selective spraying of disease-infected zones, such as vine downy mildew (Oberti et al., 2016). Despite these advancements, the adoption of high-resolution sensor-based VR systems remains limited, particularly outside the USA. For specialty crops, the most widely used system in practice is still the on–off ultrasonic-based approach, which simply detects canopy presence to activate or deactivate spraying (Miranda-Fuentes et al., 2017). The complexity of integrating newer technologies in sensing, modeling, and controls has slowed down their adoption in the field; however, as the costs of 3D sensors decline and real-time processing algorithms improve, high-resolution sensing combined with PWM control is expected to gain industry acceptance, enhancing precision in pesticide applications.

1.3.1.2 Variable Spray Rate Determined by Uploaded Prescription Maps

VRs can also be implemented using prescription maps, which predetermine application rates for specific zones within an orchard or vineyard. Unlike real-time sensor systems, which continuously adapt spray rates on-the-fly, prescription maps are generated prior to field operations using spatial datasets that capture variability in plant vigor, pest pressure, or other relevant agronomic factors. These maps are uploaded to the sprayer's control system and combined with GNSS coordinates to ensure that each zone receives the assigned rate as the machine moves through the field.

In most practical applications, prescription maps are generated using a single spatial data layer, typically a vegetation index derived from aerial or satellite imagery. The normalized difference vegetation index (NDVI) is the most common due to its accessibility and ease of processing (Campos et al., 2020; Campos et al., 2021). However, NDVI tends to saturate in high- vigor crops, which limits its utility in dense canopies. In such cases, alternative indices such as PCD may offer improved sensitivity (Proffitt et al., 2006). Although it is technically possible to integrate additional layers—such as historical yield data, soil properties, pest incidence records, or scouting observations—this is not commonly done in commercial settings, largely due to the complexity of data acquisition and processing. Instead, classification algorithms (e.g., clustering) are typically applied to the vegetation index layer alone to define relatively homogeneous management zones (Rodríguez-Lizana et al., 2021). For operational efficiency, it is generally recommended to divide the field into two or three zones, each one assigned to a specific application rate based on relative vigor or stress level. A prescription dose is assigned to each management zone, which can be determined with decision support systems (DSS) such as DOSA3D, DOSAVIÑA (Gil et al., 2019), DOSAOLIVAR, or CITRUSVOL among others (Garcerá et al., 2021). These software tools calculate the MED by considering various crop and application parameters, including canopy characteristics, sprayer configuration, and target pest or disease. Once the prescription map is generated—with each zone linked to a specific dose—it is uploaded to the sprayer's control system, typically as shapefiles or in other formats like those proposed by Rovira-Más et al. (2024). Combined with GNSS positioning, the sprayer can accurately apply the predefined product rates across the designated zones during operation.

The prescription map approach offers several advantages. First, because rate determinations are made prior to field operations, the system eliminates the need for onboard computation, thereby simplifying the sprayer's hardware architecture. This reduces the risk of real-time processing delays, operational issues, and equipment costs. Second, the use of historical or multi-temporal data enables consistency and continuous refinement over time, as prescription maps can be updated seasonally based on new measurements or agronomic insights. Additionally, pre-season planning allows application strategies to be developed independently of immediate environmental conditions, providing greater logistical flexibility for field operations. However, prescription maps also present several limitations. Because they are generated prior to field operations, they cannot account for unexpected anomalies such as localized plant stress, sudden pest outbreaks, or rapid changes in canopy development. This temporal disconnection may reduce application effectiveness under dynamic field conditions. In addition, the potential for pesticide savings is often constrained by the coarse resolution of typical management zones—commonly limited to two or three classes—which may result in only moderate reductions in spray volume, typically up to 25% (Román et al., 2021). Another key challenge to consider is the lack of standardization in prescription map formats, which complicates integration across different software platforms and sprayer control systems, thereby limiting interoperability. As noted by Rovira-Más et al. (2024), no universally accepted protocol currently exists for the creation, formatting, or sharing of prescription maps. Finally, the development and implementation of effective prescription maps requires technical expertise in geospatial analysis, remote sensing, and VR principles—skills that may not be readily available to all growers or advisors.

Table 1.1 presents a comparison between VR systems based on prescription maps and real-time sensors. While each approach has distinct advantages and limitations, ongoing advances in digital agriculture and data integration are fostering convergence between the two of them. In particular, prescription-based systems are expected to complement—and in some cases integrate with—real-time VR technologies. For instance, biotic or abiotic stress indicators (e.g., disease presence or water stress) identified through remote sensing or historical scouting data could be incorporated into prescription maps. These, in turn, can be combined with real-time canopy volume measurements from sensors such as LiDAR or RGB-D cameras to dynamically adjust spray doses in the field.

1.3.2 Flow Control

Once the target rate is determined—whether in real time or from a prescription map—the sprayer must adjust its spray output accordingly. Two primary methods exist for modulating the flow of CPPs in VR systems:

1. Changing the circuit (nozzle) pressure to force a change in the sprayed flow
2. Using PWM solenoid valves prior to the nozzles.

1.3.2.1 Real-Time Modification of the Circuit Pressure

The most popular method for regulating flow today is to vary the operating pressure in the sprayer's hydraulic circuit. As pressure increases, liquid flow through the nozzles also increases; conversely, reducing pressure lowers the output flow. This technique is widely supported by existing hardware and is relatively easy to implement on commercial sprayers.

TABLE 1.1
Comparison of VR Systems Based on Prescription Maps and Real-Time Sensors

Criterion	Prescription Maps	Real-Time Sensors
Information source	Multispectral data, historical and multi-seasonal data (yield, soil, imagery, etc.)	Data captured during operation (canopy, distance, color, etc.)
Timing of dose calculation	Prior to field operation	During field operation, in real time
Adaptation to current conditions	Limited (does not respond to unexpected changes)	High (adjusts dosage based on instantaneous canopy conditions)
Processing requirements	Low, pre-processed offline	High, requires fast and continuous onboard computation
Hardware requirements	GNSS and compatible control terminal	Sensors (ultrasonic, LiDAR, RGB-D), controllers, and additional hardware
Temporal consistency	High in stable management zones	Variable, depends on real-time data quality
Pre-treatment effort	High (data analysis, map creation, integration)	Moderate (sensor calibration and configuration)
Interoperability	Limited due to lack of standardized formats	More flexible if system is fully integrated
Initial cost	Variable (depends on data and GIS software used)	High (advanced sensors like LiDAR may be expensive)
Scalability	High in fields with consistent spatial patterns	High in fields with dynamic variability

However, the major weakness of this approach lies in its impact on droplet size. Because nozzle pressure directly influences droplet formation, any change in pressure to adjust flow also alters droplet characteristics. High pressure produces finer droplets, which are more susceptible to drift and evaporation. In contrast, lower pressures result in coarser droplets, which may reduce canopy coverage and biological efficacy. This trade-off poses a challenge for maintaining both dosage accuracy and spray quality, especially when large flow rate adjustments are required. For this reason, pressure-based flow modulation must operate within a limited range to avoid compromising coverage uniformity or increasing the risk of off-target losses. While still widely used, this method is gradually being supplemented or replaced by more advanced technologies in precision spraying systems.

1.3.2.2 Pulse Width Modulated (PWM) Solenoid Valves

PWM technology is a more advanced, flexible solution for flow control in modern VR sprayers. In PWM systems, nozzles are equipped with solenoid valves that open and close rapidly at a fixed frequency. The proportion of time that the valve is open during each cycle, known as the duty cycle (DC), determines the flow rate (Figure 1.5). The most important advantage of PWM flow control is the capability of the system to maintain constant pressure throughout operation, ensuring consistent droplet sizes and spray patterns regardless of flow changes.

The decoupling of flow rate and pressure offers several advantages. First, it ensures uniform droplet size across different application rates, which is essential for effective and efficient pesticide deposition (Grella et al., 2022). Second, PWM valves enable fine-grained and rapid flow adjustments, making it compatible with real-time, sensor-based VR and prescription map-based strategies. Third, many PWM-based sprayers support individual nozzle control, enabling precise application to variable canopy structures or targeted spot treatments. Despite their advantages, PWM systems have limitations too. One significant constraint is the working pressure. Commercial PWM valves are generally limited to a maximum of 6–8 bar (600–800 kPa), which may be insufficient for

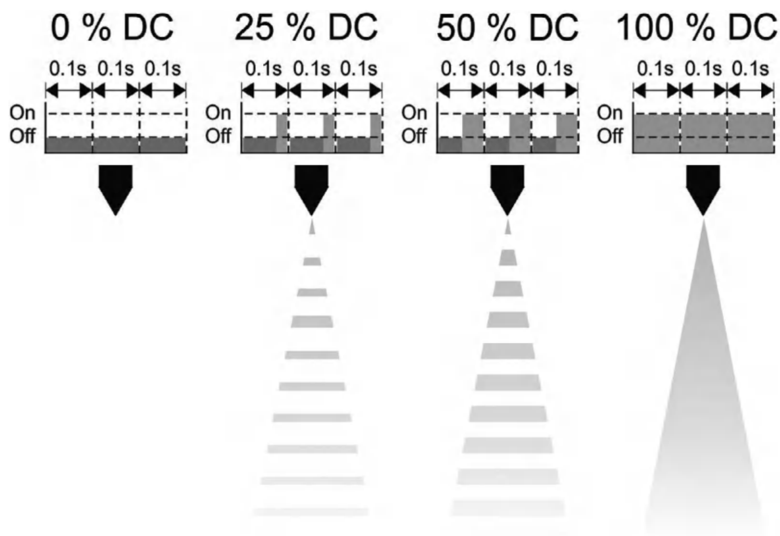

FIGURE 1.5 Operation of PWM valves at different duty cycles (DCs).

applications requiring high-pressure operations (Campos et al., 2025). Examples of such applications include dense canopy penetration and high-speed spraying. Exceeding this pressure range can compromise valve functioning or longevity. Additionally, high precision necessitates increased valve cycling frequency, which can result in mechanical wear, heat accumulation, and diminished reliability over time, especially during continuous, high-duty-cycle operations. Finally, while PWM systems aim at maintaining constant pressure, rapid changes in DC or flow demand can induce transient pressure fluctuations (Román et al., 2025; Saiz-Rubio et al., 2023). These fluctuations can affect spray pattern uniformity if not properly compensated for in the system design, for example, by using air dampers or feedback pressure control systems. Nevertheless, PWM systems are becoming the preferred flow control method in high-precision sprayers, especially when combined with advanced sensing technologies. Their ability to deliver accurate, rate-adjusted spraying while maintaining stable droplet characteristics makes it a key enabling technology for current and future VR systems.

1.4 CONTROL ALGORITHMS FOR VR APPLICATIONS

The current requirements for sustainable spraying forces machinery developers and manufacturers to reduce off-target spraying, specifically drift to the air and runoff to the soil. This is particularly important in orchards where canopies are dense and can reach high dimensions. As explained in Section 1.3, a consistent droplet size requires maintaining circuit pressure within a reduced range of variations. The control of spray flow through PWM solenoid valves enables sprayers to change flows very fast as changing flows is equivalent to changing the DC of solenoids, which are electronically actuated. Such electronic control is favorable to VR systems, as flows are rapidly changed by computer-generated commands. However, the rapid actuation of solenoids that partially- or totally open and close multiple valves creates unavoidable and unpredictable changes in pressure, which ultimately affects droplet size and the spraying beam pattern. VR systems that follow a prescription map can attenuate large changes of flow as these changes are known prior to nozzle actuation. However, sensor-based VR systems alter flows according to real-time sensor readings, and therefore cannot foresee significant pressure jumps. Nevertheless, regardless of the procedure to execute VRs, it is always convenient to include an automatic control system to grant that circuit pressure falls within reasonable ranges regardless of how fast flows are changed or how large flow magnitude varies. By bounding pressure consistently during operations, in addition to accurately reproduce prescribed rates and thus reduce off-target spray, the PWM solenoids are robustly protected from dangerous overpressures that quickly damage the mechanical parts of the valves.

The sprayer of Figure 1.3 was designed to independently and automatically control the four sectors of Figure 1.6. As shown in the figure, sectors 1 and 2 are the central sectors that deliver most of the volume to the crops, whereas sectors 3 and 4 are peripheral sectors with the highest likelihood of producing drift and runoff. Without the height of the trees as a crop parameter included in the prescription maps for making decisions on nozzle actuation, the automatic distribution of spray rate among sectors depended on the spray flow being delivered at any instant, under the grounds that small canopies required small amounts of volume, and therefore less participation of peripheral sectors 3 and 4. The mathematical formulation of such control strategy was based on the following empirical rule (Equation 1.1), where Q_c is the current flow prescribed by the map for the instant location of the sprayer, Q_{max} is the maximum flow reachable by the hydraulic system, being 65–80 L/min in the sprayer of Figure 1.3a for the traditional olive orchard and 65 L/min for the trellised orchard, Q_{1-2} is the flow delivered by central sectors (Figure 1.6), Q_{3-4} is the flow delivered by peripheral sectors, and alpha is a weight factor, which in the developed sprayer was $\alpha = 0.3$:

$$\left.\begin{array}{l} \text{if } Q_c < 0.3\cdot Q_{max} \rightarrow \left(\begin{array}{c} Q_{1-2} = Q_c \\ Q_{3-4} = 0 \end{array}\right) \\ \text{if } Q_c > 0.7\cdot Q_{max} \rightarrow \left(\begin{array}{c} Q_{1-2} = 0.5\cdot Q_c \\ Q_{3-4} = 0.5\cdot Q_c \end{array}\right) \\ \text{Otherwise} \rightarrow \left(\begin{array}{c} Q_{1-2} = \dfrac{Q_c}{2-\alpha} \\ Q_{3-4} = \dfrac{Q_c\cdot(1-\alpha)}{2-\alpha} \end{array}\right) \end{array}\right\} \tag{1.1}$$

When prescriptions maps were uploaded to the smart sprayer of Figure 1.3, and the strategy of Eq. (1.1) applied, the behavior of the sprayer was satisfactory for prescription maps with gradual changes of spray rate, which is the typical case in intensive orchards with regular canopies (Figure 1.3a). However, when tested in traditional olive orchards with old trees and missing trees,

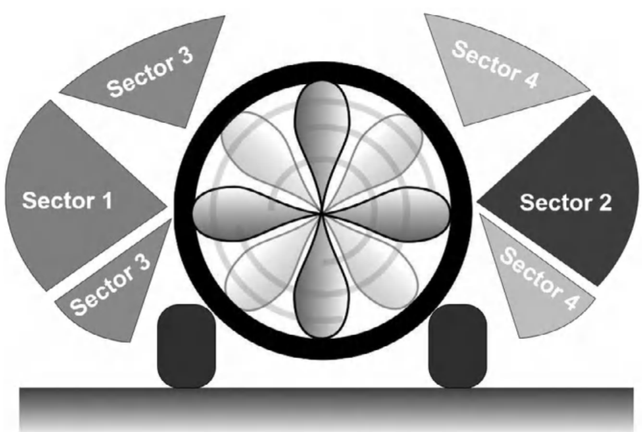

FIGURE 1.6 Multi-sector strategy for intelligent sprayers.

larger rate variations resulted in sudden peaks of pressure. The targeted pressure for the sprayer was 700 kPa (7 bar), but the solenoid valves used by the PWM system could not stand pressures above 1 MPa (10 bar); consequently, a counterweighting measure was needed to stabilize pressure under unforeseen spray rate variations. The implemented solution was given by the PD (proportional–derivative) control law of Eq. (1.2), where the (pressure) error ε was the difference between the target pressure of 700 kPa and the current pressure given by the onboard sensors, k_p was the proportional constant, and k_d was the derivative constant.

$$\text{control} = \varepsilon_k \cdot k_p + k_d \cdot \left|\varepsilon_k - \varepsilon_{k-1}\right| \tag{1.2}$$

The architecture of Figure 1.3b includes the actuation of pressure control electrovalves. In reality, there were four shut-off valves in a multi-stage arrangement, by which jumps in the control variable of Eq. (1.2) greater than 150 kPa opened the next valve if the differential was positive and closed it if the differential was negative. The electrovalves opened to the main return line to alleviate pressure and converge to the target pressure as fast as possible. Theoretically, the control system should actuate on a pressure-relief valve to reduce pressure error ε, but all the commercial valves available were too slow to grant the protection of the system, and thus the multi-stage system resulted more efficient and reactive with fast shut-off valves. Case Study 2 describes a use case where the performance of the sprayer of Figure 1.6 and its pressure control system is further discussed.

CASE STUDY 1 – VARIABLE RATE APPLIED TO TRELLISED STRUCTURES: WINE GRAPE VINEYARDS

CROP DESCRIPTION AND GENERATION OF PRESCRIPTION MAPS

This section presents the results obtained in a 0.91-ha trellised wine grape vineyard of the winery *Viñas del Vero* in Barbastro (Spain). The vineyard is planted with the *Macabeo* cultivar and follows a linear trellised training system with a 3-m row spacing, a common configuration in high-value vineyards of the region.

Wine grape vineyards have a repetitive and organized structure consisting of evenly spaced rows and uniform spacing between adjacent vines. Despite this apparent regularity, considerable spatial variability in canopy density is often observed, influenced by factors such as soil heterogeneity, topography, and water availability. These spatial differences offer a unique opportunity for implementing VR technologies tailored to site-specific crop needs (Martínez-Casasnovas et al., 2012). Prescription maps for VR in vineyards can be generated using vegetation indices such as the NDVI or PCD derived from remote sensing platforms, including drones, airplanes, and satellites (Campos et al., 2019; Román et al., 2020). These data sources provide spatial information correlated with vine vigor and canopy structure, making them suitable for defining management zones. After processing the data in a geographic information system, clustering techniques, such as unsupervised k-means classification, can be applied to delineate zones of differing canopy vigor. Each zone can then be assigned to a corresponding spray volume according to viticultural criteria. For this case study, low-vigor areas were prescribed with an application rate of 100 L/ha, medium-vigor areas 140 L/ha, and high-vigor areas 220 L/ha, in accordance with recommendations from a decision support tool (Gil et al., 2019) (Figure 1.7a). The prescription map uploaded to the sprayer was formatted in a text file as a series of GNSS-positioned points carrying the individual prescriptions, following the protocol described by Rovira-Más et al. (2024). The file contained a dense grid of 4134 points/ha (Figure 1.7b), each of them characterized by its geodetic coordinates (latitude, longitude, and altitude) and an associated flow rate in L/min, which corresponded to the vigor

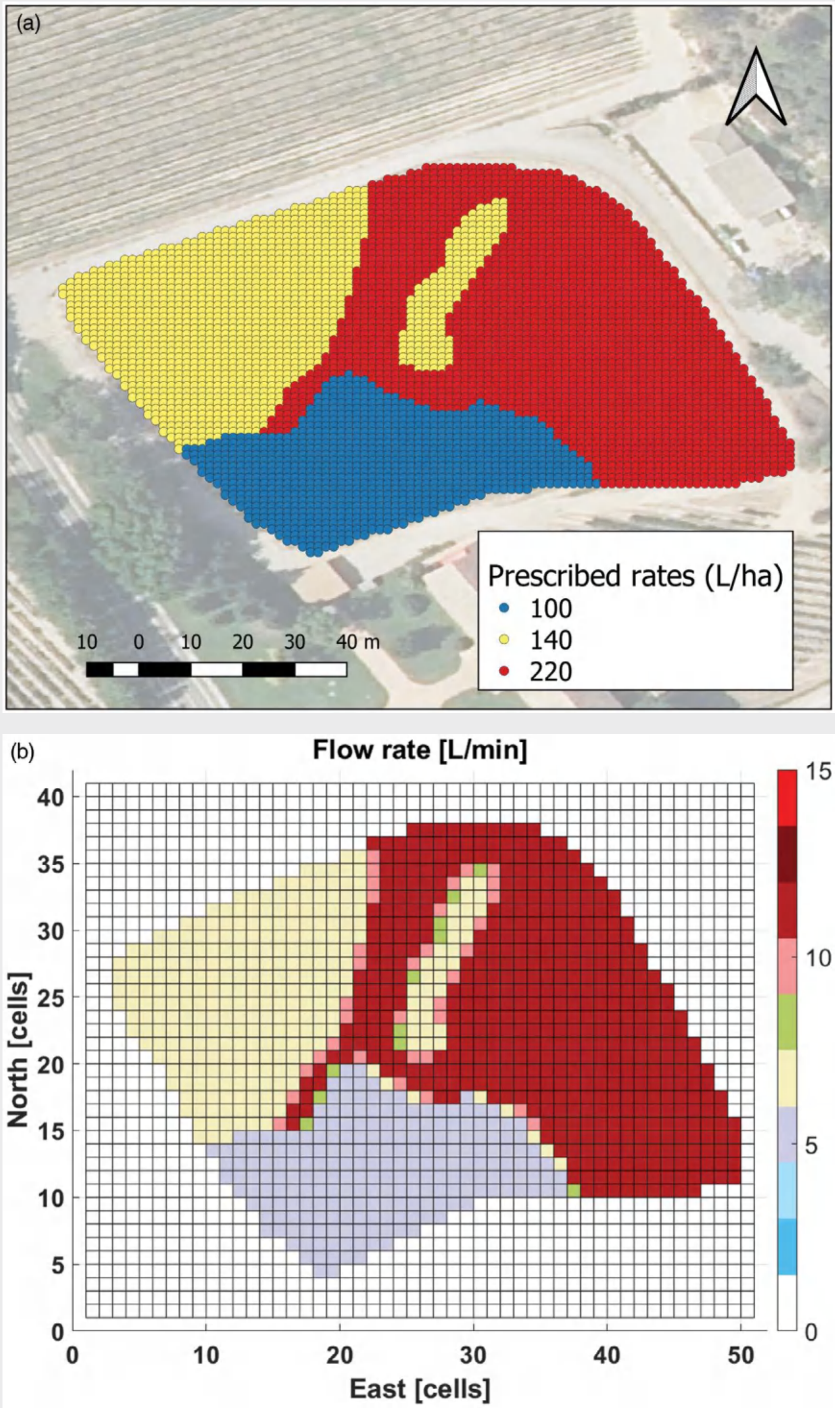

FIGURE 1.7 Prescription map for variable-rate spraying of the tested vineyard: (a) spatial classification of canopy vigor zones; (b) prescriptions expressed in plane coordinates as flow rates (L/min).

zone (Figure 1.7a) in which the point was located. This high-resolution structure enabled precise and localized flow control during applications (Román et al., 2025).

VR SPRAYER

The spraying platform was a commercial air-assisted vertical boom sprayer (Ilemo-Hardi, Lleida, Spain), configured for simultaneously treating three vineyard rows (Figure 1.8). The platform was modified to enable the electronic control of key spraying functions, particularly PWM-controlled solenoid valves (Teejet Spraying Co., Wheaton, USA), each coupled with a conventional hollow disc-cone nozzle (Albuz, Evreux, France). The outermost vertical booms on both sides of the sprayer were disabled to limit the treatment to two rows per pass instead of three, resulting in a total of 24 nozzles, 6 per boom (Saiz-Rubio et al., 2023). The PWM system was operated at a frequency of 10 Hz, with DCs ranging between 10% and 100%, allowing the real-time variation of spray flow rate at boom level while maintaining a constant pressure. The relationship between DC and actual flow rates was calibrated in the lab and input in the onboard computer for three ISO nozzle sizes (Ramos del Pino, 2023). The operation speed was set to 5 km/h, and the working pressure was maintained at 6 bar (600 kPa) to ensure the proper atomization while protecting the PWM solenoids from pressure-induced wear.

The VR sprayer was equipped with sensors to monitor operating conditions. These included two pressure transducers (Gems Sensors & Controls, Plainville, USA) installed on each side of the hydraulic circuit, and a turbine-type flowmeter (FTI Flow Technology Inc., Tempe, USA) to estimate instantaneous flow rates. A GNSS receiver (Ag Leader, Ames, USA) provided real-time positioning, enabling the precise application of the rates defined in the prescription map. The electronic system was controlled through an embedded computer interface for manual DC configuration, data logging, map-based automatic spraying, and real-time feedback on system performance. To apply the prescription map of Figure 1.7b, the onboard computer converted geodetic coordinates (latitude, longitude, altitude) from the text file into local tangent plane (LTP) coordinates (Figure 1.4), a Cartesian system with east–north axes referenced to a locally defined origin (Rovira-Más et al., 2024). This transformation enabled

FIGURE 1.8 Smart sprayer platform for vineyards.

rapid distance calculations and an efficient real-time execution of the prescribed flow rates during operation. The sprayer's computer recorded operational data at a frequency of 3–5 Hz, providing real-time information on key variables including hydraulic pressure, the total flow rate applied, and global positioning, all of which were accessible via the integrated touch-screen interface. This continuous data stream allowed for both in-field monitoring and post-operation analysis. Key performance metrics evaluated included ground speed, system pressure, and flow rate errors, with particular attention to the system's ability to accurately deliver the prescribed volumes under varying DCs and travel speeds.

RESULTS

Figure 1.9a shows the travel path recorded by the onboard GPS as the sprayer traversed the consistent pattern along the vine rows, confirming a uniform row coverage with minimal deviations. Since the sprayer treated two rows simultaneously, a total of 12 rows were covered during the operation. Recording the sprayer path during commercial applications provides valuable operational feedback, allowing operators identify untreated rows or pinpoint the exact location where the sprayer ran out of water. The sprayer consistently maintained the target speed of 5 km/h along the straight passes (Figure 1.9b), being occasional reductions and

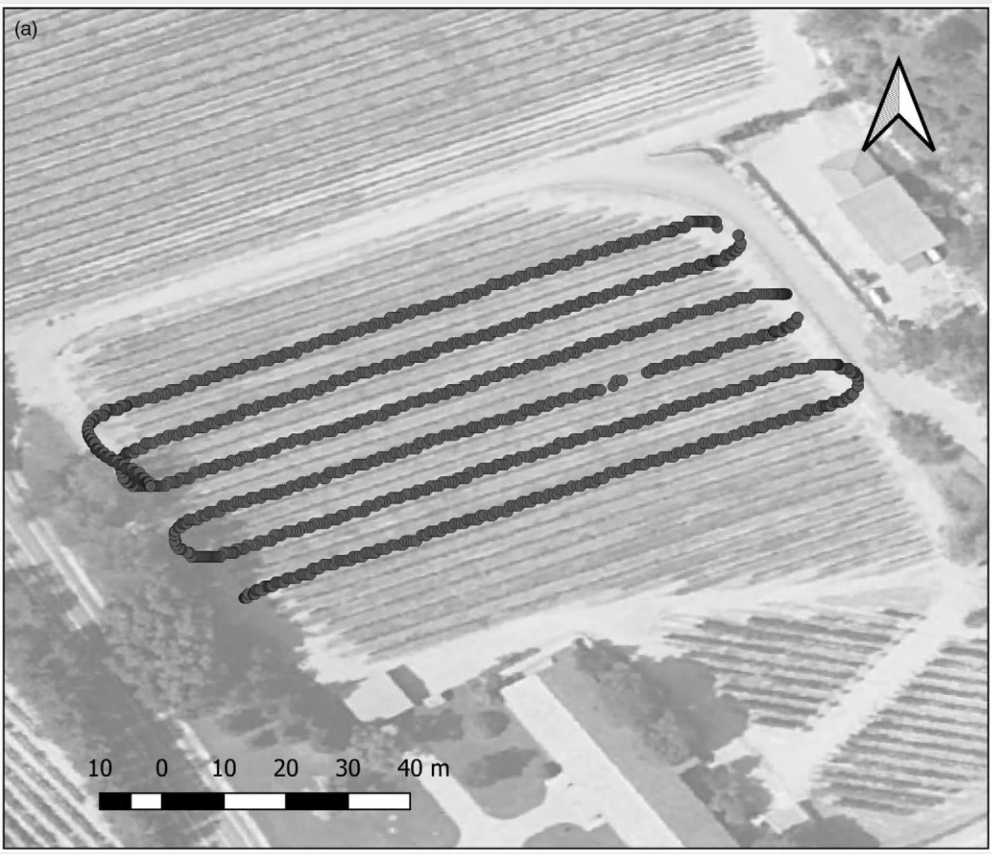

FIGURE 1.9 Sprayer travel path (a) and speed profile (km/h) during VR application in a vineyard (b). (*Continued*)

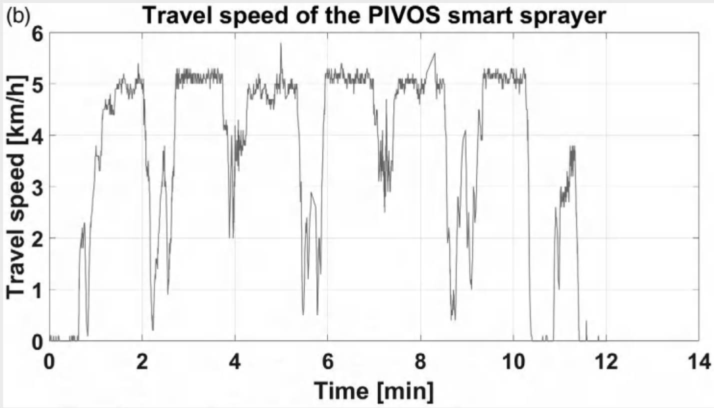

FIGURE 1.9 (Continued)

stops due to headlands. However, this uniformity in velocity is not always granted, existing the need for flow rate real-time adjustments according to vehicle speed.

With respect to flow dynamics, Figure 1.10a illustrates the temporal assignment of prescribed flow rates throughout the treatment. Discrete steps in prescribed rates correspond to transitions between low (100 L/ha), medium (140 L/ha), and high (220 L/ha) vigor zones

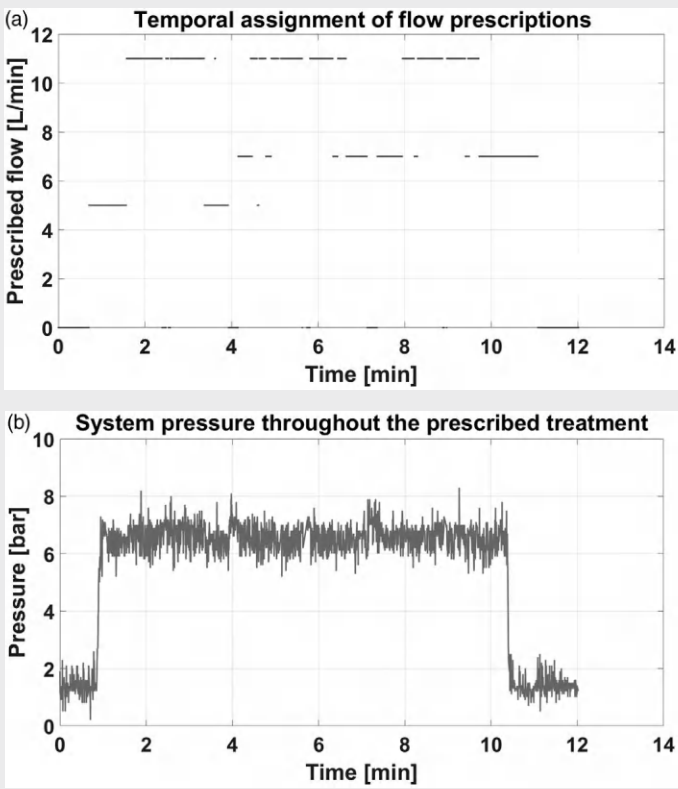

FIGURE 1.10 Prescribed flow rates (a) and system pressure during the VR spraying application (b).

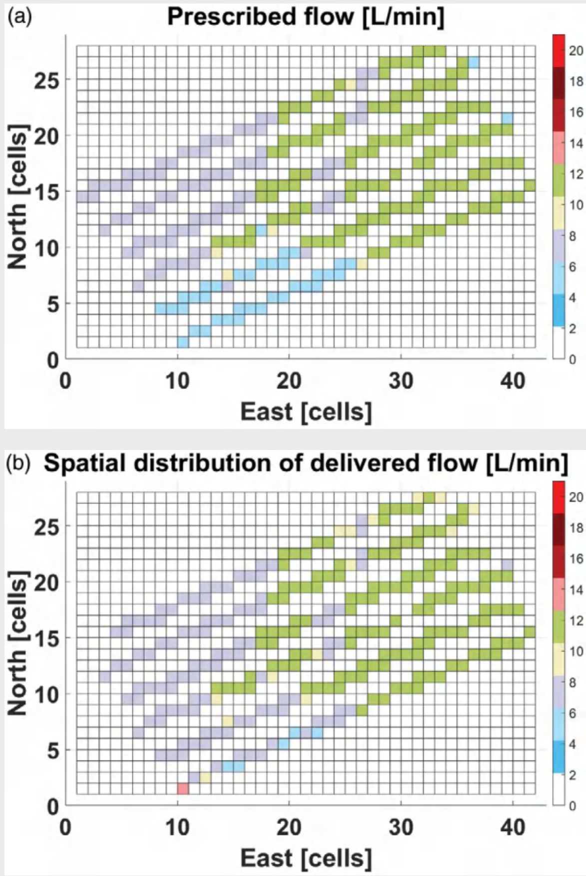

FIGURE 1.11 Prescribed (a) and delivered flow rates (b) along the travel path.

defined in the prescription map (Figure 1.7a). These volumes translated into DC of 30%, 38%, and 69%, respectively. Periods assigned with a flow of zero pointed at locations outside the rows, where the sprayer was either turning or not treating the canopy. Figure 1.10b shows the evolution of system pressure throughout the entire treatment. Pressure stabilized shortly after startup and remained consistent around the target value of 600 kPa. In particular, the mean operating pressure was 660 kPa (6.6 bar), resulting in excellent stability across the application period regardless of the frequency and magnitude of DC changes. The drop in pressure after minute 10 corresponds to the end of spraying, confirming the system shutdown.

Figure 1.11 compares the prescribed flows (a) with the actual flows (b) delivered along the VR treatment in the vineyard. The spatial pattern of the prescribed flow corresponds to the vigor-based management zones of Figure 1.7a, with lower rates assigned to the southern rows and higher rates to the central and northern areas. The map of delivered flow demonstrates that the sprayer generally followed the prescriptions, especially in medium and high flow zones, with occasional discrepancies in low-vigor zones due to overapplication.

A further analysis of system performance across canopy zones is summarized in Table 1.2. While the prescribed and delivered flow rates in the medium and high vigor zones converged,

TABLE 1.2
Main Parameters for Assessing VR Spraying Across Canopy Vigor Zones

Canopy Vigor	Target Flow (L/min)	Mean Flow (L/min)	Mean Error (L/min)	Mean Pressure (bar)	Applied Rate (L/ha)	Expected (L/ha)	Absolute Error (%)
Low	5	5.65	1.95	5.8	139.9	100	39.9
Medium	7	7.08	0.87	5.4	127.7	140	8.8
High	11	10.82	0.28	6.6	216.4	220	1.6

the low-vigor areas resulted in overapplication (Figure 1.12). The mean applied rate for low-vigor zones was 139.9 L/ha, which represents an absolute error of 39.9% when compared to the intended 100 L/ha. This error can be attributed to a combination of factors, including mechanical limitations of the PWM solenoid valve at low DCs, particularly when operating at relatively high pressures. In fact, PWM systems were originally developed for boom sprayers in arable crops, where they typically operate at significantly lower pressures. This makes them challenging for the demands of high-pressure orchard applications. An additional factor contributing to this error may be the operational range of the flowmeter, commercially rated between 3.8 and 38 L/min. At the low end of this range, such as in the 5 L/min prescriptions for low-vigor zones, sensor accuracy and resolution usually decrease, leading to noisy measurements and potential flow regulation errors. These errors could impair both real-time control and post-analysis accuracy in low-volume applications, leading to consider lower capacity flowmeters for vineyard applications. Moreover, the rate discrepancy was exacerbated by the higher sprayer speed during the first row, as the mean speed during the first row, corresponding to the low-vigor area, was approximately 4 km/h instead of the intended 5 km/h. Such slower speed increased the spray deposition rate, amplifying the overapplication effect further. If the speed had remained constant at 5 km/h, the expected error would have been reduced to 13.3%. Similarly, in the medium-vigor class, although flow rate control was relatively accurate, the applied spray volume per hectare was slightly lower

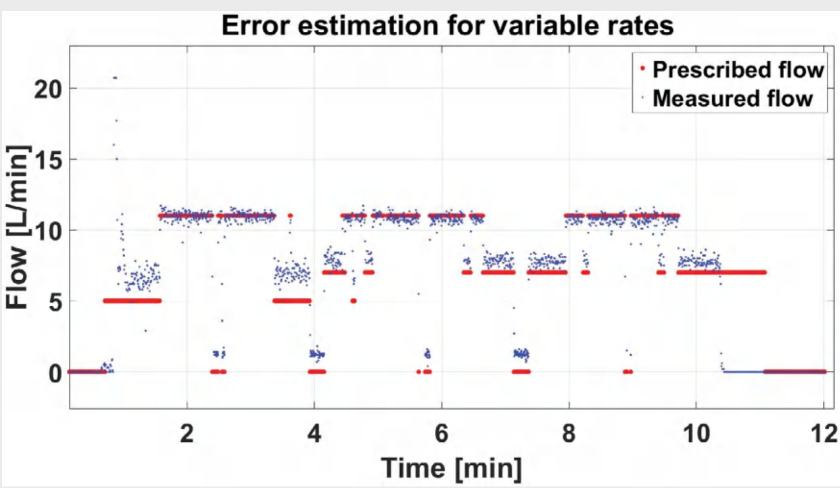

FIGURE 1.12 Prescribed and measured flow rates over time during VR application.

than prescribed, which can be attributed to higher-than-target forward speeds. This result suggests that the observed 8.8% error would likely have been reduced if the sprayer had maintained the targeted travel speed throughout the entire treatment. In contrast, high-vigor zones demonstrated near-perfect accuracy with only 1.6% error. These outcomes underscore the importance of implementing corrections and better hardware to enhance performance when applying low spray volumes in site-specific viticulture, especially when operating at the lower end of the PWM modulation range.

In addition to environmental benefits, the use of VR prescription maps also translated into a notable product savings. If a constant application rate of 220 L/ha had been used across the entire vineyard block, the total volume applied would have reached approximately 200.2 L. Instead, the vigor-based prescription resulted in an actual application of 157.8 L, yielding a 21.2% reduction in spray volume. This figure highlights the practical benefits of precision viticulture, and in particular VR technologies, demonstrating how the site-specific management of key inputs greatly contributes to resource efficiency and product savings, an approach well aligned with the sustainability objectives set forth by EU agricultural policies. Unpublished research conducted with the smart prototypes of Figures 1.3a and 1.8 have shown that the PWM-map approach developed for vineyards and olive orchards maintained biological efficacy comparable to conventional uniform applications. Specifically, no significant differences were observed in the control of downy mildew in vineyards or olive moth (*Prays oleae*) in olive orchards, supporting the feasibility of VR spraying without compromising crop protection effectiveness.

CASE STUDY 2 – VARIABLE RATE APPLIED TO TRADITIONAL FRUIT PRODUCTION: CITRUS GROVES

CROP DESCRIPTION AND GENERATION OF PRESCRIPTION MAPS

This use case evaluates the four-sector pressure-based control system of the sprayer shown in Figures 1.3 and 1.6. The sprayer was tested in a citrus orchard located in Valencia, Spain, with an area of 0.98 ha. The orange trees followed a traditional layout with a spacing of 6 m. To test the responsiveness of the control system under varying flow demands, the prescription map was outlined according to a sequence of homogeneous bands, each of them assigned to a specific flow rate as depicted in Figure 1.13. These rates simulate the most demanding spraying conditions found in Mediterranean fruit production, with typical rates ranging between 25 and 65 L/min.

VR SPRAYER

The sprayer used in this case was a commercial axial-fan blast sprayer (Mañez y Lozano S.L., Spain) customized for variable-rate applications by integrating PWM-driven nozzles and computer controls for smart actuation (Figures 1.3 and 1.6). The system incorporated 16 solenoid valves (Teejet Spraying Co., Wheaton, USA) operated at 10 Hz and hollow-cone nozzles (HCI 6005, ASJ srl, Centallo, Italy). To monitor operational parameters in real time, the sprayer was equipped with three pressure sensors (WIKA A10, Klingenberg, Germany) placed at strategic locations in the hydraulic circuit and a turbine flowmeter (Flow Technology Inc., Phoenix, USA). Spatial positioning was provided by a GNSS receiver (Ag Leader GPS 6000, Ames, USA) with a 5 Hz sampling rate.

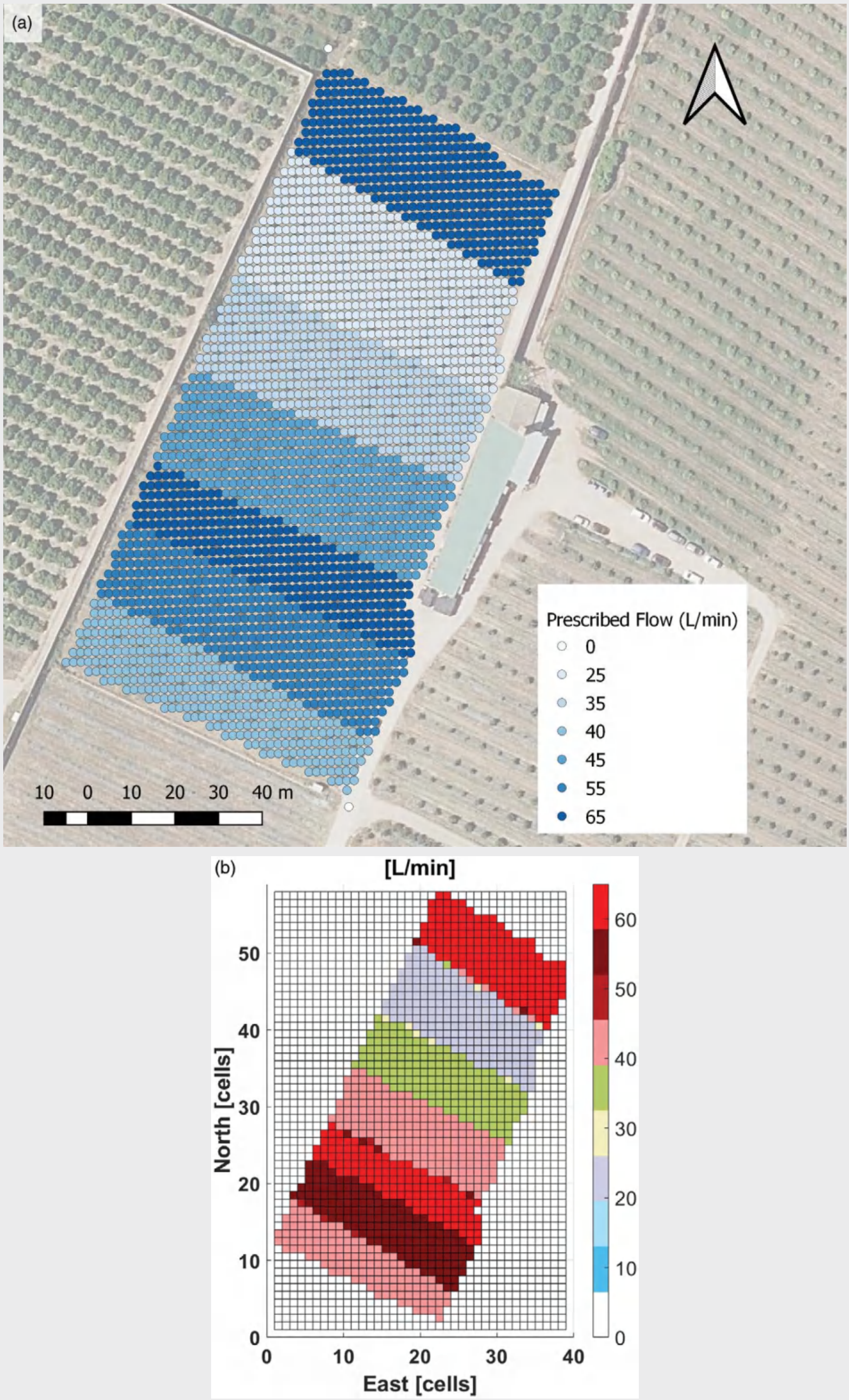

FIGURE 1.13 Prescription map for testing variable-rate spraying in an orange orchard, in coordinates (a), and in grid cells (b).

RESULTS

The working pressure set over the evaluation tests was 6 bar and the sprayer speed 3 km/h, which are typical operating conditions in Valencian citriculture. The prescribed flow rates (Figure 1.13) in the range 25–65 L/min reflected common spray volumes between 800 and 2200 L/ha. The onboard computer recorded key parameters at a frequency of 3–5 Hz, including hydraulic pressure, flow rate, and GPS positioning, all of which were also accessible through a touchscreen graphical user interface.

Figure 1.14 shows the trajectory followed by the sprayer in the orchard. According to Figure 1.15a, the average spraying speed was 2.8 km/h, and the mean pressure was 6.1 bar (Figure 1.15b), indicating stable control around the target pressure despite observed fluctuations that remained within a range unlikely to significantly affect droplet size distribution, and thus spray coverage and deposition efficiency in orchard canopies.

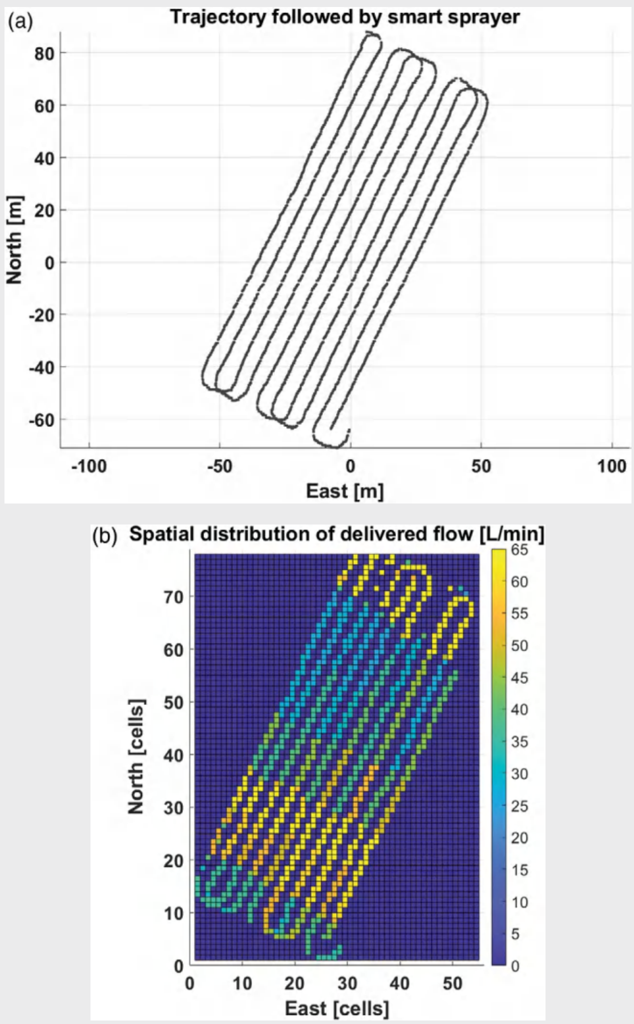

FIGURE 1.14 Smart spraying: Vehicle trajectory (a) and spatial distribution of delivered spray flow (L/min) (b).

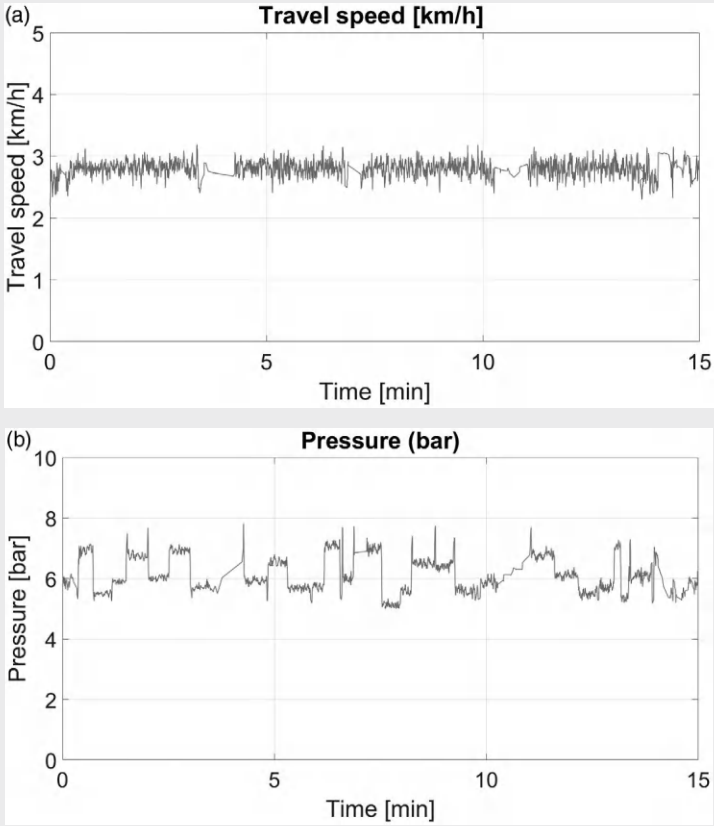

FIGURE 1.15 Smart spraying: Vehicle velocity (km/h) (a) and system pressure (bar) (b).

Overall, the smart spraying control system demonstrated the ability to follow the prescribed pattern of flows coded in the prescription map of Figure 1.13a. Flow rate errors varied with the target flows set. Table 1.3 compares target and actual flow rates, associated pressures, and resulting application volumes per hectare. As expected, higher flow demands in the range 45–65 L/min resulted in larger deviations, likely due to the increased system inertia of a

TABLE 1.3
Performance of Smart Sprayer when Applying the Map of Figure 1.13

Flow (L/min)			Absolute Error (L/min)		Pressure (bar)		Volume Rate
Target	Mean	SE	Mean	SE	Mean	SE	(L/ha)
25	27.1	2.1	2.0	2.0	6.3	0.6	962
35	32.3	3.5	2.7	3.5	6.3	0.3	1154
40	35.9	2.2	4.1	2.2	6.4	0.5	1325
45	38.9	2.2	6.1	2.1	6.1	0.5	1387
55	53.6	3.6	1.4	3.6	5.9	0.8	1909
65	62.6	2.2	2.4	2.2	5.8	0.2	2245

hydraulic configuration that was not optimized for more turbulent flows than regular spraying, and the lag in solenoid response. Still, pressure remained within the ideal range for effective spray atomization, confirming that real-time control with PWM regulation is feasible under orchard conditions, even when variable flow demands reach 65 L/min. The fact that pressure was bounded to 8 bar regardless of the flow being commanded implied that system performance was safe, as the PWM solenoid valves were mechanically limited to 10 bar. Therefore, there is a need for reliable pressure control before accurate DC actuation with the purpose of preventing mechanical stress on key components and maintaining a consistent spray profile under any orchard condition.

1.5 CONCLUSION

Supermarkets and food providers require high standards of fruit quality, resulting in the rejection of either internal or skin defects. In addition, pest attacks account for an important fraction of the fresh food that goes to waste, which is relevant in developing countries where fruit security is an issue. As a result, crop protection is key and necessary for fruit production, impacting the economical profitability of the specialty crops sector. On the other hand, the inaccurate delivery of pesticides has an important impact on human health and environmental sustainability. These two requirements of protecting the fruits and the environment at the same time can be met by making crop protection technology more accurate and trustable, in the direction outlined by the principles of smart, data-driven, AI-based, and precise agriculture.

This chapter has explained the benefits of variable rating for the sustainable spraying of orchards, where application precision and treatment effectiveness are crucial. Out of the available technologies, the best results have been found by implementing PWM-controlled nozzles, as long as the circuit pressure is kept stable and bounded regardless of the combination of DCs set by the computer at any given position of the sprayer. Although the site-specific rates have been previously coded in prescription maps for the use cases presented in Case Study 1 and 2, results are expected to be similar for real-time calculated rates, as long as onboard sensors and canopy assessment strategies are as accurate as those implemented in the prescription maps. Field experience showed that the regulation of flow rates was satisfactory through the PWM-driven nozzles in the range of 20%–80% DCs. Overall, biological efficacy was proved for the smart sprayers developed (Figures 1.3 and 1.8) with product savings up to 30% in olive groves and 21% in vineyards. Nevertheless, there is still substantial field work remaining with the goal of pushing the reduction rates of pesticide further without reducing the effectiveness at controlling the pests, for other orchard crops, pests, and environmental conditions.

ACKNOWLEDGMENTS

The research presented in this chapter was supported by projects PIVOS (PID2019-104289RB) and ADOPTA (PDC2022-133395-C42), funded by the Spanish Government, and the European Project CERBERUS (Grant 101134878). The authors would like to thank Andrés Cuenca and Montano Pérez (Universitat Politècnica de València, UPV, Spain) for assistance in the sprayer prototyping and assembly, Coral Ortiz, Enrique Ortí, and Antonio Torregrosa (UPV) for lab testing and validation, Francisco García and Ramón Salcedo (Universitat Politècnica de Catalunya, Spain) for the coding of prescription maps and field testing in vineyards, and finally Gregorio Blanco, Antonio Rodríguez-Lizana and José María Mariscal (University of Córdoba, Spain) for prescription mapping and field validation in olive groves.

REFERENCES

Barbieri, H. B., Fernandes, L. S., Pontes, J. G. D. M., Pereira, A. K., & Fill, T. P. (2023). An overview of the most threating diseases that affect worldwide citriculture: Main features, diagnose, and current control strategies. *Frontiers in Natural Products*, *2*, 1045364. https://doi.org/10.3389/fntpr.2023.1045364

Campos, J., Gallart, M., Llop, J., Ortega, P., Salcedo, R., & Gil, E. (2020). On-farm evaluation of prescription map-based variable rate application of pesticides in vineyards. *Agronomy*, *10*(1), 102. https://doi.org/10.3390/agronomy10010102

Campos, J., García-Ruíz, F., & Gil, E. (2021). Assessment of vineyard canopy characteristics from vigour maps obtained using UAV and satellite imagery. *Sensors*, *21*(7), 2363. https://doi.org/10.3390/s21072363

Campos, J., Llop, J., Gallart, M., García-Ruiz, F., Gras, A., Salcedo, R., & Gil, E. (2019). Development of canopy vigour maps using UAV for site-specific management during vineyard spraying process. *Precision Agriculture*, *20*(6), 1136–1156. https://doi.org/10.1007/s11119-019-09643-z

Campos, J., Zhu, H., Salcedo, R., Jeon, H., Ozkan, E., & Gil, E. (2025). Droplet size distributions from PWM-controlled hollow-cone nozzles operated at high modulation frequencies and pressures. *Journal of the ASABE*, *68*(1), 51–60. https://doi.org/10.13031/ja.16094

EPPO. (2012). PP 1/225(2) Minimum effective dose. *EPPO Bulletin*, *42*(2012), 403–404. https://doi.org/10.1111/epp.2612

EPPO. (2021). PP1/239(3) dose expression for plant protection products. *EPPO Bulletin*, *51*(1), pp. 10–33. https://doi.org/10.1111/epp.12704

European Commission (EC). (2009a). Regulation (EC) No 1107/2009 of the European Parliament and of the Council of 21 October 2009 concerning the placing of plant protection products on the market and repealing Council Directives 79/117/EEC and 91/414/EEC. *Official Journal of the European Union*. https://eur-lex.europa.eu/legal-content/EN/ALL/?uri=CELEX:32009R1107

European Commission (EC). (2009b). Directive 2009/127/EC of the European Parliament and of the Council of 21 October 2009 amending Directive 2006/42/EC with regard to machinery for pesticide application. *Official Journal of the European Union*. https://eur-lex.europa.eu/eli/dir/2009/127/oj/eng

European Commission (EC). (2009c). Directive 2009/128/EC of the European Parliament and of the Council of 21 October 2009 establishing a framework for Community action to achieve the sustainable use of pesticides. *Official Journal of the European Union*. https://eur-lex.europa.eu/eli/dir/2009/128/oj/eng

European Commission (EC). (2019). *The European Green Deal*. Brussels: European Commission. https://eur-lex.europa.eu/legal-content/EN/TXT/?uri=CELEX:52019DC0640

European Commission (EC). (2020). *A farm to fork strategy for a fair, healthy and environmentally-friendly food system*. Brussels: European Commission. https://eur-lex.europa.eu/legal-content/EN/TXT/?uri=CELEX:52020DC0381

Garcerá, C., Doruchowski, G., & Chueca, P. (2021). Harmonization of plant protection products dose expression and dose adjustment for high growing 3D crops: A review. *Crop Protection*, *140*, 105417. https://doi.org/10.1016/j.cropro.2020.105417

Garcerá, C., Román, C., Moltó, E., Abad, R., Insa, J. A., Torrent, X., … & Chueca, P. (2017). Comparison between standard and drift reducing nozzles for pesticide application in citrus: Part II. Effects on canopy spray distribution, control efficacy of *Aonidiella aurantii* (Maskell), beneficial parasitoids and pesticide residues on fruit. *Crop Protection*, *94*, 83–96. https://doi.org/10.1016/j.cropro.2016.12.016

Gil, E., Campos, J., Ortega, P., Llop, J., Gras, A., Armengol, E., Planas, S., & Gallart, M. (2019). DOSAVIÑA: Tool to calculate the optimal volume rate and pesticide amount in vineyard spray applications based on a modified leaf wall area method. *Computers and Electronics in Agriculture*, *160*, 117–130. https://doi.org/10.1016/j.compag.2019.03.018

Grella, M., Gioelli, F., Marucco, P., Zwertvaegher, I., Mozzanini, E., Mylonas, N., Nuyttens, D., & Balsari, P. (2022). Field assessment of a pulse width modulation (PWM) spray system applying different spray volumes: Duty cycle and forward speed effects on vines spray coverage. *Precision Agriculture*, *23*(1), 219–252. https://doi.org/10.1007/s11119-021-09835-6

Jensen, P. K., & Olesen, M. H. (2014). Spray mass balance in pesticide application: A review. *Crop Protection*, 61, 23–31. https://doi.org/10.1016/j.cropro.2014.03.006

Jeon, H., & Zhu, H. (2012). Development of a variable-rate sprayer for nursery liner applications. *Transactions of the ASABE*, *55*(1), 303–312. https://doi.org/10.13031/2013.41240

Jeon, H., & Zhu, H. (2022). Stereo vision controlled variable rate sprayer for specialty crops: Part I. Controller development. *Journal of the ASABE*, *65*(6), 1397–1410. https://doi.org/10.13031/ja.15227

Jeon, H., & Zhu, H. (2023). Investigation of depth camera potentials for variable-rate sprayers. *Journal of the ASABE*, *66*(1), 115–126. https://doi.org/10.13031/ja.15070

Jeon, H., Zhu, H., Derksen, R., Ozkan, E., & Krause, C. (2011). Evaluation of ultrasonic sensor for variable-rate spray applications. *Computers and Electronics in Agriculture*, *75*(1), 213–221. https://doi.org/10.1016/j.compag.2010.11.007

Knutson, R. D., & Smith, E. G. (1999). AFPC *p*olicy *w*orking *p*aper*, 99-2*.

Llorens, J., Gil, E., Llop, J., & Escolà, A. (2010). Variable rate dosing in precision viticulture: Use of electronic devices to improve application efficiency. *Crop Protection*, *29*(3), 239–248. https://doi.org/10.1016/j.cropro.2009.12.022

Llorens, J., Gil, E., Llop, J., & Escolà, A. (2011). Ultrasonic and LIDAR sensors for electronic canopy characterization in vineyards: Advances to improve pesticide application methods. *Sensors*, *11*(2), 2177–2194. https://doi.org/10.3390/s110202177

Martinez-Casasnovas, J. A., Agelet-Fernandez, J., Arno, J., & Ramos, M. C. (2012). Analysis of vineyard differential management zones and relation to vine development, grape maturity and quality. *Spanish Journal of Agricultural Research*, *10*(2), 326–337. https://doi.org/10.5424/sjar/2012102-370-11

Miranda-Fuentes, A., Rodríguez-Lizana, A., Cuenca, A., González-Sánchez, E. J., Blanco-Roldán, G. L., & Gil-Ribes, J. A. (2017). Improving plant protection product applications in traditional and intensive olive orchards through the development of new prototype air-assisted sprayers. *Crop Protection*, *94*, 44–58. https://doi.org/10.1016/j.cropro.2016.12.012

Morelli, M., García-Madero, J. M., Jos, Á., Saldarelli, P., Dongiovanni, C., Kovacova, M., Saponari, M., Baños Arjona, A., Hackl, E., Webb, S., & Compant, S. (2021). *Xylella fastidiosa* in olive: A review of control attempts and current management. *Microorganisms*, *9*(8), 1771. https://doi.org/10.3390/microorganisms9081771

Oberti, R., Marchi, M., Tirelli, P., Calcante, A., Iriti, M., Tona, E., Hočevar, M., Baur, J., Pfaff, J., Schütz, C., & Ulbrich, H.. 2016. Selective spraying of grapevines for disease control using a modular agricultural robot. *Biosystems Engineering*, *146*, 203–215. https://doi.org/10.1016/j.biosystemseng.2015.12.004

Ortiz, C., Torregrosa, A., Saiz-Rubio, V., & Rovira-Más, F. (2023). Vibration analysis of pulse-width-modulated nozzles in vineyard blast sprayers. *Horticulturae*, *9*(6), 703. https://doi.org/10.3390/horticulturae9060703

Proffitt, T., Bramley, R., Lamb, D., & Winter, E. (2006). *Precision viticulture—A new era in vineyard management and wine production*. Winetitles. https://hdl.handle.net/1959.11/786

Ramos del Pino, Á. (2023). *Modelado de la pulverización de viñedos mediante la caracterización precisa del ciclo de trabajo de un pulverizador con boquillas de control electrónico por pulsos* [Trabajo final de grado, Universitat Politècnica de Catalunya]. UPCommons. https://upcommons.upc.edu/handle/2117/388552

Rodríguez-Lizana, A., Pereira, M. J., Ribeiro, M. C., Soares, A., Azevedo, L., Miranda-Fuentes, A., & Llorens, J. (2021). Spatially variable pesticide application in olive groves: Evaluation of potential pesticide-savings through stochastic spatial simulation algorithms. *Science of the Total Environment*, *778*, 146111. https://doi.org/10.1016/j.scitotenv.2021.146111

Román, C., Arnó, J., & Planas, S. (2021). Map-based zonal dosage strategy to control yellow spider mite (*Eotetranychus carpini*) and leafhoppers (*Empoasca vitis* & *Jacobiasca lybica*) in vineyards. *Crop Protection*, *147*, 105690.

Román, C., Jeon, H., Zhu, H., Campos, J., & Ozkan, E. (2023). Stereo vision controlled variable rate sprayer for specialty crops: Part II. Sprayer development and performance evaluation. *Journal of the ASABE*, *66*(5), 1005–1017. https://doi.org/10.13031/ja.15578

Román, C., Llorens, J., Uribeetxebarria, A., Sanz, R., Planas, S., & Arnó, J. (2020). Spatially variable pesticide application in vineyards: Part II, field comparison of uniform and map-based variable dose treatments. *Biosystems Engineering*, *195*, 42–53. https://doi.org/10.1016/j.biosystemseng.2020.04.013

Román, C., Rovira-Más, F., Ortiz, C., Ruiz, J. I., Cuenca-Cuenca, A., Torregrosa, A., … & Blanco-Roldán, G. (2025). Influence of prescription map layout on pressure in pulse width modulation-driven blast sprayers. In *Precision agriculture'25* (pp. 263–270). Wageningen Academic. https://doi.org/10.1163/9789004725232_032

Rovira-Más, F. (2010). Sensor architecture and task classification for agricultural vehicles and environments. *Sensors*, *10*(12), 11226–11247. https://doi.org/10.3390/s101211226.

Rovira-Más, F., Saiz-Rubio, V., Cuenca, A., Ortiz, C., Pérez, M., & Ortí, E. (2024). Open-format prescription maps for variable rate spraying in orchard farming. *Journal of the ASABE*, *67*(2), 243–257. https://doi.org/10.13031/ja.15750

Saiz-Rubio, V., Ortiz, C., Torregrosa, A., Ortí, E., Pérez, M., Cuenca, A., & Rovira-Más, F. (2023). Modelling vineyard spraying by precisely assessing the duty cycles of a blast sprayer controlled by pulse-width-modulated nozzles. *Agriculture*, *13*(2), 499. https://doi.org/10.3390/agriculture13020499

Saiz-Rubio, V., & Rovira-Más, F. (2020). From smart farming towards agriculture 5.0: A review on crop data management. *Agronomy*, *10*(2), 207. https://doi.org/10.3390/agronomy10020207.

Salas, B., Salcedo, R., Garcia-Ruiz, F., & Gil, E. (2025). Field validation of a variable rate application sprayer equipped with ultrasonic sensors in apple tree plantations. *Precision Agriculture*, *26*(1), 22. https://doi.org/10.1007/s11119-024-10201-5

Salcedo, R., Zhu, H., Zhang, Z., Wei, Z., Chen, L., Ozkan, E., & Falchieri, D. (2020). Foliar deposition and coverage on young apple trees with PWM-controlled spray systems. *Computers and Electronics in Agriculture*, *178*, 105794. https://doi.org/10.1016/j.compag.2020.105794

Shen, Y., Zhu, H., Liu, H., Chen, Y., & Ozkan, E. (2017). Development of a laser-guided, embedded-computer-controlled, air-assisted precision sprayer. *Transactions of the ASABE*, *60*(6), 1827–1838. https://doi.org/10.13031/trans.12455

Wei, Z., Xue, X., Salcedo, R., Zhang, Z., Gil, E., Sun, Y., Li, Q., Shen, J., He, Q., Dou, Q., & Zhang, Y. (2022). Key technologies for an orchard variable-rate sprayer: Current status and future prospects. *Agronomy*, *13*(1), 59. https://doi.org/10.3390/agronomy13010059

Wodzicki, L. M., Madden, L. V., Long, E. Y., Zhu, H., & Ivey, M. L. L. (2023). Evaluation of a laser-guided intelligent sprayer for disease and insect management on grapes. *American Journal of Enology and Viticulture*, *74*(2). https://doi.org/10.5344/ajev.2023.23013

Xue, X., Luo, Q., Ji, Y., Ma, Z., Zhu, J., Li, Z., Lyu S, Sun D., & Song, S. (2023). Design and test of Kinect-based variable spraying control system for orchards. *Frontiers in Plant Science*, *14*, 1297879. https://doi.org/10.3389/fpls.2023.1297879

Zhang, J., Yin, H., Zhou, L., Gu, C., Qiu, W., Lv, X., Sun, H., Yu, H., & Zhang, Z. (2022). Variable rate air-assisted spray based on real-time disease spot identification. *Pest Management Science*. https://doi.org/10.1002/ps.7209

2 Image Analysis Techniques for Fruit Assessment in Apples and Grapes

Julie Tang, Annie Xu Wang, and Mark Whitty

2.1 INTRODUCTION

This chapter aims to highlight the importance of agricultural image data as an asset and help inform users across the data ecosystem as to the advantages and limitations of various agricultural image management methods and the processes which underpin these.

This will be done by:

a. Examining the decisions taken during the planning phase which will impact the entire data lifecycle.
b. Highlighting aspects of data collection which will facilitate long-term use, particularly with commercial outcomes in mind.
c. Demonstrating examples of data processing techniques and lessons learnt from real-world experience.
d. Showing the importance of decisions taken when visualizing data.

The focus of this chapter is on perennial crops, drawing primarily on experience with grapevines and apple trees. These usually rely on a permanent trellis structure or regular layout which offers the opportunity to localize imagery and management activities. The experience of the authors is drawn from a series of research activities carried out between 2010 and 2023 based at UNSW, Australia. The majority of solutions developed by the team included side-view imagery of row crops, with a range of camera styles from machine vision cameras to DSLRs to action cameras to smartphones.

The examples used in this chapter will be primarily drawn from a project called “Developing Agri-tech solutions for the Australian Apple Industry”, funded by Horticulture Innovation Australia (AP16005), led by SwarmFarm Robotics and partnering with Bosch (Gerlingen, Germany) and ADAMA (Asdod, Israel). Several images in this chapter have been adapted from unpublished material collected during this project and are used with permission. One component of this project was the development of a sensing solution to link to a variable rate chemical sprayer for apple flower thinning. After significant stakeholder engagement the sensing objective was defined as the ability to detect the flower phenology stage so that variable timing of spray application could be achieved for individual portions of a tree as shown in Figure 2.1. Field trials were undertaken at Warragul, Victoria; Tatura, Victoria, and Batlow, New South Wales, all apple-growing regions in Australia.

Inspired by asset management practice, the remainder of the chapter is split into the four key sections, planning, data collection, data processing, and data visualization. For each, examples and insight from the team are presented and conclusions drawn.

DOI: 10.1201/9781003510598-2

FIGURE 2.1 Visual representation of cells in which spray application may be varied in an apple orchard.

2.2 PLANNING

Holistic planning considers all aspects of planning including data management, data collection, data processing, and visualization. Best practice involves the documentation of a data management plan, which also lays out responsibilities for data management and gives assurance to the project leaders that systematic processes are in place.

Once the requirements of the overall system are known, a key aspect is the collection of ground-truth data as part of the data collection plan. In relation to agricultural image processing, there are two distinct methods for ground-truth data collection. The first begins with images and applies manual labeling or human counting of the content in the image. Many large image databases then collate these labeled or annotated images for training algorithms. However, for agricultural data, the final usable output more often is an aspect of the physical environment, where a quantitative measure is needed for the basis of grower action. Hence, counting objects or manually quantifying their state, for example. Phenological stage or disease severity needs physical measurement.

A major challenge in the community has been how to relate these physical measurements, which we refer to in the rest of this chapter as *ground truth* to the distinct content captured in image(s) of the plants. For a 2D sensor, identifying the extent of the area in which the physical measurement has been taken can be readily done with a visual guide. Automating this by means of making it distinct or easily detectable within the wavelength of the image sensor (e.g., RGB, hyperspectral, or LiDAR) can greatly speed up the detection and correlation of ground-truth data. Second, the user needs to ensure the section of the plant measured correlates exactly with the image, so a label is needed—preferably machine readable. Third, ensuring accurate timestamps (including local time zones) are captured by both the person taking the measurement and the image collection device enables correlation with the most relevant ground truth. This is particularly relevant when ground-truth data is of necessity captured at a lower temporal frequency than imagery. Fourth, the depth component of the image needs to be clearly defined, noting that depending on the plant, trellis style, and growth stage, physical occlusion may change dramatically.

Defining in advance the data collection processes, frequency, and volume allows resourcing to be planned for the season. The processes should include nominating who is responsible for data collection, how data entry will occur, what processes will be used to verify data, and what training is needed for each of these phases.

In the project example, which ran over four seasons (Year 1 to Year 4), the planning steps taken can be seen below.

Year 1 (2018–2019): As the first season of data collection, the team gathered background information which consisted of conducting a literature review of the sensors and body of works for image-based automation in the agriculture/tree-crop industry. Two different sensors were selected for testing due to availability at short notice: A consumer grade camera and a machine vision camera.

Several sampling sections in the field were defined to aid data collection and ground truthing. By clearly marking out these sampling sections with frames and reflective tape, the sections of plant measured in the field could be correlated to sections of imagery taken. To further ensure sections of plants measured were correlated to the exact image, QR codes were printed and appended to each frame in the field as shown in Figure 2.2.

FIGURE 2.2 QR code attached to a ground-truthing frame in the field to allow automated identification.

Images were taken in a manner ensuring the QR codes were visible and readable. Timestamps are also included when capturing the data to ensure repeated measurements from the same sampling section could be correctly attributed to ground truthing conducted on different dates.

Year 2 (2019–2020): From the image results of Year 1, it was found that the consumer grade sensor used in Year 1 was lacking sufficient controls that resulted in poor color reproduction. Additionally, the sensors produced unusable results in low light. Such limitations hindered our ability to accurately label imagery for model training. A key learning from Year 1 was that requirements on hardware need to be set early given the lead time required for hardware sourcing and integration.

A set of requirements were then generated for sensor and lens selection to test for improved visual identification of flower density and the viability of earlier stage flowering/pink detection. These requirements included a minimum number of pixels/mm based on the small object targets. A set of experiments were also generated to test the clarity of the small objects in the resulting images and the ability to effectively label or utilize the image data collected. These experiments included in-field data collection at different times of the day with timestamps clearly identifying the date and time of data collection, and at different speeds to test the limits of acceptable image clarity.

From the sampling section results of Year 1, the time-to-sample ratio required for ground truthing was found to be high. For Year 2, the sampling section areas were reduced to increase the time to sample ratio and increase the total sampling sections with the same labor footprint. The use of reflective tape on frames with clear QR codes employed in Year 1 were successful in ensuring ground-truth data collected in the field correlated with the correct images and the same process was repeated here.

Year 3 (2020–2021): A stage estimation algorithm was proposed as a new objective. A set of requirements for data collection in terms of total samples, sampling frequency, and phenological stages to count were presented. The team considered sampling time, budget constraints, and training material to assist in-field workers to identify phenological stages consistent with the model. Training material introduced assisted field workers with repeatability of measurements in-field.

Year 4 (2021–2022): The objective of this season was to further evaluate the stage estimation algorithm proposed in Year 3. Planning therefore included similar requirements to Year 3. Any stages with limited data collection in Year 3 due to factors such as weather were planned to be rectified through additional data collections during the expected stages. Timestamps were captured for all image data and dates were recorded for all ground truthing done in the field.

2.2.1 Planning Discussion

From the project example, key items in regard to planning data collection and ground truthing in an agricultural environment included the following.

To ensure images collected corresponded to ground truthing in the field, the locations for data collection need to be clearly marked. The locations were marked visually with frames and reflective tape to aid finding of each location without requiring GPS. By including QR codes and associated text at each marked sampling location, both computers and humans were able to accurately identify the sample and attribute the ground truth collected to the correct sample.

Ensuring ground truthing is consistent between different workers is key to developing a high-quality dataset. Using a visual guide with all classes of flower stages proved helpful in achieving consistency across different people doing ground-truth data collection. Making the data upload process as efficient as possible and including checks by the data processing team helped ensure the data was able to be used rapidly and quality controlled.

Additionally, selecting sufficient data across the distinct phenology stages was crucial in providing a less biased training dataset. This was especially challenging when the visual appearance of flowers (as shown in Figure 2.3) progressed rapidly through early stages with changes in weather, so ensuring field-based resources were in place, trained and ready to move rapidly was a key learning. Figure 2.3 shows a collage of eight images illustrating the phenology stages of apple flowers,

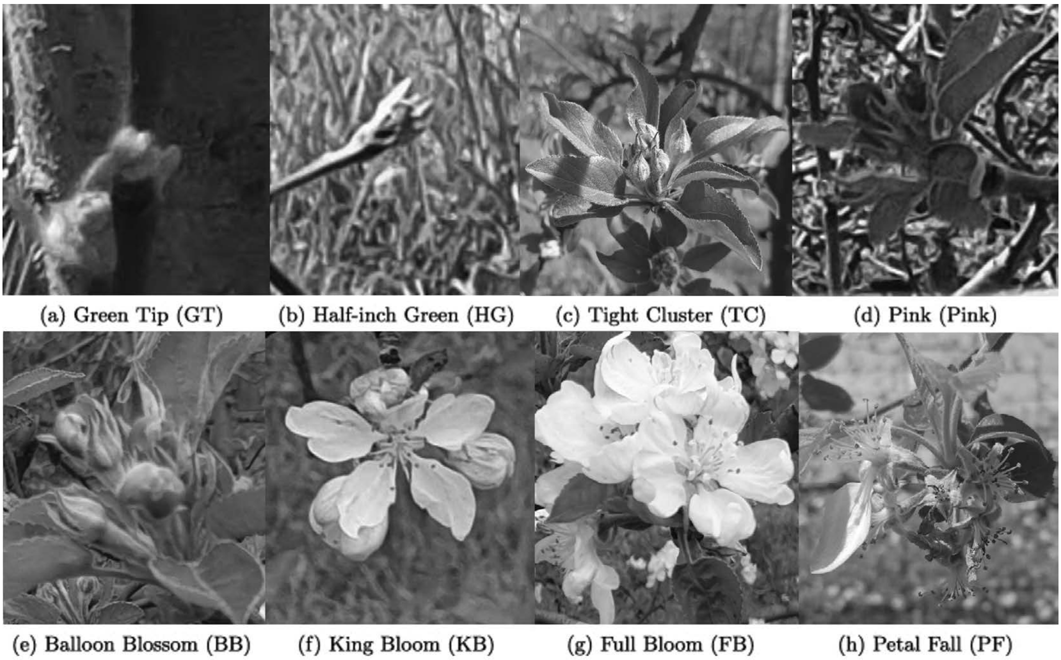

FIGURE 2.3 A collage of eight images illustrating the phenology stages of apple flowers, progressing from early bud development to blooming and petal fall. The stages are labeled as follows: (a) Green tip (GT) where fruit buds display a light green tip, (b) half-inch green (HG) showing buds that have burst, revealing small spiky leaves about half an inch in size, (c) tight cluster (TC) with buds opening into a dense green cluster of flowers surrounded by emerging spur leaves, (d) pink (pink) where the flowers begin to show a pink hue, (e) balloon blossom (BB) with the pink flowers swelling and separating, resembling small pink balloons, (f) king bloom (KB) highlighting the central flower, which is the most developed and has the highest potential for fruit production, (g) full bloom (FB) showing the surrounding pink balloon blossoms opening fully around the central king bloom, and (h) petal fall (PF) depicting flowers with petals beginning to drop.

progressing from early bud development to blooming and petal fall. The stages are labeled as follows: (a) Green tip (GT) where fruit buds display a light green tip, (b) half-inch green (HG) showing buds that have burst, revealing small spiky leaves about half an inch in size, (c) tight cluster (TC) with buds opening into a dense green cluster of flowers surrounded by emerging spur leaves, (d) pink (pink) where the flowers begin to show a pink hue, (e) balloon blossom (BB) with the pink flowers swelling and separating, resembling small pink balloons, (f) king bloom (KB) highlighting the central flower, which is the most developed and has the highest potential for fruit production, (g) full bloom (FB) showing the surrounding pink BBs opening fully around the central king bloom, and (h) petal fall (PF) depicting flowers with petals beginning to drop.

2.3 DATA COLLECTION

The data collection process can be broken into the two main steps of data collection and data validation. With agricultural image data, the data collection step consists of image and ground-truth data. Image data without corresponding ground-truth data is insufficient for evaluating a solution.

Data validation is extremely important, and, in this context, it refers to validating the image quality and ground-truth data. The image quality must be *sufficient* for the detection of objects of interest, and the ground truth in terms of any image labeling, manual sampling, or on-farm data must be correctly associated with the imagery.

In the project example which ran over four seasons, the data collection steps taken can be seen below.

- *Year 1*: Data was captured during the flowering period of the 2018–2019 season using sensors fitted on a custom-built vehicle. The corresponding ground-truth data collected was counts in defined sample locations.
- *Year 2*: Data was captured during early flowering to late flowering of the 2019–2020 season using machine vision sensors fitted on a custom-built vehicle. The corresponding ground-truth data collected was counts in defined sample locations.
- *Year 3 and Year 4*: Data was captured during budburst to late flowering of the 2020–2021 season using machine vision sensors fitted on a custom-built vehicle. The corresponding ground-truth data collected was counts in defined sample locations.

In the project example which ran over four seasons (Year 1 to Year 4), the data validation steps taken can be seen below.

- *Year 1*: Images from cameras were visually validated as they are required to be labeled by humans for use in a model. Consumer-grade cameras were found to be sufficient in a daytime setting for the detection of white flower pixels, whereas machine vision cameras were more suitable for night-time data collection. Consumer-grade cameras were not suited to resolving objects smaller than an open flower in the challenging unstructured environment.
- *Year 2*: Images from cameras were visually validated as they are required to be labeled by humans for use in a model. Machine vision grade cameras were found to be sufficient at resolving smaller objects such as early flowering and pink buds when paired with a lens with a smaller field of view—particularly at night with consistent illumination as in Figure 2.4.

Labeling these objects in daytime imagery was challenging due to lighting and the inability to distinguish *green tipped* budburst from the generally green vegetation present on-farm. Although green buds were visible, it was challenging to distinguish between leaf-buds and flower-buds. Overall, the imagery from the sensors combined with our algorithm was robust under different lighting conditions.

FIGURE 2.4 Ruggedized data capture rig with machine vision cameras working at night.

Year 3 and Year 4: The requirements set for data collection in terms of total samples, sampling frequency, and phenological stages formed the basis of our experiments. The planning minimized weather disruption due to the frequency of data capture and resulted in most stages collected to a sufficient degree. Images were visually validated and compared to the phenological stages recorded.

2.3.1 Data Collection Discussion

Visual imagery is generally identified as suitable or unsuitable through visual inspection. We found image quality needed to be of sufficient resolution to aid labeling. If imagery cannot be labeled consistently, the dataset quality is poor. Imagery can be downsampled to mimic lower quality imagery or target resolution imagery during production. However, agricultural imagery can rarely be upsampled to a higher resolution for training.

When considering agricultural imagery, the appearance of each plant is rapidly changing and careful planning is required to ensure all desired stages of the plant are captured. Lighting is also a factor that must be considered with the capture of imagery. The ability to distinguish the sampling area from background from the imagery is paramount to ground truthing. Overall, if the image quality is insufficient for ground truthing, the dataset quality is likely to be poor.

In the project example, data collection was undertaken with data validation methods in mind. Data needed to be validated rapidly due to the rapidly changing nature of plants in agriculture. Where data was considered unsuitable, recollection of datasets were conducted where possible.

2.4 DATA PROCESSING

Data processing in the realm of computer vision/deep learning consists of preprocessing, model training, and model inference. Preprocessing refers to the initial changes to the image dataset in preparation for training.

2.4.1 Preprocessing

Preprocessing is a critical step in data-driven modeling, particularly in deep learning, as it significantly influences model performance and accuracy. One key preprocessing technique is data normalization, which involves subtracting the mean and dividing by the standard deviation. This method has been consistently applied across all our training experiments. Another essential technique is data augmentation, which is particularly valuable when working with limited datasets, as it maximizes the utility of the available data. By introducing random variations during training, augmentation helps prevent overfitting and enhances the model's ability to identify meaningful patterns. Care must be taken to ensure any augmentations used during training are reasonable when considering the agricultural environment. During Year 2 to Year 3 of the project example, random horizontal and vertical flips, along with HSV augmentation, were applied to further improve model robustness and reduce overfitting during training. These augmentations attempted to simulate differences in data capture and lighting that may be present in an agricultural environment.

2.4.2 Training Models

The training datasets comprised images captured during both day and night across flowering stages. The input resolution was configured to 320×640 pixels, yielding approximately 15×15 pixels per apple flower.

In the first two years of the project, a custom fully convolutional network-based semantic segmentation framework was chosen to segment apple flowers as it was the state-of-the-art framework at the time. It was adapted to FCNs-Edge (Wang et al., 2020) because of the final detail and complex flower shapes and challenging lighting conditions which made comparable methods inaccurate at the object resolution. For efficiency, the VGG-16 architecture was utilized. This network was initialized with pre-trained ImageNet weights, and no layers were frozen during training, allowing for the adjustment of all weights based on the apple flower dataset. The process was carried out on both a local machine equipped with an NVIDIA GPU and a cloud-based machine, depending on datasets and settings.

For years two and three, despite improvements in image quality, heavy occlusion, and the flower complexity led to a different approach, whereby a custom VGG-based classification model, named DeepPhenology, was utilized to estimate the distribution across eight phenological stages of apple flowers. This removed the need to label individual flowers but provided more useful outputs for growers to understand their crop. To evaluate robustness, all daytime and night-time images from a specific field quadrant were initially withheld to create a test set, enabling performance assessment across all phenological stages. The remaining daytime and night-time images were randomly divided into training and validation sets with a 70 and 30% split, respectively. Training was conducted on a desktop computer, requiring approximately 2 hours to complete 200 epochs.

2.4.3 Running Batches

When processing results on the edge-device, the processing is limited to the edge-device's hardware capabilities. It is important to acknowledge the hard requirements of the project. In this scenario, the hard requirements included that the accuracy of the model is reasonable, and the model is run on an edge-device in near real-time as the grower will need to review the results in the morning.

For the accuracy of the model, the speed and accuracy of different image input sizes were tested and a trade-off between acceptable *real-time* processing was obtained.

Several factors were found to impact the speed of model inference. We tested the speed of different batch sizes, and in our scenario, it was found that consecutive processing with a batch size of one outperformed parallel processing with a batch size of two. This was likely a result of limited memory on the edge-device resulting in storage on slower media. Temperature of the device also impacted the speed of model inference and therefore we recommend tests to be run in conditions representative of envisaged deployment conditions.

Additionally, the number of images in the data stream impacts the speed of processing a block. Although imagery can be captured at a fairly high speed, if the processing of each image takes longer than the frame capture time, a buffer of images is built up. As the buffer increases, the memory of the system is utilized for non-real-time processes. Therefore, limiting the number of necessary images to be processed is ideal for reducing the speed of processing a block. In our scenario, we reduced the amount of overlap between image frames by accounting for the expected physical distance between each image frame captured.

Additional considerations included reducing the number of samples and comparing the results to manual counts to identify if a trade-off in accuracy for speed is suitable to the application.

2.5 DATA PROCESSING DISCUSSION

In Year 1 and Year 2, data was recorded in ROS bag files which required the transfer of 10 GB+ files when the required image data was less than 100 MB per file. This resulted in significant delays to processing when used with cloud resources as standard storage mediums are not solid-state or have a sufficiently fast write speed. By extracting the data from ROS bag files at defined GPS locations, the time taken to process raw field data into a dataset was minimized.

When validating the trained models, some results significantly deviated from the in-field manual count ground-truth data. On review, results were valid for what could be seen in the image and therefore the model was valid.

For example, our model FCNs-Edge was trained for pixel detection of three colors. The accuracy of the model is dependent on the accuracy of the labeling which will vary from image to image. Some images had very few pixels of specific colors labeled as in Figure 2.5 and therefore if a few

FIGURE 2.5 The relative number of pixels of the white (outlined in green) and pink (outlined in pink) classes of flowers was quite different.

pixels were missed, the accuracy of that class declines significantly. The object may have been detected and only a subset of pixels missed. We identified that some images had fairly low F1 scores but visually the color detection was sound and therefore the model was considered valid. Figure 2.5 shows a close-up image of a tree branch with clusters of large white flowers and tiny pink buds. The white flowers are outlined in green, highlighting their shape, while the small pink buds are scattered across the branch and marked with magenta outlines, emphasizing the size comparison between the flowers and the pink buds.

In another example, the model DeepPhenology (Wang et al., 2021) was trained on manual in-field counts completed on both sides of a plant. As seen in Figure 2.6, it was found that significant

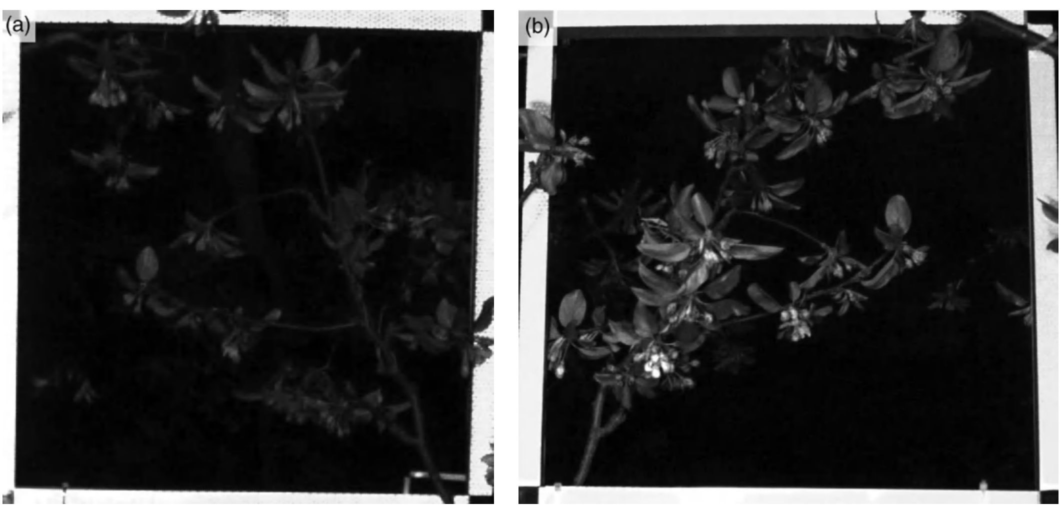

FIGURE 2.6 The visual appearance, and hence, class distribution, may vary greatly from different sides, (a) and (b), of the same quad.

occlusion in some images result in poor performance as there is expectation of similar distribution of object classes visible in the image compared to those that were occluded.

Visually, the result was valid for what could be seen in the image and therefore the model was valid. Overall, we decided to collect imagery from both sides of the plant to get a more accurate idea of the phenological distribution rather than relying on imagery from a single side of the plant.

Additionally, with DeepPhenology, we detected stages of the flowering. We combined the flowering of king bloom, full bloom, and petal fall to evaluate the percentage bloom of the plant. Rather than evaluating the accuracy of each class separately, we found percentage bloom to be in line with grower metrics and expectations on when a spray event should be triggered. Therefore, the accuracy of the model became the similarity in percentage flowering between the ground-truth data and the model output.

Overall, when working with computer vision models in agriculture, it is important to consider the purpose of the model in addition to the accuracy metrics generally used in computer vision. As the applications of computer vision are widespread, some accuracy metrics are better placed for some industries than others. As agriculture remains a small subset of available open-source computer vision datasets, widely used metrics may not give a good representation of true usefulness of the model. Therefore, care needs to be taken in understanding the purpose of the model and a suitable metric generated to capture the accuracy.

2.6 DATA VISUALIZATION

Once data has been processed, its user and use-case also defines the format in which it needs to be presented. In many cases, validation of the data with a human in the loop is necessary, particularly where critical decisions are being made as a result—for example an appropriate type and amount of chemical application. Hence data must be visualized in a manner which is effective. This section will provide examples of relevant forms of visualization and discuss the implications of these.

First, the purpose of the visualization should be defined prior to its generation. This may help define whether one or multiple visualizations are needed and avoid attempting to present too many results in one graph or equivalently avoid using many graphs to convey a point which would be more succinctly communicated.

Second, the audience must be considered. The level of experience or training with visualizations may vary dramatically, as will familiarity of the users. On farms where labor is seasonal, ensuring users can rapidly orient the data is important. The location where the visualization is being used and the medium through which is displayed will impact the effectiveness of communication. An example is the generation of a spray map, where data needs to be easily visualized and checked to instill confidence. Figure 2.7 shows a composite image demonstrating a spray map interface example from the apple flower project. The left bottom section displays a detailed spray map with color-coded blocks representing the spray density based on different apple flower stages, accompanied by a graph on the right showing the percentage distribution of these stages over time. Above the map, there are checkboxes for selecting among eight apple flower stages and a sliding bar to adjust spray density as growers could adjust thresholds until known patterns appeared and once satisfied could export the result to a spray map.

For field-based users, where digital displays are used, avoiding reflections, being able to view screens comfortably in direct and bright light conditions, and ensuring appropriate contrast is helpful. Viewers may also need to use devices at night. Visualization which requires a reliable internet connection to display results is not effective where internet connectivity is temporally or spatially inconsistent. In such cases, caching the data, or providing printed copies may be more effective and should be considered in the planning workflow. Office-based visualizations often need a computer, and as such can provide more detail where greater screen area is available.

Disseminating results to a wider audience of stakeholders should be considered. This may extend well beyond farm-based users to advertising media, insurance agents, crop buyers, and more. Having

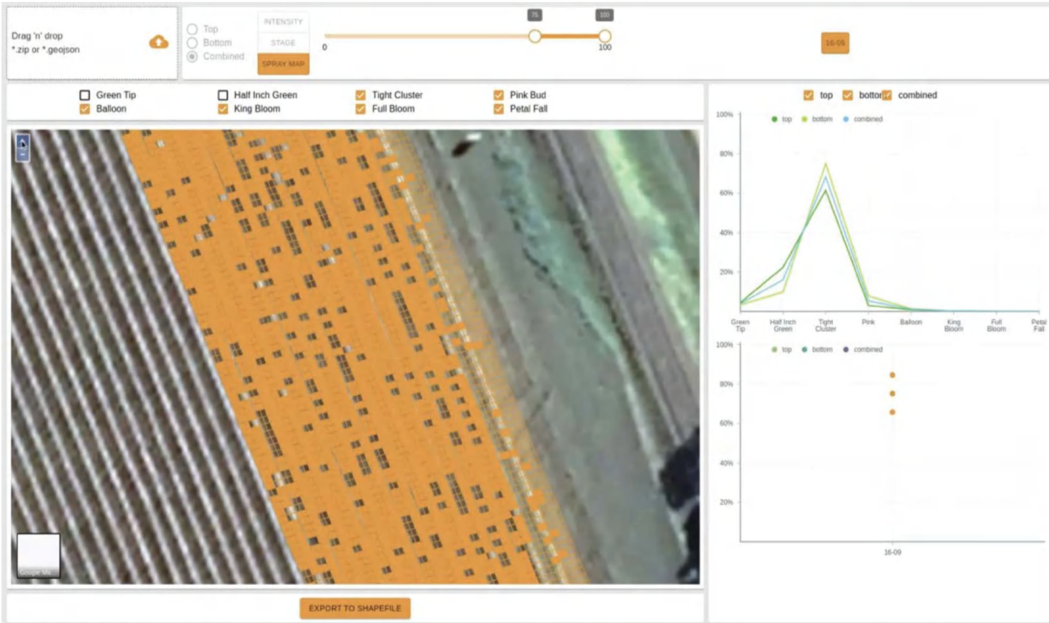

FIGURE 2.7 Adjustable thresholds for processed image data allowed growers to adapt the locations of spray application.

a visualization which is appropriate to each of these audiences, given different levels of data permissions would be helpful.

Third, different forms of visualization are appropriate to convey different messages. For many applications, qualitative trends and identification of outliers is important to identify areas of interest for further inspection or differential treatment. However quantitative values are needed in situations where there is an interface to other data sources or where treatments are being prescribed on the basis of the data.

For example, restrictions around chemical application for flower thinning often require adherence to specific concentration rates. Varying these may not be permitted under legal frameworks, so determining where to spray rather than adjusting the concentration may be a more effective means of treatment. In this case, while at first glance a quantitative prescription map may be needed, simply a binary yes/no application for each tree or location may be sufficient. Therefore, a qualitative map may suffice as a basis, as long as an appropriate threshold is set, as shown in Figure 2.7.

In many cases historical records may exist, whether obtained with different technologies or by different service providers. Showing data in the same spatial format and to a consistently color scale or representation is important to allow user comparison to previously obtained data. Defining the representation at the outset and communicating this to users is helpful. Where possible, initiatives and standards such as those promoted by Collabriculture (http://collabriculture.com/) allow portability of data between users and service providers.

The performance of image processing algorithms can be evaluated in a plethora of manners. Traditional computer vision work has been compared to large common datasets of labeled imagery (footnote: https://en.wikipedia.org/wiki/List_of_datasets_in_computer_vision_and_image_processing). In most cases this is devoid of a real understanding of what exists in the scene at the moment and place of capture. Where this becomes an issue in agriculture is with occlusion, usually due to foliage. Relating the actual *ground truth* with what is in the image, on an image-by-image basis takes significant resources, care, and attention. Many approaches have been taken to resolve this (Hill & Whitty, 2021). Therefore, when performance of an algorithm is presented, it is important to clearly articulate on what basis the performance has been measured—against labeled images or against an in-field measurement—as there may be significant difference.

As a side note, where performance is presented, the basis also needs to be expressed. In some cases, an image would nominally contain one object, whereas in other applications an image could contain 1000 or more objects of interest. Measuring performance per image versus per instance, causes challenges if a straightforward average is taken rather than a weighted average. Similarly, accuracy over a single image versus a dataset or a plurality of datasets will give different results if a simple average is taken, so the basis needs to be clear.

Where quantitative results are presented, using a table format allows these to be extracted and imported for direct comparison by future users if they are not directly provided as data files.

Fourth, color is a key ingredient in effective visualization. Colorblind-friendly palettes and perceptually uniform color maps (https://colorcet.com/) can be used to improve accessibility. Where visualizations are printed on a grayscale printer, the choice of base color palette should also be considered and tested. Figure 2.8 shows a poor choice of color scheme in a map which when converted to grayscale makes several colors indistinguishable

Similarly, when presented in formats where display contrast is limited, such as older computer projectors or screens used in an outdoor setting, effort should be put into increasing the contrast over a reasonable range of values in the visualization. The range of values, and whether linear, logarithmic or other color scales applied should be considered to ensure the intent of the visualization is conveyed.

Fifth, results may not necessarily need a custom-designed visualization to be effective. For qualitative results, overlaying detection results on an image is the default output for many image processing tools. Where a pixel-level segmentation is applied, web-based tools such as Juxtapose shown in Figure 2.9 allow viewers to effectively hide and reveal the results over the base image, allowing the segmented areas to more clearly be identified. However, there are cases where more complex visualizations are needed as per Figure 2.10.

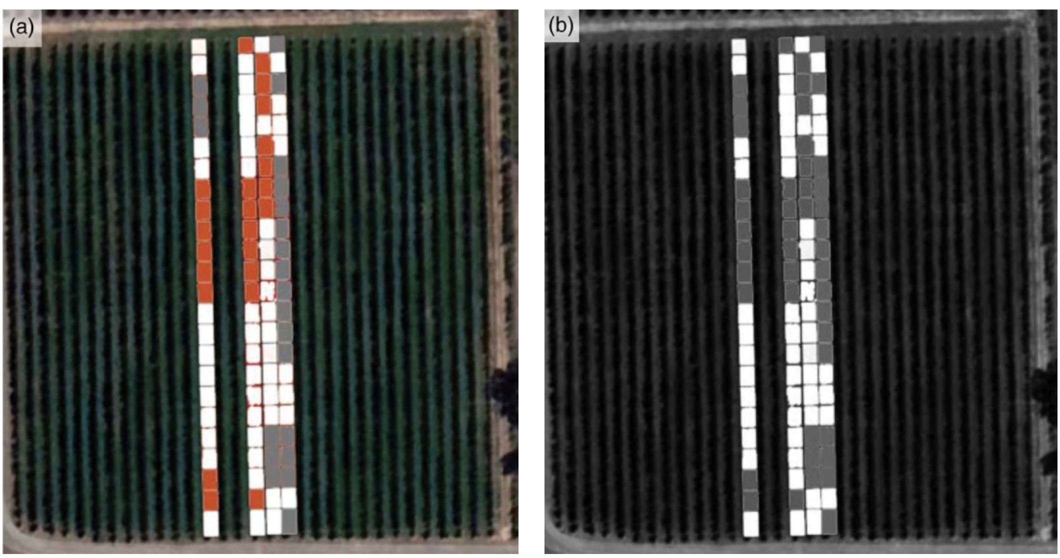

FIGURE 2.8 A color scheme in the image at left, which when converted to grayscale results in the color differentiation being completely lost. This may occur for example if an image is printed on a grayscale printer, or if a poor color range is chosen. (a) Graphic with poor color scheme. (b) The same graphic when converted to grayscale, making spatial patterns indistinguishable.

FIGURE 2.9 Example of a tool for rapidly visualizing an original image and processed result, allowing quick identification of qualitative performance.

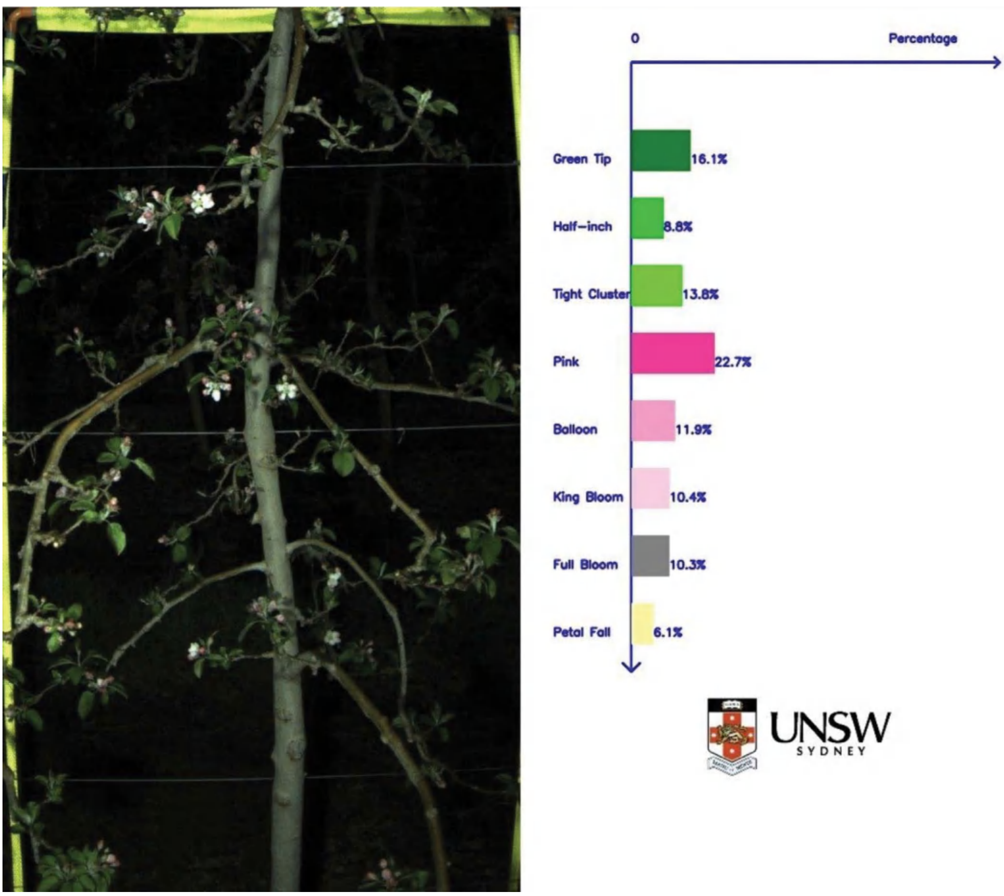

FIGURE 2.10 Example of an automatically generated visualization combining an image and a flower phenology distribution in a single display.

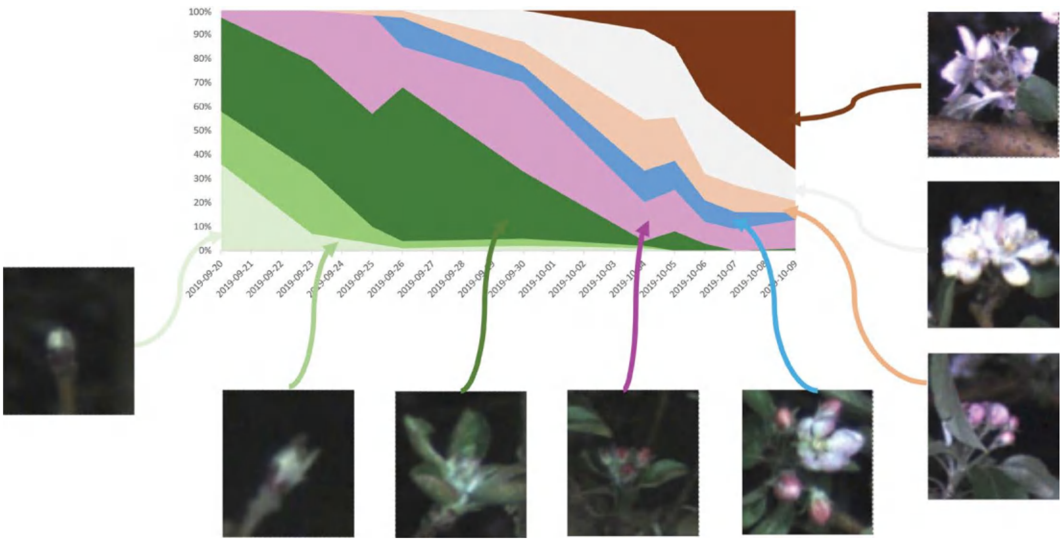

FIGURE 2.11 Stacked area chart showing the change in distribution of apple flower phenology over time from 2019/09/20 to 2019/10/09.

For quantitative results, including processed or ground-truth values in the filename has proven to be an effective means of visual identification, particularly when labeling images. It also allows a cross-check of this data, whether encapsulated as metadata or stored in a separate database.

Sixth, when comparing visualization of the same target object over time, placing these side by side in chronological order, with a clear legend showing dates of capture, to the same scale and size, using a consistent color scale can make this effective.

If not adjacent, giving the user the ability to flick between images rapidly or adjust the degree of transparency can help in identifying differences and trends. Specifically, calculating and presenting differences between maps can highlight areas of interest. Showing a change in distribution over time can also be achieved with a stacked area chart as in Figure 2.11.

Finally, visualization is inherently a Human–Machine Interface (HMI) topic, yet the method for storage of data may different whether it is to be human-read or machine-read. The level of caching of data will vary given the limited rate for a human to visually process the imagery, while later consumption by an algorithm will be at a different rate. Visualization tools take time to develop, so the trade-off between development time and how frequently they will be used and the value they add should be considered. Some growers may only use a visualization once a day for three weeks, yet base critical management decisions off it.

For assurance purposes, a timestamped and static snapshot of the imagery context is essential and may even be included in the filename if not the file metadata. For example, an original image may be labeled with the following:

- Metadata of collection (e.g., timestamp, location, operator, camera parameters, weather, purpose, data series)
- Metadata of ground truth (e.g., associated manual measurements and methods or corresponding data sources)
- Metadata of storage (e.g., where stored, when uploaded, who uploaded)

An image containing the results of processing may also contain the following:

- Configuration of processing (e.g., when generated; what version of the data pipeline was used: The algorithm, the preprocessing parameters, the software libraries)

This metadata allows traceability right through the workflow to enable identification of any errors. Given the value of decisions users may make on the basis of this data, ensuring there is an ability to identify any source of error facilitates remediation and builds confidence in the system.

In summary, a range of aspects of visualization impact the effectiveness of the overall image management system in an agricultural context. Many of these aspects have been well-demonstrated in individual cases; however, a holistic viewpoint is presented here as a basis for future implementations.

2.7 CONCLUSION

This chapter has sought to share lessons learnt from a decade of experience in agricultural image processing; the advantages and limitations of various image management methods, and the processes which underpin these.

When examining the decisions taken during the planning phase which will impact the entire data lifecycle, clearly defining ground-truthing methods for in-field data collection allows robust data to be collected. This was supported by multiple phases of quality control checks done as efficiently as possible. Planning to ensure sufficient data was collected in times of rapidly changing visual appearance was a logistical challenge.

Through highlighting aspects of data collection which will facilitate long-term use, particularly with commercial outcomes in mind, made clear that humans are still a key part of data quality validation. Regardless, data validation is essential and must be considered rather than a *try it and see* approach where opportunities for data collection may be infrequent.

By demonstrating examples of data processing techniques and lessons learnt from real-world experience, it was discovered that there is a nexus between edge computing and cloud processing. The end-to-end logistics of moving large datasets must be considered in advance with an appreciation of the volume of data to be managed.

Finally, the importance of decisions taken when visualizing data was illustrated through lessons including defining the purpose of each visualization, understanding the audience, identifying relevant visualization forms, choosing color judiciously, selection of visualization tools, and consistency in display.

In summary, while technical obstacles are often a key focus of computer vision projects in agriculture, there remain many non-trivial aspects of managing agricultural image data which have been aggregated in this chapter.

REFERENCES

Hill, G. N., & Whitty, M. A. (2021). Embedding metadata in images at time of capture using physical Quick Response (QR) codes. *Information Processing & Management*, *58*(3), 102504.

Wang, X. A., Tang, J., & Whitty, M. (2020). Side-view apple flower mapping using edge-based fully convolutional networks for variable rate chemical thinning. *Computers and Electronics in Agriculture*, *178*, 105673, https://doi.org/10.1016/j.compag.2020.105673.

Wang, X. A., Tang, J., & Whitty, M. (2021). DeepPhenology: Estimation of apple flower phenology distributions based on deep learning. *Computers and Electronics in Agriculture*, *185*, 106123.

3 Digital Tools in the Context of Agriculture 4.0 for Integrated Management of Orchard Crops

Stanley Best, José Maldonado, Melany Navarro, and Valentina De la Barrera

3.1 INTRODUCTION

This chapter examines in detail the importance of irrigation in the context of climate change, where alterations in precipitation patterns, the increased frequency of extreme events, and the seasonal distribution of water pose challenges for Chilean and global agricultural production.

Advanced tools and methodologies are explored for site characterization and definition of management zones, which allow measuring the spatial variability of soil physicochemical characteristics and monitoring crop development and condition. This knowledge is essential to design more efficient irrigation strategies adapted to the specific needs of each farm.

In addition, the theoretical basis of crop water requirement is addressed, answering key questions such as *how much water is required?* And *when is the optimal time to irrigate* using digital tools? Crop type, soil properties, evapotranspiration, and irrigation uniformity are considered in this analysis. Finally, the potential of Internet of Things (IoT) systems in irrigation scheduling is examined, and a comprehensive methodology—from variable collection and evaluation to water monitoring validated with vegetative information and management control—is presented to implement responsible and sustainable irrigation practices in modern agriculture.

3.2 THE IMPORTANCE OF IRRIGATION IN A CLIMATE CHANGE CONTEXT

There are three global phenomena that are conditioning the development of agriculture, also known as *drivers of change*: (1) climate change; (2) the increase in demand for food; and (3) technological innovation processes. These factors will define the agenda for crop development in the coming years, each with a different level of impact.

Climate change is already affecting agriculture in the region, manifesting itself in an increase in events such as droughts, floods, and extreme weather phenomena. This has led to the implementation of mitigation measures at the local level, such as early warnings and timely technical adjustments in the control and management of water resources (Ministerio del Medio Ambiente (MMA), 2011). In this context, climate change generates challenges for production due to uncertainty in yields and the frequency of extreme events.

On the other hand, technological advances applied by more innovative farmers with greater investment capacity contribute to increasing the competitiveness gap between corporate agriculture and medium and small producers (Best, 2011; Best et al., 2014). In its Second National Communication (MMA, 2011), the Government of Chile highlighted the vulnerability of various sectors to expected future climate scenarios.

DOI: 10.1201/9781003510598-3

The increase in temperature, changes in precipitation patterns, and soil erosion caused by storms and desertification processes seriously impact agricultural productivity. In much of Chile, yield losses are expected in rainfed areas and in those with irrigation restrictions due to water scarcity (Agrimed & Asagri, 2011). In addition, water supply limitations and the reduction of the phenological period caused by the thermal rise increase crop stress (MMA, 2011). These drought phenomena are associated with *La Niña*, whose most intense event in the last decade (2010–2020) lasted about 18 months and generated abnormally dry conditions throughout the country (Orrego et al., 2020; Vicencio, 2020).

The mega drought in Chile has intensified, accumulating 11 consecutive years of water deficit with precipitation drops of −20% to −40% in the central zone and −10% to −20% in the south, which has drastically reduced river and reservoir flows (González, 2020; Orrego et al., 2020). NASA's MODIS spectroradiometer detected an annual retreat of about 10 m in permanent snow elevation since the year 2000 (MMA, 2011). In turn, subway aquifers have been depleted after successive lean seasons, decreasing natural infiltration and increasing losses in unlined channels (Agrimed & Asagri, 2011).

Faced with this scenario, producers agree that, without the construction of reservoirs, it is impossible to project local agriculture for the global challenges of the food market; however, these infrastructures must be complemented with technologies that increase water use efficiency (Best, 2011; González, 2020; PwC, 2019). Tools such as soil sensors, spatial modeling, and the NDVI index allow evaluating the variability of vegetative development and optimizing irrigation scheduling (Fuentes-Peñailillo et al., 2024). It should be noted that the decrease in precipitation, associated with the increase in temperatures, is not distributed homogeneously in the region. There are areas where the thermal increase is greater than in others, which generates a differential impact on both the water problem and the thermal changes that directly influence the phenological development of plants (Vargas & Best, 2019).

For those who do not have systems for monitoring climatic variables, there is the possibility of accessing quality meteorological information using data from stations close to the farm, available, for example, at agrometeorologia.cl. In Chile, INIA's meteorological network (www.agromet.cl) offers a set of stations distributed throughout the country that record the main agroclimatic variables with good accuracy. However, the quality of these data decreases when the farm is more than 20 km from a weather station of this network.

To mitigate this limitation, there are applications that allow access to global information (Kamilaris et al., 2017). These combine data from existing stations with information from meteorological satellites and, using mathematical models, project climate variables beyond the ideal location of the stations. This makes it easier to obtain information adjusted to the local values of the property, with a margin of approximately ±0.25°C of accuracy.

3.3 VARIABILITY OF ORCHARD CONDITIONS

On the other hand, there are still unexplored areas in terms of crop response to the diverse soil and climate conditions present in the country. This demands the incorporation of new *Agriculture 4.0* technologies that allow the development of research aimed at solving management requirements from a site-specific perspective, i.e., considering the particular conditions of each farm, where productive factors (soil, climate, plant) present spatial variations. Thus, in order to face the challenges imposed by the changes in production paradigms resulting from climate change and market conditions, it is essential to adopt new technologies that allow for more efficient and timely decisions on agronomic management. The technologies used in Agriculture 4.0 generate significant positive environmental externalities, such as the reduction in the use of pesticides and the mitigation of their effects, the promotion of more efficient fertilization that minimizes groundwater contamination, and the reduction of greenhouse gas emissions, among other benefits (Best et al., 2014; Boletín Agrometeorológico – Ñuble, 2019). However, these technologies have a clear intervention logic, ranging from the capture of information and its interpretation to the implementation of corrective actions.

Thus, considering the above, from a practical management perspective, it becomes essential to develop a zoning management of orchards based on their tree water status. This zoning would become a key tool for making pertinent decisions, due to the high heterogeneity of soils and the need for adequate management during critical crop periods. For this purpose, it is essential to assess plant water status with high spatial and temporal resolution.

The information generated would be a valuable resource for quality management in a production-scale orchard, allowing the optimization of processes such as ripening control, differentiated harvesting, irrigation management, plant vigor development, and production balance, among others. However, before analyzing the system at the spatio-temporal level, it is necessary to ask some questions: What is the magnitude of the variation in water stress (in space and time) expected in a commercial-scale orchard? Is this variation significant enough to provide a relevant tool for orchard quality management? And finally, does the magnitude of variation in quality justify the implementation of this zoning?

3.3.1 Methodology of Intervention of an Irrigation System

The proposed intervention methodology should be aligned with the technologies that are feasible to implement, considering both the capabilities of the agronomic team of the companies and the availability and aptitude of producers to adopt and apply them in the management of their crops. Given the considerable impact that climate change is having on the normal development of crops (Santibáñez et al., 2014), an intervention logic is proposed in the areas of irrigation management.

First, priority is given to the collection of technical information to characterize the existing variability at the site and climate level in the different production units. Then, this collected information is analyzed to generate the necessary indicators to facilitate the interpretation of what is happening in the pasture. Finally, specific management strategies are developed based on the variable climatic conditions, with the objective of mitigating the adverse effects of climate change and improving the sustainability of production (Vargas & Best, 2019).

3.3.2 Tools for Site Characterization and Definition of Management Areas

To understand the variability of a site and its impact on productivity and, therefore, on crop profitability, it is essential to know the soil characteristics, both in terms of physical (topography, texture, moisture retention, depth, etc.) and chemical (fertility level, electrical conductivity (EC), percentage of organic matter, etc.) and biological (bacterial activity indexes, etc.) conditions. These are the key factors the authors are working with. However, it is curious that this type of information is rarely found in producers' records, despite the fact that evaluations such as those of soil physical characteristics are usually carried out only once. The possible explanation for this situation lies in the fact that farmers often consider this information costly to obtain and do not clearly visualize the benefits it could bring them in the short, medium, and long term to improve the productivity and quality of their crops. For this reason, it is crucial to have monitoring tools that allow farmers to know the state of their land, identify conditions of productive variability, and make the necessary corrective decisions, whether at planting time, in the application of inputs, or in the subsequent follow-up of the crop's evolution.

3.3.3 Measurement of Spatial Variability of Physico-Chemical Characteristics

The equipment for measuring soil electrical conductivity associated with existing altimetry is used as a support tool for the physical-hydric characterization of soil in order to provide information to

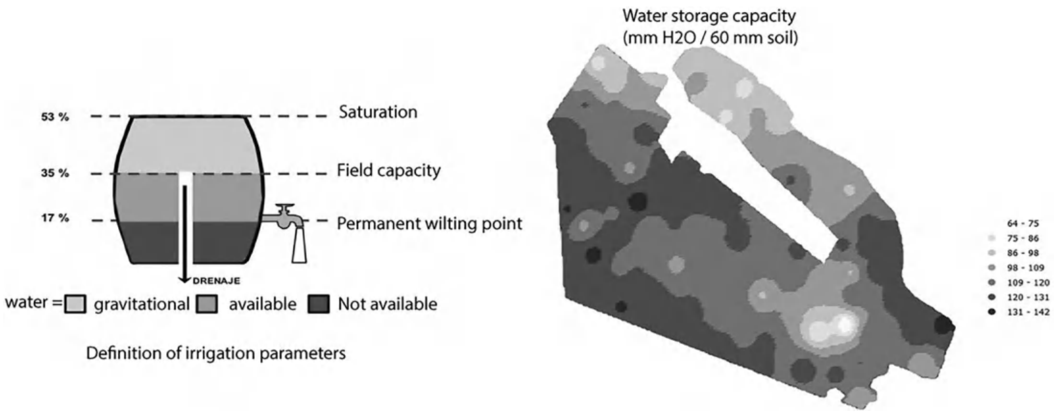

FIGURE 3.1 Zoning with EM 38 equipment; sampling points; maps of sand content, clay content, and storage capacity.

measure its variability and thus explain the spatial variation of water stress detected in plants (Best et al., 2014).

This equipment is very useful for the definition of zones of dissimilar conditions within a field, which allows locating with great accuracy measurement points to obtain an edaphic characterization of the sector. This is also useful to evaluate the conditions in which a variable irrigation system is developed and also for the definition of the optimum fertilization with the support of appropriate equipment.

To build a conductivity map, representative and georeferenced sampling points are determined. Once the samples are collected, they are sent to the laboratory to analyze texture characteristics and water storage capacity; with the results obtained, it is feasible to perform an analysis that allows generating a spatial representation of these variables. These maps are essential for defining the irrigation strategy, since they allow determining the amount of water that can be applied per zone. Figure 3.1 shows a spatial representation of the amount of water, in millimeters, that can be stored in 60 cm of soil. If more water is applied than the soil can hold, it will begin to percolate, generating unnecessary losses. With this information, a correct irrigation system can be designed, which will greatly facilitate more uniform irrigation management.

There is also a key tool in irrigation related to measuring the topography of a field. Traditionally, this task is done with surveyors and total stations, which involves many hours of field work and high cost. However, the introduction of GPS, especially geodetic GPS (stationary or installed in drones), has allowed the survey of altimetric data with greater precision, efficiency, and a greater amount of data, which generates a better representation of the area under study (Nirmal, 2024). With this information, it is possible to design irrigation systems appropriate to the topography and to construct drainage systems in areas with high soil moisture.

3.3.4 Spatial Measurement of Soil Compaction

Compaction is produced by the mechanical compression of soil particles and their aggregates (sets of soil particles grouped into a single block). It can be measured with a soil penetrometer. The deeper and easier the penetration of the probe of this instrument, the lower the compaction and, consequently, the better the condition of the soil. A low resistance (<2000 KPa) indicates that the soil is not very compacted. Less compaction facilitates the development of deep roots, the vertical flow of water, and the increase of spaces (pores) in the soil. This increase in pores correlates with greater aggregate structure and higher organic matter content. It is important to note that compaction of surface layers restricts root growth and vertical water flow, which can lead to a considerable reduction in yield.

Currently, there are mobile penetrometers that allow the creation of spatial compaction planes, which is crucial to evaluate the need for subsoiling in the specific areas of the farm that require it, thus avoiding the unnecessary costs of this practice if it were carried out on the entire surface. In addition, there is equipment that evaluates compaction at different depths, which defines the effective soil depth, a relevant factor with an impact on the productive and economic response of the crop (Vargas et al., 2015).

3.3.5 Multitemporal Segmentation Tools Using Satellite Imagery

Another site segmentation tool that can be useful to identify homogeneous response zones, allowing the focus of the sampling points for the physical and hydraulic characterization of soils, is the analysis of the *historical stability of vegetational indices*. This analysis is based on the grouping in clusters of the analyzed elements of the vegetational index map (such as MSAVI, NDVI, and other vegetation indices) in different seasons, obtained through statistical classification of the data. The purpose is to classify *n* objects into groups, using a set of vegetational maps of several years from the same locality. The groups are formed according to the degree of similarity between the members of each cluster.

This zonation method is less accurate than that achieved with the use of the M38 equipment, which directly measures soil properties. Therefore, it is recommended to increase the sampling level by 20% more to achieve adequate zonation (Vargas & Best, 2019). However, in places where this type of equipment is not available, the clustering system turns out to be a superior option for the definition of the sampling points than the traditional method, also allowing a clear definition of the zones.

3.3.6 Tools for Monitoring Crop Development and Status (Diagnosis and Monitoring)

There are multiple ways to efficiently monitor crops, ranging from the use of satellites to sensors in the field. One of the tools that has experienced the greatest growth in recent years is plant monitoring using biophysical indicators obtained from satellite platforms. Currently, there are monitoring systems available at different costs, and even free of charge, depending on the level of image resolution and frequency of revision. Among the most popular is the Sentinel (2A) family of satellites, which are free and have a weekly revision frequency, which is sufficient to detect problems and correct them in a timely manner; however, in areas with frequent cloudy conditions, a higher frequency of satellite passes may be required, being able to access Planet images, which have a daily frequency at quite reasonable costs (Best et al., 2014, 2023).

The use of this type of system allows to perform a spatial evaluation of the crop condition (activity, development, and environmental conditions) in stages after planting. This evaluation is useful to adjust irrigation or fertilizer doses by environments, as well as to detect early weed infestations. In the latter case, it is also useful to conduct a sampling, which can be not only soil sampling but also foliar sampling, to evaluate the nutritional level of the plant and its deficiency condition. This allows homogeneous applications (with an adequate average) or at a variable rate. In addition, possible water problems can be identified when significant drops in this index are observed between different dates, which makes it easier to focus soil moisture sampling by using sensors or by making test pits, as will be explained later in this chapter.

In order to represent the variability of soil conditions and considering the variability detected, sampling points are defined. Then, soil samples are taken for physical (sand, silt, clay) and hydraulic (water storage capacity) analysis, which will contemplate a sample distribution ideally based on international standards (1 sample/ha) and on the variability found. This will allow, on the one hand, to generate a spatial representation of the physical and hydraulic conditions of the soil associated with zones of homogeneous characteristics, and on the other hand, to guide irrigation management, defining irrigation zones according to the water storage capacity of the soil.

3.3.7 Analytical and Control Systems

The use of high-frequency information allows continuous monitoring with a sufficient level of detail to detect anomalies. These, in turn, can be analyzed through data management and analysis platforms, which facilitate the generation of prescriptions. This approach is already being implemented in other countries and is also starting in Chile (Vargas & Best, 2019).

Another form of crop monitoring that has been used in recent years is the use of drones and unmanned aerial vehicles (UAVs) on farms. These platforms offer the advantage of high resolution and flexibility in image capture, but their high cost has limited their adoption, which has generated a moderate development of this technology for the moment.

3.4 THEORETICAL BASIS FOR CROP WATER REQUIREMENTS

Prolonged water stress is generally associated with the gradual depletion of water in the soil. Despite advances in the definition of yield and associated quality, there is still a gap in the evaluation of the variables that determine them. Among these variables, according to the authors' experience and the literature consulted (Best et al., 2023; Ferreyra & Sellés Van, 2007; Kool et al., 2014), the most important corresponds to orchard water management.

3.4.1 The Importance of Irrigation

Water plays an essential role in the life of plants and crops, being a key component in the cycle of production processes. Its functions include the following:

- It constitutes more than 60% of the fresh weight of vegetables.
- It transports nutrients, gases, and dissolved organic products through plants.
- Maintains cell turgor, giving firmness to plant tissues.
- It participates in chemical and biochemical processes.
- It plays a central role in perspiration.

The difference between water absorbed and water lost by transpiration is used in metabolic processes linked to plant growth and fruit and seed production. However, the proportion of water retained by plants, although low (less than 5%), is not a fixed value but rather a dynamic parameter that varies according to the physiological state of the plant and the surrounding environmental conditions (Peters et al., 2025).

3.4.2 Water Balance

The water balance is the balance between inputs and outputs of water in the system (Kool et al., 2014), described by the following equation:

$$\mathbf{P + I = E + Pe + \Delta S + ET} \tag{3.1}$$

where,

P is precipitation (mm/day);

I is irrigation input (mm/day);

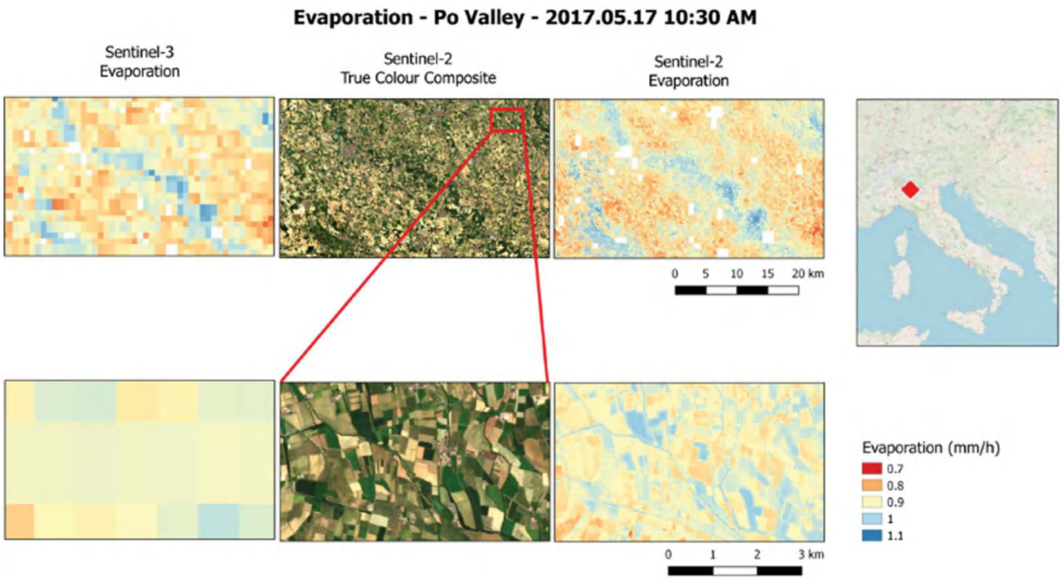

FIGURE 3.2 Example flowchart for estimating ET using the Sen ET model. (From ESA, 2020.)

E is surface runoff (mm/day);
Pe is deep percolation (mm/day);
ΔS is the change in soil water storage (mm/day);
ET is evapotranspiration (mm/day).

To maintain the water balance in the soil, one of the water inputs that can be managed is irrigation, which is translated as the water input to meet the evapotranspiration requirements of crops; for this, the water demand and evapotranspiration of the crop must be calculated (Kool et al., 2014).

Currently, the reference evapotranspiration (ETo) can be obtained through various online platforms that use meteorological stations distributed throughout Chile, allowing the determination of ETo for specific locations. On the other hand, through the Sen-ET model, the energy balance method has been implemented, developing an open-source complement in Python for SNAP, and its website is available at https://www.esa-sen4et.org/. Alternatively, the USGS has developed the same energy balance model on the basis of Landsat satellites, available on their website (https://eeflux-level1.appspot.com/).

Although these models are valuable tools, they have limitations in terms of frequency and accuracy in the evaluation of water stress (Figure 3.2). Therefore, it is recommended to integrate them with real field data obtained from sensors, which will be detailed later.

3.5 MONITORING WITH IoT SYSTEMS FOR IRRIGATION SCHEDULING

3.5.1 Soil Moisture Condition Monitoring Sensors

The use of soil moisture sensors has proven to be a fundamental tool in modern agriculture, allowing accurate and real-time monitoring of water content at different depths (Best et al., 2023). This continuous measurement capability facilitates irrigation optimization, adjusting programs according to actual water needs and avoiding over- or under-watering.

In addition, the permanent recording of soil moisture offers significant water and energy savings by avoiding unnecessary irrigation and reducing excessive pumping. Maintaining a balanced moisture level favors nutrient absorption and maximizes crop yields, improving product quality and the profitability of crops. At the same time, early identification of deficiencies, excesses, or water stress allows timely corrective actions to be taken, such as adjusting irrigation frequency or duration and applying emergency irrigation when necessary.

Finally, these sensors integrate with irrigation automation and control systems, enabling fully automated irrigation based on real-time data. The connection with actuators dynamically adjusts both the frequency and volume of water delivered, simplifying management and ensuring a fast and accurate response to changes in soil conditions and plant demands.

For the proper use of this type of technology, certain considerations must be taken into account, such as:

- Perform test pits in different environments to identify the characteristics of the soil profile by stratum.
- Have information on soil water retention capacity, obtained through physical analysis (field capacity and permanent marching point) for each stratum.

3.5.1.1 Definition of the Irrigation Sensor Location

Multispectral images, through a multitemporal analysis, make it possible to identify the specific areas of each quarter and make accurate diagnoses, overcoming decisions based solely on intuition. These diagnoses must be supported by reliable information and based on clearly defined indices, which is essential for making appropriate decisions in crop irrigation management. Thus, the correct location of sensors (Figure 3.3) in strategic and representative areas of the farm is key to ensuring success in the use of this type of tool.

Correct interpretation of soil moisture data is key to efficient irrigation. First, it is essential to establish moisture thresholds that indicate the minimum level at which plants begin to experience stress and the maximum level at which waterlogging or lack of oxygen can occur. These limits should be defined according to the specific water requirements of each crop and the soil's retention capacity.

In addition, the frequency and depth of measurements are essential. Sensors must provide continuous and frequent data to detect patterns, trends, and sudden changes in moisture that require

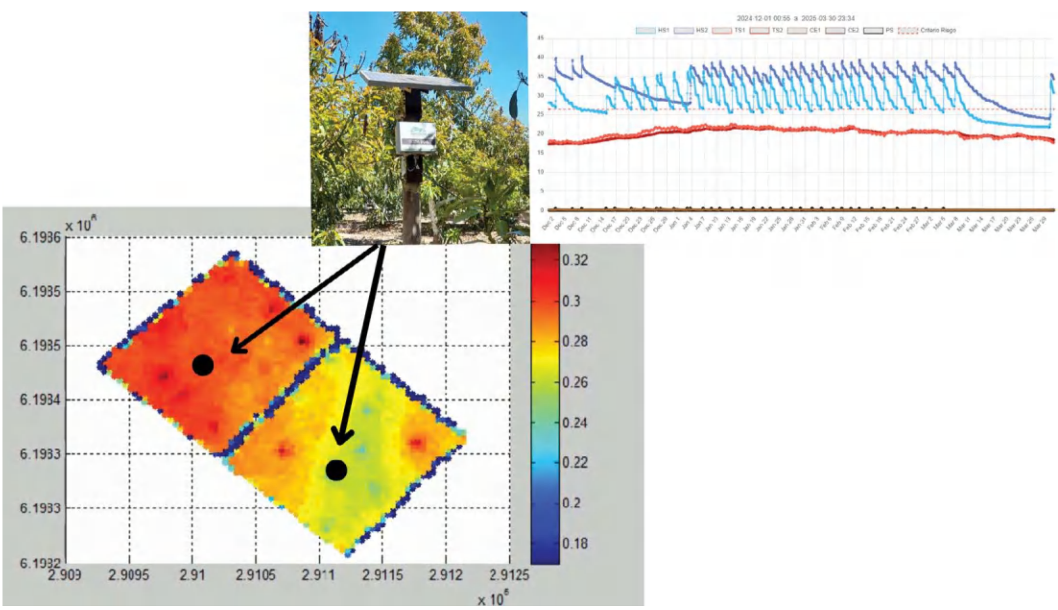

FIGURE 3.3 Proper placement of soil moisture sensors for two irrigation sectors.

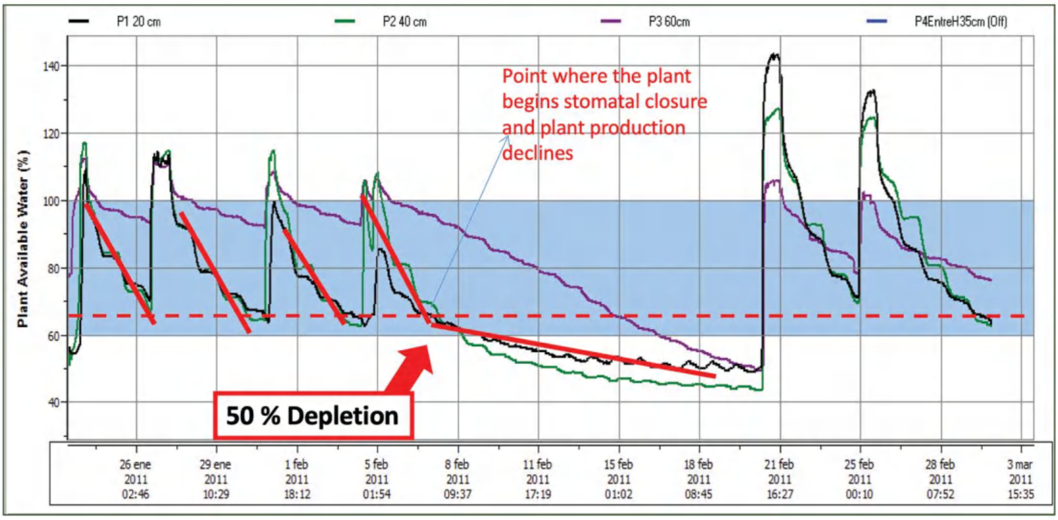

FIGURE 3.4 Definition of the irrigation threshold or irrigation criterion (IC) on a soil moisture monitoring graph. (From Ferreyra & Sellés Van, 2007.)

immediate irrigation adjustments. Measuring at different depths provides insight into how moisture varies along the soil profile and ensures that water reaches the root system, avoiding shallow or insufficient irrigation.

Finally, the interpretation of sensor data must be integrated with other agronomic and climatic factors, such as crop phenological stage, weather conditions, soil texture, and water-holding capacity. This holistic approach provides a complete picture of water needs (Figure 3.4) and allows for accurate planning of both the amount and frequency of water applied (Fuentes-Peñailillo et al., 2024).

It is important to note that, although the selection of the evaluation point is made in a highly representative area of the field, the sensor measurements are still punctual. Therefore, it is necessary to extrapolate the observed conditions to the rest of the field to assess its potential stress state. This can be achieved by a spatial representation of the rate of change in vegetational indices, such as NDVI.

3.5.2 Indicators of Water Status by Plant Measurements

Water status indicators obtained from plant measurements have historically been used mainly in environmental physiology and irrigation research, but their practical application in irrigation scheduling has been limited. However, there is growing interest in methods that are based directly on plant responses to water stress, as they offer a closer approximation to the real needs of the crop.

While designing an optimized irrigation system to manage spatial variability is key, ensuring proper scheduling—both in frequency and volume of irrigation—is equally essential to improve profitability. Without accurate estimation of plant water status, yield targets will not be met, and developing indices or practical tools to effectively assess water status remains a challenge.

For the production of high-quality wine, efficient water management is essential. Therefore, the water status of grapevines has been extensively studied, finding significant correlations with production and quality (García & González, 2020; Muñoz et al., 2007). One of the most widely used methodologies is the measurement of xylem water potential (Ψ) at dawn and midday, a biophysical parameter suitable for establishing water stress levels and irrigation needs in fruit trees (Naor, 2001) and *Cabernet Sauvignon* grapevines, which also correlates positively with stomatal conductance (Acevedo-Opazo et al., 2010).

Xylem water potential (Ψ), measured at midday, is considered a standard indicator of plant water status, as it reflects the moment of highest stress in the soil-plant-atmosphere continuum (Acevedo-Opazo et al., 2010). Both Ψ and leaf potential have been used as key parameters in irrigation scheduling in fruit trees, although their measurement with a Scholander pump is arduous, costly in time and labor, and destructive, as it requires leaf extraction; however, given the standards developed by research and its ease of use, it is still a widely used tool in the fruit- and wine-growing world in Chile (Selles Van et al., 2002). On the other hand, integrating these measurements with remote sensing systems facilitates the generation of models that more accurately represent the spatial variability of water stress.

Infrared (IR) thermography uses the temperature difference between the canopy (Tc) and the air (Ta) as a proxy for water deficit, where high Tc-Ta values indicate stress and low values indicate well-watered plants. Infrared thermography (IRT) sensors, which are lighter and have a better field of view, capture thermal images that, after calibration, allow rapid and non-destructive detection of water problems (Best et al., 2009). This methodology speeds up field sampling by enabling a greater number of repetitions in less time than Ψ-based techniques (Jones et al., 2002).

On this basis, the Crop Water Stress Index (CWSI) correlates plant temperature with plant water status, ranging from 0 (optimum) to 1 (maximum stress) depending on the vapor pressure deficit (Jackson et al., 1981). Studies have confirmed its relationship with xylem potential (Yuan et al., 2004), making the CWSI an effective tool for assessing water stress in vineyards without the costs and complexity of direct Ψ measurement (Best et al., 2012).

3.5.3 Application Systems Variable Associated with Segmentation Found (Actuators)

One of the challenges associated with the use of technological tools in agriculture is the connectivity available. Although coverage and access to connectivity in rural areas of Chile have improved in recent years, they are still insufficient. The country's mountainous geography also represents an additional obstacle. In addition, although the network reaches the main buildings on farms, coverage within the fields themselves is often limited. This makes it difficult to install sensors and actuators, although, given that these devices have a low transmission consumption (GPRS), it has been possible to introduce this type of equipment in the field. However, the flow of more complex information, such as images, is still restricted to offline work.

Once the correct operation of the irrigation system has been evaluated, and the zoning of the work area and the site-specific irrigation management (how much and when to irrigate) have been carried out, it is necessary to have intelligent machinery capable of receiving digital prescriptions and transforming them into automated actions that place the inputs in the correct place and quantity. In terms of irrigation, there are several tools that support this task, among them variable irrigation systems (VRI), such as those used in center pivot equipment.

Once the variable prescription is established in digital format, it is loaded into the pivot control panel (Figure 3.5(a)), which, by means of a GPS system and depending on the type of dosing system

FIGURE 3.5 (a) Variable prescription over a storage capacity map; (b) center-pivot with section-by-section variable irrigation; (c) irrigation control on a web platform. (From TristateKS; Lindsay.)

used (solenoid valves or pivot speed control), precisely regulates the amount of water to be applied along the entire transect. In the case of fruit trees, the use of variable irrigation is more restricted and has been translated rather into the realization of a good initial irrigation design that adapts to the conditions of soil variability (as described above), allowing a greater uniformity in each irrigation sector.

3.6 CONCLUSION

Agriculture 4.0, driven by smart sensors, the IoT, artificial intelligence, and data analytics, is redefining agricultural irrigation management. By integrating real-time information on soil moisture, weather conditions, and crop-specific requirements, these technologies enable highly accurate water allocation, reducing losses and increasing productivity in a sustainable way. This approach makes traditional agriculture more efficient and resilient to global challenges such as climate change and water scarcity.

However, access to these innovations is still limited in many rural areas. In order to democratize Agriculture 4.0, it is essential to design public policies, offer subsidies, and implement training programs that facilitate technological adoption among small- and medium-sized producers. This is the only way to ensure the equitable implementation of advanced tools, strengthening the competitiveness of the sector and promoting a fair distribution of its benefits.

Beyond their immediate utility, Agriculture 4.0 solutions open a wide field of research and development of adaptive systems that improve resilience to future challenges. These technologies not only respond to present needs but also act as a driver of permanent change, preparing the sector to proactively address production and conservation requirements. Their success will depend on effective collaboration between governments, research institutes, companies, and farmers to overcome adoption barriers and maximize positive impact at local and global scales.

REFERENCES

Acevedo-Opazo, C., Ortega-Farías, S., & Fuentes, S. (2010). Effects of grapevine (*Vitis vinifera* L.) water status on water consumption, vegetative growth and grape quality: An irrigation scheduling application to achieve regulated deficit irrigation. *Agricultural Water Management*, *97*, 956–964.

Santibáñez Quezada, F., Varnero, T., Santibáñez Varnero, P., Caroca Torres, C., González Mendoza, P., Perry Cavieres, P., Gajardo Alarcón, N., Franchi Pérez, J., Melillán Furicoyán, C. & Coronado Diaz, P. (2011). *Portafolio de propuestas para el programa de adaptación del sector silvoagropecuario en Chile al Cambio Climático*. Santiago, Chile. http://www.agrimed.cl/informaciones_detalle.asp?Solicitud=9&Tipo_Contenido=Proyectos%20en%20ejecuci%F3n

Agrometeorología Chile. (2022). *Agrometeorología Chile: Información y pronósticos meteorológicos para la agricultura*. https://agrometeorologia.cl/

Best, S. (2011). *Handbook de agricultura de precisión* [online]. https://hdl.handle.net/20.500.14001/68410

Best, S., De LaBarrera, V., & Maldonado, J. (2023). *Proyecto INIA-INDAP de evaluación digital del riego: Tecnificación del soporte de los grupos SAT con foco en el uso eficiente del riego*. Recuperado de https://heyzine.com/flip-book/f11792d295

Best, S., Gatica, G., & León, L. (2009). Development of an assessment model of water stress of a Var. Merlot vineyard, based on the use of infrared thermography. In *En Frutic Chile 2009*: Proceedings of the 8th Fruit, Nut and Vegetable Production Engineering Symposium (pp. 1133–1149). Progap-INIA.

Best, S., León, G., Méndez, A. L., Flores, F., & Aguilera, C. H. (2014). *Adopción y desarrollo de tecnología en agricultura de precisión*. Retrieved from https://hdl.handle.net/20.500.14001/68414

Best, S., León, G. L., Quintana, L. R., Flores, P. F., Aguilera, C. H., Concha, C. V., & Thomas, P. (2012). *Olivicultura de precisión: nuevas tecnologías aplicables a olivicultura*. Boletín INIA (253). Retrieved from https://biblioteca.inia.cl/handle/20.500.14001/7659

Boletín Agrometeorológico – Ñuble. (2019). *Boletín Nacional de Análisis de Riesgos Agroclimáticos para las Principales Especies Frutales y Cultivos, y la Ganadería*. INIA. http://riesgoclimatico.inia.cl/public/boletines/eyJpdiI6IkE0VTZ2Q0pjK0NnVnJMaFRlTkdpTGc9PSIsInZhbHVlIjoia2hjMnZlRHd1cWFtY1lGaHh5Nkdndz09IiwibWFjIjoiOTZiOGJkYTUyYTE5NWY5YzQ5NTE5YWE3Yjk1OGUxZGU0YjkzZjU2YzNmZTEyODc1ZWEzNDRkMjQ4NjhiN2RjMCJ9

ESA. (2020). *Sen4ET – Satellite-based solutions for estimating crop water requirements*. European Space Agency. https://www.esa-sen4et.org/

Ferreyra, E., & Sellés Van, S. G. (Eds.). (2007). *Manejo del riego y suelo en palto*. Boletín INIA No. 160. Retrieved from https://hdl.handle.net/20.500.14001/7110

Fuentes-Peñailillo, F., Gutter, K., Vega, R., & Carrasco, G. (2024). Transformative technologies in digital agriculture: Leveraging internet of things, remote sensing, and artificial intelligence for smart crop management. *Journal of Sensor and Actuator Networks*, *13*(4), 39. https://doi.org/10.3390/jsan13040039

García, M., & González, S. (2020). Determinación del estado hídrico del viñedo mediante el uso de imágenes térmicas y su influencia en la calidad y producción de la uva. *ResearchGate*. Recuperado de https://www.researchgate.net/publication/347913004

González, U. J. (Ed.). (2020). *Agricultura de la nueva región de Ñuble: una caracterización sectorial*. Colección Libros INIA No. 39. Retrieved from https://hdl.handle.net/20.500.14001/3622

Jackson, R. D., Idso, S. B., Reginato, R. J., & Pinter, P. J. (1981). Canopy temperature as a crop water stress indicator. *Water Resources Research*, *17*, 1133–1138.

Jones, H. G., Stoll, M., Santos, T., Sousa, C., Chavez, M., & Grant, O. (2002). Use of infrared thermography for monitoring stomatal closure in the field: Application to grapevine. *Journal of Experimental Botany*, *53*, 2249–2260.

Kamilaris, A., Kartakoullis, A., & Prenafeta-Boldú, F. X. 2017. A review on the practice of big data analysis in agriculture. *Computers and Electronics in Agriculture*, *143*, 23. Elsevier BV. https://doi.org/10.1016/j.compag.2017.09.037

Kool, D., Agam, N., Lazarovitch, N., Heitman, J. L., Sauer, T. J., & Ben-Gal, A. (2014). A review of approaches for evapotranspiration partitioning. *Agricultural and Forest Meteorology*, *184*, 56–70.

Ministerio del Medio Ambiente (MMA), Gobierno de Chile. (2011). *Segundo Comunicado Nacional sobre Cambio Climático*. https://mma.gob.cl/wpcontent/uploads/2014/11/SegundoComunicadoCC.pdf

Muñoz, H., González, Y., & Sellés Van, S. G. (Eds.). (2007). *Seminario Internacional Manejo de Riego y Suelo en Vides para Vino y Mesa*. Serie Actas INIA No. 39. https://hdl.handle.net/20.500.14001/8543

Naor, A. (2001). Irrigation and crop load influence fruit size and water relations in field-grown *Spadona* pear. *Journal of the American Society for Horticultural Science*, *126*, 252–255.

Nirmal, S. B. (2024). Applications of drone and unmanned aerial vehicle (UAV) surveying for planning for cities. *International Journal for Research in Applied Science and Engineering Technology*, *12*(3), 885.

Orrego, R., Valenzuela, A., Balbontin, C., Castillo, D., Fernández, F., Donoso, G., Matus, I., Tay, J., Espinoza, S., Tay, K., León, L., Salvo Del Pedregal, J., Campos, C., Fuentes Bustamante, M., & Ruiz, R. (2020). *Boletín Nacional de Análisis de Riesgos Agroclimáticos para las Principales Especies Frutales y Cultivos y la Ganadería*. INIA. https://www.agromet.cl/bolet%C3%ADn-agroclim%C3%A1tico-inia-mar-2020

Orrego, V. R., Campos, M. C., & Fuentes, B. M. (2020). *El clima de la Región de Ñuble: factor determinante para el progreso agrícola*. INIA. https://hdl.handle.net/20.500.14001/3625

Peters, R. L., Arend, M., Zahnd, C., Hoch, G., Arndt, S. K., Cernusak, L. A., Poyatos, R., Zhorzel, T., & Kahmen, A. (2025). Uniform regulation of stomatal closure across temperate tree species to sustain nocturnal turgor and growth. *Nature Plants*. https://doi.org/10.1038/s41477-025-01957-3

PwC. (2019). *Soluciones basadas en drones para agricultura*. https://www.pwc.com/co/es/assets/video/PwC-Soluciones-Drones-Para-Agricultura.pdf

Santibáñez, F., Santibáñez, P., & Solis, L. (2014). *Agricultural systems vulnerability to climate change* [Publication details not available].

Selles Van, S. G., Ferreyra, E., & Montaldo, P. (2002). Cámara de presión: instrumento para controlar el riego a través de mediciones del estado hídrico de las plantas. *Aconex*, *76*, 18–22. https://hdl.handle.net/20.500.14001/28875

Vargas, Q. P., & Best, S. (2019). *Introducción a la agricultura 4.0* [online]. INIA. https://hdl.handle.net/20.500.14001/68862

Vargas, S.R. del P., Serrato, C. F., & Torrente Trujillo, A. (2015). Variabilidad espacial de Las propiedades físicas de un suelo Fluventic Ustropepts en la cuenca baja del río Las Ceibas – Huila. *Ingeniería y Región*, *13*, 113. https://doi.org/10.25054/22161325.713

Vicencio, J. (2020). *La Niña se establece en el Océano Pacífico*. Boletín S2S – Pronóstico Subestacional y Estacional, 162. chrome-extension://efaidnbmnnnibpcajpcglclefindmkaj/https://climatologia.meteochile.gob.cl/publicaciones/boletinTendenciasClimaticas/boletinTendenciasClimaticas-202009.pdf

Yuan, G., Luo, Y., Sun, X., & Tang, D. (2004). Evaluation of a crop water stress index for detecting water stress in winter wheat in the North China Plain. *Agricultural Water Management*, *64*, 29–40.

4 Geostatistical Modeling of Multispectral Data for Monitoring *Xylella fastidiosa* in Olive Groves

Antonella Belmonte, Gabriele Buttafuoco, and Annamaria Castrignanò

4.1 INTRODUCTION

In 2015, the United Nations launched a strong call to action establishing 17 Sustainable Development Goals (SDGs) to respond to the impact of the multiple and interconnected crises facing the world and provide high-level political guidance on transformative and accelerated action toward the target year of 2030 (United Nations, 2015). Among these SDGs, the SDG 2 aims to: *End hunger, achieve food security and improved nutrition, and promote sustainable agriculture* (United Nations, 2015). Smart Agriculture offers a broad range of technologies to attempt to meet the goals of the United Nations. Precision agriculture, often seen as a subset of Smart Agriculture, is *a management strategy that gathers, processes, and analyzes temporal, spatial, and individual data and combines it with other information to support management decisions according to estimated variability for improved resource use efficiency, productivity, quality, profitability, and sustainability of agricultural production* (www.ispag.org/about/definition). Therefore, precision (or smart) agriculture has the potential to improve food production and food security using sustainable management of agriculture. However, to enhance food security, the challenge is to move beyond a diagnostic or simply a knowledge phase to a more prescriptive one of applying these principles and technologies (Hatfield & Kitchen, 2013). That could be achieved through the integration of spatial information at field scale with the most effective management practices to be implemented within the field. A significant contribution for improved management precision practices could come from remote sensing data combined with soil maps and agronomic assessments (Hatfield & Kitchen, 2013). However, remote sensing platforms often provide data not much suitable for site-specific applications because of spatial resolution or temporal availability. In order to overcome many critical issues related to remote sensing platforms, the exploration of unmanned aerial vehicles (UAVs) in agriculture has been developed (van der Merwe et al., 2020). There are different types of UAVs and their classification is based on weight, endurance, altitude, and operational radius (Acharya et al., 2021; Qi et al., 2018). Also, their design (aerodynamic configuration) includes many different forms, features, and functions: Fixed-wing, single-rotor, multi-rotor, and hybrid (van der Merwe et al., 2020). The different UAV platforms have advantages and disadvantages, and most commonly used flight platforms are multi-rotor and fixed-wing UAVs. The latter differ in both the weight they can carry (payload capacity) and the flight time (endurance): Fixed-wing UAVs have high endurance and medium-high payload capacity, whereas multi-rotor UAVs have low endurance and low payload capacity. However, the most important difference is probably the ability of vertical takeoff and landing for multi-rotor, which is not possible for fixed-wing UAVs (van der Merwe et al., 2020).

DOI: 10.1201/9781003510598-4

Three major components are required for UAV surveys: (1) A system for data collection including aerial platform and sensors, (2) a system for data processing to generate surface models and orthomosaics, and (3) data analysis for images visualization, extraction, and interpretation (Acharya et al., 2021). The sensors carried by the UAVs are the core of the system. Those most commonly used alone or in combination are the following: (1) RGB (red, green, and blue) imaging sensors, (2) multispectral (MS) sensors, (3) hyperspectral sensors, (4) thermal sensors, (5) LiDAR (light detection and ranging) sensors, and (6) microwave sensors (Acharya et al., 2021; van der Merwe et al., 2020). The choice of sensors depends on the specific application and each of them has advantages and disadvantages over the others as well as different costs.

4.2 UNMANNED AERIAL VEHICLE APPLICATION IN SMART AGRICULTURE

In Smart Agriculture, UAV, commonly known as drones, can play a crucial role by providing farmers with detailed and real-time insights into their crops and fields (Kakarla et al., 2022; van der Merwe et al., 2020; do Amaral et al., 2022). The data collected by UAV platforms are based on reflectance measurements and the success or failure of UAV technology in fulfilling the objectives of their applications depend on the quality of reflectance measurements (van der Merwe et al., 2020). For this reason, depending on the type of application, the type of sensor is chosen. For example, RGB sensors are the least expensive and most common passive sensors used and are useful in applications where the interest is in the visible light spectrum (400–700 nm) to calculate some vegetation indices (Vis) relatively easy to interpret even by relatively inexperienced people (Kakarla et al., 2022; van der Merwe et al., 2020). MS sensors are an advancement compared to RGB sensors because they can provide spectral reflectance measurements beyond what naked eyes can see. These sensors are used to calculate several VIs (e.g., NDVI) that are used for identifying plant stress and crop yield prediction (Kakarla et al., 2022). Hyperspectral sensors can measure hundreds of discrete bands at narrow wavelength ranges usually within 400–2,400 nm, but this fine spectral resolution leads to increased equipment costs, complexity, data processing times, and high storage space (Kakarla et al., 2022; Mulla, 2013; van der Merwe et al., 2020). However, hyperspectral sensors can allow to detect, identify, and distinguish plant diseases with similar visual symptoms that for RGB and multispectral sensors would be a very complex or impossible task (Abdulridha et al., 2020a; Hariharan et al., 2019).

Thermal sensors measure the energy radiated in the infrared range (7,000–12,000 nm) based on the objects' temperature (Kakarla et al., 2022). The field surface temperature can be used for precision irrigation applications (Kakarla et al., 2022) or detecting leaf wetness (Swarup et al., 2020) and trees fruits maturation (Gan et al., 2020).

Finally, LiDAR sensors use a laser to emit light and measure the time taken by light to reflect off an object and return to the sensor (Kakarla et al., 2022; van der Merwe et al., 2020). LiDAR sensors were used to create digital elevation and surface models of the Earth's surface and, specifically in agriculture, for 3D modeling of farms and farm buildings (Kakarla et al., 2022; van der Merwe et al., 2020). However, they can be used to measure many attributes of vegetation such as crop height, crop density, and canopy size (Kakarla et al., 2022).

There is now a well-established body of literature on the many possible applications of UAVs in agriculture. Citing just a few examples from the many available in the worldwide literature, there are applications for crop monitoring and health assessment (Ampatzidis & Partel, 2019; Abdulridha et al., 2020b; Kerkech et al., 2020; Moriya et al., 2021), yield estimation (Li & Wu, 2023; Saravia et al., 2023; Wahab et al., 2018), water management (Gago et al., 2015; van der Merwe et al., 2020), nutrients in crop and soil for application of agronomic inputs (Jiang et al., 2023; Mazur et al., 2023; Wang et al., 2023; YU et al., 2023), planting and seedling emergence (Sankaran et al., 2015), modeling and mapping soil variability (Belmonte et al., 2022; Romano et al., 2023), weed detection and mapping (Ajayi et al., 2023; Rasmussen et al., 2013; Sapkota et al., 2023), crop damage assessment after weather events, and a variety of other causes including insects and diseases (Belmonte et al., 2023; Castrignanò et al., 2021a, 2021b; Chin et al., 2023; van der Merwe et al., 2020).

4.3 UAV DATA ANALYSIS

Nowadays, new technologies such as Internet of Things (IoT) (Atzori et al., 2010) give relevant potential in Smart Agriculture allowing the acquisition of real-time environmental data. Such IoT devices include UAV, which can provide services regarding fields' management, by acquiring images at high resolution. However, some issues had to be solved before adoption of UAV in the agriculture domain, such as the data collection and processing methods. In agricultural field UAVs provide the temporal and spatial resolution necessary to study, different targets such as phenology, yield accumulated throughout specific crop growth stages and individual plant production, and so on, but there is still no standardized workflow or well-established techniques for analyzing and visualizing the information acquired. Before managing the information of UAV data, it is necessary to apply the following operations.

4.3.1 Preprocessing Operations

After pre-flight setup for UAV data acquisition, such as selection of platform, sensor, and flight mission, the UAV flight brings back a large amount of raw data. Nonetheless, raw data are not yet adapted for retrieval of information and drawing inference because UAV platforms are rarely engineered for in-flight data processing. UAV image preprocessing is a basic and vital factor that influences spectral accuracy and quantitative analysis of data and sensor corrections are the fundamental initial steps required to obtain geometrically consistent products from the raw data. This aspect of the measurement process involves noise (Li et al., 2010), vignetting (Zheng et al., 2009), and lens distortion correction (Wang et al., 2009).

The next steps involve the band registration to improve spatial coherence between bands and the radiometric correction to transform the digital number (DN) values into spectral reflectance.

Two radiometric correction methods are often employed for UAV-data: Vicarious calibration correction (Doelling et al., 2018) and pre-flight correction. The empirical linear calibration (ELC) method, one of the most widely applied vicarious correction methods, is based on a regression analysis of spectral image data over actual measured values (Turner et al., 2014) and has been employed in several crop monitoring studies. Differently pre-flight calibration used laboratory-calibrated parameters (e.g., calibration coefficients) to characterize the sensor.

These preprocessing operations are available in commercial packages, such as Agisoft PhotoScan® and Pix4dMapper®. After these preprocessing methods it is possible to analyze UAV agricultural images by applying different techniques.

4.3.2 Photogrammetric Techniques

These techniques allow extracting three-dimensional digital surface model (DSM) or terrain model (DTM) (de Castro et al., 2018; Torres-Sánchez et al., 2018; Ziliani et al., 2018) and/or orthophotos regarding the vegetation. DTM is a topographic model of the bare Earth without taking into account objects that may exist in the site, either natural or artificial (e.g., trees, vegetation, buildings); instead, DSM represents elevations of human-made and natural features. A DSM measures the top-most surface of an area, including all exposed objects such as treetops and buildings. UAV data generates 3D models with a much higher spatial resolution compared to other remote sensing technologies, given the lower flight altitude, through the acquisition of many overlapping images. From the 3D models orthoimage is generated, in which the distortions produced by terrain relief and camera tilts are removed, thus, merging the characteristics of an image with the geometric qualities of a map.

An orthoimage has a uniform scale, so it can be utilized as a base map to measure true distances and can be utilized to calculate other 3D parameters; therefore, it is a valid representation of the Earth's surface. The generation of orthophotos requires accurate estimation of the internal and external camera parameters. For UAV data, photogrammetric techniques rely mainly on structure from motion (SfM) (Westoby et al., 2012) algorithms that generate the sparse 3D point cloud, corresponding to the locations of the estimated feature points, to retrieval the 3D model and correspondent orthoimages. The 3D representation of vegetation features by output of relevant models was usually favored in cases where multispectral or hyperspectral data could not be acquired.

4.3.3 Calculation of Various Vegetation Indices

Spectral signatures are the combination of reflected, absorbed, and transmitted or emitted electromagnetic radiation (EM) by elements at varying wavelengths, which can uniquely identify an object (Figure 4.1).

In remote sensing applications, the spectral signature information is applied to retrieve the VIs. VIs are obtained by mathematically matching a number of spectral bands based on the physical characters of vegetation in order to retrieve relevant information such as biomass, vigor, and crop stress. VIs are regarded as very robust and adequate metrics for monitoring crop growth and health in qualitative and quantitative vegetation analysis. They are widely used to get information from UAV images for Smart Agriculture.

Based on sensor acquisition, VIs can be classified as RGB-based VIs, multispectral VIs, and hyperspectral VIs (HVIs). RGB-based VIs take three bands (RGB bands) to build VIs and are mainly used for high-resolution imaging applications on agricultural environment such as plant counting, plant density estimation, canopy cover, among others. Multispectral VIs are spread further to cover the near-infrared (NIR) band in addition to the visible light spectrum. They are used primarily in plant health monitoring on the red and NIR bands. HVIs cover a greater number of spectral bands allowing more targeted studies of vegetation to be done. One of the first indices was the Ratio Vegetation Index (RVI). This index brings out the contrast between vegetation and soil. It can be used to estimate and monitor biomass especially in densely vegetated areas; it is sensitive to the optical properties of the soil and to atmospheric effects when the vegetation cover is less than 50% (Xue & Su, 2017).

The most used multispectral vegetation index is the normalized differential vegetation index (NDVI), calculated from the *NIR* and *red* bands. Visible radiation toward red is absorbed by

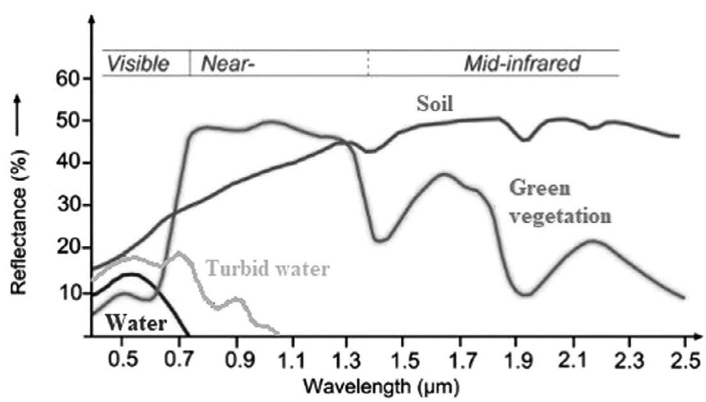

FIGURE 4.1 Generalized reflectance spectra of some Earth surface materials. (From SEOS project https://seos-project.eu/remotesensing/remotesensing-c01-p06.html. Introduction to Remote Sensing: 1. Physical Basics, modified.)

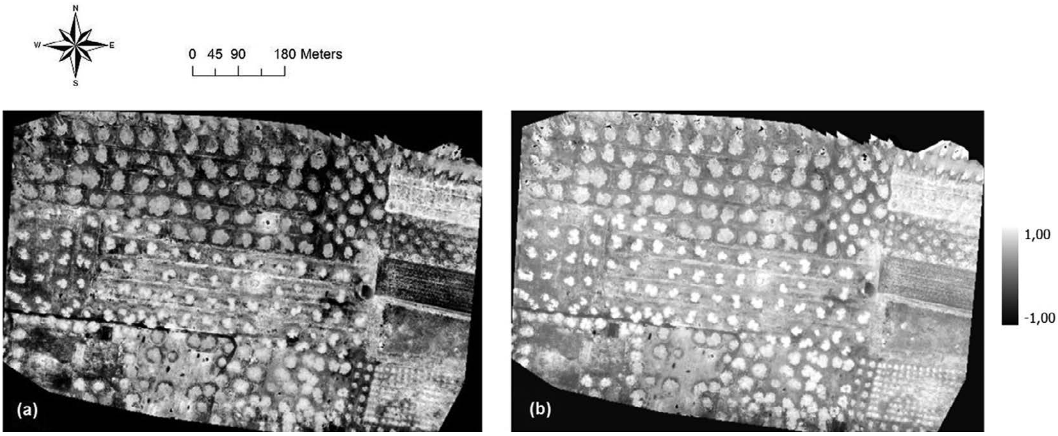

FIGURE 4.2 Example of NDVI (a) and GNDVI (b) products acquired by UAV on olive groove.

chlorophyll, while NIR radiation is highly reflected. Thus, vegetation can be discriminated from the soil in the image and unhealthy plants can be detected. Therefore, the higher the NDVI value, the better the health status of the vegetation. NDVI produced from multispectral UAV images has been demonstrated to be very effective in predicting yield and tracking fertilizer application levels indicated the potential for early detection of nitrogen deficiency in rice and wheat field experiments (Guan et al., 2019).Other VIs, such as NDRE (Normalized Difference Red Edge) or GNDVI (Green Normalized Difference Vegetation Index), are mathematically based on NDVI expression by swapping the red band with the red edge and green, respectively.

NDRE uses the red-edge band, which can penetrate leaves much more deeply than the red light used in NDVI. Thus, where there is full canopy, it is appropriate to use NDRE because NDVI saturates. Differently GNDVI is generally applied to determine water and nitrogen uptake in the crop canopy. An example of the application of these VIs is shown in Figure 4.2.

Some VIs that are based on visible bands other than NIR, such as Green Red Vegetation Index (GRVI) and Red Edge Ratio (RER), have also been used in Smart Agriculture with specific applications. The performance of GRVI and RER has been studied to track the effects of water stress on cotton respect to NDVI and crop water stress index (CWSI) (Ballester et al., 2019). The GRVI and RER appear to be good predictors of fiber quality, providing cotton producers with the opportunity to design specific harvesting plans in cases of large fiber quality variability, helping to avoid discount prices. Hyperspectral remote sensing is gaining momentum in crop monitoring, especially as it allows the development of new VIs by acquiring a large volume of data in very fine wavelengths that are highly correlated HVIs. That information richness can be distilled to a few physically meaningful variables. Generally, HVIs use the finest spectral sampling to create a narrowband equivalent to a broadband VI.

A UAV-based approach employing hyperspectral sensing technologies could reliably deliver VIs, detecting both healthy and unhealthy portions of a crop field. With the aid of this information, possibly matched with spectral calibration data, a farmer could detect infected areas in the field and make timely decisions to rescue the endangered portion of crop production (Meiyan et al., 2022). Using UAV data has shown as some HVIs have advantages in maize aboveground biomass (AGB) estimation at the field scale and can be adopted for precise nutrient management on farms (Zhang et al., 2021).

4.3.4 Novel Techniques: Machine Learning and Deep Learning

Artificial intelligence (AI) systems perform by learning from a vast amount of training data, parsing the data for correlations and patterns, and afterward employing these patterns to forecast future state. The science of computer algorithms that enhance automatically with experience and represent from the beginning a basic idea in AI research is called machine learning (ML). ML algorithms build a model based on sample data, called *training data* to make predictions or judgments without being explicitly codified. ML algorithms typically comprise three main phases: Learning, testing, and self-adjustment. The learning phase comes from the training data, in which the computer makes a set of rules and reasoning from the data. These workarounds are then matched against a set of test data, which produces a score that quantifies the goodness or accuracy of the models created. The algorithm then employs these test scores to determine whether to generate the final model if the scores are high (good) or to keep training in search of better possibilities.

Deep learning (DL) is a subset of an ML algorithms family that is based on representation learning and artificial neural networks (ANNs). In DL, the word *deep* describes the employment of many layers in the network. DL is a current form of algorithms that has a great number of layers of limited size, allowing for practical application and optimization while preserving theoretical universality under mild conditions.

The simplest way to represent the relationship between DL and ML is to see them as AI, with the original idea of ML at its core, which later developed into DL and is the basis for the widespread use of AI.

DL algorithms process data using various features, which are represented hierarchically through different levels of abstraction. The great potential of DL is depicted from its advances and applications in different domains. By assessing millions of samples, image recognition technology can learn to recognize and feature objects in images.

ML and DL techniques in Smart Agriculture are widely applied to exploit the information acquired by the UAVs.

Allowing for the large amounts of data picked up from agricultural fields, ML can be employed to build up the performance of UAV-based systems for Smart Agriculture, by extracting knowledge for several vegetative parameters. ML is applied for different purposes and in many cases. There are two kinds of learning, supervised or unsupervised algorithms, that use classification, regression, and clustering methods.

Classification techniques are mostly applied for disease detection (Albetis et al., 2018; Kerkech et al., 2018) and weed mapping (Bah et al., 2018; Franco et al., 2018; Gao et al., 2018; Huang et al., 2018; Lambert et al., 2018). Two precise classification methods are the random forest family (Oliveira et al., 2020; Wan et al., 2018; Zheng et al., 2018) and the ANNs algorithm (Bah et al., 2018; Franco et al., 2018; Gao et al., 2018; Huang et al., 2018).

These techniques utilize mainly the intensity, the RGB colors, spectral information, or other features retrieved from the image, and, in some cases, they also consider the information retrieved from the neighborhood of each pixel. The high accuracy of classification algorithms is reached using VIs as features in the model. Usually, ANNs as classification algorithms show an accuracy that may reach 99% for weed mapping (dos Santos Ferreira et al., 2017); but depending on the crop the method accuracy changes (Bah et al., 2018).

Regression algorithms are widely employed in UAV applications for Smart Agriculture for different purposes, such as to estimate spectral VIs by evaluating data acquired from RGB images (Khan et al., 2018), with generally good results; or to analyze the correlation of some VIs with vegetation features such as leaf area index (Fan et al., 2018; Maimaitijiang et al., 2017), biomass index (Fan et al., 2018; Maimaitijiang et al., 2017; Oliveira et al., 2020), and nitrogen (Ballester et al., 2017; Oliveira et al., 2020; Zheng et al., 2018). For evaluating leaf nitrogen content, in a comparison of different regression algorithms, random forests reached the best results among 14 algorithms, with the coefficient of determination (R^2) being up to 0.79 (Zheng et al., 2018). Another use of the regression algorithms is the prediction of crop water status, by mining information from RGB, multispectral, and thermal sensors (Poblete et al., 2017; Quebrajo et al., 2018; Romero et al., 2018). Within this contest, ANNs give generally good results (R^2 up to 0.87 by operating and taking information from some spectral bands).

Another application of ML techniques is the recognition of objects through Object-Based Image Analysis (OBIA) within agricultural images from UAVs (de Castro et al., 2018; Pádua et al., 2022), and their classification for recognition and detection of weeds or species discrimination. With respect to traditional image classification algorithm, which classifies each pixel, OBIA combines small pixels together into vector objects. The UAV images have very high spatial resolution, so pixel-based classifications have become much less effective. This is due to the significant change in the relationship between pixel size and object size with advancements in technology (e.g., UAVs cameras resolution). Therefore, object-oriented classification algorithms are growing in popularity.

DL techniques are also applied to help farmers to solve and facilitate many agriculture-related applications. DL and UAV-based remote sensing technologies have recently been changing the way of approaching agriculture. They have been emerging as powerful new innovative techniques for automatic and accurate crop classification. UAVs allow farmers the ability to survey small and medium-sized farmland and crops using a wide variety of sensors. On the other hand, DL endures decision-making and automatic crop classification.

The match of UAV and DL models should provide snapshot information on crop status, soil type, and disease and pest attack, which has been infeasible in recent decades. Accurate and automatic crop classification employing UAV data and DL techniques is a fundamental task for many Smart Agriculture applications, including crop yield estimation (Ashapure et al., 2020; Yang et al., 2019), crop detection/monitoring (Théau et al., 2020; Tu et al., 2020), water stress monitoring (Zhang et al., 2019), and precise spraying of pesticides and liquid fertilizers (Khan et al., 2021).

The future approach to manage the UAV data (in particular, multispectral data) is based on transformers (Vaswani et al., 2017) method. These approaches have recently been proposed for segmentation using multispectral data (Montán López, 2022; Tao et al. 2022). The effective handling of multispectral data when using transformers is today a relevant research goal for UAV image data.

4.4 PEST CONTROL: STUDY CASES

4.4.1 Foreword

Plant diseases cause appreciable yield losses; therefore, proper identification of disease etiological agents is essential to save time and money by preventing or limiting crop damage (Singh et al., 2018). In the past, diseases were only being recognized using traditional methods; these methods were often subjective, depending strictly on the observer, time-consuming, and inaccurate. Furthermore, human investigation based on visual survey is generally expensive and, in many cases, impractical for a reliable diagnosis in the early stages of infection (Qin et al., 2021).

Therefore, a real technological revolution is needed to solve the problems mentioned before at a reasonable cost and with reduced environmental impact. Many researchers have used high-resolution images collected by satellites, aircraft, and drones to detect plant diseases (Mahlein, 2016; Martinelli et al., 2015). Although satellites and aircrafts can cover large areas in a short period of time, they have poor spatial and temporal image resolution compared to drones and are highly susceptible to weather conditions (Martinelli et al., 2015).

As it has already been highlighted previously in this chapter, drones are currently widely used in many Smart Agriculture applications, and surely many more will be developed. In this section of the chapter, the application of drones to plant disease detection (Veroustraete, 2015) will be specifically treated. One of the main advantages of using drones is the early detection of diseases and thus the ability to reduce the spread of infections to minimize crop damages (Devi & Priya, 2021; Kitpo & Inoue, 2018). It has also been proved how decision support systems (DSSs) using drones can lead to better timely decisions, thus drastically reducing yield and economic losses (Sinha, 2020). Drones can be equipped with digital, multispectral, hyperspectral, thermal, and fluorescence sensors that provide high spatial and temporal resolution of plant diseases. Then, they can help farmers to detect infection even at earlier stages than it would be possible with traditional methods. The acquired data can also be processed in real time to give predictions about the occurrence and spread of infection. This information can then be provided to farmers, enabling them to make appropriate decisions about timely disease management. Therefore, Smart Agriculture can greatly benefit plant disease detection with the use of drone technology due to both its low cost and high flexibility (Shahi et al., 2023; Yamamoto et al., 2023).

Recently, a systematic review of the papers on plant disease detection using drones has been published (Chin et al., 2023). The results of this review show that most studies (58%) used field images and very few papers used images of leaves (14%) or plants (28%). Investigation of small objects, such as leaves and plants, required higher-resolution surveys than visual ones, and thus, the use of high-resolution sensors. The most used algorithm was convolutional neural network (CNN), probably because this algorithm has been the basis of complex DL-based models, and many researchers have approached the mentioned problem as a classification task.

However, effective algorithms are needed to analyze images collected by drones for disease detection. Traditional ML methods have a shortfall due to their reliance on manual feature extraction methods, which are particularly unsuccessful in complex environments such as agricultural ones. More recently DL algorithms put themselves as a promising new alternative for autonomous monitoring of crop diseases. Actually, without any human assistance, they can perform feature extraction, providing farmers with the data they need to monitor and then manage plant diseases (Abbas et al., 2023).

Nevertheless, it must be kept in mind that ML is based exclusively on algorithms. Although it has undoubtedly important advantages, it should be used with caution because it can be susceptible to over-fitting and lack of transparency (Heuvelink & Webster, 2022; Spiegelhalter, 2019). ML is essentially a nonspatial technique, because it is based on regression between dependent (target) and independent (auxiliary) variables but does not account for their geographic position. The problem is not to use *spatial* (geo-referenced) variables (Hengl et al., 2018; Wadoux et al., 2019) but to explicitly introduce a spatial correlation function of observations into the calculation algorithm. ML works very well with large datasets (*big data*) and it is in these situations which is gathering considerable success even in mapping the degree of plant infestation (Shahi et al., 2023). At present, drones can provide sufficient large coverage of radiometric data (big data) to be put in relation to plant health at a very fine spatial resolution.

As pointed out earlier, both ML and traditional spatial statistics are unable to describe the degree of spatial association of an infected plant population because they do not take into account the spatial correlation commonly existing between geo-referenced observations. To analyze both numerical (level of infection) and categorical (infected or not) spatial data, it is necessary to use another type of spatial statistics, known as geostatistics, which was for the first time formalized by Matheron (1963). These analysis and interpolation techniques are explicitly based on spatial dependence functions between observations to improve prediction precision. They have also been utilized to characterize the spatial distribution of insects by entomologists who studied population dynamics (Barrigossi et al., 2001; Castrignanò et al., 2012; Ellsbury et al., 1998).

Actually, there are few papers in the scientific literature in which the spread of plant infection is explicitly related to the location of the monitored plants. This section aims to present some case studies in which the spatial distribution of *Xylella fastidiosa* (Xf) was studied with multivariate geostatistical techniques to improve disease control from the perspective of Smart Agriculture.

Xf is a pathogen that is widespread throughout the world, but since 2013 it has made its entry into southeastern Italy, seriously threatening the renowned production and even the survival of olive trees growing in the Apulia region. The rather aggressive bacterium can affect, besides olive trees, vines, oleanders, and some citrus species, leading to their quick desiccation. This is known as olive rapid decline syndrome (OQDS) when observed on olive trees (Bleve et al., 2016; Saponari et al., 2016). Challenges in the control of this bacterium arise from the possible absence of symptoms over a rather long incubation period of 6–18 months and from the uneven distribution of the bacterium, which makes early identification of the infected plants rather difficult. When desiccation appears macroscopically visible, it is actually too late, and the plant is irrevocably destined to death. Currently, the most accurate method of detecting the presence of bacterial Xf is using laboratory genetic analysis as PCR (polymerase chain reaction) technique (Delong & Zhou, 2015). This is a sophisticated and complex technique that reproduces small segments of DNA multiple times. PCR is more sensitive than ELISA (enzyme-linked immunosorbent assay) technique (Lequin, 2005), which is sensitive to antibodies or antigens of a given pathogen but can produce more false negatives. In any case, both techniques use high-cost analytical instruments and take some days before producing results. Their main limitation is that they can be applied only in the laboratory and not in the field to guide timely operational choices by farmers. It is obvious from what has been said before that there is a need for the use of alternative methods based on spectral analysis of radiation reflected by plants and received by multi- or hyperspectral drone-borne radiometer sensors.

Indeed, the relative intensity of reflected radiation (spectral signature) by the plant is a function of wavelength of incident light and contains much useful information for plant management. More specifically, the shape of this curve depends on photosynthetic activity in the visible region (350–750 nm) and the structure of plant leaves and canopy (size, number of leaf layers, arrangement, etc.) in the NIR region (NIR, 750–1,000 nm).

About the benefits of using drones in the fight against Xylella, all the considerations made earlier apply. Xf indeed poses a serious threat to olive production in Italy that the Ministry of Economic Development (MiSE) has funded a 3.5 million Euros research project called REDoX (Remote Early Detection of Xylella), aimed at detecting and monitoring Xf using multispectral, hyperspectral, and thermal images obtained from aircraft, UAVs, and satellites. The REDoX project is coordinated by the Apulian Aerospace Technology District (DTA).

Below, two case studies are reported concerning the use of multispectral data recorded by a drone-borne radiometer flying over three olive groves with Xylella-infected plants located in the Apulia region (southeastern Italy).

CASE STUDY 1: DATA FUSION APPROACH

Given the aggressiveness and spreading ability of the Xf bacterium, best practices for disease control should focus on early detection of infection, preferably before symptoms of the disease become manifest so that decisions on preventive actions can be made in a timely manner. To achieve this, diagnosis needs to be based on a very fine spatial scale survey, even at within-plant scale, and covering a wide area. For what was stated above, UAV could be an ideal solution to the problem of carrying out very fine-scale monitoring of the olive grove with frequent repetitions over time. However, the use of only one sensor or one type of vegetation health measurement may be of limited value because of the multiple processes and complex interactions that take place in the plant also due to influences of other types of stresses. Recently, ground penetrating radar (GPR), based on the principle of electromagnetic signal reflection, has been used for detection of the internal structure of the trunks, partly related to water content and sap circulation in vessels.

Thus, the idea was to employ multiple sensing sources, using outputs from remote and proximal sensors as auxiliary information, to supplement the sparsely sampled data of a laboratory-measured variable to assess the risk of bacterial infection. This process of fusing spatially heterogeneous data required a (geo)statistically well-defined approach to spatially estimate a specific indicator of plant infection status from the auxiliary information set. A probabilistic approach to assessing the risk of infection was preferred because its estimation is based on variables that are generally subject to great uncertainty due to the highly random nature of disease spread and the inevitable limitation of sampling. In particular, multivariate non-parametric geostatistics has been used, which is a set of (geo)statistical techniques mainly aimed at estimating uncertainty. More specifically, an approach known as probability cokriging proposed by Journel (1989) was used, which allows the calculation of probability of infection occurrence using all available information. To jointly analyze binary data with numerical data, it was necessary to transform the latter into data with uniform distribution varying between 0 and 1.

Geostatistics also makes it possible to solve the crucial problem called *change of support*, which arises when several variables with *different support* need to be analyzed jointly. The complete specification of the term *support* includes the geometrical shape, size, and spatial orientation of the measurement volume. The support can be as small as a point or as large as the entire field. In geostatistics it is possible to solve the problem of *change of support* by resorting to block cokriging.

Summing up, the objective of the paper from Castrignanò et al. (2021a) was to develop a multi-step method of risk assessment of Xf infection using non-parametric multivariate geostatistics, which combined data from remote (radiometric) on-board UAV and proximal sensors with data from visual inspection in the field and diagnostic laboratory tests on the plant, to provide probabilistic maps of Xf infection in olive trees. The interested reader who wants to know more details about the defined approach is referred to the previously mentioned article and associated bibliography.

The study site (Figure 4.3) was a commercial, centenarian, olive grove (cv. Ogliarola Salentina) located at Oria-Brindisi (southeastern Italy) and was chosen because at the time of monitoring (September 2017) only few plants among the 61 showed initial macroscopic symptoms (wilted shoots) of the disease.

The main final outcome of the work was the probability map of disease occurrence (Figure 4.4).

From the observation of Figure 4.4, it is evident that the bacterium through the insect vector had entered from the eastern edge of the field and was probably spreading in the E–W

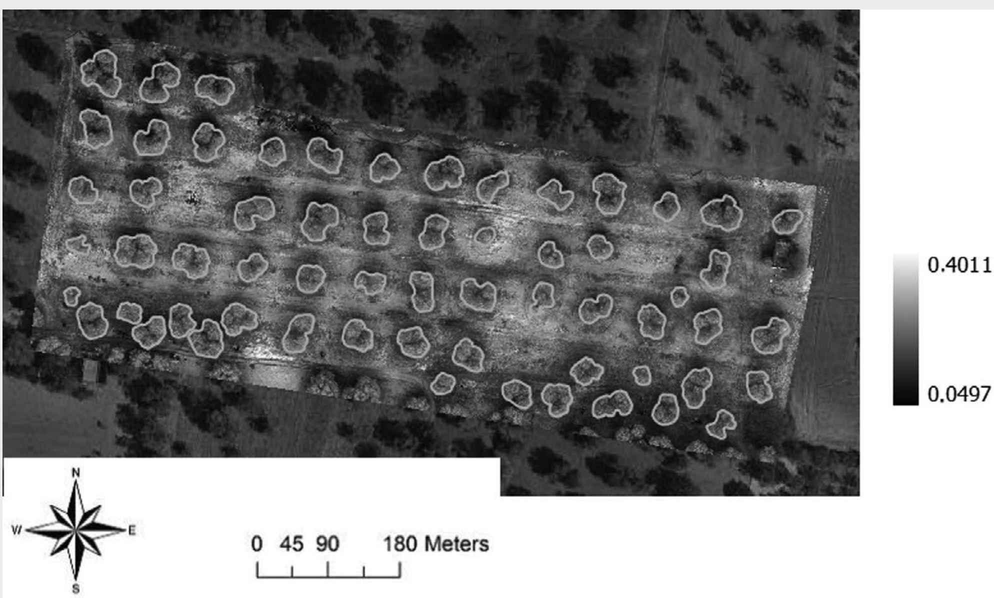

FIGURE 4.3 Study area within an olive grove. Drone red-edge image of the olive tree canopies (red polygons).

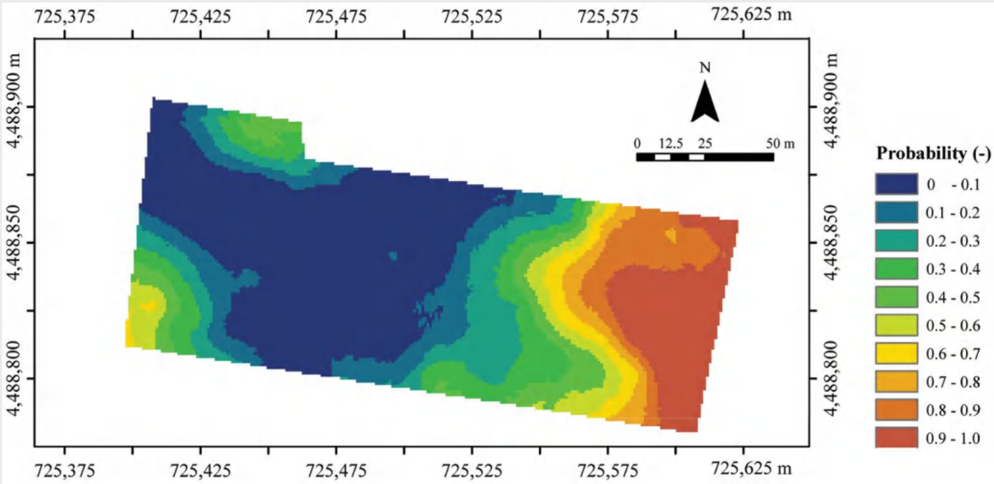

FIGURE 4.4 Probability map of disease occurrence for of *Xylella fastidiosa* subsp. *Pauca* infection.

direction. However, there were two other foci at the NW and SW corners from which the bacterium might also be spreading. Indeed, considering these considerations, it is not easy to predict the spatial and temporal evolution of the spreading process. To follow the evolution of the disease, leaf samples were taken six months later, in March 2018, and analyzed in the laboratory. After only six months, almost all plants were found to be infected, even those located in the central area of the field despite having a low probability of infection at the time of the first survey.

These results highlight the extreme rapidity of disease spread and the need for preventive action with containment measures even on plants that are asymptomatic, or in the very early stages of infection. Moreover, rather weak spatial correlations were found between the infection indicator variable and auxiliary (radiometric, geophysical, from visual inspection, and laboratory analysis) variables. This was probably because of the *change of support* which was centimeter for drone measurements and degraded by three spatial scales for laboratory measurements. Since spatial relationships are a function of the scale of investigation and the infection by Xf is essentially a point event, all measurements should be made at a very fine scale. Obviously, this will entail substantial changes in survey planning in the fight against Xylella, even with considerable expenditure of financial resources, but for this purpose drone recording can bring considerable support.

CASE STUDY 2: EARLY DETECTION OF XF USING A COMBINED APPROACH OF GEOSTATISTICS AND DISCRIMINANT ANALYSIS

Xf is a bacterium that lives and reproduces in the xylem, causing a blockage of water and nutrient transport, which results in a browning of the leaves until a desiccation of the entire aerial portion of the plant. Unfortunately, currently there is no cure, and the only solution to stop the epidemic spread of the disease is the uprooting of infected trees. As repeatedly emphasized, a more efficient disease management strategy would be to identify asymptomatic plants or those infected in the early stages so to reduce the spread of the pathogen. Currently, the most common approach to assessing the degree of infection is the visual rating which, even though relatively easy to learn, has, however, several disadvantages: Subjective, time-consuming, expensive, and destructive if the leaves need to be harvested and then brought to the laboratory. Certainly, it would be desirable to have an automated method that is fast, reliable, relatively inexpensive for pathogen detection, so allowing real-time monitoring and then site- and time-specific management of the infection.

The presence of any pathogen in the plant causes stress that affects chlorophyll functionality and thus its spectral signature, even before it appears macroscopically. Therefore, a drone coupled with a multispectral radiometer can be an efficient scouting tool in this regard. Whenever one wants to analyze the fine-resolution data from drone with other data from different sources, the problem of *change of support* arises unavoidably as already observed in the previous case study. In this second case study, a semi-automatic method of detecting asymptomatic or at the very early stages of Xf infection plants is proposed through an efficient combination of geostatistics with statistical discriminant analysis explicitly taking the *change of support* into account.

The study area concerned three olive groves in Apulia (southeastern Italy): The first olive grove (Field 1) was the same as the previous case study, the second (Field 2) and third (Field 3) regarded two neighboring olive groves in the same province (Brindisi). However, the olive trees in the three fields differed in age (100 years old in Field 1 and 3; 50–60 years old in Field 2), variety, and morphological characteristics of the trunks and canopy. To build the prediction model, it was first necessary to define the variables: Both response variable and predictors. For the former, the level of severity of the infection through visual rating was used. However, in this particular case only two classes were defined: Class 0, corresponding to asymptomatic plants and those with a degree of leaf wilting in each sector of no more than 5%; Class 1, including all other plants. For the predictors, the four-band radiometric data from the drone were employed. The total dataset analyzed concerned the drone data collected from the three olive groves in four successive flights carried out from September 2017 to August 2019. The processing of the multi-source data required the development of an integrated multi-step approach: (1) Extraction of the olive tree canopies from the drone images; (2) degradation of the drone data from centimeter resolution to plant scale. To this end, a multivariate geostatistical technique known as polygon cokriging was applied, which for each variable (band) produced two types of output: The expected value and the standard deviation of the expected value for each canopy; (3) determination of the discriminating statistical model. Indeed, two types of models were constructed: A parametric one and a non-parametric one, which were compared with cross-validation. Although overall results did not change appreciably between the two models (overall accuracy = 0.69), the non-parametric model performed better (Table 4.1). In early detection Class 0, an accuracy of 0.77 was obtained with a probability of misclassification of 0.23.

The results were not indeed the best, nevertheless those obtained with the non-parametric model are undoubtedly encouraging and could be further improved with better calibration of the parameters and the use of a hyperspectral rather than multispectral sensor on board the drone. Effectively, the former makes it possible to choose those fairly narrow-band wavelengths that are particularly discriminating for Xf-infected plants, as already verified by other authors (Zarco-Tejada et al., 2018).

What makes the proposed approach in combination with UAV data particularly useful as a decision-making tool is that, besides the prediction of the most likely class of infection, it also provides its posterior probability, which is a measure of its uncertainty. In decision-making it is quite critical indeed to have such a piece of information which is strongly related to the level of risk associated with a decision based on that prediction. Therefore, in planning management of infection control, priority for action should be given to those plants for which the prediction is most uncertain.

TABLE 4.1
Confusion Matrix for Xylella Severity Classes Using the Non-Parametric Method with the Absolute Counts and the Percentages

Observed Class	Predicted Class		
	0	1	Total
0	1835	538	2373
	77.33%	22.67%	100%
1	730.00	992.00	1722
	42.30%	57.61%	100%
Total	2565.00	1530.00	4095
	62.64%	37.36%	100%
Prior Probability	0.58	0.42	

A DSS aimed at identifying asymptomatic plants or in the early stages of Xylella infection, could easily be designed with the appropriate informatization of the illustrated approach. However, it should be emphasized that, due to the particular techniques used, especially the geostatistical ones, the prediction of the most probable level of infection could not be done in real time, but with the necessary involvement of an operator, and even on a cloud computer. Nevertheless, the system is flexible enough to include other classification techniques, such as ML, that would allow better automation, although it would introduce determinism that might be risky in decision-making.

These promising results seem to encourage the application of UAV technology for early detection of Xylella infection especially when combined with hyperspectral sensors, therefore it is expected that it will soon become a powerful tool for plant disease control by farmers.

4.5 CONCLUSIONS

The proposed Smart Agriculture approach offers considerable appeal for managing plant infection. However, the use of drones for the automatic control of infected plants is still far from being fully accomplished. This is due to various problems that need to be solved: (1) Difficulty in isolating the canopy from the background because of the porous nature of the foliage, particularly in olive trees; (2) some infections produce variations in the spectral signature at very specific wavelengths, for which it would be advantageous to use hyperspectral radiometers; (3) other types of stress may coexist in the plant that produce effects similar to those due to infection.

Although the results with drone-borne radiometers are very promising, undoubtedly better results would be obtained from the joint use (fusion) of not only remote but also proximal sensors of different types.

REFERENCES

Abbas, A., Zhang, Z., Zheng, H., Alami, M. M., Alrefaei, A. F., Abbas, Q., Naqvi, S., Rao, A. H., Mosa, M. J., Abbas, A., Hussain, Q., Hassan, A., & Zhou, M. Z. (2023). Drones in plant disease assessment, efficient monitoring, and detection: A way forward to smart agriculture. *Agronomy*, *13*(6), 1524. https://doi.org/10.3390/agronomy13061524

Abdulridha, J., Ampatzidis, Y., Qureshi, J., & Roberts, P. (2020). Laboratory and UAV-based identification and classification of tomato yellow leaf curl, bacterial spot, and target spot diseases in tomato utilizing hyperspectral imaging and machine learning. *Remote Sensing*, *12*(17), 2732. https://doi.org/10.3390/rs12172732

Acharya, B. S., Bhandari, M., Bandini, F., Pizarro, A., Perks, M., Joshi, D. R., Wang, S., Dogwiler, T., Ray, R. L., Kharel, G., & Sharma, S. (2021). Unmanned aerial vehicles in hydrology and water management: Applications, challenges, and perspectives. *Water Resources Research*, *57*(11). https://doi.org/10.1029/2021WR029925

Ajayi, O. G., Ashi, J., & Guda, B. 2023. Performance evaluation of YOLO v5 model for automatic crop and weed classification on UAV images. *Smart Agricultural Technology*, *5*, 100231. https://doi.org/10.1016/j.atech.2023.100231

Albetis, J., Jacquin, A., Goulard, M., Poilvé, H., Rousseau, J., Clenet, H., Dedieu, G., & Duthoit, S. (2018). On the potentiality of UAV multispectral imagery to detect *Flavescence dorée* and grapevine trunk diseases. *Remote Sensing*, *11*(1), 23. https://doi.org/10.3390/rs11010023

Ampatzidis, Y., & Partel, V. (2019). UAV-based high throughput phenotyping in citrus utilizing multispectral imaging and artificial intelligence. *Remote Sensing*, *11*(4), 410. https://doi.org/10.3390/rs11040410

Ashapure, A., Jung, J., Chang, A., Oh, S., Yeom, J., Maeda, M., Maeda, A., Dube, N., Landivar, J., Hague, S., & Smith, W. (2020). Developing a machine learning based cotton yield estimation framework using multi-temporal UAS data. *ISPRS Journal of Photogrammetry and Remote Sensing*, *169*, 180–194. https://doi.org/10.1016/j.isprsjprs.2020.09.015

Atzori, L., Iera, A., & Morabito, G. (2010). The internet of things: A survey. *Computer Networks*, *54*(15), 2787–2805. https://doi.org/10.1016/j.comnet.2010.05.010

Bah, M., Hafiane, A., & Canals, R. (2018). Deep learning with unsupervised data labeling for weed detection in line crops in UAV images. *Remote Sensing*, *10*(11), 1690. https://doi.org/10.3390/rs10111690

Ballester, C., Hornbuckle, J., Brinkhoff, J., Smith, J., & Quayle, W. (2017). Assessment of in-season cotton nitrogen status and lint yield prediction from unmanned aerial system imagery. *Remote Sensing*, *9*(11), 1149. https://doi.org/10.3390/rs9111149

Ballester, C., Brinkhoff, J., Quayle, W.C., & Hornbuckle, J. (2019). Monitoring the effects of water stress in cotton using the green red vegetation index and red edge ratio. *Remote Sensing*, *11*(7), 873. https://doi.org/10.3390/rs11070873

Barrigossi, J. A. F., Young, L. J., Crawford, C. A. G., Hein, G. L., & Higley, L. G. (2001). Spatial and probability distribution of Mexican bean beetle (*Coleoptera*: *Coccinellidae*) egg mass populations in dry bean. *Environmental Entomology*, *30*(2), 244–253. https://doi.org/10.1603/0046-225X-30.2.244

Belmonte, A., Gadaleta, G., & Castrignanò, A. (2023). Use of geostatistics for multi-scale spatial modeling of *Xylella fastidiosa* subsp. *pauca* (*Xfp*) infection with unmanned aerial vehicle image. *Remote Sensing*, *15*(3), 656. https://doi.org/10.3390/rs15030656

Belmonte, A., Riefolo, C., Lovergine, F., & Castrignanò, A. (2022). Geostatistical modelling of soil spatial variability by fusing drone-based multispectral data, ground-based hyperspectral and sample data with change of support. *Remote Sensing*, *14*(21), 5442. https://doi.org/10.3390/rs14215442

Bleve, G., Marchi, G., Ranaldi, F., Gallo, A., Cimaglia, F., Logrieco, A. F., Mita, G., Ristori, J., & Surico, G. (2016). Molecular characteristics of a strain (Salento-1) of *Xylella fastidiosa* isolated in Apulia (Italy) from an olive plant with the quick decline syndrome. *Phytopathologia Mediterranea*, *55*(1), 139–146.

Castrignanò, A., Belmonte, A., Antelmi, I., Quarto, R., Quarto, F., Shaddad, S., Sion, V., Muolo, M. R., Ranieri, N. A., Gadaleta, G., Bartoccetti, E., Riefolo, C., Ruggieri, S., & Nigro, F. (2021a). A geostatistical fusion approach using UAV data for probabilistic estimation of *Xylella fastidiosa* subsp. *pauca* infection in olive trees. *Science of the Total Environment*, *752*, 141814. https://doi.org/10.1016/j.scitotenv.2020.141814

Castrignanò, A., Belmonte, A., Antelmi, I., Quarto, R., Quarto, F., Shaddad, S., Sion, V., Muolo, M. R., Ranieri, N. A., Gadaleta, G., Bartoccetti, E., Riefolo, C., Ruggieri, S., & Nigro, F. (2021b). Semi-automatic method for early detection of *Xylella fastidiosa* in olive trees using UAV multispectral imagery and geostatistical-discriminant analysis. *Remote Sensing*, *13*(1). https://doi.org/10.3390/rs13010014

Castrignanò, A., Boccaccio, L., Cohen, Y., Nestel, D., Kounatidis, I., Papadopoulos, N. T., De Benedetto, D., & Mavragani-Tsipidou, P. (2012). Spatio-temporal population dynamics and area-wide delineation of *Bactrocera oleae* monitoring zones using multi-variate geostatistics. *Precision Agriculture*, *13*(4), 421–441. https://doi.org/10.1007/s11119-012-9259-4

Chin, R., Catal, C., & Kassahun, A. (2023). Plant disease detection using drones in precision agriculture. *Precision Agriculture*, *24*(5), 1663–1682. https://doi.org/10.1007/s11119-023-10014-y

de Castro, A., Torres-Sánchez, J., Peña, J., Jiménez-Brenes, F., Csillik, O., & López-Granados, F. (2018). An automatic random forest-OBIA algorithm for early weed mapping between and within crop rows using UAV imagery. *Remote Sensing*, *10*(3), 285. https://doi.org/10.3390/rs10020285

Delong, R. K., & Zhou, Q. 2015. Polymerase chain reaction (PCR). In *Introductory experiments on biomolecules and their interactions* (pp. 59–66). Elsevier. https://doi.org/10.1016/B978-0-12-800969-7.00006-2

Devi, A. K., & Priya, R. 2021. Plant disease identification using the unmanned aerial vehicle images. *Turkish Journal of Computer and Mathematics Education*, *12*(10), 2396–2399.

do Amaral, L.R., de Freitas, R.G., Júnior, M.R.B., & da Silva Simões, I.O.P. (2022). Application of drones in agriculture. In D. Marçal de Queiroz, D.S.M. Valente, F. de Assis de Carvalho Pinto, A. Borém, & J.K. Schueller (Eds.), *Digital agriculture*. Springer. https://doi.org/10.1007/978-3-031-14533-9_7

Doelling, D., Helder, D., Schott, J., Stone, T., & Pinto, C. T. (2018). Vicarious calibration and validation. In *Comprehensive remote sensing* (pp. 475–518). Elsevier. https://doi.org/10.1016/B978-0-12-409548-9.10329-X

dos Santos Ferreira, A., Matte Freitas, D., Gonçalves da Silva, G., Pistori, H., & Theophilo Folhes, M. (2017). Weed detection in soybean crops using ConvNets. *Computers and Electronics in Agriculture*, *143*, 314–324. https://doi.org/10.1016/j.compag.2017.10.027

Ellsbury, M. M., Woodson, W. D., Clay, S. A., Malo, D., Schumacher, J., Clay, D. E., & Carlson, C. G. (1998). Geostatistical characterization of the spatial distribution of adult corn rootworm (*Coleoptera*: *Chrysomelidae*) emergence. *Environmental Entomology*, *27*(4), 910–917. https://doi.org/10.1093/ee/27.4.910

Fan, X., Kawamura, K., Xuan, T. D., Yuba, N., Lim, J., Yoshitoshi, R., Minh, T. N., Kurokawa, Y., & Obitsu, T. (2018). Low-cost visible and near-infrared camera on an unmanned aerial vehicle for assessing the herbage biomass and leaf area index in an Italian ryegrass field. *Grassland Science*, *64*(2), 145–150. https://doi.org/10.1111/grs.12184

Franco, C., Guada, C., Rodríguez, J. T., Nielsen, J., Rasmussen, J., Gómez, D., & Montero, J. 2018. Automatic detection of thistle-weeds in cereal crops from aerial RGB images (pp. 441–452). https://doi.org/10.1007/978-3-319-91479-4_37

Gago, J., Douthe, C., Coopman, R. E., Gallego, P. P., Ribas-Carbo, M., Flexas, J., Escalona, J., & Medrano, H. 2015. UAVs challenge to assess water stress for sustainable agriculture. *Agricultural Water Management*, *153*, 9–19. https://doi.org/10.1016/j.agwat.2015.01.020

Gan, H., Lee, W. S., Alchanatis, V., & Abd-Elrahman, A. 2020. Active thermal imaging for immature citrus fruit detection. *Biosystems Engineering*, *198*, 291–303. https://doi.org/10.1016/j.biosystemseng.2020.08.015

Gao, J., Liao, W., Nuyttens, D., Lootens, P., Vangeyte, J., Pižurica, A., He, Y., & Pieters, J. G. 2018. Fusion of pixel and object-based features for weed mapping using unmanned aerial vehicle imagery. *International Journal of Applied Earth Observation and Geoinformation*, *67*, 43–53. https://doi.org/10.1016/j.jag.2017.12.012

Guan, S., Fukami, K., Matsunaka, H., Okami, M., Tanaka, R., Nakano, H., Sakai, T., Nakano, K., Ohdan, H., & Takahashi, K. (2019). Assessing correlation of high-Resolution NDVI with fertilizer application level and yield of rice and wheat crops using small UAVs. *Remote Sensing*, *11*(2), 112. https://doi.org/10.3390/rs11020112

Hariharan, J., Fuller, J., Ampatzidis, Y., Abdulridha, J., & Lerwill, A. (2019). Finite difference analysis and bivariate correlation of hyperspectral data for detecting laurel wilt disease and nutritional deficiency in avocado. *Remote Sensing*, *11*(15), 1748. https://doi.org/10.3390/rs11151748

Hatfield, J. L., & Kitchen, N. R. (2013). The role of precision agriculture in food production and security. In M. Oliver, T. Bishop, & B. P. Marchant (Eds.), *Precision agriculture for sustainability and environmental protection* (Vol. 9780203128, pp. 20–33). Routledge. https://doi.org/10.4324/9780203128329

Hengl, T., Nussbaum, M., Wright, M. N., Heuvelink, G. B. M., & Gräler, B. (2018). Random forest as a generic framework for predictive modeling of spatial and spatio-temporal variables. *PeerJ*, *6*, e5518. https://doi.org/10.7717/peerj.5518

Heuvelink, G. B. M., & Webster, R. (2022. Spatial statistics and soil mapping: A blossoming partnership under pressure. *Spatial Statistics*, *50*, 100639. https://doi.org/10.1016/j.spasta.2022.100639

Huang, H., Deng, J., Lan, Y., Yang, A., Deng, X., & Zhang, L. (2018). A fully convolutional network for weed mapping of unmanned aerial vehicle (UAV) imagery. *PLoS One*, *13*(4), e0196302. https://doi.org/10.1371/journal.pone.0196302

Jiang, J., Wu, Y., Liu, Q., Liu, Y., Cao, Q., Tian, Y., Zhu, Y., Cao, W., & Liu, X. (2023). Developing an efficiency and energy-saving nitrogen management strategy for winter wheat based on the UAV multispectral imagery and machine learning algorithm. *Precision Agriculture*, *24*(5), 2019–2043. https://doi.org/10.1007/s11119-023-10028-6

Journel, A. G. 1989. *Fundamentals of geostatistics in five lessons*. American Geophysical Union. https://doi.org/10.1029/SC008

Kakarla, S. C., Costa, L., Ampatzidis, Y., & Zhang, Z. (2022). Applications of UAVs and machine learning in agriculture (pp. 1–19). https://doi.org/10.1007/978-981-19-2027-1_1

Kerkech, M., Hafiane, A., & Canals, R. (2018). Deep leaning approach with colorimetric spaces and vegetation indices for vine diseases detection in UAV images. *Computers and Electronics in Agriculture*, *155*, 237–243. https://doi.org/10.1016/j.compag.2018.10.006

Kerkech, M., Hafiane, A., & Canals, R. (2020). VddNet: Vine disease detection network based on multispectral images and depth map. *Remote Sensing*, *12*(20), 3305. https://doi.org/10.3390/rs12203305

Khan, S., Tufail, M., Khan, M. T., Khan, Z. A., Iqbal, J., & Wasim, A. (2021). Real-time recognition of spraying area for UAV sprayers using a deep learning approach. *PLoS One*, *16*(4), e0249436. https://doi.org/10.1371/journal.pone.0249436

Khan, Z., Rahimi-Eichi, V., Haefele, S., Garnett, T., & Miklavcic, S. J. (2018). Estimation of vegetation indices for high-throughput phenotyping of wheat using aerial imaging. *Plant Methods*, *14*(1), 20. https://doi.org/10.1186/s13007-018-0287-6

Kitpo, N., & Inoue, M. (2018). Early rice disease detection and position mapping system using drone and IoT architecture. 2018 12th South East Asian Technical University Consortium (SEATUC), 1–5. https://doi.org/10.1109/SEATUC.2018.8788863

Lambert, J. P. T., Hicks, H. L., Childs, D. Z., & Freckleton, R. P. (2018). Evaluating the potential of unmanned aerial systems for mapping weeds at field scales: A case study with *Alopecurus myosuroides*. *Weed Research*, *58*(1), 35–45. https://doi.org/10.1111/wre.12275

Lequin, R. M. (2005). Enzyme immunoassay (EIA)/Enzyme-linked immunosorbent assay (ELISA). *Clinical Chemistry*, *51*(12), 2415–2418. https://doi.org/10.1373/clinchem.2005.051532

Li, D., & Wu, X. (2023). Individualized indicators and estimation methods for tiger nut (*Cyperus esculentus* L.) tubers yield using light multispectral UAV and lightweight CNN structure. *Drones*, *7*(7), 432. https://doi.org/10.3390/drones7070432

Li, F., Barabas, J., Mohan, A., & Raskar, R. (2010). Analysis on errors due to photon noise and quantization process with multiple images. *2010 44th Annual Conference on Information Sciences and Systems (CISS)*, 1–6. https://doi.org/10.1109/CISS.2010.5464908

Mahlein, A.-K. (2016). Plant disease detection by imaging sensors – Parallels and specific demands for precision agriculture and plant phenotyping. *Plant Disease*, *100*(2), 241–251. https://doi.org/10.1094/PDIS-03-15-0340-FE

Maimaitijiang, M., Ghulam, A., Sidike, P., Hartling, S., Maimaitiyiming, M., Peterson, K., Shavers, E., Fishman, J., Peterson, J., Kadam, S., Burken, J., & Fritschi, F. (2017). Unmanned aerial system (UAS)-based phenotyping of soybean using multi-sensor data fusion and extreme learning machine. *ISPRS Journal of Photogrammetry and Remote Sensing*, *134*, 43–58. https://doi.org/10.1016/j.isprsjprs.2017.10.011

Martinelli, F., Scalenghe, R., Davino, S., Panno, S., Scuderi, G., Ruisi, P., Villa, P., Stroppiana, D., Boschetti, M., Goulart, L. R., Davis, C. E., & Dandekar, A. M. (2015). Advanced methods of plant disease detection. A review. *Agronomy for Sustainable Development*, *35*(1), 1–25. https://doi.org/10.1007/s13593-014-0246-1

Matheron, G. (1963). Théorie des droites de correspondance. *Revue de statistique appliquée*, *11*(4), 13–23.

Mazur, P., Gozdowski, D., Stępień, W., & Wójcik-Gront, E. (2023). Does drone data allow the assessment of phosphorus and potassium in soil based on field experiments with winter rye? *Agronomy*, *13*(2), 446. https://doi.org/10.3390/agronomy13020446

Meiyan, S., Qizhou, D., ShuaiPeng, F., Xiaohong, Y., Jinyu, Z., Lei, M., Baoguo, L., & Yuntao, M. (2022). Improved estimation of canopy water status in maize using UAV-based digital and hyperspectral images. *Computers and Electronics in Agriculture*, *197*, 106982. https://doi.org/10.1016/j.compag.2022.106982

Montán López, J. A. (2022). The use of multispectral images and deep learning models for agriculture: The application on Agave [Instituto Tecnológico y de Estudios Superiores de Monterrey]. https://hdl.handle.net/11285/650159

Moriya, É. A. S., Imai, N. N., Tommaselli, A. M. G., Berveglieri, A., Santos, G. H., Soares, M. A., Marino, M., & Reis, T. T. (2021). Detection and mapping of trees infected with citrus gummosis using UAV hyperspectral data. *Computers and Electronics in Agriculture*, *188*, 106298. https://doi.org/10.1016/j.compag.2021.106298

Mulla, D. J. (2013). Twenty five years of remote sensing in precision agriculture: Key advances and remaining knowledge gaps. *Biosystems Engineering*, *114*(4), 358–371. https://doi.org/10.1016/j.biosystemseng.2012.08.009

Oliveira, R. A., Näsi, R., Niemeläinen, O., Nyholm, L., Alhonoja, K., Kaivosoja, J., Jauhiainen, L., Viljanen, N., Nezami, S., Markelin, L., Hakala, T., & Honkavaara, E. (2020). Machine learning estimators for the quantity and quality of grass swards used for silage production using drone-based imaging spectrometry and photogrammetry. *Remote Sensing of Environment*, *246*, 111830. https://doi.org/10.1016/j.rse.2020.111830

Pádua, L., Matese, A., Di Gennaro, S. F., Morais, R., Peres, E., & Sousa, J. J. (2022). Vineyard classification using OBIA on UAV-based RGB and multispectral data: A case study in different wine regions. *Computers and Electronics in Agriculture*, *196*, 106905. https://doi.org/10.1016/j.compag.2022.106905

Poblete, T., Ortega-Farías, S., Moreno, M., & Bardeen, M. (2017). Artificial neural network to predict vine water status spatial variability using multispectral information obtained from an unmanned aerial vehicle (UAV). *Sensors*, *17*(11), 2488. https://doi.org/10.3390/s17112488

Qi, S., Wang, F., & Jing, L. (2018). Unmanned aircraft system pilot/operator qualification requirements and training study. *MATEC Web of Conferences*, *179*, 03006. https://doi.org/10.1051/matecconf/201817903006

Qin, J., Wang, B., Wu, Y., Lu, Q., & Zhu, H. (2021). Identifying pine wood nematode disease using UAV images and deep learning algorithms. *Remote Sensing*, *13*(2), 162. https://doi.org/10.3390/rs13020162

Quebrajo, L., Perez-Ruiz, M., Pérez-Urrestarazu, L., Martínez, G., & Egea, G. (2018). Linking thermal imaging and soil remote sensing to enhance irrigation management of sugar beet. *Biosystems Engineering*, *165*, 77–87. https://doi.org/10.1016/j.biosystemseng.2017.08.013

Rasmussen, J., Nielsen, J., Garcia-Ruiz, F., Christensen, S., & Streibig, J. C. (2013). Potential uses of small unmanned aircraft systems (UAS) in weed research. *Weed Research*, *53*(4), 242–248. https://doi.org/10.1111/wre.12026

Romano, N., Szabó, B., Belmonte, A., Castrignanò, A., Dor, E., Ben, Francos, N., & Nasta, P. (2023). Mapping soil properties for unmanned aerial system–based environmental monitoring. In *Unmanned aerial systems for monitoring soil, vegetation, and riverine environments* (pp. 155–178). Elsevier. https://doi.org/10.1016/B978-0-323-85283-8.00010-2

Romero, M., Luo, Y., Su, B., & Fuentes, S. (2018). Vineyard water status estimation using multispectral imagery from an UAV platform and machine learning algorithms for irrigation scheduling management. *Computers and Electronics in Agriculture*, *147*, 109–117. https://doi.org/10.1016/j.compag.2018.02.013

Sankaran, S., Khot, L. R., & Carter, A. H. (2015). Field-based crop phenotyping: Multispectral aerial imaging for evaluation of winter wheat emergence and spring stand. *Computers and Electronics in Agriculture*, *118*, 372–379. https://doi.org/10.1016/j.compag.2015.09.001

Sapkota, R., Stenger, J., Ostlie, M., & Flores, P. (2023). Towards reducing chemical usage for weed control in agriculture using UAS imagery analysis and computer vision techniques. *Scientific Reports*, *13*(1), 6548. https://doi.org/10.1038/s41598-023-33042-0

Saponari, M., Boscia, D., Altamura, G., D'Attoma, G., Cavalieri, V., Zicca, S., Morelli, M., Tavano, D., Loconsole, G., Susca, L., Potere, O., Savino, V., Martelli, G., Palmisano, P., Dongiovanni, F., Saponari, C., Fumarola, A., & Carolo, G., M. Di. (2016). Pilot project on *Xylella fastidiosa* to reduce risk assessment uncertainties. *EFSA Supporting Publications*, *13*(3). https://doi.org/10.2903/sp.efsa.2016.EN-1013

Saravia, D., Valqui-Valqui, L., Salazar, W., Quille-Mamani, J., Barboza, E., Porras-Jorge, R., Injante, P., & Arbizu, C. I. (2023). Yield prediction of four bean (*Phaseolus vulgaris*) cultivars using vegetation indices based on multispectral images from UAV in an arid zone of Peru. *Drones*, *7*(5), 325. https://doi.org/10.3390/drones7050325

Shahi, T. B., Xu, C.-Y., Neupane, A., & Guo, W. (2023). Recent advances in crop disease detection using UAV and deep learning techniques. *Remote Sensing*, *15*(9), 2450. https://doi.org/10.3390/rs15092450

Singh, A. K., Ganapathysubramanian, B., Sarkar, S., & Singh, A. (2018). Deep learning for plant stress phenotyping: Trends and future perspectives. *Trends in Plant Science*, *23*(10), 883–898. https://doi.org/10.1016/j.tplants.2018.07.004

Sinha, J. P. (2020). Aerial robot for smart farming and enhancing farmers' net benefit. *The Indian Journal of Agricultural Sciences*, *90*(2), 258–267. https://doi.org/10.56093/ijas.v90i2.98997

Spiegelhalter, D. (2019). *The art of statistics: How to learn from data*. Pelican.

Swarup, A., Lee, W. S., Peres, N., & Fraisse, C. (2020). Strawberry plant wetness detection using color and thermal imaging. *Journal of Biosystems Engineering*, *45*(4), 409–421. https://doi.org/10.1007/s42853-020-00080-9

Tao, C., Meng, Y., Li, J., Yang, B., Hu, F., Li, Y., Cui, C., & Zhang, W. (2022). MSNet: Multispectral semantic segmentation network for remote sensing images. *GIScience & Remote Sensing*, *59*(1), 1177–1198. https://doi.org/10.1080/15481603.2022.2101728

Théau, J., Gavelle, E., & Ménard, P. (2020). Crop scouting using UAV imagery: A case study for potatoes. *Journal of Unmanned Vehicle Systems*, *8*(2), 99–118. https://doi.org/10.1139/juvs-2019-0009

Torres-Sánchez, J., de Castro, A. I., Peña, J. M., Jiménez-Brenes, F. M., Arquero, O., Lovera, M., & López-Granados, F. (2018). Mapping the 3D structure of almond trees using UAV acquired photogrammetric point clouds and object-based image analysis. *Biosystems Engineering*, *176*, 172–184. https://doi.org/10.1016/j.biosystemseng.2018.10.018

Tu, Y.-H., Phinn, S., Johansen, K., Robson, A., & Wu, D. (2020. Optimising drone flight planning for measuring horticultural tree crop structure. *ISPRS Journal of Photogrammetry and Remote Sensing*, *160*, 83–96. https://doi.org/10.1016/j.isprsjprs.2019.12.006

Turner, D., Lucieer, A., Malenovský, Z., King, D. H., & Robinson, S. A. (2014). Spatial co-registration of ultra-high resolution visible, multispectral and thermal images acquired with a micro-UAV over Antarctic moss beds. *Remote Sensing*, *6*(5), 4003–4024. https://doi.org/10.3390/rs6054003

Muir, M. A. K. (2015). Global Sustainable Development Report 2015. Department of Economic and Social Affairs. United Nations. https://www.researchgate.net/publication/305943226_Global_Sustainable_Development_Report_2015

van der Merwe, D., Burchfield, D. R., Witt, T. D., Price, K. P., & Sharda, A. (2020). Chapter one – Drones in agriculture.. D. L. Sparks, Ed. Advances in Agronomy. Academic Press, Vol. 162, pp. 1–30). https://doi.org/10.1016/bs.agron.2020.03.001

Vaswani, A., Shazeer, N., Parmar, N., Uszkoreit, J., Jones, L., Gomez, A. N., Kaiser, L., & Polosukhin, I. (2017). Attention Is All You Need. In Proceedings of the 31st International Conference on Neural Information Processing Systems (NIPS'17). Curran Associates Inc., Red Hook, NY, USA, 6000–6010. https://doi.org/10.48550/arXiv.1706.03762

Veroustraete, F. 2015. The rise of the drones in agriculture. *EC Agriculture*, *2*.

Wadoux, A. M. J.-C., Padarian, J., & Minasny, B. (2019). Multi-source data integration for soil mapping using deep learning. *SOIL*, *5*(1), 107–119. https://doi.org/10.5194/soil-5-107-2019

Wahab, I., Hall, O., & Jirström, M. (2018). Remote sensing of yields: Application of UAV imagery-derived NDVI for estimating maize vigor and yields in complex farming systems in sub-Saharan Africa. *Drones*, *2*(3), 28. https://doi.org/10.3390/drones2030028

Wan, L., Li, Y., Cen, H., Zhu, J., Yin, W., Wu, W., Zhu, H., Sun, D., Zhou, W., & He, Y. (2018). Combining UAV-based vegetation indices and image classification to estimate flower number in oilseed rape. *Remote Sensing*, *10*(9), 1484. https://doi.org/10.3390/rs10091484

Wang, A., Qiu, T., & Shao, L. (2009). A simple method of radial distortion correction with centre of distortion estimation. *Journal of Mathematical Imaging and Vision*, *35*(3), 165–172. https://doi.org/10.1007/s10851-009-0162-1

Wang, Y., Feng, C., Ma, Y., Chen, X., Lu, B., Song, Y., Zhang, Z., & Zhang, R. (2023). Estimation of nitrogen concentration in walnut canopies in Southern Xinjiang based on UAV multispectral images. *Agronomy*, *13*(6), 1604. https://doi.org/10.3390/agronomy13061604

Westoby, M. J., Brasington, J., Glasser, N. F., Hambrey, M. J., & Reynolds, J. M. (2012). 'Structure-from-Motion' photogrammetry: A low-cost, effective tool for geoscience applications. *Geomorphology*, *179*, 300–314. https://doi.org/10.1016/j.geomorph.2012.08.021

Xue, J., & Su, B. (2017). Significant remote sensing vegetation indices: A review of developments and applications. *Journal of Sensors*, *2017*, 1–17. https://doi.org/10.1155/2017/1353691

Yamamoto, S., Nomoto, S., Hashimoto, N., Maki, M., Hongo, C., Shiraiwa, T., & Homma, K. (2023). Monitoring spatial and time-series variations in red crown rot damage of soybean in farmer fields based on UAV remote sensing. *Plant Production Science*, *26*(1), 36–47. https://doi.org/10.1080/1343943X.2023.2178469

Yang, Q., Shi, L., Han, J., Zha, Y., & Zhu, P. (2019). Deep convolutional neural networks for rice grain yield estimation at the ripening stage using UAV-based remotely sensed images. *Field Crops Research*, *235*, 142–153. https://doi.org/10.1016/j.fcr.2019.02.022

Yu, F., Bai, J., Jin, Z., Guo, Z., Yang, J., & Chen, C. (2023). Combining the critical nitrogen concentration and machine learning algorithms to estimate nitrogen deficiency in rice from UAV hyperspectral data. *Journal of Integrative Agriculture*, *22*(4), 1216–1229. https://doi.org/10.1016/j.jia.2022.12.007

Zarco-Tejada, P. J., Camino, C., Beck, P. S. A., Calderon, R., Hornero, A., Hernández-Clemente, R., Kattenborn, T., Montes-Borrego, M., Susca, L., Morelli, M., Gonzalez-Dugo, V., North, P. R. J., Landa, B. B., Boscia, D., Saponari, M., & Navas-Cortes, J. A. (2018). Previsual symptoms of *Xylella fastidiosa* infection revealed in spectral plant-trait alterations. *Nature Plants*, *4*(7), 432–439. https://doi.org/10.1038/s41477-018-0189-7

Zhang, L., Zhang, H., Niu, Y., & Han, W. (2019). Mapping maize water stress based on UAV multispectral remote sensing. *Remote Sensing*, *11*(6), 605. https://doi.org/10.3390/rs11060605

Zhang, Y., Xia, C., Zhang, X., Cheng, X., Feng, G., Wang, Y., & Gao, Q. (2021). Estimating the maize biomass by crop height and narrowband vegetation indices derived from UAV-based hyperspectral images. *Ecological Indicators*, *129*, 107985. https://doi.org/10.1016/j.ecolind.2021.107985

Zheng, H., Li, W., Jiang, J., Liu, Y., Cheng, T., Tian, Y., Zhu, Y., Cao, W., Zhang, Y., & Yao, X. (2018). A comparative assessment of different modeling algorithms for estimating leaf nitrogen content in winter wheat using multispectral images from an unmanned aerial vehicle. *Remote Sensing*, *10*(12), 2026. https://doi.org/10.3390/rs10122026

Zheng, Y., Lin, S., Kambhamettu, C., Jingyi Yu, & Sing Bing Kang. (2009). Single-image vignetting correction. *IEEE Transactions on Pattern Analysis and Machine Intelligence*, *31*(12), 2243–2256. https://doi.org/10.1109/TPAMI.2008.263

Ziliani, M., Parkes, S., Hoteit, I., & McCabe, M. (2018). Intra-season crop height variability at commercial farm scales using a fixed-wing UAV. *Remote Sensing*, *10*(12), 2007. https://doi.org/10.3390/rs10122007

5 UAV Remote Sensing for Fertilization Rating in Olive Groves

Eliseo Roma and Pietro Catania

5.1 INTRODUCTION

5.1.1 Olive Grove

According to FAO estimates, the world population will exceed 9.6 billion by 2050 (Godfray et al., 2010). Therefore, there will need to be a change in agricultural systems that will have to increase production efficiency by increasing production and minimizing inputs used; increasing environmental and economic sustainability (Tilman et al., 2011). These changes are leading to a radical change in cultivation techniques involving more agronomic and plot management practices.

Olive trees are mainly cultivated in Europe (61% of the world's surface area), particularly in the Mediterranean area from where it originates (FAOSTAT, 2022), followed by the continents of Africa (20%) and Asia (15%). It is a dual-purpose species as it is cultivated for the production of table olives and for oil, although the latter covers more than 80% of production. The world's largest producers are Italy, Spain, and Greece. However, new continents have also started massive cultivation in recent years, given the market demand for EVOO (extra virgin olive oil). The cultivation systems, varieties, and agronomic techniques adopted so far vary greatly depending on the region. In fact, in Mediterranean areas there is still a high presence of plots cultivated with traditional systems characterized by wide planting distances that are not always regular (Di Vaio et al., 2012). However, as production requirements tend to be ever greater, new intensive and super-intensive cultivation systems are being developed, which are capable of reaching densities of more than 1000 plants per hectare (Connor et al., 2014). These new systems make it possible to mechanize manual operations entirely, cutting costs considerably, but at the same time require efficient management of agronomic techniques and higher inputs (Figure 5.1).

5.1.2 Spatial Variability and Smart Agriculture

The variability in olive groves is determined by the growing conditions of each plant. Those conditions are linked to the soil, weather trends, and human input. Therefore, it is not easy to understand how all these factors spatially vary and how their modifications can determine a change in the vegetative activity and plant production. However, there are various technologies and sensors that can directly or indirectly detect many of the main parameters that influence plants. For olive groves, several studies show that knowledge of soil variability and in particular organic matter (SO), soil nitrogen (TN) and partially electrical conductivity (EC) can explain the crop variability found (Gargouri et al., 2006; Huang et al., 2006; Roma et al., 2023). Instead, in order to know the conditions of vegetative growth and consequently, productivity, scientific research has focused on the identification of biophysical (Caruso et al., 2019a; Torres-Sánchez et al., 2015), spectral (Catania et al., 2023), and thermal (Berni et al., 2009) parameters. The most important biophysical parameters are canopy height (CH), canopy area (CA), canopy volume (CV), and, in rare cases, perimeter and canopy porosity.

 DOI: 10.1201/9781003510598-5

	Traditional < 200 plants/ha	Intensive 250-500 plants/ha	Super intensive > 500 plants/ha
Cost	***	**	**
Yield	*	**	***
Mechanization	*	*	***
Inputs	*	**	***
Profitability	*	**	***

FIGURE 5.1 Schematic representation of costs, yield, level of mechanization, and number of inputs used on average in the three planting systems [* low; ** medium; *** high].

Instead, spectral parameters are based on the behavior observation of particular reflection bands in the spectrum and combining them to calculate vegetation indices (VI, Lee et al., 2010). Vegetation index can be categorized in different ways and there are several of them (Xue & Su, 2017). The most commonly used vegetation index in olive groves is the normalized difference vegetation index (NDVI, Rouse et al., 1974) followed by modified soil-adjusted vegetation index (MSAVI, Qi et al., 1994), and also some simple band ratios. The NDVI uses the reflectance in the red and infrared bands of crops and allows a good indication of biomass, nutritional, productive, and physiological status, as it depends on the chlorophyll content and the leaf area index (LAI), expressing a value ranging from 0 to 1. Other indices allow the detailed evaluation of certain pigments such as chlorophyll in order to understand the health or even identify the phytosanitary status of the crop. Unfortunately, there are no standard ranges to determine the true condition of plants due to the diverse factors involved. From the experience of the authors, healthy olive trees, compared to other plants, due to the presence of small, leathery leaves and a not very high LAI, the NDVI values have hardly higher average values per plant of 0.8–0.9 and the average is around 0.7. These values are to be considered purely indicative as they may vary depending on age, cultivar, cultivation techniques, etc.

Finally, the thermal parameters are related to the identification of the canopy temperature, but more important is the calculation of the stress indices. In the latter case, the most important stress index and widely used in olive growing is the crop water stress index (CWSI, Idso, 1982; Jackson et al., 1981).

Soil, crop, and climate variables measured using the various sensors and technologies are used to create the base maps describing the differences in spatial conditions. Then, by integrating and interconnecting this information, it is possible to obtain prescription maps for variable rate applications (VRA). Site-specific management of variability yields greater economic and environmental benefits than uniform plot management. The scale of applicability of VRA can vary depending on the agronomic context; the grove can be managed by homogeneous zones, by sectors, or even by individual plants. Several studies have been able to affirm the savings achieved in the use of fertilizers and pesticides (Campos et al., 2020). The VRA application regarding fertilization leads to a reduction in fertilizer use of around 30%, resulting in increased sustainability (Roma et al., 2023; Van Evert et al., 2017).

5.1.3 Platform of Remote Sensing to Detect the Variability

Precision agriculture makes use of technologies capable of acquiring geo-referenced information from different platforms in order to obtain different data that will be processed and used for site-specific management of the agro-ecosystem. Acquisition platforms are able to capture information of spatial and temporal variability and are classified according to their distance from the target object as: remote platforms, proximal platforms and ground platforms (Roma & Catania, 2022). Between them, there are great differences in terms of cost, usability, practicality, operating techniques, etc. Within the remote platforms we find: Satellites (Gómez et al., 2011), aircraft (Senay et al., 1998), and drones (Caruso et al., 2019b), with different modes of operation that determine their uses in agriculture.

It is clear that UAV (unmanned aerial vehicles) systems are a monitoring tool that lends itself well to future developments in precision agriculture, whose future directions (decision support systems (DSS), crop development models, etc.) require high-precision and accurate information to improve site-specific management.

5.1.4 Drones: Classification and General Applications

In order to overcome certain limitations associated with the use of satellites and aircraft, such as low versatility and reduced spatial resolution, UAVs, or more commonly known as Drones, have become increasingly popular and used in the last decade.

Such platforms have numerous advantages due to their wide operational flexibility. In fact, they can be equipped with different types of sensors, making these platforms suitable for a multitude of surveys. Their most evident benefits are associated with the speed of data acquisition and the ability to fly below 120 m, which allows for high geometric resolution and consequently very detailed information. Recent innovations in such platforms have significantly reduced the costs of purchase and use. Furthermore, the temporal resolution allows surveys to be carried out at certain times related to agronomic conditions; however, this advantage can be negated by weather conditions.

UAVs need to address certain technical limitations, such as battery efficiency, communication distance, and payload. There are different models on the market that can be classified according to the flight mode adopted (Figure 5.2). In this case, we distinguish two macro-categories, namely fixed-wing and propeller-driven. Fixed-wing UAVs exploit aerodynamic thrust and lift force and are mainly used for spraying and photography over a wide radius in orographically homogeneous areas. The macro-category of rotary-wing UAVs can be subdivided into helicopters and multi-rotors. The

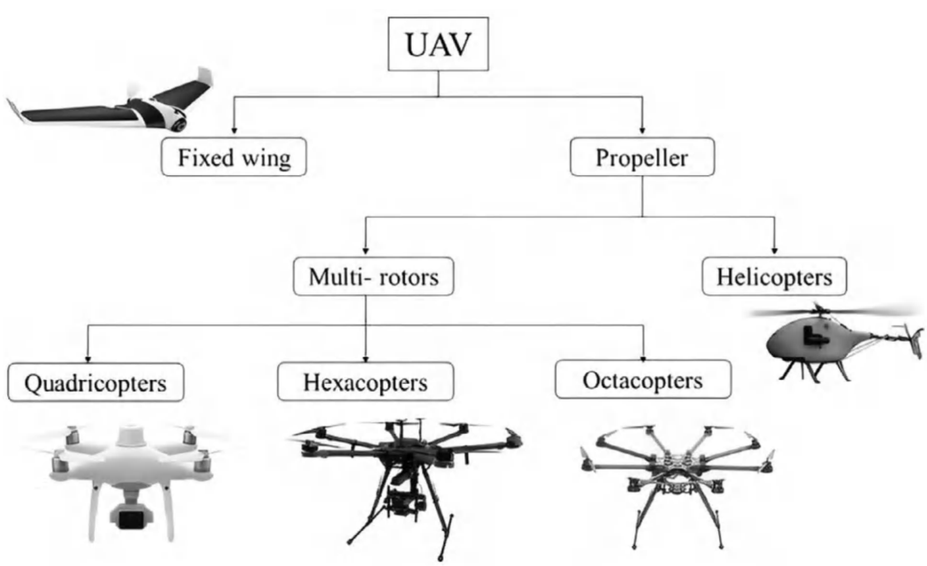

FIGURE 5.2 Overview of drone typologies classified according to wing configuration.

helicopter type is characterized by a large propeller on top of the aircraft. However, multi-rotor models are characterized by several rotors that allow movement. Depending on the different number of rotors, they are distinguished into: quadricopters, hexacopters, and octocopters. These categories of drones are more widely used due to their versatility in fragmented areas and uneven terrain. This is due to a vertical landing and take-off mode and an easy variation in altitude according to terrain profile.

At construction level, the main components that characterize UAVs are as follows: frame, propellers, brushless motors, central management unit (control unit or flight control) of the flight, ECS (electronic speed control), IMU (inertial measurement unit) systems, which include accelerometers, gyroscopes, compass, magnetometer and altimeter, the PMU (power management unit), the flight management system (navi control), a GNSS (global navigation satellite system) module, the communication systems (generally radio) between the platform and the radio control and finally the payload composed of gimbal and sensors.

Since drones are equipped with a GNSS system, they are able to capture geo-referenced frames containing geometric, spectral, and thermal information through various sensors. These sensors can be CMOS (complementary metal oxide semiconductor) or CCD (charge-coupled device) type and influence the final pixel size and the effect of noise in the images. Depending on their construction technology, sensors are classified as active and/or passive if they make use of external illumination sources or not. Another classification is based on the type of wavelengths acquired and their amplitude.

In precision agriculture, the main types of sensors used for UAV monitoring activities are RGB, multispectral, hyperspectral, thermal, and LiDAR (light detection and ranging) cameras. RGB cameras are mainly used for topographic land surveys, monitoring vegetation growth, acquiring biophysical information of the canopy (diameter, area, and volume; Figure 3a); it is also possible to detect the evolution of phenological phases and quantify the yield of certain crops.

Multispectral sensors generally use a few bands (3–10) with a high amplitude (15–70 nm) and allow the quantification of the ecophysiological state of crops through the calculation of VI, such as NDVI. Hyperspectral technology captures images capable of acquiring a high number of bands (1000–2500), with a low amplitude (1–5 nm) up to the point of describing the entire spectral signature of the target object (Figure 5.3). However, their use in agriculture is still limited due to their high cost and processing difficulty.

Another category of sensors are thermal sensors, which measure the thermal output of vegetation. This type of sensor is mainly used for water resource management. Finally, there are LiDAR sensors, known as one of the most accurate methods for acquiring geometric data. LiDAR, RGB, and multispectral cameras, by means of photogrammetric reconstruction, allow the acquisition of dense point clouds for the estimation of CV and reliable crop surface models (CSM).

5.1.5 Advantages and Disadvantages of Drones

In all countries, the use of UAV platforms is regulated by law and the regulations governing their use can vary greatly. Some data concerning the European Union (EU) are given here, given the importance of olive growing in these areas. As of 31 December 2020, implementing regulation (EU) No. 947/2019 on rules and procedures for the operation of unmanned aircraft became applicable; from which each member state has produced its own regulations depending on the authority responsible for the use of airspace. In general, according to these regulations in agriculture, a special license is required for the use of such platforms called A1–A3, which allows the operation of a UAS (Unmanned Aerial System) with an operational mass at take-off between 250 g and 25 kg, in VLOS (visual line of sight) conditions, in areas where reasonably no persons are involved and at least 150 m from residential, commercial, industrial or recreational areas.

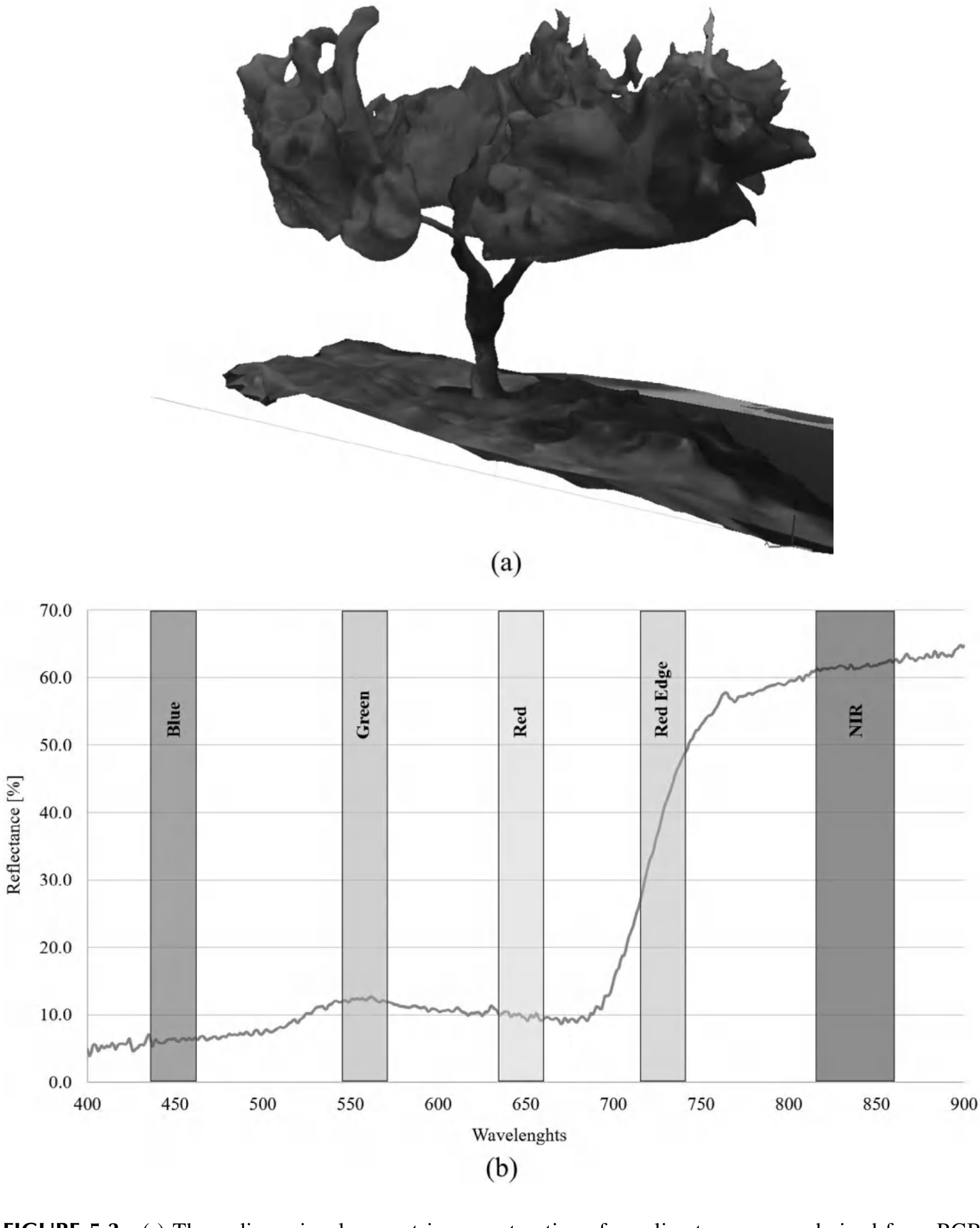

FIGURE 5.3 (a) Three-dimensional geometric reconstruction of an olive tree canopy derived from RGB imagery; (b) canopy reflectance signature across the VIS–NIR spectral range.

5.1.6 Process to Acquire the Data: Main Parameters to Set a Flights

Regardless of the type of drone, it is necessary to know how the different flight variables can affect the final data acquisition and the entire processing process. The process of drone image acquisition starts with good flight planning. Flights can be performed by setting different parameters that can affect the entire data construction and evaluation process. There are no standard settings that can be adopted, so different settings are found in literature. The settings, however, depend mainly on the quality of the sensors that are carried by the drone. Naturally, high-quality sensors allow more accurate data to be obtained under the same conditions and can facilitate certain operational choices. Weather conditions can also greatly influence the choice of a few parameters such as the drone's forward speed, image overlap, and flight height.

Flight planning software is sold associated with the drone, but different software can be used.

Whichever software is used, the main parameters must be set, such as area to be surveyed, flight mode, image acquisition mode, flight altitude, image overlay, camera inclination, drone travel speed, and flight path orientation. Identifying the area to be surveyed is the first step in order to properly design the flight plan. Regardless of the size of the area to be covered, the edges must be increased in order to obtain an adequate reconstruction even in the outer parts. The flight mode refers to the possibility of flying in automatic or manual mode and whether it is possible to fly at a constant altitude or following contour lines (Figure 5.4). The best combination of flight is the automatic mode with the mode that follows the morphology of the terrain. This allows the overlapping of images with the same pixel size to be perfectly maintained. In agriculture, given the extensions, manual flight is never practiced, except in rare cases, while it is not always possible to perform the flight that follows orography.

The image capture mode means at what time the drone should proceed with the capture. Generally, there are three modes: equal time interval, equal distance interval, and hover capture. In some higher-cost drones, there may also be other modes that are little used. The first two modes are very similar and provide significant battery savings. Both modes cause the drone to shoot every certain time or when a precise distance is reached. Therefore, in these modes, the time between a shot and the drone's forward speed must be set. On the other hand, the third mode should be used when there is a lot of wind and/or low image overlap, but you still want to obtain a good reconstruction. The most important parameter that can significantly influence all other parameters and the obtaining of an excellent photogrammetric product is the flight height. The height of flight depends on various factors including level of detail, legislation, and quality of the object to be evaluated. The level of detail is expressed with the ground surface distance (GSD) and tends to be minimized; the range usually varies from 2 to 7 cm. However, its reduction may invalidate the data due to high noise. For small objects, the size of the GSD must be at least 1/3 of that of the object to ensure the presence of at least one pure pixel. High-resolution sensors are able to generate pixels of a few centimeters. The last condition allows for a very good level of detail with the lowest battery consumption. At the legislative level, in the EU, the limit imposed is 120 m above the starting height. In the olive tree, given the low crown densities in all types of planting, the signal-to-noise ratio is significantly lowered. In fact, an increasingly common practice is to raise the flight height, which generally remains between 70 and 100 m. In this way, the level of detail decreases but the discretization of the acquired objects succeeds in improving the final quality of the data.

The overlapping of the images is intended in the lateral and frontal parts. Smaller values of overlap significantly decrease flight times and thus battery consumption, while larger values allow better photogrammetric reconstruction. However, in the olive grove there is no standard reference value but conventionally one should stay between 60% and 70%. Several papers have pointed out that a non-perfectly orthogonal camera tilt can allow for a better geometric reconstruction of the plants. However, the effects of this parameter from a spectral point of view have not been well investigated.

The forward speed of the drone depends on the weather conditions and the mode of image acquisition. In the case of high winds, it is preferable to enter the hover capture mode, so the forward speed is used for the drone to move between shooting points. In the case of high overlap and low altitude, this distance can be very low, so it is preferable to adopt low speeds. In contrast, if one of the other two modes is adopted, speed becomes a determining factor. Generally higher speeds result in shorter flight time and greater stability in windy conditions. Unfortunately, a high value can cause a high distortion of the acquired images, which can be compensated for with a higher altitude and image overlap.

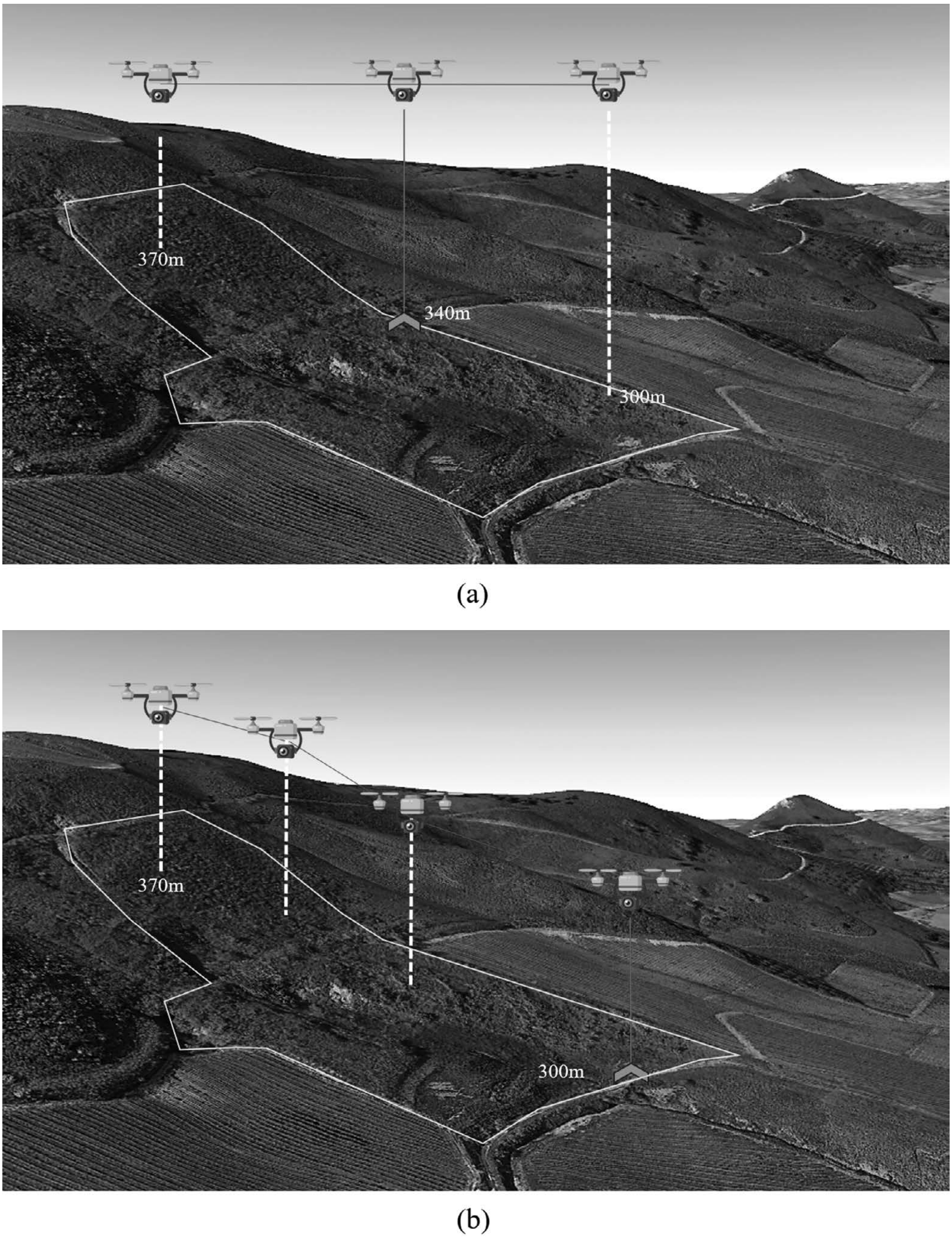

FIGURE 5.4 Representation of two flight-mode configurations for drone-based multispectral surveys: (a) flight conducted at a constant altitude; (b) flight following terrain contour lines.

The direction of the flight paths is generally entered automatically on many software packages to determine the path with the least expenditure of energy. However, in the study by Catania et al. (2022), it was observed that in row crops, such as SHD (Super High Density) plants, a perpendicular configuration of the routes respect to the rows is preferable to a parallel configuration.

Once the flight is scheduled, there are certain operations to be performed in the field to improve the quality of the acquisition process. Among the main operations to be performed at

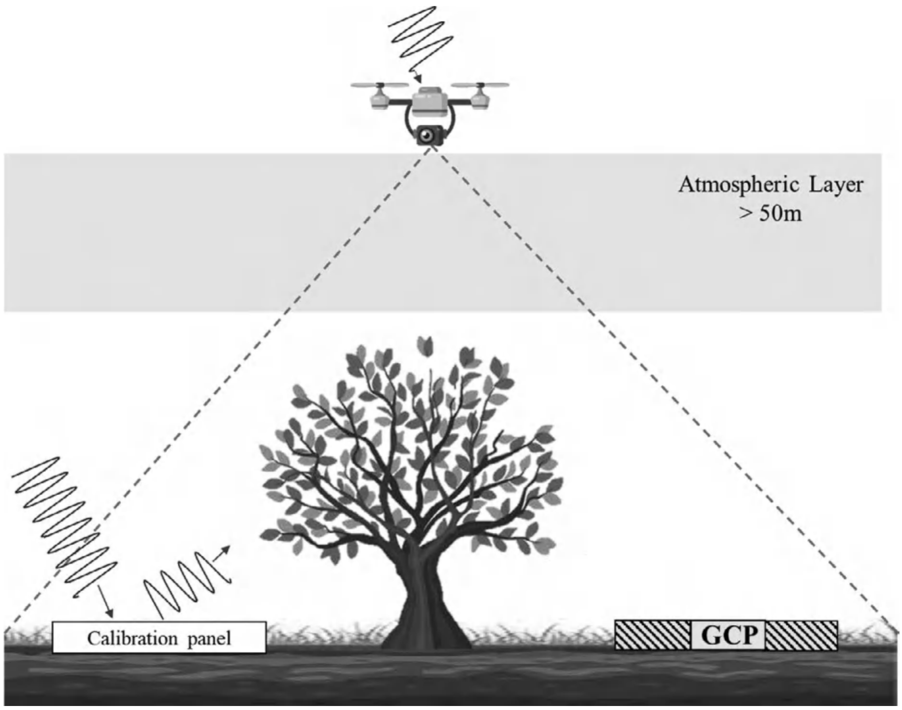

FIGURE 5.5 Schematic representation of the calibration panel and Ground Control Points (GCPs), illustrating their function and placement during drone image acquisition.

the time of flight is the positioning of one or more calibration panels and ground control points (GCPs, Figure 5.5).

The calibration panel can be used for different purposes in order to improve image quality. In the case of multispectral, hyperspectral, and RGB images, the panel is of fundamental importance as it allows the reflectance data of different objects to be obtained during the photogrammetric process. Many drone companies already integrate the drone itself with a light sensor that is placed in the apex. This sensor does not require the presence and therefore the positioning of calibration panels. However, the layer of atmosphere between the sensor and the object can slightly affect the acquisition. In fact, depending on the climatic conditions, slight variations can be observed on the actual reflectance conditions, which are generally overestimated with the use of the brightness sensor alone. Unfortunately, panels are very expensive and time-consuming to place, especially in very large areas. In addition, the panel must have known reflectance characteristics that are certified by laboratories. Although the use of these panels can be mitigated in spectral chambers, in the case of thermal imaging they can play a decisive role. Indeed, the atmosphere may have little influence at spectral level but can have great influences from a thermal point of view. Furthermore, drones do not have sensors that allow the image to be perfectly calibrated, so it is necessary to have a ground reference.

Frequently, those who use drone thermography exploit these images to obtain water stress indices such as the aforementioned CWSI. By using these objects at a known temperature, it is not only possible to calibrate the images well, but also to use them as a reference for stress calculations (Cohen et al., 2005; Maes & Steppe, 2012).

GCPs have the function of geometrically correcting the images in order to obtain a better photogrammetric reconstruction. GCPs must be positioned at the end and in the center of the field, and by using GNSS handheld systems, their coordinates must be determined with very high precision and accuracy. GCPs must be positioned at known points, e.g., large stones and edges of buildings, which can also be used for subsequent flights, decreasing the positioning time of the GCPs. The use of GCPs is necessary when the flight cannot be carried out in RTK (real-time kinematic) mode to reduce the error from half a meter to a few centimeters.

The number of panels and GCPs that must be positioned is not fixed; however, a higher number and a homogeneous distribution allow good results to be obtained.

Once the panels and GCPs have been positioned, the flight can be carried out, securing the drone's landing and take-off zone.

5.1.7 Data Analysis: Photogrammetric Process and GIS

Once the images have been acquired, they and the associated metadata are stored in specific folders on the SD card. The images are processed using photogrammetry to obtain two important raster files, the orthomosaic and the digital elevation model (DEM, Figure 5.6) saved in .tiff. Various photogrammetric software exists on the market. These two rasters allow us to obtain different information depending on the type of sensors that were used to acquire them. As far as surveys with LiDAR sensors are concerned, this type of data is processed using different software, suitable precisely for the reconstruction of the 3D model of the objects investigated. However, the latter type of survey will not be explored in this chapter due to the importance of this technology in precision olive cultivation.

The photogrammetric process consists of several consequential steps following the loading of the images into the software. The first step is the alignment of the images. This is one of the most computationally complex processes but can be speeded up depending on the parameters set. Furthermore, if the image acquisition is done in RTK mode, the calculation time is reduced. The second step concerns calibration (in reflectance or thermal) and geometric calibration. Reflectance calibration is performed using the calibration panels and/or the light sensor. Once the images have been calibrated, the dense-could is constructed, which is the most computationally intensive

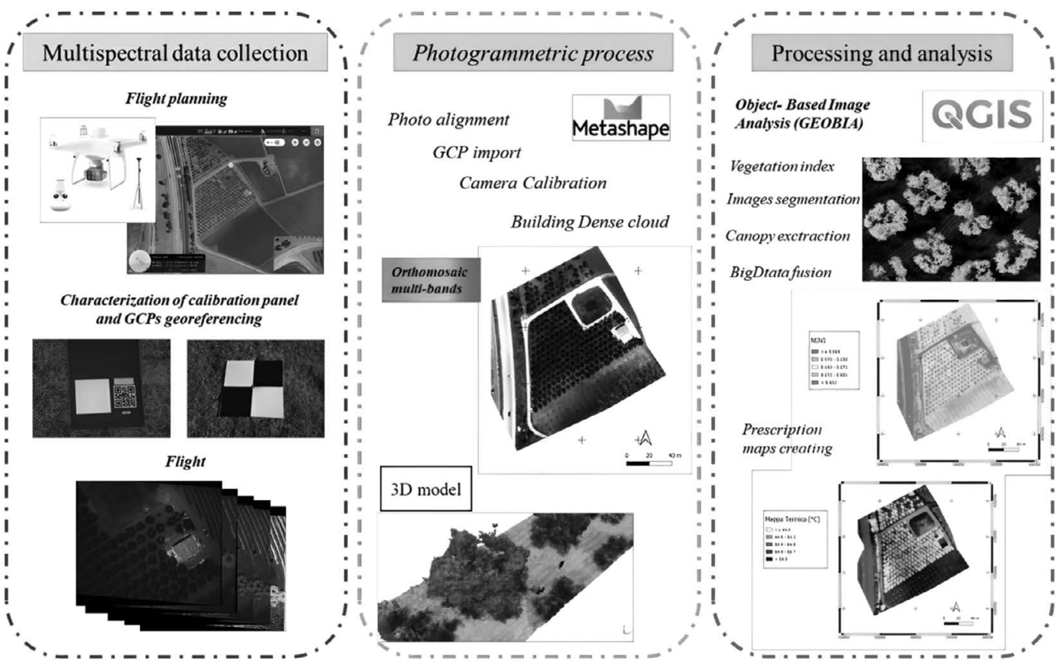

FIGURE 5.6 Main steps of the multispectral data collection, photogrammetric process and Object-Based Image Analysis (OBIA).

process. The mesh is then created, although this is not always necessary. Finally, the DEM and finally the orthomosaic can be obtained from the dense-cloud or the mesh. The orthomosaic if obtained from multi-hyperspectral images will contain a different number of bands depending on the camera while or only the three RGB bands.

5.1.8 Variability Detection: Vigor Maps

The photogrammetric process is concluded by obtaining two rasters containing both spectral and geometric information of the entire plot. Whether or not a digital terrain model (DTM) is available, it is possible to obtain the CSM. This information is becoming more and more interesting for smart and precision olive grove management because it allows height and CV values to be obtained. The orthomosaic remains the main product that is used to extract the spectral and geometric information of individual plants by exploiting the different bands. Using the information obtained from the VIs, it is possible to create continuous maps over the entire plot that can describe the spatial-temporal distribution of a given variable, such as the vigor map that can be used to monitor vegetative growth (Figure 5.7) or be linked to production.

The maps created need to be validated in the field because, as previously mentioned, the same NDVI value can be caused by various factors and does not always express the same condition between different zones. Therefore, once the maps have been created, it is necessary to have references on the ground that really allow the state of the plants to be understood and, depending on agronomic observation, to decide on thresholds to identify areas of low, medium, and high vigor.

Understanding variability allows the application of VRA inputs through the use of prescription maps. The elementary application plot can refer to individual plants, parts of the plot, between plots or by management zones (MZ). The level of detail of the prescription maps depends on many variables, the most important of which include the type of planting and the operation of the VRA machines.

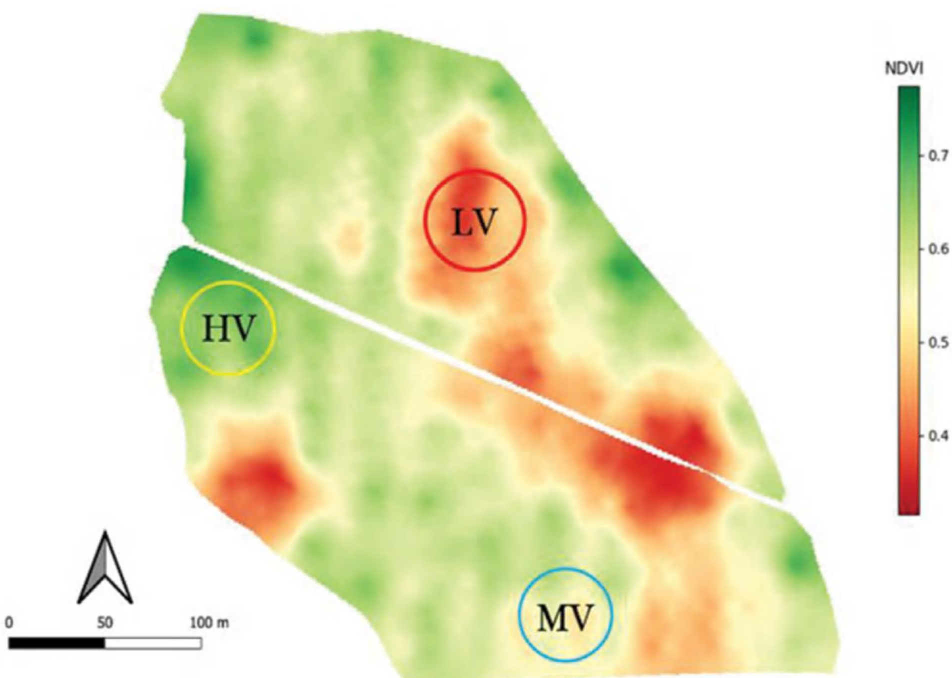

FIGURE 5.7 Continuous NDVI-based canopy vigour map and spatial patterns of different vigour levels within the vineyard.

CASE STUDY

In this section, the entire process of obtaining a nitrogen fertilization prescription map from multispectral images acquired by drone will be shown. Precisely, the steps that will be described are as follows: flight planning and flight execution (Step 1), photogrammetric reconstruction (Step 2), GIS processing for the extrapolation of geo-referenced information (Step 3) and finally the creation of the prescription map (Step 4).

EXPERIMENTAL SITE

The study area is located in Segesta (Trapani, Italy) with flat orography and a surface area covers of 5860 m^2. According to the Koppen–Geiger's classification, the climate of the area is classified as Mediterranean hot summer climates (Kottek et al., 2006). The soil moisture regime is xeric, bordering with aridic, and the temperature regime is thermic. According to the United States Department of Agriculture (USDA) classification, the soil belongs to the sandy–clay–loam granulometric class. The plot has 20-year-old olive grove cultivated according to ordinary management practices without irrigation system. The olive grove is cultivated with a traditional training system and a plant layout is 5 × 5.5 m; the direction of the rows is NE–SW at an angle of 60° to the North. The total number of trees considered in the tests was 211.

INSTRUMENTS

Multispectral data acquisition was performed using a rotary-wing quadcopter Phantom 4 Multispectral drone (DJI, Shenzhen, China). It is equipped with four rotors (quadcopter) capable of autonomously flying over the predetermined route by the waypoints. It has a solar irradiance sensor on the top, which allows pre-calibrated images to be obtained. It is also able to compensate for image position, as the relative positions of the CMOS sensor centers of the six cameras and the phase center of the on-board D-RTK antenna are stored in the EXIF (Exchangeable Image File Format) information of each image. The positioning system consists of a multi-frequency GNSS capable of receiving and decoding signals from the main satellites constellation NAVSTAR (GPS, Global Positioning System), GLONASS, BeiDou, and Galileo, with possibility of RTK correction. The flight speed can be modified during the flight and depending on flight mode. The max speed is 50 km/h during the flight, thus in ascending and descending 6 and 3 m/s, respectively. The speed precision is 0.03 m/s. Flight data is automatically recorded on the internal storage of the aircraft. This includes flight telemetry, aircraft status information, and other parameters. The DJI intelligent flight battery has a capacity of 5870 mAh, a voltage of 15.2 V, and a smart charge/discharge functionality. It should only be charged using an appropriate charger and is capable of a flight time of approximately 27 minutes. Regular calibration is required for optimal performance.

The Phantom 4 remote controller is a multi-function wireless communication device that integrates the video downlink system and aircraft remote control system. The video downlink and aircraft remote control system operate at 2.4 or 5.8 GHz with a maximum distance of transmission of 7 km.

The acquisitions of the multi-spectral images are carried out using a DJI multispectral camera implemented as payload in the UAV above described. The multispectral camera has six 1/2.9 in. CMOS sensors, such as an RGB sensor for visible light imaging and a multi-imager system formed of five narrow monochrome sensors for multispectral imaging with a final resolution of 2.08 MP pixels. The lens has a FOV (field of view) of 62.7 degrees, a focal length of 5.74 mm and an aperture of f/2.2. The maximum final image size is generally 1600 × 1300 (4: 3.25). The spectral centers of the monochromatic sensors are 450 nm (Blue), 560 nm (Green), 650 nm (Red), 730 nm (Red-Edge), 840 nm (NIR, Near Infrared). The narrow bands have a spectral resolution of ±16 and ±26 only for NIR band.

The sensors acquire the image as a global shutter (all pixels are acquired at the same time) and save the data in .jpeg and .tiff format in float at 32 bit (FP32).

STEP 1: FLIGHT SCHEDULE

Before the multispectral data collection, the flight has been planned using the specific and official DJI software. In particular the following was set: flight altitude, the GSD, investigation surface, speed, path, camera setting, gimbal orientation, time of the flight, side overlap, and the forward overlap (Figure 5.8).

The GCP and calibration panel were positioned to make the geometric and the radiometric calibration in the photogrammetric process. Six GCPs were placed evenly at the edges and center of the plot on a solid platform. The GCPs were georeferenced using a GNSS instrument, specifically the Stonex S7-G with external antenna and RTK correction. The flight was performed in automatic flight configuration following the routes and waypoints predetermine in excellent weather conditions with high light intensity and low wind speed at 12 noon to minimize shadowing. Image acquisition was carried out with the hover capture mode with

FIGURE 5.8 DJI flight-planning software interface.

an average speed of 15 m/s. The image overlap ratio, front overlap ratio and side overlap ratio were 70%, while the gimbal pitch was set at 90 degrees (downwards).

STEP 2: PHOTOGRAMMETRIC PROCESS

The photogrammetric process will not be described in detail because the steps that must be performed to obtain the orthomosaic and the DEM depend on the flight settings and the quality of the acquired data. However, the steps that have been described in the previous section are those that have been applied.

STEP 3: GEOBIA PROCESS

Once the orthomosaic and the DEM were obtained, they were processed in a GIS (Geographic Information System) environment in order to correctly detect the physiological state and vigor of the plants. In this specific case, QGIS version 3.2 software was used (Figure 5.9).

The first operation to be performed concerns the identification and segmentation of individual crowns. The main aim of segmentation is to identify and separate the different parts or objects in an image so that they can be analyzed or processed individually. For image analysis on olive groves, the best performance is obtained by segmenting from NDVI images processed from images acquired in the summer and midday due to the lack of weeds and the lower shadow effect. In addition, it is advisable to start from images that have already been cropped through the perimeter of each plot, so that there are fewer objects to discriminate. Therefore, the first step involves calculating the NDVI using the raster calculator and then cropping using the appropriate tool (Figure 5.10).

Once the NDVI clipped image is obtained, one can proceed with segmentation. The basic technique is thresholding as it is simpler and also quite accurate. It divides an image into regions using a threshold, so that pixels with a value above the threshold are assigned to one region and those below the threshold to another. Multiple thresholds can also be used

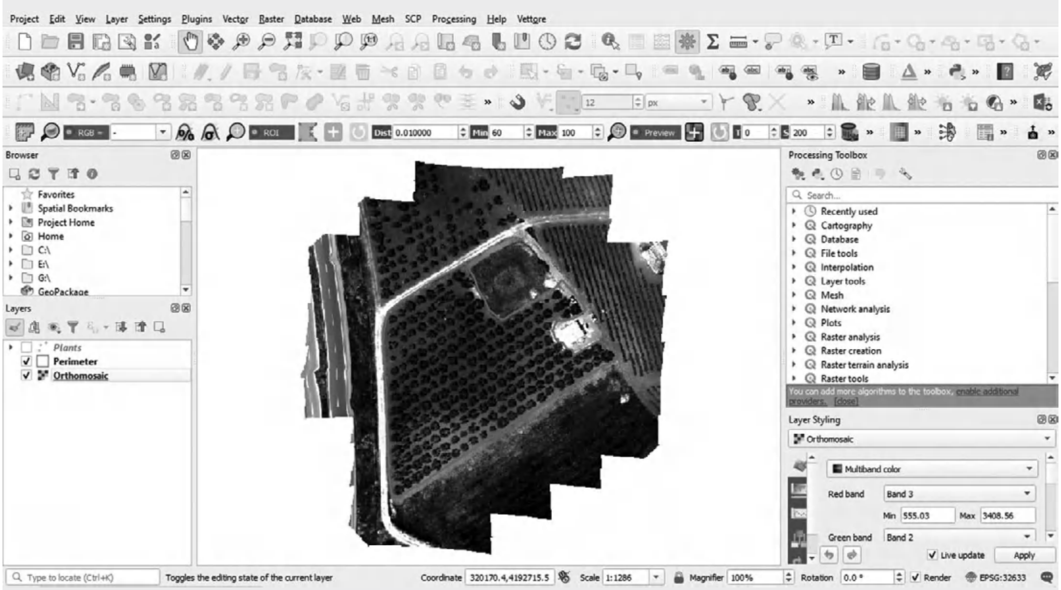

FIGURE 5.9 Example of a standard QGIS workspace used for geospatial data visualization and analysis.

depending on the complexity of the images. The threshold value depends on the image you are working with. If you were working with an NDVI image, in the olive grove, you could use a threshold value of 0.25 for the separation between soil and vegetation. This way, unfortunately, some information is lost and depending on the soil type may not be sufficient. Indeed, as can be seen in the figure below, the frequency histogram well identifies two peaks, one related to soil and one to vegetation. However, their separation cannot be precise due to the presence of non-pure pixels (Figure 5.11).

All other methods include more or less sophisticated algorithms for image segmentation. These are implemented directly in the processing or in the libraries of SAGA, GRASS or the Python Script already present in QGIS. The choice of algorithm depends on the specific application, image characteristics, and segmentation aim. In many cases, it is necessary to experiment with different techniques and adapt them to the specific requirements of the problem. Furthermore, with the advent of deep learning, many image segmentation solutions rely on convolutional neural networks trained on large datasets to achieve advanced results.

For simplicity's sake, we present the use of the k-means algorithm as it provides excellent results in the olive grove. This algorithm is implemented in SAGA and is also able to work

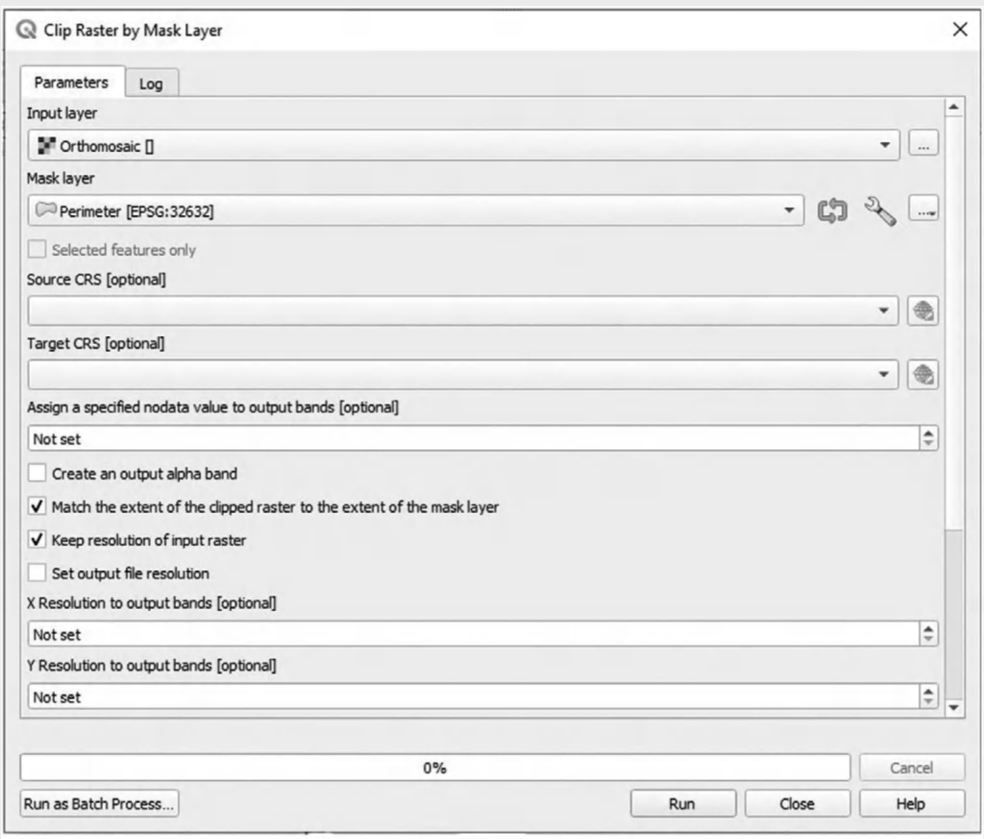

(a)

FIGURE 5.10 (a) Illustration of the orthomosaic cropping process using a mask pre-determined; (b) NDVI map generation through the Raster Calculator tool, using the red (Clipped_mask@3) and NIR (Clipped_mask@5) bands extracted from the orthomosaic. (*Continued*)

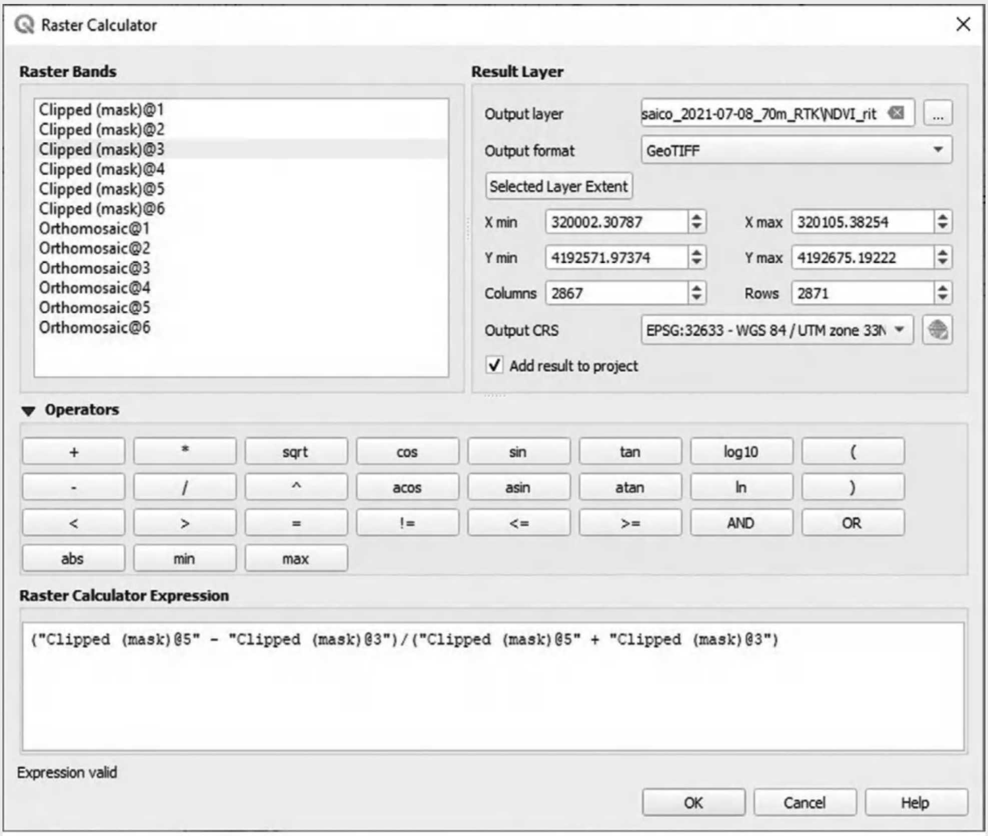

(b)

FIGURE 5.10 (Continued)

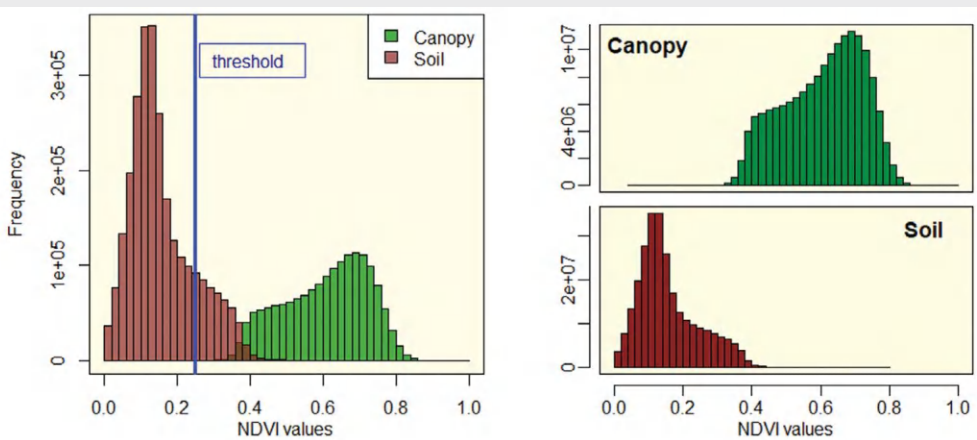

(a) (b)

FIGURE 5.11 (a) Frequency histogram division using the thresholding method for image segmentation; (b) frequency histograms of vegetation (top) and soil (bottom) segmented pixels obtained through an unsupervised algorithm.

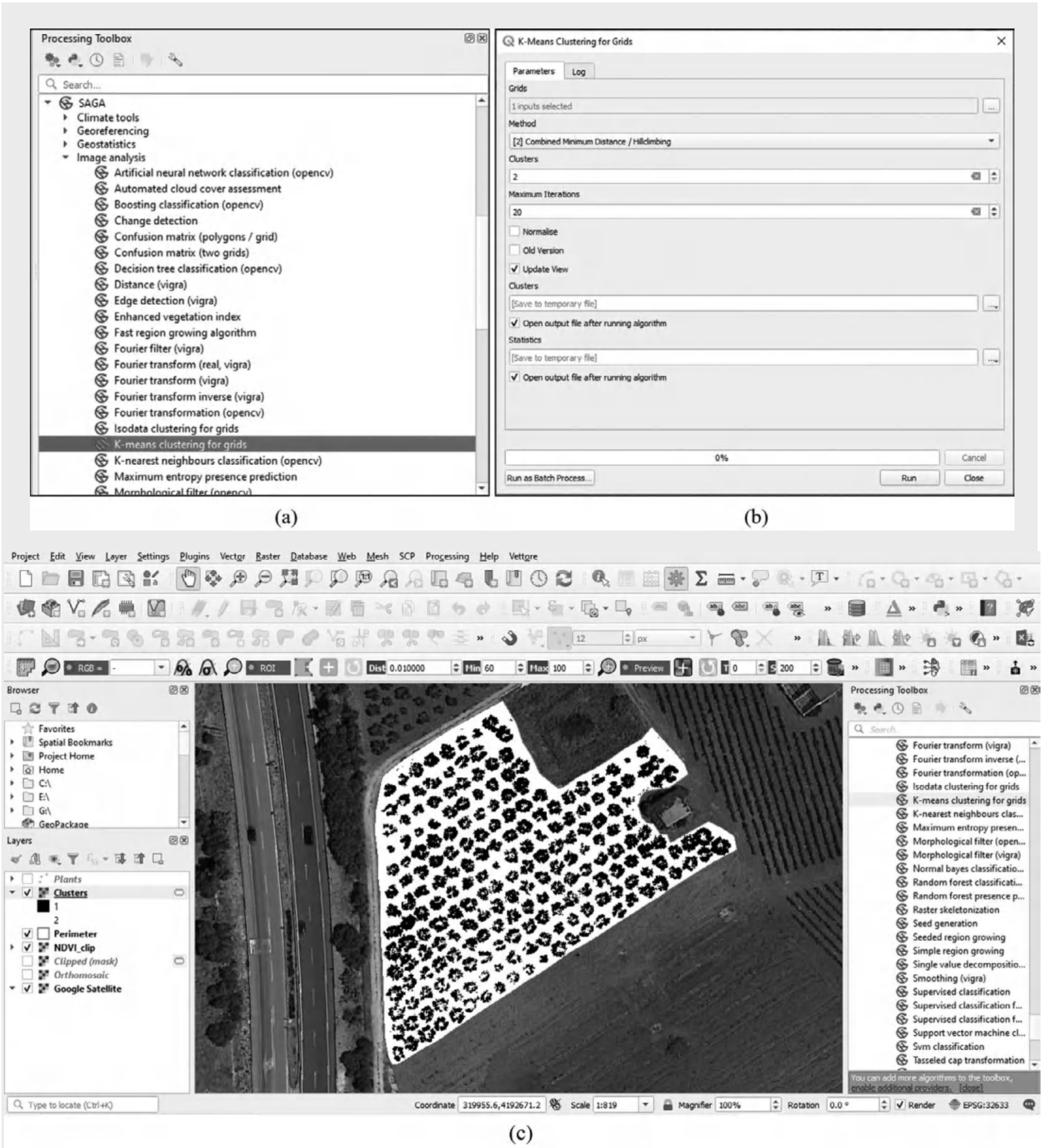

FIGURE 5.12 Application of the NDVI image segmentation process using the unsupervised K-means algorithm implemented in QGIS through the SAGA library: (a) tool path; (b) parameter settings for image binarization; (c) algorithm output.

on several images simultaneously (Figure 5.12). The number of homogeneous regions is predetermined by the operator and generally, under the previously mentioned conditions, two classes are included. In some cases, segmentation into three classes may be required due to the presence of weeds or shadows.

Once the segmentation is carried out, one is left with a 2-bit (black–white) image that allows one to distinguish well between two homogeneous regions that correspond to soil and vegetation. At this stage, the image must be classified in order to label the data perfectly. In

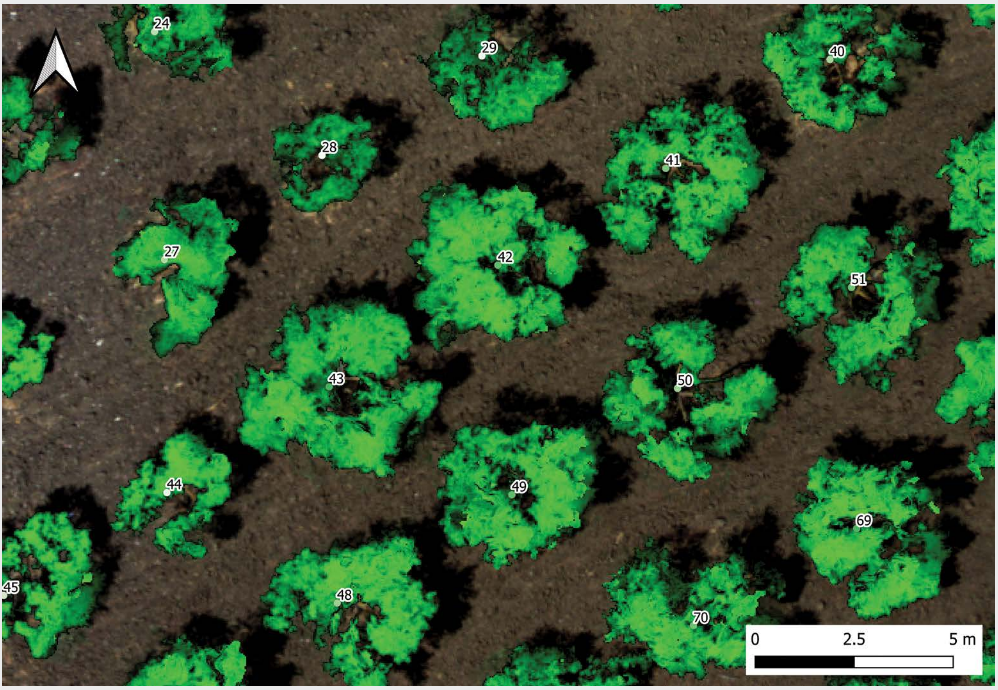

FIGURE 5.13 Raster representation of individual tree crowns obtained from the segmentation and classification process carried out through Object-Based Image Analysis (OBIA) of multispectral drone imagery.

this case, even looking at the image, it is possible to identify whether black corresponds to vegetation or the reverse.

Once the classification is complete, it remains to be able to distinguish the individual crowns. In this case, an initial vectorization of the raster image must be carried out, excluding the ground. Thus, we will obtain a different number of polygons that can be associated with the individual plants depending on the distance between them (less than 2 m). Of course, we must have or construct a point layer that allows us to really know how many plants and where they are in the plot. Polygons that do not correspond to the query can be deleted safely. At this point, we will have obtained the individual canopies that we can investigate to find out the real biometric and spectral conditions (Figure 5.13).

Various information can be extracted from the individual canopies in vector format. The toolbox to use is *Zonal statistics*, which allows statistics to be obtained for each given vector. In our case, we will use the crowns as a vector and the NDVI map as the image from which to extract the information (Figure 5.14).

From this processing we will obtain the NDVI data for each plant which we will insert in the attributes table. If we use the DEM as input image, it is possible to obtain the height and volume for each plant. The average value of each canopy in space identifies its vigor condition, as they are well correlated.

STEP 4: PRESCRIPTION MAPS

The aim of the previous processing was to obtain a map that correlates well with the nutritional and physiological conditions for variable rate fertilization. The next step is to associate

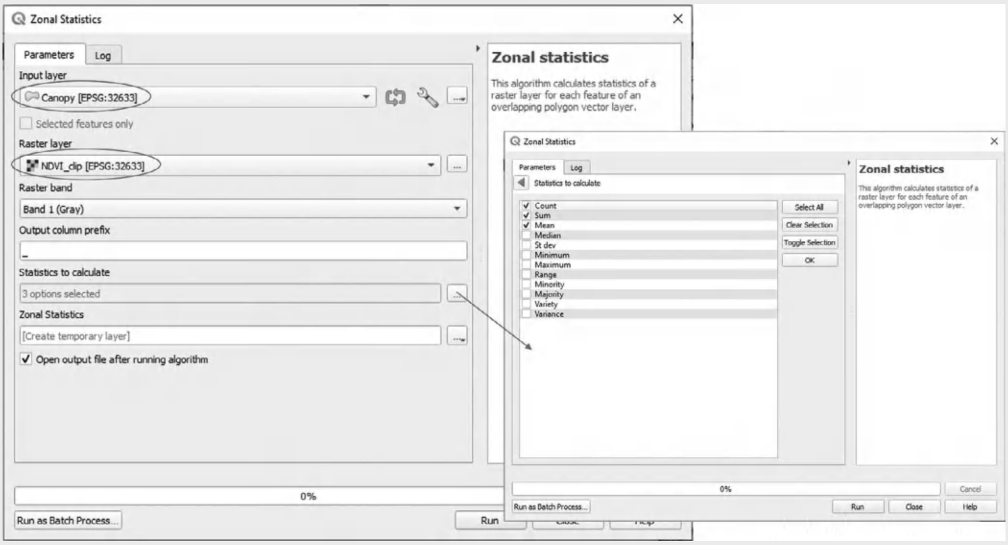

FIGURE 5.14 GIS tool employed for extracting individual plant information from multiple thematic maps.

the attribute table of each plant with a point data corresponding to the centroids of each canopy. Subsequently, using geostatistical algorithms, the continuous vigor map of the entire plot can be derived (Figure 5.15). It is advisable to check that the vigor conditions are really different by comparing them with the data taken in the field. If this is not the case, it is advisable to identify the best variable to estimate the real vegetative and productive conditions in

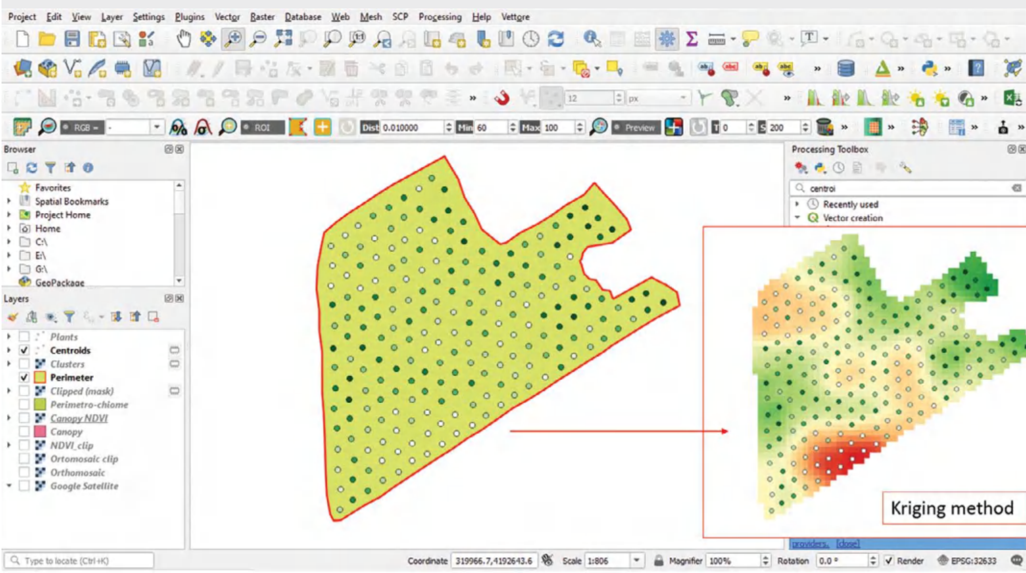

FIGURE 5.15 Obtaining the continuous vigor map by geostatistical interpolation of the previously extracted information per plant.

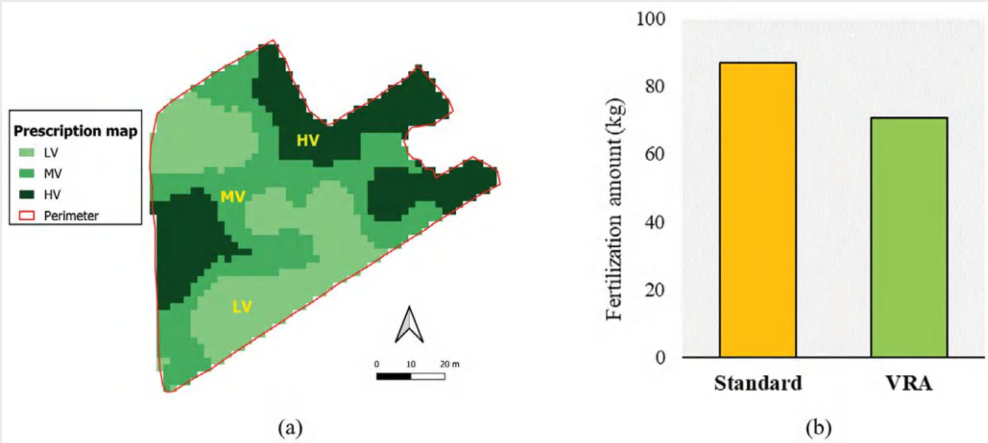

FIGURE 5.16 Fertilization prescription map, differentiated for high (HV), medium (MV), and low (LV) vigor level (a). Fertilizer savings actually obtained by performing a site-specific distribution compared with the amount distributed without variable rate application (VRA) (b).

the field. If data from foliar sampling are available, it is possible to obtain an NDVI correlation curve and foliar nitrogen content, which is an excellent indicator of nutrient conditions.

As can be seen from the figure above, three zones can be distinguished, at low, medium, and high levels. To conclude, prescription maps can indicate the optimal fertilizer doses to be applied in different parts of the field according to the nutritional needs of the crops. Therefore, the prescription map is nothing more than the result of several pieces of geo-referenced information being combined. In this case study, only vigor conditions were examined because the plot had a small size and therefore low variability in terms of soil and climate. Therefore, it was sufficient to reconnect the highest and lowest quantity to the high- and low-volume classes by means of a simple linear correlation in order to determine the quantity to be distributed for each plot (Figure 5.16).

The area covered by the three vigor areas is 32%, 37%, and 32% for high, medium, and low vigor, respectively. Considering a variable dose depending on the level of vigor of 150, 120, and 100 kg/ha, a considerable saving of fertilizer is obtained. The case just reported, at a detailed scale for homogeneous zones, yielded a 19% saving in fertilizer. However, there are also more precise applications in the literature that go down to the individual plant down to 30% savings, with consequent economic and environmental benefits (Roma et al., 2023).

5.2 CONCLUSIONS

The world olive-growing industry has at its disposal numerous technologies that allow the improvement in the use of resources to optimize crop productivity and quality. Among these, the use of drones is achieving great success due to their great versatility of use in EU countries characterized by high farm fragmentation and spatial-temporal variability of crops and land. In this chapter, an attempt has been made to provide a picture of the real advantages and disadvantages of the application of these platforms in olive grove, examining an application case of the whole operational process.

However, while we are at an important moment in the evolution of precision agriculture in olive groves, the chapter concludes with a look into the future. Future developments in precision agriculture promise to be even more revolutionary. New technologies such as artificial intelligence, machine learning and advanced connectivity appeared to boost the improvement of platforms, sensors and machines. Among the most important aims in the field of precision olive cultivation is the need for algorithms that are increasingly able to segment, classify, and process images in order to obtain easy-to-use and highly accurate predictive growth models and DSS. However, the scientific achievements so far allow a practical application in all types of olive farms.

In conclusion, precision olive cultivation represents a way toward a more sustainable and efficient future for olive growing. It will continue to guide the growth and prosperity of the sector as olive growers and researchers explore new frontiers and to increase the economic and environmental sustainability of farms.

REFERENCES

Berni, J. A., Zarco-Tejada, P. J., Suárez, L., & Fereres, E. (2009). Thermal and narrowband multispectral remote sensing for vegetation monitoring from an unmanned aerial vehicle. *IEEE Transactions on Geoscience and Remote Sensing*, *47*(3), 722–738.

Campos, J., Gallart, M., Llop, J., Ortega, P., Salcedo, R., & Gil, E. (2020). On-farm evaluation of prescription map-based variable rate application of pesticides in vineyards. *Agronomy*, *10*(1), 102.

Caruso, G., Zarco-Tejada, P. J., González-Dugo, V., Moriondo, M., Tozzini, L., Palai, G., Rallo, G., Hornero, A., Primicerio, J., & Gucci, R. (2019a). High-resolution imagery acquired from an unmanned platform to estimate biophysical and geometrical parameters of olive trees under different irrigation regimes. *PLoS ONE*, *14*(1), e0210804.

Caruso, G., Zarco-Tejada, P. J., González-Dugo, V., Moriondo, M., Tozzini, L., Palai, G., Rallo, G., Hornero, A., Primicerio, J., & Gucci, R. (2019b). High-resolution imagery acquired from an unmanned platform to estimate biophysical and geometrical parameters of olive trees under different irrigation regimes. *PLoS ONE*, *14*(1), e0210804.

Catania, P., Ferro, M. V., Roma, E., Orlando, S., & Vallone, M. 2022. *Evaluation of different flight courses with UAV in vineyard* (pp. 457–467). Springer. https://doi.org/10.1007/978-3-031-30329-6_47

Catania, P., Roma, E., Orlando, S., & Vallone, M. (2023). Evaluation of multispectral data acquired from UAV platform in olive grove. *Horticulturae*, *9*(2), 133.

Cohen, Y., Alchanatis, V., Meron, M., Saranga, Y., & Tsipris, J. (2005). Estimation of leaf water potential by thermal imagery and spatial analysis. *Journal of Experimental Botany*, *56*(417), 1843–1852.

Connor, D. J., Gómez-del-Campo, M., Rousseaux, M. C., & Searles, P. S. (2014). Structure, management and productivity of hedgerow olive groves: A review. *Scientia Horticulturae*, *169*, 71–93.

Di Vaio, C., Marallo, N., Nocerino, S., & Famiani, F. (2012). Mechanical harvesting of oil olives by trunk shaker with a reversed umbrella interceptor. *Advances in Horticultural Science*, *26*(3–4), 176–179. https://doi.org/10.13128/ahs-22675

FAOSTAT. (2022). *Statistics, food and agriculture organization of the United Nations, Rome. 2022*. https://www.fao.org/faostat.

Gargouri, K., Sarbeji, M., & Barone, E. (2006). *Assessment of soil fertility variation in an olive grove and its influence on olive tree nutrition*. In Second international seminar on biotechnology and quality of olive tree products around the mediterranean basin (pp. 5-10). Italy: Marsala-MazaradelVallo.

Godfray, H. C. J., Beddington, J. R., Crute, I. R., Haddad, L., Lawrence, D., Muir, J. F., Pretty, J., Robinson, S., Thomas, S. M., & Toulmin, C. (2010). Food security: The challenge of feeding 9 billion people. *Science*, *327*(5967), 812–818.

Gómez, J., Zarco-Tejada, P., García-Morillo, J., Gama, J., & Soriano, M. (2011). Determining biophysical parameters for olive trees using CASI-airborne and QuickBird-satellite imagery. *Agronomy Journal*, *103*(3), 644–654.

Huang, S.-W., Jin, J.-Y., Yang, L.-P., & Bai, Y.-L. (2006). Spatial variability of soil nutrients and influencing factors in a vegetable production area of Hebei Province in China. *Nutrient Cycling in Agroecosystems*, *75*(1), 201–212.

Idso, S. B. (1982). Non-water-stressed baselines: A key to measuring and interpreting plant water stress. *Agricultural Meteorology*, *27*(1–2), 59–70.

Jackson, R. D., Idso, S., Reginato, R., & Pinter Jr, P. (1981). Canopy temperature as a crop water stress indicator. *Water Resources Research*, *17*(4), 1133–1138.

Kottek, M., Grieser, J., Beck, C., Rudolf, B., & Rubel, F. (2006). *World map of the Köppen-Geiger climate classification updated. Meteorologische Zeitschrift*, *15*(3), 259–263. https://doi.org/10.1127/0941-2948/2006/0130

Lee, W.-S., Alchanatis, V., Yang, C., Hirafuji, M., Moshou, D., & Li, C. (2010). Sensing technologies for precision specialty crop production. *Computers and Electronics in Agriculture*, *74*(1), 2–33.

Maes, W., & Steppe, K. (2012). Estimating evapotranspiration and drought stress with ground-based thermal remote sensing in agriculture: A review. *Journal of Experimental Botany*, *63*(13), 4671–4712.

Qi, J., Chehbouni, A., Huete, A. R., Kerr, Y. H., & Sorooshian, S. (1994). A modified soil adjusted vegetation index. *Remote Sensing of Environment*, *48*(2), 119–126.

Roma, E., & Catania, P. (2022). Precision oliviculture: Research topics, challenges, and opportunities—A review. *Remote Sensing*, *14*(7), 1668.

Roma, E., Laudicina, V. A., Vallone, M., & Catania, P. (2023). Application of precision agriculture for the sustainable management of fertilization in olive groves. *Agronomy*, *13*(2), 324. https://doi.org/10.3390/agronomy13020324

Rouse, J. W., Haas, R. H., Schell, J. A., Deering, D. W., & Harlan, J. C. (1974). *Monitoring the vernal advancement and retrogradation (green wave effect) of natural vegetation*. NASA/GSFC Type III final report, Greenbelt, MD: NASA/ GSFC.

Senay, G. B., Ward, A. D., Lyon, J. G., Fausey, N. R., & Nokes, S. E. (1998). Manipulation of high spatial resolution aircraft remote sensing data for use in site-specific farming. *Transactions of the ASAE*, *41*(2), 489.

Tilman, D., Balzer, C., Hill, J., & Befort, B. L. (2011). Global food demand and the sustainable intensification of agriculture. *Proceedings of the National Academy of Sciences*, *108*(50), 20260–20264.

Torres-Sánchez, J., López-Granados, F., Serrano, N., Arquero, O., & Peña, J. M. (2015). High-throughput 3-D monitoring of agricultural-tree plantations with unmanned aerial vehicle (UAV) technology. *PLoS ONE*, *10*(6), e0130479.

Van Evert, F. K., Gaitán-Cremaschi, D., Fountas, S., & Kempenaar, C. (2017). Can precision agriculture increase the profitability and sustainability of the production of potatoes and olives? *Sustainability*, *9*(10), 1863.

Xue, J., & Su, B. (2017). Significant remote sensing vegetation indices: A review of developments and applications. *Journal of Sensors*, *2017*.

6 Smart Agriculture for Peach Orchard Management

Irene Borra-Serrano, José Manuel Peña, Joe Mari Maja, Juan Carlos Melgar, Kelly Nascimento-Silva, and Ana de Castro

6.1 INTRODUCTION

Fruit orchards require site-specific management at the individual tree level. Some management activities must occur at a specific growth stage, while others require precise timing for maximum efficiency (Zhang et al., 2021). Regular assessments of tree structure and health status provide critical data for this approach (Tu et al., 2020). Additionally, historical data across multiple growing seasons is essential, as it provides valuable information on the endogenous growth factors and long-term orchard management (Zude-Sasse et al., 2021). Poor orchard management may require years of corrective practices (Raman et al., 2022). Site-specific orchard management offers multiple benefits: reducing labor costs, overcoming the limitation of visual assessments, cutting production costs, maximizing yield and quality, increasing grower income, and lowering environmental footprint of fruit production (Sarron et al., 2018; Usha & Singh, 2013; Zhang et al., 2021; Zude-Sasse et al., 2016). In that context, precise management strategies help regulate flower density per tree to prevent overloading, which can lead to poor fruit quality and excessive strain on trees (Dennis, 2000). Insufficient fruit exposure to sunlight affects total soluble solids and sugar content, impacting peach quality (Alcobendas et al., 2013). Tree structural characteristics like canopy volume and projected area are useful indicators of growth status and help determine pruning strategies or address soil heterogeneity (Castillo-Ruiz et al., 2015; Jiménez-Brenes et al., 2017; Miranda-Fuentes et al., 2015). Proper irrigation management directly influences peach quality and yield while limiting excessive vegetative growth (Alcobendas et al., 2013; Chai et al., 2015). Therefore, efficient irrigation strategies based on tree-specific water needs are crucial for optimizing water productivity (Conesa et al., 2019). Early disease detection and identification are equally important to prevent the spread of pests and safeguard production, though diagnostics can be complex (De Castro et al., 2015).

Smart Agriculture, or precision agriculture, leverages technology and data-driven approaches to optimize orchard management, considering the spatial and temporal variability. Remote sensing is a key component, enabling data collection from a distance via imaging sensors or radar. The increasing volume of publications and reviews on remote sensing for precision agriculture underscores its growing importance. For an in-depth discussion, refer to Maes and Steppe (2019) and Segarra et al. (2020).

Among the most transformative remote sensing technologies, uncrewed aerial vehicle (UAV) stands out as a promising tool for site-specific orchard management (De Castro et al., 2021). UAV-based assessments facilitate frequent, high-resolution crop monitoring and detailed analyses of inter- and intra-field variability providing growers with crucial insights for decision-making (Mulla, 2013). UAV can operate at low altitudes capturing highly detailed spatial data that enables individual tree identification, digital surface model generation, and the integration of various sensors (Dandois & Ellis, 2013; De Castro et al., 2021). Essential orchard management tasks—such as monitoring tree size, growth or mortality, disease detection, and water need—rely on accurate tree detection and segmentation (Popescu et al., 2023). Several works have successfully segmented individual

DOI: 10.1201/9781003510598-6

trees in different orchard species, achieving over 95% accuracy in apple and pear crown delineation (Dong et al., 2020). UAVs can support tree monitoring throughout the entire growing season, from flowering to dormancy between production cycles.

Despite the benefits, UAV deployment in orchards presents challenges due to the absence of standardize operational protocols, as flight variables (e.g., altitude and overlap settings) significantly affect data quality and usability (Roth et al., 2018; Torres-Sánchez et al., 2018). Zhang et al. (2021) and Zude-Sasse et al. (2021) have identified gaps in UAV applications, emphasizing the need for systemic flight planning. Tu et al. (2020) proposed flight planning protocols tailored for horticultural tree crops using a multispectral camera, emphasizing the importance of high forward overlap (>80%), nadir image capture, and optimal solar elevation. Other studies have refined flight settings for specific crops, such as lychee, where a 70 m altitude was found optimal for balancing accuracy, area coverage, and processing time (Johansen et al., 2018). For olive tree volume estimation, Torres-Sánchez et al. (2018) determined that a 95% forward overlap combined with 60% side overlap was optimal for data reconstruction and computational efficiency.

More than 65% of UAV research in orchard management focuses on three primary areas: resource efficiency, geometric traits, and productivity (Zhang et al., 2021). This chapter focuses on UAV imagery captured by passive sensors. While other technologies, e.g., active sensors such as LiDAR, offer other capabilities, these are beyond the scope of the chapter (for more details, see Colaço et al., 2018).

Spectral data from UAV sensors enables precise flowering status estimation, addressing challenges such as flowers counting, which is affected by the occlusion by branches and leaves, variable lighting conditions, and color similarity (Horton et al., 2017; Zhang et al., 2021). Examples include the enhanced bloom index (EBI) for almond floral phenology (Chen et al., 2019), colored photogrammetric point cloud for flower density assessments in almond trees (López-Granados et al., 2019) and NIR and blue bands threshold for peach blossoms detection (Horton et al., 2017).

Passive sensors provide detailed spectral information, making them well-suited for detecting plant stress and monitoring vegetation health (Abdulridha et al., 2018; De Castro et al., 2015). High-resolution thermal imagery has been used to assess plant water stress at the field scale. For instance, Park et al. (2017) developed a method to estimate the crop water stress index (CWSI) in nectarine and peach orchards, demonstrating a strong correlation with the stem water potential (Ws). Similarly, drought responses affecting photosynthetic pigment content can be detected using NIR-vegetation indices like the PRI (photochemical reflectance index) (Ballester et al., 2018). A comprehensive list of vegetation indices for orchard water stress can be found in Zhang et al. (2021). Nutritional status monitoring is another way to achieve higher productivity, e.g., nitrogen via the modified canopy chlorophyll content index (M3CI) in pear (Perry et al., 2018).

Biotic stressors such as diseases and pests also impact fruit quality and yield, potentially leading to tree mortality, as seen with huanglongbing (HLB) or citrus greening and laurel wilt in avocado. Early detection is critical to mitigating economic losses and UAVs allow on demand and rapid large-scale scouting (De Castro et al., 2019; Torres-Sánchez et al., 2015). However, disease detection using imagery is challenging due to differential symptomology along the disease life cycle, mixed disease stages, and overlapping stressors under field conditions (Matese et al., 2024). In the review by Terentev et al. (2022), it was highlighted a mismatch between many articles revised not coinciding in the bands to use for the same diseases, which means there is still advancements required to fully use HSI (hyperspectral imaging). Besides, if the disease onset occurs in the lower part of the canopy, data collection is restricted by the sensor angle (i.e., side vs nadir) (Matese et al., 2024). In summary, the spectral data is influenced by biochemical changes (Terentev et al., 2022), foliar symptoms and crop structure, particularly in heterogenous woody crops (Di Gennaro et al., 2022). The majority of the research has been done in wheat for rust diseases detection or fusarium head blight. There is a limited amount of studies in fruit trees. Moriya et al. (2021) reported better results for citrus gummosis using HSI than multispectral imagery; Deng et al. (2020) and Schoofs et al. (2020) identified crucial wavelengths to detect citrus huanglongbing and fire blight in pear orchards, respectively. Using a multispectral sensor for pest detection, early symptoms of peach flatheaded root borer (PFRB) infestation were detected, and the discrimination between healthy and damaged trees achieved 85% accuracy in the work by Arapostathi et al. (2024). More examples can be found in Popescu et al. (2023).

The spectral response characteristics of passive sensor are crucial for accurately interpreting and utilizing data. Hyperspectral sensors offer superior selectivity and spectral uniformity, and fidelity compared to visual or multispectral sensors due to their design (Proctor & He, 2015). Moreover, they provide richer spectral information to identify and distinguish subtle changes due to stress (Matese et al., 2024) and to quantify biophysical and biochemical parameters of vegetation (Huang et al., 2004), mainly due to the narrow contiguous spectral bands of HSI (Omia et al., 2023). The measurement of the (entire) spectra at narrow bands facilitates the use of vegetation indices based on a narrow band absorbance range, e.g., the PRI and the use of techniques such as spectral unmixing or continuum removal (Proctor & He, 2015). HSI results in a hyperspectral cube with two spatial dimensions and one wavelength dimension (Kuswidiyanto et al., 2022). Nevertheless, the high dimensionality of the data results in wavelengths datasets with a high correlation that requires dimensionality reduction (Matese et al., 2024). The deployment of hyperspectral sensors on a UAV capable of recording more than 200 bands has significant technical difficulties (Ram et al., 2024). As the data collected can be quite large, data management is crucial and requires large amounts of data storage (Mishra et al., 2017; Wong, 2009). For years, their higher cost together with the technical risk and the complex data handling have hindered the adoption of hyperspectral sensors even being a cutting-edge technology (Matese et al., 2024).

Hyperspectral sensors are classified on the basis of their operation, i.e., acquisition mode and hypercube construction. There are two main types of sensors: (1) push broom, a line-scanning approach that captures the spectral data in lines, and (2) snapshot, where single images are obtained for each band. The pre-processing of the data is required before any data extraction or analysis due to the influence of elements such as atmospheric effects, light scattering or canopy geometry (Mishra et al., 2020; Ram et al., 2024). All those factors, plus varied results in specific applications and crops, hinder to identify with certainty best practices to use HSI (Matese et al., 2024). Hyperspectral sensors require radiometric correction, which is fundamental to compare spectral data in case of different environmental light conditions (Herrero-Huerta et al., 2014; Iqbal et al., 2018). Radiometric correction for multispectral imagery for horticultural purposes was covered in Tu et al. (2018), where it was concluded that flying at low altitudes and trees canopy geometry increase the illumination influence on the spectral bands. A geometrical correction could also be required due to lens distortion, vignetting or spatial shift between single bands (Di Gennaro et al., 2022). A possible solution to the spatial shift is the methodology proposed by Honkavaara et al. (2017) where selected bands are used as references. Workflow, data collection, calibration recommendations, and applications for hyperspectral sensors can be found in several reviews, such as Proctor and He (2015), Matese et al. (2024), Ram et al. (2024) among others. Briefly, the processing steps after HSI data acquisition by Di Gennaro et al. (2022) are as follows: (1) geometrical distortion correction, (2) dark current removal to remove noise signals, (3) radiometric correction, and (4) bands mosaicking and georeferencing.

6.2 INTRODUCTION TO CASE STUDIES

Peach (*Prunus persica* (L.) Batsch) is a widely grown deciduous tree from the Rosaceae family and one of the most common and productive crops of the temperate zone (Cao et al., 2014), being China the first producer followed by Spain and Italy (FAOSTAT, 2022). Commercial peach production encounters several problems related to the susceptibility to many fungal and bacterial diseases, as well as proper irrigation management being crucial in the early growing years, affecting both to fruit yield and quality and the trees longevity (Luo et al., 2022). Management decisions and practices, e.g., soil management, nutrient, or water application, are key to ensure and improve production.

Some of the most economically important peach diseases in the main production countries are brown rot caused by *Monilinia* spp., bacterial spot caused by X*anthomonas arboricola* pv. *pruni* (*Xap*), *Armillaria* root rot, bacterial canker caused primarily by *Pseudomonas syringae*, powdery mildew caused by *Podosphaera pannosa* and peach rust caused by *Tranzschelia discolor* (Luo et al., 2022). A detailed description and their distribution can be found in the review by Luo et al. (2022). The first case study is about one of the diseases that affect peach production, peach rust caused by *T. discolor*. It is a fungus that overwinters in woody tissue where infectious spores are moved by wind and rain and produce yellow lesions in leaves (Soto-Estrada et al., 2007). Symptoms initiate as pale green spots on both sides of the leaf during spring and can also affect fruit (Luo et al., 2022). The diagnostic is by visual inspection, samples collections or laboratory analysis, which implies cost and time. Two management strategies for disease control were evaluated, potassium foliar fertilization (nutrient application) and root-collar excavation (soil management), via HSI.

Peach production is limited during the first three years after plantation, as most of the resources are used for vegetative growth, which is crucial for the tree architecture development and future production (Zambrano-Vaca et al., 2020). Therefore, irrigation management is a key component to ensure adequate water supply during early tree growth stages and may be accompanied by fertilization application to mitigate water stress, e.g., silicon (Si), classified as a beneficial element for crop growth and development (Marschner, 2012). Fertilization tends to be done without knowing the real need (Zhou & Melgar, 2019) and this fact can lead to excessive canopy foliage and internal shading that reduce fruit quality (Layne, 2011). Site-specific fertilizer applications would bring significant agronomic and economic benefits. Therefore, peach production can be improved by knowing the health status of the trees at crucial decision-making times such as when site-specific fertilization application has to be applied. Monitoring the effect of Si application on water stress via HSI is presented in the second case study of the chapter.

The research presented in both case studies was part of a research program to develop methodologies to be included in the integrated pest management (IPM) strategies for peach orchards.

CASE STUDY 1

INTRODUCTION

Management practices, from nutrient application to soil management, are key to ensure and improve yield but also costly and time-consuming. Therefore, it is essential to examine whether they fulfill their aim. In this case study, the outcomes of potassium (K) foliar fertilization and root-collar excavation practices to prevent damage caused by the fungus *T. discolor* in peach production were evaluated. Peach rust can cause a significant impact on yield and at a severe infection level the tree shed leaves early that diminishes nutrient translocation. The repetitive early defoliation may result in the tree weakening and lower production (Adaskaveg et al., 2012). The two practices of interest in this work have different effects. Potassium foliar application improves yield, diameter, and weight fruit and root-collar excavation, i.e., permanent soil removal at the trunk base, which aims to prevent tree mortality progression and extend tree longevity. Preventative root-collar excavation practice has been used and proven to be effective for Armillaria root rot on replant sites (Miller et al., 2020). The evaluation of the two management practices to assess whether their effect on disease damage had an impact on the spectral signature was based on hyperspectral data analysis. The potential of HSI as a tool to monitor factors affecting the peach orchard was assessed. The objectives were (1) optimize an image processing and spectral data retrieval protocol, (2) quantification of the measures effect and influence on the spectral signature and (3) identification of the best wavebands to discriminate affected trees. An accurate and early identification of the disease trees is crucial to define management strategies to promote trees health.

MATERIALS AND METHOD

The experimental field was part of an IPM research program in peach at the Clemson University's Musser Fruit Research Center located in Seneca, South Carolina USA (34.601°N, −82.873°W, WGS84). The experimental orchard consisted of 85 peach trees, five-year-old *PF-23* trees on Guardian® rootstock trained to the perpendicular-V system, under the common growing management practices of the region. The peach trees were planted in five rows of 17 trees each, at a distance of 1.5 m between them and 6 m between rows, on a sandy loam soil. The design was a split-plot design with two factors, being the K fertilization and the soil management (Figure 6.1). The fertilization was applied by hand underneath the trees' canopies with the following pattern: three rows with the standard K rate (1 kg/ha) and two with five times the standard K rate (5 kg/ha). For the soil management, per row, half of the tress were non-excavated and half were under root collar excavation. The following four treatments combinations were evaluated: non-excavated+K, non-excavated+5K, excavated+K, and excavated+5K. Peach rust presence assessment consisted on rating visually the degree of defoliation and also laboratory analysis. Four stages of disease presence were defined based on the assessment: healthy (no defoliation), low (<20% defoliation), medium (20%–50%), and high (>50%).

The aerial images were captured in September 2019 using a Senop HSC-2 hyperspectral camera (Senop Oy, Oulu, Finland) mounted on a DJI Matrice 600 Pro UAV (DJI Technology Co., Ltd, Shenzhen, China). The specifications of the camera were as follows: spectral range

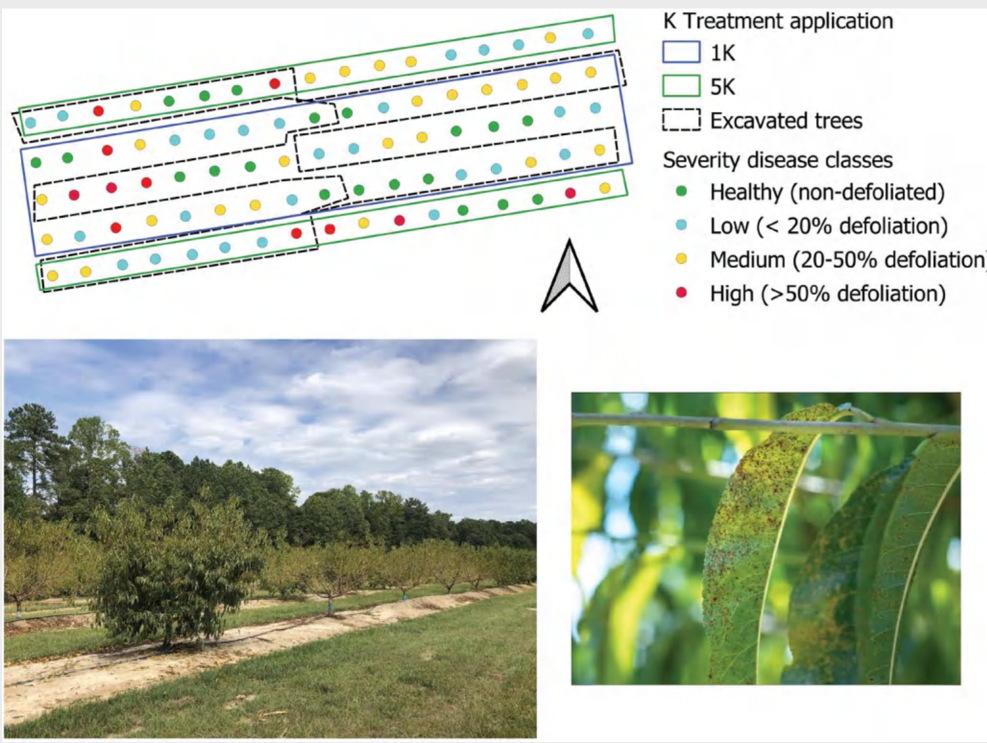

FIGURE 6.1 Experimental design and spatial distribution of the trees classified by disease severity stage, picture of the experiment, and yellow lesions detail.

of 500–900 nm with a 1.0 nm bandwidth, 1-megapixel resolution (1024 × 1024 pixels), and 12 bits radiometric resolution. As the flight was performed at 50 m altitude, the images had a 5 cm/pixel spatial resolution. Image processing was conducted using Agisoft Metashape Professional (Agisoft LLC, St. Petersburg, Russia). The orthomosaicked image was built following the protocol described in De Castro et al. (2018), resulting in a unique image of 203 spectral bands. Radiometric correction was performed using ENVI (ENVI, Research Systems Inc., Boulder, CO, USA) with the empirical line method (Smith & Milton, 1999). This method adjusted the digital values of the HSI to match reference reflectance spectra, converting them into reflectance values. The calibration reference spectra were obtained from two field calibration targets placed during image capture, one with 2% reflectance (black) and another with 83% (white).

An object-based image analysis (OBIA) algorithm was developed for automatic tree delimitation and spectral data retrieval in eCognition Developer 9 (Trimble GeoSpatial, Munich, Germany) software. The algorithm consisted of five steps: (1) segmentation, (2) tree and bare soil classification, (3) tree edges buffering, (4) spectral information retrieval, and (5) data exportation for analysis. Only the central part of the canopy, i.e., ten pixels, was considered to avoid mixed pixels and then the averaged spectral values for each tree were extracted. The spectral data was grouped in four classes corresponding to disease severity (healthy, low, medium, and high). The difference between the groups was analyzed with ANOVA (analysis of variance) test at the 0.01 significance level by a Tukey Honestly Significant Difference (HSD) range test carried out in the JMP software (version 12, SAS Institute Inc., Cary, NC, USA). Moreover, spectral data between classes was compared to determine spectral variations in the wavebands.

RESULTS AND DISCUSSION

Significant differences were obtained in the analysis for either management practices and the severity classes nonetheless in different regions of the spectrum, i.e., spectral bands. In the case of healthy trees, the hyperspectral signature for each K-treatment (1K and 5K) was significantly different and could be distinguished using specific wavelengths in the red-edge (699) and NIR (771 and 886) region (Figure 6.2). The effect of the K nutrient treatment could be related to the number of pigments in the leaves, such that the caused biochemical and cell structure alterations lead to changes in those spectral regions.

Similar regions were depicted in the work by De Castro et al. (2015) on laurel wilt and phytophthora root rot in avocado. In the case of soil management, the differences were found in the visual spectral region: green (510–520, 524–528, 540–597, 532–536, 601–617) and red (639–707) wavelengths. Hence, discrimination between conventional soil management and root collar excavation was achieved confirming that soil treatment around the roots also affected the spectral profiles, mainly due to changes in the physiological status of the trees. When the four disease classes were compared, differences in the spectral data were observed in the Green (510, 514–520), Red (653–667, 671–679), and NIR (854, 896–900) regions. The red-edge did not appear to be sensible enough to detect differences between disease levels. The distinction between the healthy trees class and the lower disease level was significant. In the case of medium and high disease level, as they presented very similar spectral values, it was difficult to differentiate them. An accurate and early identification of affected trees is key to act and prevent the spread of the disease to the healthy trees. From the data analyzed it was possible to detect lower disease level and distinguish them from healthy trees, which would allow early management decision to be taken. The results confirmed the potential of hyperspectral data to differentiate between disease levels and evaluate treatments effects in

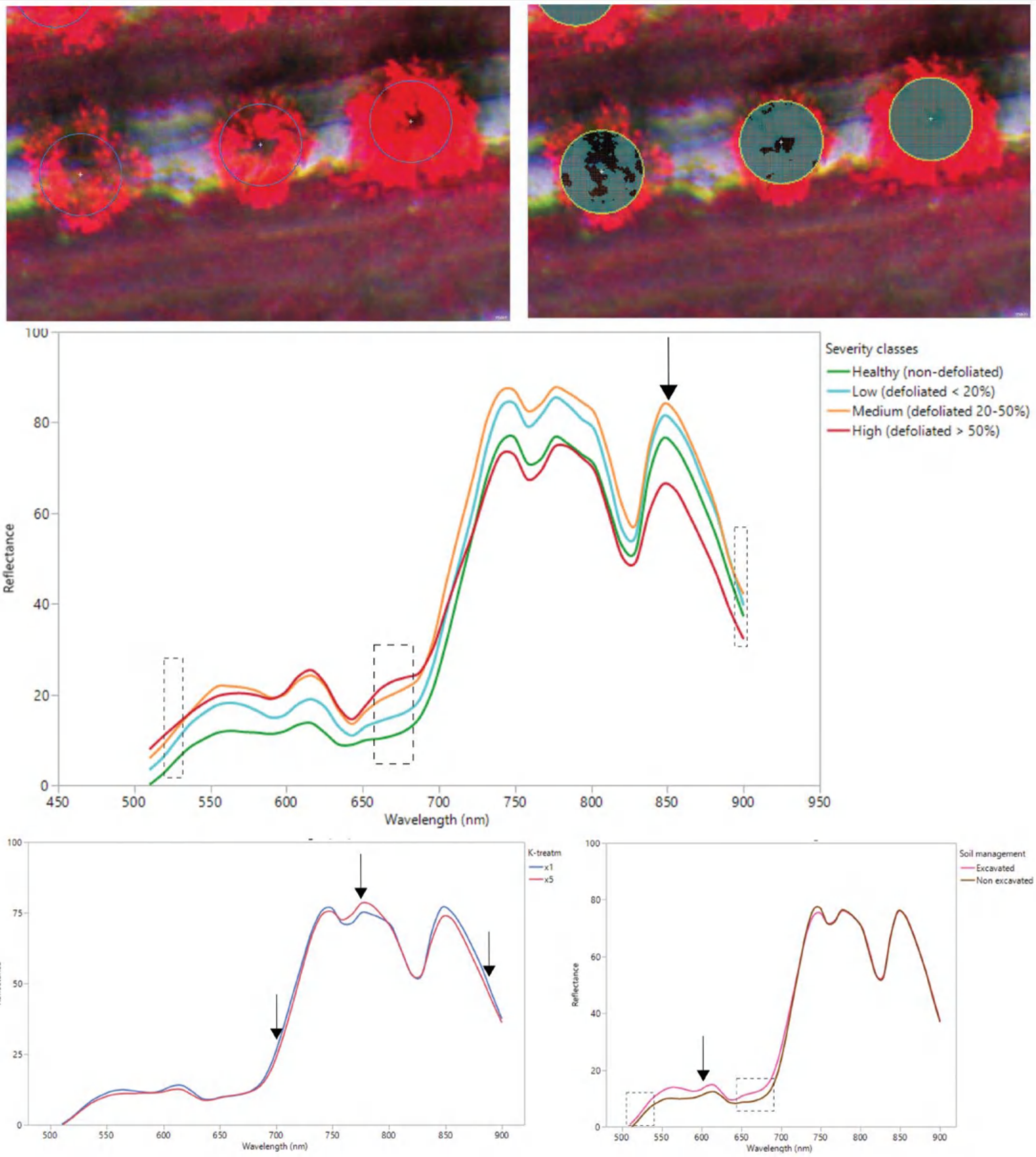

FIGURE 6.2 Zoom of three peach trees with canopy section considered and pixels selected to extract spectral data marked by a blue circle; spectral signature divided by severity classes with significant region marked by a box or arrow; and spectral signature of healthy tree class with significant wavelengths marked by practice (K-treatment and root-collar excavation).

peach trees by spectral signature analysis as significant differences were obtained and spectral signature variations detected. In order to decrease processing time and increase speed to establish strategies to perform site-specific management, a possibility could be to reduce the number of wavelengths and only consider the crucial ones or the most sensible to the effects. Further research could be carried out by combining spectral bands in (vegetation) ratios to enhance the discrimination power of the hyperspectral data.

CASE STUDY 2

INTRODUCTION

In commercial young peach tree fields, water scarcity is common during the first years as it is a non-irrigated production system (Zambrano-Vaca et al., 2020). A demonstrated practice to improve crop tolerance to biotic and abiotic stresses, including the mitigation of drought effects, is the exogenous application of Si (Fernández-Escobar, 2019; Ma, 2004). Silicon exerts its protective effects through morpho-physiological, biochemical or molecular processes. One fundamental mechanism through Si is to bolster the accumulation of Si in the cell walls, thus forming a cuticle-Si double layer, improving the plants' architecture, reducing leaf water loss, and maximizing water use efficiency (Debona et al., 2017; Ma et al., 2001). As plant physiology is sensible to stress and changes occur, e.g., stomatal closure that leads to decrease leaf gas exchange, imagery, and sensors can be used to achieve stress detection based on (hyper)spectral data (De Castro et al., 2021). In this case, the effect of Si treatments and water regimes is monitored via the hyperspectral signature response of peach trees.

MATERIALS AND METHOD

The experiment consisted of 60 two-year-old peach trees [*P. persica* (L.) Batsch cv. Contender] established in 19-L plastic pots placed in a shade house located at the Clemson University's Musser Fruit Research Farm (Seneca, SC, USA; lat. 34.61°N, long. 82.87°W). The experimental design consisted of ten subsets of six trees each, where half of them were irrigated and the other half were subjected to water stress by withholding irrigation. The subsets were supplied with two Si products: pure Si (Sigma Aldrich, St. Louis, MO, USA) containing 99+ % Si and a commercial brand (YaraVita Actisil® (Bio Minerals N.V., Destelbergen, Belgium)), whose active compound is choline-stabilized orthosilicic acid (containing 0.5% Si, w/v), in doses of 2 and 4 ppm at several moments throughout the study. Two subsets, one irrigated and one non-irrigated, were kept as control. Tree water status was monitored by measuring stem water potential using a Scholander-type pressure bomb (PMS Instrument Co., Albany, OR, USA; Scholander et al., 1965). Shortly before the image acquisition, the 60 pots were moved outdoors and subsequently returned to the shade house.

Three UAV flights with a hexacopter drone model DJI Matrice 600 Pro (DJI Technology Co., Ltd, Shenzhen, China) were carried out at 20 m altitude. Imagery was captured with the hyperspectral camera model Senop HSC-2 (Senop Oy, Oulu, Finland) on 19 September, 2 October, and 13 November 2019, during the central hours of the day to avoid shading. The camera has a spectral range of 500–900 nm, 1.0 nm of bandwidth, 1 megapixel of resolution (1024 × 1024 pixels), and 12 bits of radiometric resolution. At this flight altitude, the images had a 2.5 cm/pixel size as spatial resolution. The workflow to analyze the hyperspectral information included the following steps: (1) radiometric correction of the images to convert digital numbers (raw pixel values) to reflectance via empirical line method in ENVI (ENVI, Research Systems Inc., Boulder, CO, USA), (2) individual trees delineation via image segmentation and classification using an OBIA algorithm, (3) tree canopy (pure pixels) hyperspectral signatures extraction in eCognition Developer 9 (Trimble GeoSpatial, Munich, Germany) software, and (4) spectral data analysis in the JMP software (version 12, SAS Institute Inc., Cary, NC, USA).

RESULTS AND DISCUSSION

The results of the comparisons between each subset or treatment are here presented. The purpose of the analysis carried out was to detect reflectance differences. Significant differences

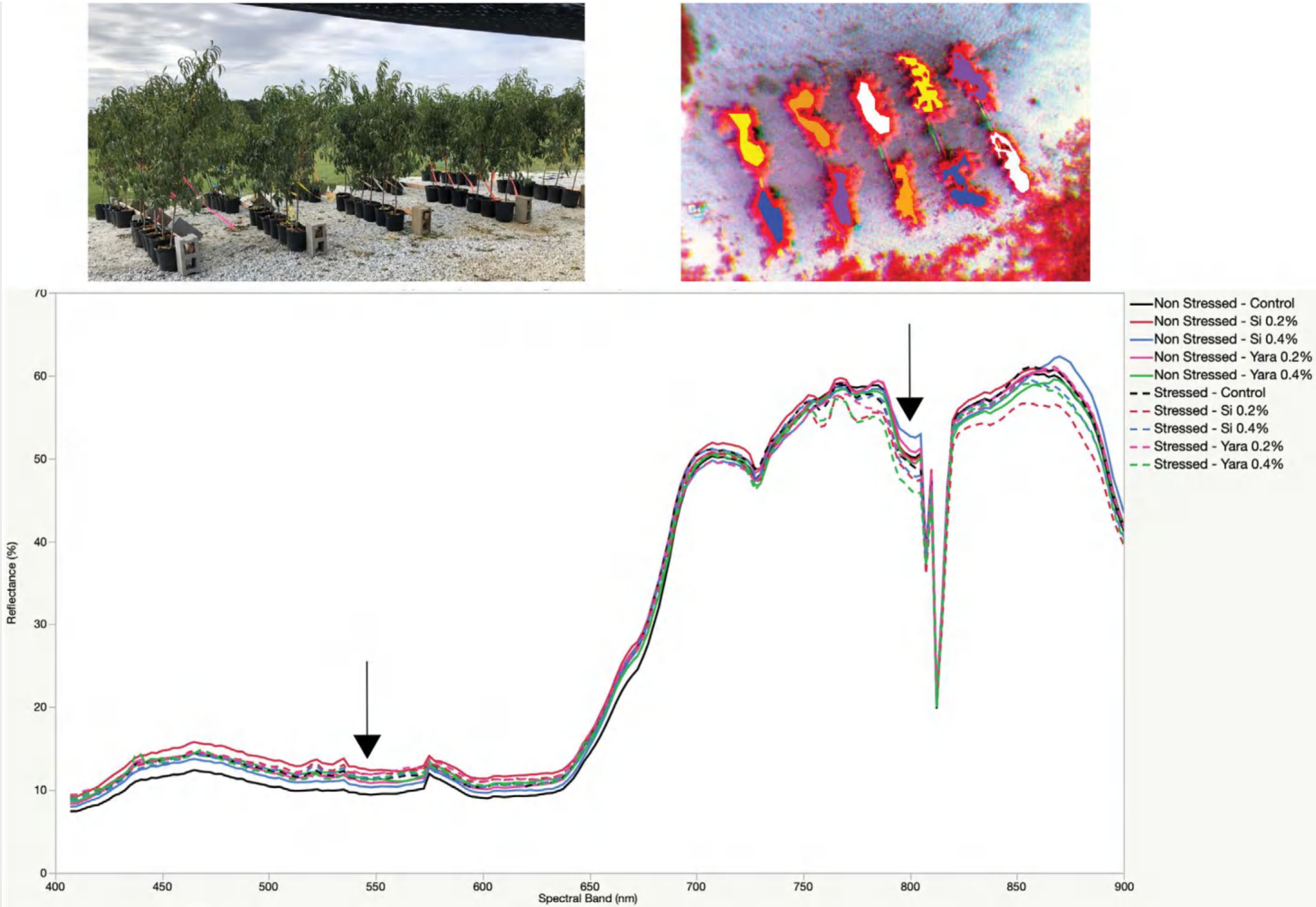

FIGURE 6.3 Picture of the experimental; pixels selected to extract spectral data; and spectral signature per treatment with most significant wavelengths marked by an arrow.

in the green and near-infrared regions were found already at the first date. Monitoring these wavelengths provides valuable insights into plant status and water stress. An effect on the spectral signature occurred in those regions as plant physiology changed due to water stress, e.g., chlorophyll degradation or leaf turgor pressure that reduces reflectance. Canopy structure could also be affected and alter light reflection. The camera characteristics and its sensitivity allowed to capture the subtle changes in the spectral data.

The most striking differences were found between (1) irrigated trees without Si application (control) and irrigated trees with pure 2 ppm dose of Si application in the green region; and (2) between irrigated trees with 4 ppm dose of pure Si and non-irrigated trees (stressed) with 2 ppm dose of commercial Si application in the infrared region (Figure 6.3). Similar spectral regions were found significant in the first case study presented in the chapter.

6.3 CONCLUSIONS

By the two cases presented, the potential of using hyperspectral data to examine and monitor peach orchards and their threats have been proved. In both cases, rapid and reliable data collection and the monitoring of each individual tree were possible. Health tree status monitoring via technical solutions based on UAV and HSI would greatly benefit and facilitate orchard management decisions. Further works and advancements in HSI are needed to reduce the constraints and widespread its use.

DECLARATION

This research was funded by the following projects: PID2023-150108OB-C31 and PID2023-150108OB-C32 from the Spanish MCIU/AEI/10.13039/501100011033, FSE+ and the project ECOdigital (ref. MMT24-ICA-01) and DIgitalWeeds (ref. MMT24-INIA-01) of the MOMENTUM CSIC program, and the European Union – NextGenerationEU, through the Recovery, Transformation and Resilience Plan (PRTR).

REFERENCES

Abdulridha, J., Ampatzidis, Y., Ehsani, R., & de Castro, A. I. (2018). Evaluating the performance of spectral features and multivariate analysis tools to detect laurel wilt disease and nutritional deficiency in avocado. *Computers and Electronics in Agriculture*, *155*(December), 203–111. https://doi.org/10.1016/J.COMPAG.2018.10.016

Adaskaveg, J. E., Duncan, R. A., Hasey, J. K., & Day, K. R. (2012). *UC IPM pest management guidelines: Peach*. Publication 3454. Davis, CA: University of California Agriculture and Natural Resources. http://www.ipm.ucdavis.edu/PMG/selectnewpest.peach.html

Alcobendas, R., Mirás-Avalos, J. M., Alarcón, J. J., & Nicolás, E. (2013). Effects of irrigation and fruit position on size, colour, firmness and sugar contents of fruits in a mid-late maturing peach cultivar. *Scientia Horticulturae*, *164*(December), 340–347. https://doi.org/10.1016/J.SCIENTA.2013.09.048

Arapostathi, E., Panopoulou, C., Antonopoulos, A., Katsileros, A., Karellas, K., Dimopoulos, C., & Tsagkarakis, A. (2024). Early detection of potential infestation by *Capnodis tenebrionis* (L.) (Coleoptera: Buprestidae), in stone and pome fruit orchards, using multispectral data from a UAV. *Agronomy*, *14*(1), 20. https://doi.org/10.3390/AGRONOMY14010020

Ballester, C., Zarco-Tejada, P. J., Nicolás, E., Alarcón, J. J., Fereres, E., Intrigliolo, D. S., & Gonzalez-Dugo, V. (2018). Evaluating the performance of xanthophyll, chlorophyll and structure-sensitive spectral indices to detect water stress in five fruit tree species. *Precision Agriculture*, *19*(1), 178–193. https://doi.org/10.1007/S11119-017-9512-Y

Cao, K., Zheng, Z., Wang, L., Liu, X., Zhu, G., Fang, W., Cheng, S., Zeng, P., Chen, C., Wang, X., Xie, M., Zhong, X., Wang, X., Zhao, P., Bian, C., Zhu, Y., Zhang, J., Ma, G. Chen, C., Li, Y., Hao, F., Li, Y., Huang, G., Li, Y., Li, H., Guo, J., Xu, X., & Wang, J. (2014). Comparative population genomics reveals the domestication history of the peach, *Prunus persica*, and human influences on perennial fruit crops. *Genome Biology*, *15*(7), 1–15. https://doi.org/10.1186/s12870-024-05437-2

Castillo-Ruiz, F. J., Jiménez-Jiménez, F., Blanco-Roldán, G. L., Sola-Guirado, R., Agüera-Vega, J., & Castro-Garcia, S. (2015). Analysis of fruit and oil quantity and quality distribution in high-density olive trees in order to improve the mechanical harvesting process. *Spanish Journal of Agricultural Research*, *13*(2), e0209–e0209. https://doi.org/10.5424/SJAR/2015132-6513

Chai, Q., Gan, Y., Zhao, C., Xu, H. L., Waskom, R. M., Niu, Y., & Siddique, K. H. M. (2015). Regulated deficit irrigation for crop production under drought stress. A review. *Agronomy for Sustainable Development*, *36*(1), 1–21. https://doi.org/10.1007/S13593-015-0338-6

Chen, B., Jin, Y., & Brown, P. (2019). An enhanced bloom index for quantifying floral phenology using multi-scale remote sensing observations. *ISPRS Journal of Photogrammetry and Remote Sensing*, *156*(October), 108–120. https://doi.org/10.1016/J.ISPRSJPRS.2019.08.006

Colaço, A. F., Molin, J. P., Rosell-Polo, J. R., & Escolà, A. (2018). Application of light detection and ranging and ultrasonic sensors to high-throughput phenotyping and precision horticulture: Current status and challenges. *Horticulture Research*, *5*(1), 1–11. https://doi.org/10.1038/s41438-018-0043-0

Conesa, M. R., Conejero, W., Vera, J., Ramírez-Cuesta, J. M., & Ruiz-Sánchez, M. C. (2019). Terrestrial and remote indexes to assess moderate deficit irrigation in early-maturing nectarine trees. *Agronomy*, *9*(10), 630. https://doi.org/10.3390/AGRONOMY9100630

Dandois, J. P., & Ellis, E. C. (2013). High spatial resolution three-dimensional mapping of vegetation spectral dynamics using computer vision. *Remote Sensing of Environment*, *136*, 259–276. https://doi.org/10.1016/j.rse.2013.04.005

de Castro, A. I., Ehsani, R., Ploetz, R., Crane, J. H., & Abdulridha, J. (2015). Optimum spectral and geometric parameters for early detection of laurel wilt disease in avocado. *Remote Sensing of Environment*, *171*, 33–44. https://doi.org/10.1016/j.rse.2015.09.011

de Castro, A. I., Jiménez-Brenes, F. M., Torres-Sánchez, J., Peña, J. M., Borra-Serrano, I., & López-Granados, F. (2018). 3-D characterization of vineyards using a novel UAV imagery-based OBIA procedure for precision viticulture applications. *Remote Sensing*, *10*(4), 584. https://doi.org/10.3390/rs10040584

de Castro, A. I., Shi, Y., Maja, J. M., & Peña, J. M. (2021). UAVs for vegetation monitoring: Overview and recent scientific contributions. *Remote Sensing*, *13*(11), 2139. https://doi.org/10.3390/RS13112139.

de Castro, A. I., Rallo, P., Suárez, M. P., Torres-Sánchez, J., Casanova, L., Jiménez-Brenes, F. M., Morales-Sillero, A., Jiménez, M. R., & López-Granados, F. (2019). High-throughput system for the early quantification of major architectural traits in olive breeding trials using UAV images and OBIA techniques. *Frontiers in Plant Science*, *10*(November), 447848. https://doi.org/10.3389/FPLS.2019.01472

Debona, D., Rodrigues, F. A., & Datnoff, L. E. (2017). Silicon's role in abiotic and biotic plant stresses. *Annual Review of Phytopathology*, *55*, 85–107. https://doi.org/10.1146/ANNUREV-PHYTO-080516-035312

Deng, X., Zhu, Z., Yang, J., Zheng, Z., Huang, Z., Yin, X., Wei, S., & Lan, Y. (2020). Detection of citrus huanglongbing based on multi-input neural network model of UAV hyperspectral remote sensing. *Remote Sensing*, *12*(17), 2678. https://doi.org/10.3390/RS12172678

Dennis, Jr., F. G. (2000). The history of fruit thinning. *Plant Growth Regulation*, *31*(1), 1–16. https://doi.org/10.1023/A:1006330009160.

Di Gennaro, S. F., Toscano, P., Gatti, M., Poni, S., Berton, A., & Matese, A. (2022). Spectral comparison of UAV-based hyper and multispectral cameras for precision viticulture. *Remote Sensing*, *14*(3), 449. https://doi.org/10.3390/RS14030449

Dong, X., Zhang, Z., Yu, R., Tian, Q., & Zhu, X. (2020). Extraction of information about individual trees from high-spatial-Resolution UAV-acquired images of an orchard. *Remote Sensing*, *12*(1), 133. https://doi.org/10.3390/RS12010133

FAOSTAT. (2022). *FAOSTAT statistical database*. Rome: Food and Agriculture Organization of the United Nations (FAO).

Fernández-Escobar, R. (2019). Olive nutritional status and tolerance to biotic and abiotic stresses. *Frontiers in Plant Science*, *10*(September), 1151. https://doi.org/10.3389/FPLS.2019.01151

Herrero-Huerta, M., Hernández-López, D., Rodriguez-Gonzalvez, P., González-Aguilera, D., & González-Piqueras, J. (2014). Vicarious radiometric calibration of a multispectral sensor from an aerial trike applied to precision agriculture. *Computers and Electronics in Agriculture*, *108*(October), 28–38. https://doi.org/10.1016/J.COMPAG.2014.07.001

Honkavaara, E., Rosnell, T., Oliveira, R., & Tommaselli, A. (2017). Band registration of tuneable frame format hyperspectral UAV imagers in complex scenes. *ISPRS Journal of Photogrammetry and Remote Sensing*, *134*(December), 96–109. https://doi.org/10.1016/J.ISPRSJPRS.2017.10.014

Horton, R., Cano, E., Bulanon, D., & Fallahi, E. (2017). Peach flower monitoring using aerial multispectral imaging. *Journal of Imaging*, *3*(1), 2. https://doi.org/10.3390/JIMAGING3010002

Huang, Z., Turner, B. J., Dury, S. J., Wallis, I. R., & Foley, W. J. (2004). Estimating foliage nitrogen concentration from HYMAP data using continuum removal analysis. *Remote Sensing of Environment*, *93*(1–2), 18–29. https://doi.org/10.1016/J.RSE.2004.06.008

Iqbal, F., Lucieer, A., & Barry, K. (2018). Simplified radiometric calibration for UAS-mounted multispectral sensor. *European Journal of Remote Sensing*, *51*(1), 301–313. https://doi.org/10.1080/22797254.2018.1432293

Jiménez-Brenes, F. M., López-Granados, F., Castro, A. I., Torres-Sánchez, J., Serrano, N., & Peña, J. M. (2017). Quantifying pruning impacts on olive tree architecture and annual canopy growth by using UAV-based 3D modelling. *Plant Methods*, *13*(1), 55. https://doi.org/10.1186/s13007-017-0205-3

Johansen, K., Raharjo, T., & McCabe, M. F. (2018). Using multi-spectral UAV imagery to extract tree crop structural properties and assess pruning effects. *Remote Sensing*, *10*(6), 854. https://doi.org/10.3390/RS10060854

Kuswidiyanto, L. W., Noh, H. H., & Han, X. (2022). Plant disease diagnosis using deep learning based on aerial hyperspectral images: A review. *Remote Sensing*, *14*(23), 6031. https://doi.org/10.3390/RS14236031

Layne, D.R. (2011). Simple, innovative practices to get high quality fruit to the early market in China. E.S.P.S. Invited seminar on February 7, 2011. Available in: http://www.clemson.edu/extension/peach/video_everything_about_peaches/esps_seminar.html

López-Granados, F., Torres-Sánchez, J., Jiménez-Brenes, F. M., Arquero, O., Lovera, M., & De Castro, A. I. (2019). An efficient RGB-UAV-based platform for field almond tree phenotyping: 3-D architecture and flowering traits. *Plant Methods*, *15*(1), 1–16. https://doi.org/10.1186/S13007-019-0547-0

Luo, C. X., Schnabel, G., Hu, M., & De Cal, A. (2022). Global distribution and management of peach diseases. *Phytopathology Research*, *4*(1), 1–15. https://doi.org/10.1186/S42483-022-00134-0

Ma, J. F. (2004). Role of silicon in enhancing the resistance of plants to biotic and abiotic stresses. *Soil Science and Plant Nutrition*, *50*(1), 11–18. https://doi.org/10.1080/00380768.2004.10408447

Ma, J. F., Miyake, Y., & Takahashi, E. (2001). Chapter 2 silicon as a beneficial element for crop plants. *Studies in Plant Science*, *8*(C), 17–39. https://doi.org/10.1016/S0928-3420(01)80006-9

Maes, W. H., & Steppe, K. (2019). Perspectives for remote sensing with unmanned aerial vehicles in precision agriculture. *Trends in Plant Science*, *24*(2), 152–164. https://doi.org/10.1016/j.tplants.2018.11.007

Marschner, P. (2012). *Marschner's mineral nutrition of higher plants* (3rd ed., pp. 1–651) Elsevier Inc. https://doi.org/10.1016/C2009-0-63043-9

Matese, A., Prince Czarnecki, J. M., Samiappan, S., & Moorhead, R. (2024). Are unmanned aerial vehicle-based hyperspectral imaging and machine learning advancing crop science? *Trends in Plant Science*, *29*(2), 196–209. https://doi.org/10.1016/J.TPLANTS.2023.09.001

Miller, S. B., Gasic, K., Reighard, G. L., Henderson, W. G., Rollins, P. A., Vassalos, M., & Schnabel, G. (2020). Preventative root-collar excavation reduces peach tree mortality caused by Armillaria root rot on replant sites. *Plant Disease*, *104*(5), 1274–1279. https://doi.org/10.1094/PDIS-09-19-1831-RE

Miranda-Fuentes, A., Llorens, J., Gamarra-Diezma, J. L., Gil-Ribes, J. A., & Gil, E. (2015). Towards an optimized method of olive tree crown volume measurement. *Sensors*, *15*(2), 3671–3687. https://doi.org/10.3390/S150203671

Mishra, P., Polder, G., & Vilfan, N. (2020). Close range spectral imaging for disease detection in plants using autonomous platforms: A review on recent studies. *Current Robotics Reports*, *1*(2), 43–48. https://doi.org/10.1007/s43154-020-00004-7.

Mishra, P., Shahrimie, M., Asaari, M., Herrero-Langreo, A., Lohumi, S., Diezma, B., & Scheunders, P. (2017). Close range hyperspectral imaging of plants: A review. *Biosystems Engineering*, *164*(December), 49–67. https://doi.org/10.1016/J.BIOSYSTEMSENG.2017.09.009

Moriya, E., Saito, A., Imai, N. N., Garcia Tommaselli, A. M., Berveglieri, A., Santos, G. H., Soares, M. A., Marino, M., & Tiedtke Reis, T. (2021). Detection and mapping of trees infected with citrus gummosis using UAV hyperspectral data. *Computers and Electronics in Agriculture*, *188*(September), 106298. https://doi.org/10.1016/J.COMPAG.2021.106298

Mulla, D. J. (2013). Twenty five years of remote sensing in precision agriculture: Key advances and remaining knowledge gaps. *Biosystems Enginieering*, *114*, 358–371. https://doi.org/10.1016/j.biosystemseng.2012.08.009

Omia, E., Bae, H., Park, E., Kim, M. S., Baek, I., Kabenge, I., & Cho, B. K. (2023). Remote sensing in field crop monitoring: A comprehensive review of sensor systems, data analyses and recent advances. *Remote Sensing*, *15*(2), 354. https://doi.org/10.3390/RS15020354

Park, S., Ryu, D., Fuentes, S., Chung, H., Hernández-Montes, E., & O'Connell, M. (2017). Adaptive estimation of crop water stress in nectarine and peach orchards using high-Resolution imagery from an unmanned aerial vehicle (UAV). *Remote Sensing*, *9*(8), 828. https://doi.org/10.3390/RS9080828

Perry, E. M., Goodwin, I., & Cornwall, D. (2018). Remote sensing using canopy and leaf reflectance for estimating nitrogen status in red-blush pears. *HortScience*, *53*(1), 78–83. https://doi.org/10.21273/HORTSCI12391-17

Popescu, D., Ichim, L., & Stoican, F. (2023). Orchard monitoring based on unmanned aerial vehicles and image processing by artificial neural networks: A systematic review. *Frontiers in Plant Science*, *14*(November), 1237695. https://doi.org/10.3389/FPLS.2023.1237695

Proctor, C., & He, Y. (2015). Workflow for building a hyperspectral UAV: Challenges and opportunities. *International Archives of the Photogrammetry, Remote Sensing and Spatial Information Sciences – ISPRS Archives*, *40*(1W4), 415–419. https://doi.org/10.5194/isprsarchives-XL-1-W4-415-2015

Ram, B. G., Oduor, P., Igathinathane, C., Howatt, K., & Sun, X. (2024). A systematic review of hyperspectral imaging in precision agriculture: Analysis of its current state and future prospects. *Computers and Electronics in Agriculture*, *222*(July), 109037. https://doi.org/10.1016/J.COMPAG.2024.109037

Raman, M. Govindasamy, Carlos, E. F., & Sankaran, S. (2022). Optimization and evaluation of sensor angles for precise assessment of architectural traits in peach trees. *Sensors*, *22*(12), 4619. https://doi.org/10.3390/S22124619

Roth, L., Hund, A., & Aasen, H. (2018). PhenoFly planning tool: Flight planning for high-resolution optical remote sensing with unmanned areal systems. *Plant Methods*, *14*(1), 1–21. https://doi.org/10.1186/S13007-018-0376-6

Sarron, J., Malézieux, E., Bassirou Sané, C. A., & Faye, E. (2018). Mango yield mapping at the orchard scale based on tree structure and land cover assessed by UAV. *Remote Sensing*, *10*(12), 1900. https://doi.org/10.3390/RS10121900

Scholander, P. F., Bradstreet, E. D., Hemmingsen, E. A., & Hammel, H. T. (1965). Sap pressure in vascular plants: Negative hydrostatic pressure can be measured in plants. *Science*, *148*(3668), 339–346.

Schoofs, H., Delalieux, S., Deckers, T., & Bylemans, D. (2020). Fire blight monitoring in pear orchards by unmanned airborne vehicles (UAV) systems carrying spectral sensors. *Agronomy*, *10*(5), 615. https://doi.org/10.3390/AGRONOMY10050615

Segarra, J., Buchaillot, M. L., Araus, J. L., & Kefauver, S. C. (2020). Remote sensing for precision agriculture: Sentinel-2 improved features and applications. *Agronomy*, *10*(5), 641. https://doi.org/10.3390/agronomy10050641

Smith, G. M., & Milton, E. J. (1999). The use of the empirical line method to calibrate remotely sensed data to reflectance. *International Journal of Remote Sensing*, *20*(13), 2653–2662. https://doi.org/10.1080/014311699211994

Soto-Estrada, A., Förster, H., DeMason, D. A., & Adaskaveg, J. E. (2007). Initial infection and colonization of leaves and stems of cling peach by *Tranzschelia discolor*. *Phytopathology*, *95*(8), 942–950. https://doi.org/10.1094/PHYTO-95-0942

Terentev, A., Dolzhenko, V., Fedotov, A., & Eremenko, D. (2022). Current state of hyperspectral remote sensing for early plant disease detection: A review. *Sensors*, *22*(3), 757. https://doi.org/10.3390/S22030757

Torres-Sánchez, J., López-Granados, F., Borra-Serrano, I., & Peña, J. M. (2018). Assessing UAV-collected image overlap influence on computation time and digital surface model accuracy in olive orchards. *Precision Agriculture*, *19*(1), 115–133. https://doi.org/10.1007/s11119-017-9502-0

Torres-Sánchez, J., López-Granados, F., Serrano, N., Arquero, O., & Peña, J. M. (2015). High-throughput 3-D monitoring of agricultural-tree plantations with unmanned aerial vehicle (UAV) technology. *PLoS ONE*, *10*(6), e0130479. https://doi.org/10.1371/journal.pone.0130479

Tu, Y. H., Phinn, S., Johansen, K., & Robson, A. (2018). Assessing radiometric correction approaches for multi-spectral UAS imagery for horticultural applications. *Remote Sensing*, *10*(11), 1684. https://doi.org/10.3390/RS10111684

Tu, Y. H., Phinn, S., Johansen, K., Robson, A., & Wu, D. (2020). Optimising drone flight planning for measuring horticultural tree crop structure. *ISPRS Journal of Photogrammetry and Remote Sensing*, *160*(February), 83–96. https://doi.org/10.1016/J.ISPRSJPRS.2019.12.006

Usha, K., & Singh, B. (2013). Potential applications of remote sensing in horticulture—A review. *Scientia Horticulturae*, *153*(April), 71–83. https://doi.org/10.1016/J.SCIENTA.2013.01.008

Wong, G. (2009). Snapshot hyperspectral imaging and practical applications. *Journal of Physics: Conference Series*, *178*(1), 012048. https://doi.org/10.1088/1742-6596/178/1/012048

Zambrano-Vaca, C., Zotarelli, L., Beeson, R. C., Morgan, K. T., Migliaccio, K. W., Chaparro, J. X., & Olmstead, M. A. (2020). Determining water requirements for young peach trees in a humid subtropical climate. *Agricultural Water Management*, *233*(April), 106102. https://doi.org/10.1016/J.AGWAT.2020.106102

Zhang, C., Valente, J., Kooistra, L., Guo, L., & Wang, W. (2021). Orchard management with small unmanned aerial vehicles: A survey of sensing and analysis approaches. *Precision Agriculture*, *22*(6), 2007–2052. https://doi.org/10.1007/S11119-021-09813-Y

Zhou, Q., & Melgar, J. C. (2019). Ripening season affects tissue mineral concentration and nutrient partitioning in peach trees. *Journal of Plant Nutrition and Soil Science*, *182*(2), 203–209. https://doi.org/10.1002/JPLN.201800304

Zude-Sasse, M., Akbari, E., Tsoulias, N., Psiroukis, V., Fountas, S., & Ehsani, R., et al. (2021). Sensing in precision horticulture. In Kerry, R. & Escolà, A. (Eds.), *Sensing approaches for precision agriculture* (pp. 221–251). Springer. https://doi.org/10.1007/978-3-030-78431-7_8

Zude-Sasse, M., Fountas, S., Gemtos, T. A., & Abu-Khalaf, N. (2016). Applications of precision agriculture in horticultural crops. *European Journal of Horticultural Science*, *81*(2), 78–90. https://doi.org/10.17660/EJHS.2016/81.2.2

7 Decision-Support Systems for Greenhouse Horticulture

Lucio Colizzi, Emanuela Guerriero, Tommaso Adamo, and Nunzia Lomonte

Smart Agriculture empowers farmers to collect and analyze data at a granular level, facilitating informed decisions tailored to specific site conditions. By leveraging Internet of Things (IoT) devices such as sensors, actuators, and drones, real-time data on parameters such as soil moisture, temperature, and crop health can be collected and transmitted for analysis.

Effective data modeling strategies are pivotal for managing the diverse and voluminous data generated by IoT devices in agricultural settings. This includes categorization, classification, and pre-processing techniques to streamline data management, enhance data quality, and facilitate decision-making processes. Moreover, robust data security measures are imperative to safeguard sensitive agricultural data from unauthorized access and breaches.

The proposal of template-based data models, including relational structures and potentially extended by NoSQL data structures, offers a comprehensive approach to meet any data requirement within the context of Smart Agriculture. This approach ensures flexibility and scalability, enabling stakeholders to harness valuable insights and drive informed decision-making for a more efficient and sustainable future in agriculture.

7.1 INTRODUCTION

7.1.1 Background on Smart Agriculture

In recent years, agriculture has undergone a significant transformation with the advent of Smart Agriculture. Smart Agriculture combines the use of advanced technologies, such as IoT, data analytics, and artificial intelligence (AI), to optimize agricultural practices and enhance productivity while minimizing resource consumption.

Traditional farming methods often relied on uniform approaches, treating entire fields or crops as homogeneous entities. However, with the emergence of Smart Agriculture, farmers can now gather and analyze data at a granular level, enabling them to make informed decisions based on site-specific conditions. This approach allows for precise management of inputs, such as water, fertilizers, and pesticides, leading to improved resource efficiency and reduced environmental impact.

The integration of IoT systems has played a crucial role in enabling Smart Agriculture. IoT devices, such as sensors, actuators, and drones, are deployed throughout agricultural fields to collect real-time data on various parameters, including soil moisture, temperature, humidity, crop health, and weather conditions. These devices communicate with each other and transmit data to a central system for analysis and decision-making.

The availability of comprehensive data from IoT systems provides farmers with valuable insights into the condition of their crops and soil, helping them optimize irrigation schedules, detect diseases or pests early, and apply targeted interventions. Moreover, advanced analytics techniques, such as machine learning algorithms, enable the extraction of valuable patterns and trends from the collected data, further enhancing the efficiency and effectiveness of agricultural practices.

DOI: 10.1201/9781003510598-7

Overall, Smart Agriculture has the potential to revolutionize the way crops are cultivated, making agriculture more sustainable, productive, and economically feasible. By harnessing the power of IoT systems and data organization strategies, farmers can make data-driven decisions and optimize resource allocation for maximum yields while minimizing environmental impact.

7.1.2 Importance of Data Organization in IoT Systems

In the context of IoT systems applied to Smart Agriculture, data organization plays a crucial role in ensuring the effectiveness and efficiency of agricultural operations. The sheer volume and variety of data generated by IoT devices in agricultural settings necessitate robust data organization strategies to make sense of the information and derive actionable insights.

Proper data organization allows for the systematic storage, retrieval, and analysis of data collected from various sources within an IoT system. It involves structuring the data in a coherent and meaningful manner, making it easier to manage, process, and interpret. Effective data organization enhances the quality and reliability of the data, enabling accurate decision-making in agricultural practices.

One key aspect of data organization is the categorization and classification of the collected data. By grouping similar types of data together, such as soil moisture readings, crop growth measurements, or weather data, farmers and researchers can quickly access and analyze specific information relevant to their objectives. This classification facilitates data retrieval and reduces the time and effort required to extract valuable insights from the vast amounts of data.

Data organization also encompasses data pre-processing and filtering techniques. IoT systems generate massive amounts of raw data, which may contain noise, outliers, or irrelevant information. Pre-processing steps, such as data cleansing, normalization, and outlier detection, help to improve the data quality and eliminate inaccuracies that could potentially mislead decision-making processes.

Furthermore, data organization strategies in IoT systems consider data compression and optimization methods. As data volumes continue to grow exponentially, efficient compression techniques reduce storage requirements and enhance data transmission efficiency. This allows for faster data transfer and real-time analytics and minimizes the impact on network bandwidth.

Data security and privacy considerations are another critical aspect of data organization in IoT systems. As agricultural data contains sensitive information about crops, farming practices, and potentially personal data, it is essential to implement robust security measures to protect against unauthorized access, data breaches, and cyber threats. Data organization strategies should incorporate encryption, access controls, and secure data-sharing protocols to ensure data integrity and confidentiality.

Effective data organization in IoT systems for Smart Agriculture is of paramount importance. It enables efficient data management, facilitates data analysis, improves decision-making, and safeguards data security and privacy. By implementing sound data organization strategies, farmers, researchers, and stakeholders can unlock the full potential of IoT systems, harnessing valuable insights to optimize agricultural practices and achieve sustainable, productive, and environmentally friendly outcomes.

7.1.3 Purpose of the Chapter

The purpose of this chapter is to delve into the strategies for organizing data in IoT systems applied to Smart Agriculture. By examining the various aspects of data organization, including categorization, pre-processing, compression, security, and privacy, this chapter aims to provide readers with a comprehensive understanding of how to effectively manage and utilize the vast amounts of data generated in agricultural IoT environments.

Specifically, this chapter will explore the significance of data organization in IoT systems and highlight its role in optimizing agricultural operations. It will emphasize the importance of structured data management in enabling data-driven decision-making and the extraction of valuable insights for improved resource allocation, crop monitoring, and yield optimization. Additionally, this chapter will discuss the challenges associated with data organization in IoT systems applied to Smart Agriculture, such as handling diverse data types, ensuring data quality, addressing scalability issues, and safeguarding data security and privacy. It will present strategies and best practices for addressing these challenges, providing practical guidance for implementing effective data organization approaches.

Furthermore, this chapter will showcase case studies of successful implementations of data organization strategies in real-world Smart Agriculture scenarios. These case studies will demonstrate how data organization techniques have been applied to optimize irrigation management, crop monitoring, and livestock tracking, highlighting the positive impact on agricultural productivity, resource efficiency, and environmental sustainability.

Overall, the purpose of this chapter is to equip readers with the knowledge and tools necessary to design and implement robust data organization strategies within IoT systems for Smart Agriculture. By understanding the importance of data organization and learning from practical examples, readers will be better equipped to harness the power of data in their agricultural practices, ultimately contributing to the advancement of sustainable and efficient farming techniques.

7.2 OVERVIEW OF IoT SYSTEMS IN SMART AGRICULTURE

7.2.1 Definition and Components of IoT Systems

In order to understand the role of IoT systems in Smart Agriculture, it is essential to define what IoT systems are and explore their key components.

IoT systems refer to networks of interconnected devices, sensors, and actuators that collect, exchange, and analyze data through the internet. These devices, often embedded with sensors and connected to the internet, enable the seamless integration and communication of physical objects and digital systems.

The components of IoT systems consist of the following:

1. *Sensors*: These are devices that gather data from the physical environment. In the context of Smart Agriculture, sensors are deployed in fields, greenhouses, and livestock areas to measure various parameters such as soil moisture, temperature, humidity, light intensity, crop growth, and livestock behavior. The data collected by sensors forms the foundation for data-driven decision-making in agriculture.
2. *Actuators*: Actuators are devices that perform actions based on the data received from sensors. In Smart Agriculture, actuators are used to control irrigation systems, adjust lighting conditions, open or close vents in greenhouses, activate machinery, and automate various processes. They enable remote control and automation of agricultural operations based on real-time data analysis.
3. *Communication Infrastructure*: IoT systems rely on communication infrastructure to transmit data between devices and central systems. This infrastructure can include wired and wireless networks, such as Wi-Fi, cellular networks, or low-power wide-area networks (LPWAN). It enables seamless connectivity and data exchange between sensors, actuators, and central control systems.
4. *Data Processing and Analytics*: IoT systems generate vast amounts of data from multiple sources. Data processing and analytics tools play a crucial role in extracting valuable insights from this data. Advanced analytics techniques, including machine learning algorithms and data visualization tools, are employed to derive meaningful information,

patterns, and trends from the collected data. These insights aid in making data-driven decisions for optimizing agricultural practices.

5. *Cloud System*: It represents the central control system and acts as the brain of the IoT system, managing and coordinating the flow of data between devices, processing the collected data, and executing commands to actuators based on the analysis and predefined rules. This central system may be located on-site or in the cloud, providing a centralized platform for data management, analysis, and control.

Understanding the definition and components of IoT systems provides a solid foundation for comprehending their application in Smart Agriculture. By harnessing the power of interconnected devices, data collection, and advanced analytics, IoT systems facilitate the optimization of agricultural processes, resource utilization, and decision-making for sustainable and efficient farming practices.

7.2.2 Role of IoT in Smart Agriculture

The integration of IoT technology has revolutionized the field of Smart Agriculture enhancing agricultural practices and enabling more efficient resource management. The role of IoT in Smart Agriculture is multifaceted and encompasses several key aspects:

- *Data Collection and Monitoring*: IoT devices, such as sensors and drones, are deployed throughout agricultural fields to collect real-time data on various parameters, including soil moisture, temperature, humidity, crop health, and weather conditions. These devices enable continuous and precise monitoring of crop and environmental conditions, providing farmers with valuable insights into the state of their crops and enabling proactive decision-making.
- *Precision Resource Management*: IoT systems play a crucial role in optimizing the management of resources in agriculture. By collecting data on soil moisture levels, temperature, and crop health, IoT devices allow for precise irrigation scheduling, reducing water waste and ensuring optimal hydration for crops. Similarly, IoT-enabled systems can monitor nutrient levels in the soil and apply fertilizers in a targeted manner, minimizing waste and maximizing crop health.
- *Disease and Pest Management*: Early detection and timely intervention are critical in combating diseases and pests in agriculture. IoT devices equipped with advanced sensors can detect signs of diseases or pests, such as changes in leaf temperature or pest activity, enabling farmers to take proactive measures. This facilitates the use of targeted treatments, reducing the need for excessive pesticide application and minimizing environmental impact.
- *Automation and Efficiency*: IoT systems enable automation and remote control of various agricultural processes. Actuators and smart devices can be programmed to perform tasks such as adjusting irrigation systems, opening or closing vents, or activating machinery based on real-time data inputs. This automation leads to increased efficiency, reduced labor requirements, and improved overall productivity.
- *Data-Driven Decision-Making*: The data collected by IoT devices in Smart Agriculture forms the foundation for data-driven decision-making. Advanced analytics techniques, such as machine learning algorithms, can be applied to the collected data to extract valuable patterns, trends, and predictive insights. This enables farmers to make informed decisions about crop management, resource allocation, and risk mitigation strategies, leading to improved yields and profitability.
- *Environmental Sustainability*: IoT systems contribute to environmental sustainability by optimizing resource usage and reducing the environmental impact of agriculture. By

precisely monitoring soil moisture and crop health, farmers can apply water and fertilizers only where and when needed, minimizing waste and nutrient runoff. Additionally, IoT-enabled pest and disease management strategies help reduce reliance on chemical treatments, promoting ecological balance and minimizing the ecological footprint of farming practices.

IoT technology plays a pivotal role in Smart Agriculture by enabling data collection, precision resource management, disease and pest management, automation, data-driven decision-making, and environmental sustainability. The integration of IoT systems in agriculture holds great potential for increasing productivity, efficiency, and sustainability while minimizing resource consumption and environmental impact.

7.2.3 Benefits and Challenges of IoT Data Management

IoT data management in Smart Agriculture brings about a multitude of benefits for farmers and stakeholders. By effectively managing the data generated by IoT devices, farmers can make informed decisions, optimize resource usage, and enhance productivity. However, this endeavor is not without its challenges, particularly in the absence of standardized frameworks and integration possibilities.

When it comes to the benefits of IoT data management, one of the most significant advantages is the enhanced decision-making it enables. By collecting and analyzing real-time data on crop conditions, resource usage, and environmental factors, farmers gain valuable insights that aid in making data-driven decisions. This leads to optimized irrigation schedules, improved fertilization strategies, and more effective pest control measures, resulting in increased yields and enhanced crop quality.

Another key benefit is the improved resource efficiency that IoT data management offers. By closely monitoring and analyzing IoT data, farmers can allocate resources, such as water and fertilizers, based on the specific needs of each crop or field. This targeted approach minimizes waste, increases overall efficiency, and saves costs while promoting sustainable agricultural practices.

IoT data management also enables predictive analytics, leveraging advanced techniques such as machine learning algorithms. By analyzing historical and real-time data, farmers can predict and mitigate potential risks such as crop diseases, pest outbreaks, or unfavorable weather conditions. This proactive approach minimizes crop losses and maximizes productivity, allowing for better risk management in agricultural operations. The ability to remotely monitor and control agricultural operations is another benefit of IoT data management. By accessing real-time data on crop health, environmental conditions, and machinery performance, farmers can address issues promptly and make adjustments as needed, without needing to be physically present on the farm. This remote monitoring capability enhances operational efficiency and provides flexibility in managing agricultural practices.

Furthermore, effective IoT data management facilitates collaboration and knowledge sharing among farmers, researchers, and stakeholders. By securely sharing and analyzing data, valuable insights and best practices can be exchanged, fostering innovation and collective learning in the field of Smart Agriculture. This collaborative approach paves the way for continuous improvement and the adoption of new and more efficient techniques.

Despite the numerous benefits, there are challenges associated with IoT data management in Smart Agriculture. One prominent challenge is the lack of standardized frameworks and protocols. The absence of common standards hampers seamless integration and interoperability between different IoT systems and solutions. As a result, solutions developed in isolation may have limited compatibility and integration possibilities, hindering the overall efficiency and effectiveness of IoT data management.

Ensuring data security and privacy is another significant challenge. IoT data management involves handling vast amounts of sensitive agricultural and environmental data. It is imperative to implement robust encryption, access controls, and secure data-sharing protocols to protect data integrity and confidentiality. This becomes even more critical considering the potential risks associated with unauthorized access or data breaches.

Maintaining data quality and reliability is also a challenge in IoT data management. IoT data may be prone to errors, noise, and inconsistencies. Effective data cleansing, validation, and quality assurance processes are necessary to ensure the reliability and accuracy of the collected data. Managing data from diverse sources and addressing issues such as missing or incomplete data require careful attention and appropriate methodologies. Scalability and infrastructure pose additional challenges in IoT data management. As the number of IoT devices and the volume of data generated continue to grow, scalable infrastructure becomes crucial. This includes robust networks, storage systems, and computational resources that can handle and process large-scale IoT data efficiently.

Last, cost and return on investment are important considerations. Implementing IoT data management solutions in Smart Agriculture requires initial investment in devices, sensors, connectivity, and analytics platforms. Farmers need to assess the potential return on investment and evaluate the economic feasibility of adopting IoT data management solutions in their specific agricultural operations.

7.3 DATA COLLECTION IN SMART AGRICULTURE

7.3.1 Sensors and IoT Devices for Data Collection

In Smart Agriculture, sensors and IoT devices play a crucial role in collecting data from the environment and crops. These devices come in various types, each designed to capture specific parameters and provide valuable insights for farmers. Let's explore different types of sensors commonly used in IoT systems for data collection:

- *Capacitive Sensors*: Capacitive sensors are widely used in Smart Agriculture to measure soil moisture levels. These sensors work by detecting changes in the electrical capacitance caused by the presence or absence of water in the soil. They provide real-time data on soil moisture, enabling farmers to determine optimal irrigation schedules and prevent over- or under-watering.
- *Resistive Sensors*: Resistive sensors are used to measure soil temperature. These sensors work by assessing the electrical resistance of the material, which changes with temperature variations. By monitoring soil temperature, farmers can make informed decisions regarding crop planting, growth, and disease prevention.
- *Photometric Sensors*: Photometric sensors are utilized to measure light intensity and photoperiods in agricultural settings. These sensors help farmers optimize lighting conditions for crops, especially in indoor or greenhouse environments. By ensuring adequate light levels, farmers can promote photosynthesis, regulate plant growth, and maximize crop yields.
- *Weather Sensors*: Weather sensors are essential for monitoring environmental conditions in and around farms. These sensors measure parameters such as temperature, humidity, wind speed, and rainfall. Accurate weather data allows farmers to assess the potential impact of weather events, plan irrigation schedules, and implement preventive measures against adverse weather conditions.
- *Nutrient Sensors*: Nutrient sensors are used to measure soil nutrient levels, such as nitrogen, phosphorus, and potassium. These sensors provide valuable information for efficient fertilization management, allowing farmers to apply fertilizers precisely and avoid excessive or inadequate nutrient supply. This promotes optimal crop growth and minimizes environmental impact.

In recent years, there has been a surge in the development of low-cost IoT technologies that find applications in professional agricultural settings. These technologies, including low-cost sensors, wireless connectivity, and cloud-based data platforms, enable cost-effective implementation of IoT systems in smaller-scale farms and facilitate data-driven decision-making for farmers with limited resources.

By leveraging these sensors and IoT devices, farmers can capture real-time data on key agricultural parameters, allowing for precise and targeted management of crops, resources, and environmental conditions. The integration of emerging low-cost technologies further expands the accessibility of IoT solutions, making data-driven agriculture more attainable for a broader range of farmers.

The use of sensors and IoT devices for data collection is instrumental in Smart Agriculture. Capacitive sensors, resistive sensors, photometric sensors, weather sensors, and nutrient sensors enable farmers to gather crucial data on soil moisture, temperature, light intensity, weather conditions, and nutrient levels. Additionally, emerging low-cost technologies contribute to the affordability and widespread adoption of IoT systems in professional agricultural applications.

7.3.2 Sensors' Calibration

In Smart Agriculture, accurate sensor measurements are crucial for making informed decisions and optimizing agricultural processes. However, sensors can experience drift, errors, or inconsistencies over time, leading to unreliable data. To ensure the reliability and accuracy of sensor readings, calibration processes are necessary. Let's explore the importance and methods of calibrating sensors in Smart Agriculture.

Over time, factors such as environmental conditions, sensor aging, and exposure to contaminants can affect the performance of sensors. Calibration allows for the adjustment or correction of sensor readings to align them with known reference values. By calibrating sensors, farmers can ensure that the collected data accurately reflects the actual conditions of the crops and the environment. This ensures that subsequent decisions, such as irrigation scheduling, nutrient management, or pest control, are based on reliable and precise information.

Laboratory calibration involves sending sensors to specialized facilities equipped with precise reference instruments. Here, sensors are tested against known reference values under controlled conditions. The calibration process typically involves exposing the sensors to specific stimuli or known values and comparing their responses to the reference values. Any deviations or errors are documented, and calibration coefficients or correction factors are determined to adjust future sensor readings.

On-site calibration involves calibrating sensors directly in the field or agricultural setting where they are deployed. This method reduces the downtime associated with sending sensors off-site for calibration. On-site calibration may utilize portable calibration equipment or reference sensors placed in close proximity to the sensors being calibrated. The readings of the reference sensors are used to calibrate and adjust the readings of the deployed sensors, ensuring accurate measurements in real-time agricultural operations.

With the advancements in IoT technology, automated calibration processes are gaining traction in Smart Agriculture. In this approach, sensors are calibrated automatically using integrated calibration algorithms and software. The calibration algorithms continuously monitor sensor performance, comparing it with known reference values or historical data. If deviations or errors are detected, the algorithms can automatically adjust the sensor readings in real-time, ensuring accurate and reliable data collection.

Ensuring the effectiveness of sensor calibration in Smart Agriculture requires following certain best practices. Adhering to the manufacturer's guidelines and recommendations for sensor calibration processes and intervals is crucial. Manufacturers often provide specific instructions and calibration procedures tailored to their sensor models, which should be followed meticulously.

Another important practice is maintaining a comprehensive record of calibration history. This includes documenting calibration dates, results, and any adjustments made to the sensors. By keeping track of this information, it becomes possible to monitor the performance of sensors over time and troubleshoot any potential issues that may arise.

Regular quality control checks are essential to validate the accuracy and reliability of sensor measurements. These checks can involve comparing sensor readings against known reference values or conducting side-by-side comparisons with multiple sensors in the same location. By implementing these checks, any inconsistencies or discrepancies can be identified and addressed promptly.

Environmental considerations play a significant role in sensor calibration. Extreme temperatures, humidity, dust, or contaminants can affect sensor accuracy. To mitigate these effects, measures should be taken to protect sensors from environmental influences during calibration and in their regular operation. This may involve providing proper shielding, sealing, or insulation to ensure optimal sensor performance.

By implementing these best practices, Smart Agriculture can rely on accurate and consistent sensor measurements. Following manufacturer guidelines, documenting calibration history, conducting quality control checks, and considering environmental factors contribute to the reliability and effectiveness of sensor calibration. This, in turn, enables data-driven decision-making and optimization of agricultural practices, leading to increased productivity and sustainable resource management.

Let’s look at a concrete example of calibrating a simple sensor that measures soil moisture.

Calibrating a capacitive soil moisture sensor is a necessary process to obtain accurate measurements. The sensor consists of two electrodes that are inserted into the soil. The resistance between the electrodes varies depending on the water content of the soil.

Calibration involves measuring the resistance of the sensor under known moisture conditions. For this purpose, it is necessary to use a soil sample with a known moisture content.

7.3.2.1 Materials and Equipment Required

- Capacitive soil moisture sensor
- Soil sample with known moisture content
- Arduino or other microcontroller
- Development board
- USB cable
- Power supply
- PC

7.3.2.2 Procedures

1. Connect the sensor to the microcontroller.
2. Power on the microcontroller.
3. Write a code to measure the resistance of the sensor.
4. Insert the sensor into the soil sample.
5. Read the resistance of the sensor.
6. Repeat steps 4–5 for different soil moisture values.
7. Create a calibration table that shows the resistance of the sensor as a function of the soil moisture content.

7.3.2.3 Example Code

The following code can be used to measure the resistance of a capacitive soil moisture sensor:

```
#include <Arduino.h>

// Sensor pin
const int sensorPin = A0;
```

```
// Resistance value under minimum moisture conditions
const int minResistance = 1000;

// Resistance value under maximum moisture conditions
const int maxResistance = 10;

void setup()
{
  // Initialize serial
  Serial.begin(9600);
  // Set the sensor pin as input
  pinMode(sensorPin, INPUT);
}

void loop() {
  // Read the sensor resistance
  int resistance = analogRead(sensorPin);

  // Calculate the moisture content
  float moisture = (resistance - minResistance) / (maxResistance
- minResistance);

  // Print the moisture value
  Serial.println(moisture);

  // Wait 1 second
  delay(1000);
}
```

7.3.2.4 Calibration Table

The calibration table should show the following values:

- Soil moisture content
- Sensor resistance

Table 7.1 shows a calibration table for a capacitive soil moisture sensor.

The calibration provided is linear. The resistance of the sensor varies linearly with the soil moisture content. This means that a simple linear function can be used to convert resistance values to moisture values.

TABLE 7.1
Percentage of Moisture Content and Related Sensor Resistance

Soil Moisture Content (%)	Sensor Resistance (Ohms)
0	1000
25	500
50	250
75	125
100	10

In particular, the linear function that can be used for calibration is as follows:

$$\text{moisture} = (\text{resistance} - \text{minResistance}) / (\text{maxResistance} - \text{minResistance}) \tag{7.1}$$

where

- moisture is the soil moisture content, expressed as a percentage
- resistance is the resistance value read from the sensor
- minResistance is the resistance value under minimum moisture conditions
- maxResistance is the resistance value under maximum moisture conditions

The code example provided uses this linear function to convert resistance values to moisture values.

However, it is important to note that linear calibration may not always be accurate. In some cases, the resistance of the sensor may vary nonlinearly with the soil moisture content. In these cases, it may be necessary to use a nonlinear calibration.

There are several methods for nonlinear calibration. One of the most common methods is to use a polynomial function to convert resistance values to moisture values.

For example, the following second-degree polynomial function can be used for nonlinear calibration:

$$\text{moisture} = a + b * \text{resistance} + c * \text{resistance}^2 \tag{7.2}$$

where

- a, b, and c are the coefficients of the polynomial function

The coefficients of the polynomial function can be determined experimentally by measuring the resistance of the sensor under known moisture conditions.

Table 7.2 shows a summary of the differences between linear and nonlinear calibration.

7.3.3 Types of Data Generated in Smart Agriculture

In the realm of Smart Agriculture, a wide range of data is generated, providing valuable insights for informed decision-making and optimized agricultural practices. Let's explore the various types of data that are commonly generated in this field:

- *Environmental Data*: Environmental data encompasses information about the surrounding conditions in which crops are grown. This includes data on temperature, humidity, rainfall, wind speed, solar radiation, and air quality. Monitoring and analyzing environmental data

TABLE 7.2
Linear vs. Nonlinear Features

Feature	Linear Calibration	Nonlinear Calibration
Relationship between resistance and moisture	Linear	Nonlinear
Accuracy	May not be accurate for all cases	More accurate for cases where the resistance–moisture relationship is nonlinear
Complexity	Simpler	More complex
Implementation	Can be implemented using a simple linear function	Requires a more complex polynomial function

enables farmers to understand the impact of these factors on crop growth, nutrient uptake, disease prevalence, and overall plant health.

- *Soil Data*: Soil data involves collecting information about the soil properties, composition, and characteristics. This includes data on soil moisture content, pH levels, nutrient levels, organic matter content, electrical conductivity (EC), and soil compaction. By analyzing soil data, farmers can make informed decisions regarding irrigation schedules, fertilizer application, soil amendments, and crop rotation strategies.
- *Crop Data*: Crop data pertains to the growth and development of specific crops. This includes data on crop phenology, growth rates, plant height, leaf area index, flowering stages, and fruiting parameters. Monitoring crop data helps farmers optimize planting schedules, assess crop health and productivity, detect potential pest or disease outbreaks, and make timely interventions for improved yield and quality.
- *Yield Data*: Yield data refers to information about the quantity and quality of harvested crops. This includes data on crop yields per unit area, weight, size, nutritional content, and market value. Analyzing yield data allows farmers to evaluate the effectiveness of different management practices, identify areas for improvement, and make strategic decisions regarding crop selection, planting density, and post-harvest handling.
- *Machinery and Equipment Data*: Smart Agriculture often involves the use of advanced machinery and equipment. Data generated by these devices includes information on fuel consumption, machinery performance, equipment usage patterns, and maintenance records. Analyzing machinery and equipment data helps optimize operational efficiency, reduce costs, and ensure timely maintenance and repairs.
- *Pest and Disease Data*: Monitoring and collecting data on pest and disease occurrences is crucial for effective pest management strategies. This includes data on pest populations, disease prevalence, symptoms, and progression. By analyzing pest and disease data, farmers can implement timely control measures, reduce crop losses, and minimize the use of pesticides.
- *Remote Sensing Data*: Remote sensing data involves capturing information about the crops and environment using satellites, drones, or other remote sensing technologies. This includes data on vegetation indices, infrared imagery, and multispectral data. Remote sensing data provides valuable insights into crop health, stress levels, water requirements, and overall field conditions.

The following sections explore the crucial topic of data organization specifically related to the impact of IoT technologies in Smart Agriculture. There will be an examination of how these technologies can be leveraged to optimize the management of essential agronomic inputs, including water, fertilizers, and energy. By effectively organizing and utilizing this data, farmers can make informed decisions regarding resource allocation, leading to improved efficiency, sustainability, and productivity in agricultural operations. Furthermore, these technologies can even enable autonomous systems to make decisions and take actions on behalf of farmers, further streamlining and optimizing agricultural operations.

The proper organization of data in IoT systems is fundamental for harnessing the full potential of Smart Agriculture. It enables farmers to access real-time information, gain actionable insights, and implement precise and targeted interventions. By optimizing the use of agronomic inputs, more sustainable and environmentally friendly agricultural practices are possible.

In the upcoming sections strategies and considerations for organizing IoT data in the context of Smart Agriculture are explored, with a focus on maximizing the impact of these technologies in optimizing water, fertilizer, and energy inputs.

7.3.4 Data Acquisition and Transmission Methods

In the context of Smart Agriculture, data acquisition and transmission methods play a crucial role in capturing and delivering real-time data for analysis and decision-making. Let's explore some key approaches and technologies utilized in this process.

7.3.4.1 Publish–Subscribe Model

One widely adopted method is the *publish–subscribe model* (Figure 7.1). In this model, data is published by the source or sensor and is made available to multiple subscribers who have expressed interest in receiving specific types of data. It enables efficient data distribution, allowing subscribers to receive only the data they need, reducing unnecessary network traffic, and improving scalability.

MQTT is a lightweight, publish–subscribe, machine-to-machine (M2M) messaging protocol that is ideal for IoT applications. It was designed to be energy and bandwidth efficient, making it ideal for devices with limited resources.

MQTT is a transport-level protocol that runs over TCP/IP. It is an asynchronous protocol, so clients do not need to be always connected to the broker to receive messages.

MQTT uses three fundamental commands:

- *PUBLISH*: A client publishes a message to a topic.
- *SUBSCRIBE*: A client subscribes to a topic to receive messages.
- *UNSUBSCRIBE*: A client unsubscribes from a topic.

MQTT is a very popular protocol for IoT applications. It is used in a variety of applications:

- *Remote Monitoring*: MQTT can be used to collect data from sensors and remote devices.
- *Remote Control*: MQTT can be used to control remote devices, such as lights, thermostats, and locks.
- *Device-to-Device Communication*: MQTT can be used to enable devices to communicate with each other.

Here are some of the benefits of MQTT:

- *Efficiency*: MQTT is an energy- and bandwidth-efficient protocol, making it ideal for devices with limited resources.
- *Scalability*: MQTT is a scalable protocol that can be used in large-scale applications.
- *Security*: MQTT supports a variety of security mechanisms, including TLS and SSL.
- *Compatibility*: MQTT is an open-source protocol that is compatible with a variety of platforms and devices.

MQTT is an important protocol for IoT applications. It is a versatile, reliable, and scalable protocol that can be used in a variety of applications.

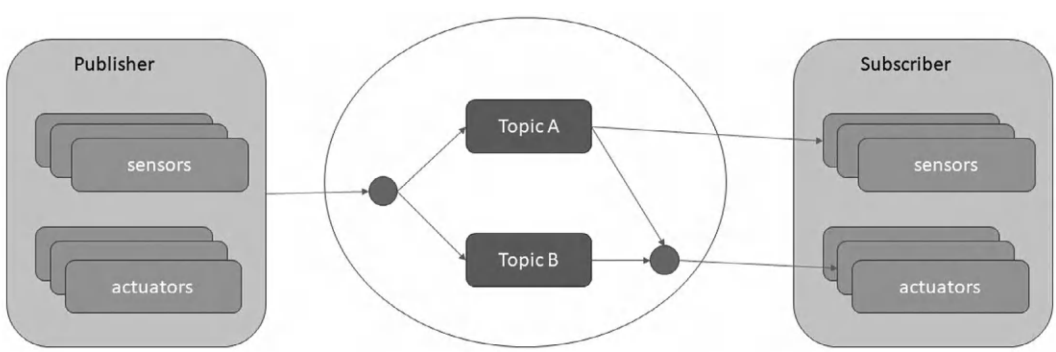

FIGURE 7.1 Publish–subscribe architecture model.

Example Scenario: A farmer has a field of wheat and wants to monitor the levels of macronutrients in the soil to ensure that the plants receive the nutrients they need to grow healthy.

Solution: The farmer installs nutrient sensors in the soil at different points in the field. The sensors send the nutrient level data to an MQTT broker. The broker publishes the data on a channel that can be read by a mobile app or monitoring software.

In this case, a generic MQTT message is composed of two fields: The *data* field, which encapsulates the structure of the application data that the system must transmit, and the *topic* field, which indicates the topic to which the data field refers. To format a data packet thus constituted, a standard format known as JSON (JavaScript Object Notation) can be used.

JSON provides a lightweight, human-readable data interchange format that is easy to parse and generate in different programming languages. It offers flexibility in structuring data and is widely supported by IoT devices and platforms.

Here's an example of a JSON file that could be used in the context of Smart Agriculture:

```
{
   "sensorId": "001",
   "timestamp": "2023-03-07 09:30:00",
   "temperatures": 25.3,
   "humidity": 62.1,
   "soilMoisture": 34.7,
   "crop": "Tomato",
   "location."
    {
      "latitude": 39.1234,
      "longitude": -121.5678
   }
}
```

This JSON file represents a data reading from a sensor in a Smart Agriculture system. It includes information such as the sensor ID, timestamp, temperature, humidity, soil moisture, crop type, and location coordinates. By utilizing JSON and adhering to data formatting standards, data can be effectively transmitted, processed, and integrated into the overall Smart Agriculture ecosystem.

Considering the example of the wheat field, the JSON message that the system will send to the broker will have a structure similar to the following:

```
{
   "topic": "nutrients",
   "date":
    {
      "N": 100,
      "P": 50,
      "K": 20
    }
 }
```

It is clear that this method of representing data, in addition to being automatically interpretable by a machine, is also highly human-readable.

7.3.4.2 Push–Pull Model

Another common approach is the *push–pull method*, where data is actively pushed from the source to the central data management system, ensuring real-time data availability. Conversely, in the *pull–push method*, the central system requests data from the sources as needed.

Here is an example of how the push–pull model can be used in Smart Agriculture:

- *Push*: A soil moisture sensor in a field continuously pushes data to a central data management system. This ensures that the system always has the latest data on soil moisture levels.
- *Pull*: The central data management system can pull data from other sources as needed, such as weather data from a weather station or crop data from a yield monitor. This allows the system to get a complete picture of the agricultural operation.

The push–pull model is particularly well-suited for Smart Agriculture because it allows for real-time data availability. This is important because farmers (or automatic DSS systems) need to be able to make quick decisions based on data, such as when to irrigate or apply fertilizer.

Here is a specific example of how the push–pull model could be used in a Smart Agriculture application:

- A farmer sets up a network of soil moisture sensors in a field. The sensors are connected to a gateway that pushes the data to a central data management system.
- The central data management system also receives data from a weather station and a yield monitor.
- The system uses the data to create a real-time map of the field, showing the soil moisture levels, crop growth, and weather conditions.
- The farmer can use this map to make informed decisions about when to irrigate, apply fertilizer, and harvest the crops.

7.3.4.3 Request–Response Model

A request–response model is a communication pattern in which one entity (the client) sends a request to another entity (the server), and the server responds to the request. The client may send the request to obtain data, perform an action, or change the state of the server. The server may respond with data, a confirmation that the action was performed, or an error message.

Request–response models are often used in IoT systems, where the client is typically an *IoT node* and the server is a *microservice*. For example, an IoT node may send a request to a microservice to get the current temperature, to turn on a solenoid, or to set a timer. The microservice would then process the request and send back a response.

Here is a specific example of a request–response model in an IoT system:

1. An IoT node that is monitoring the temperature in a greenhouse sends a request to a REST microservice to get the current temperature.
2. The microservice receives the request and queries the temperature sensor.
3. The microservice retrieves the temperature data and prepares a response.
4. The microservice sends the response back to the IoT node.
5. The IoT node receives the response and updates its display to show the current temperature.

Request–response models are a simple and effective way to implement communication between IoT nodes and microservices. However, they can be inefficient if the client needs to send a lot of requests to the server, or if the server needs to process a lot of requests at the same time.

One way to overcome these limitations is to combine request–response models with other methods, such as the push–pull method. In a push–pull system, the server can push data to the client without being prompted. This can reduce the number of requests that the client needs to send, and it can also reduce the load on the server.

For example, in an IoT system, the server could push temperature data to the client every few seconds. This would allow the client to keep its display up-to-date without having to send a request to the server each time.

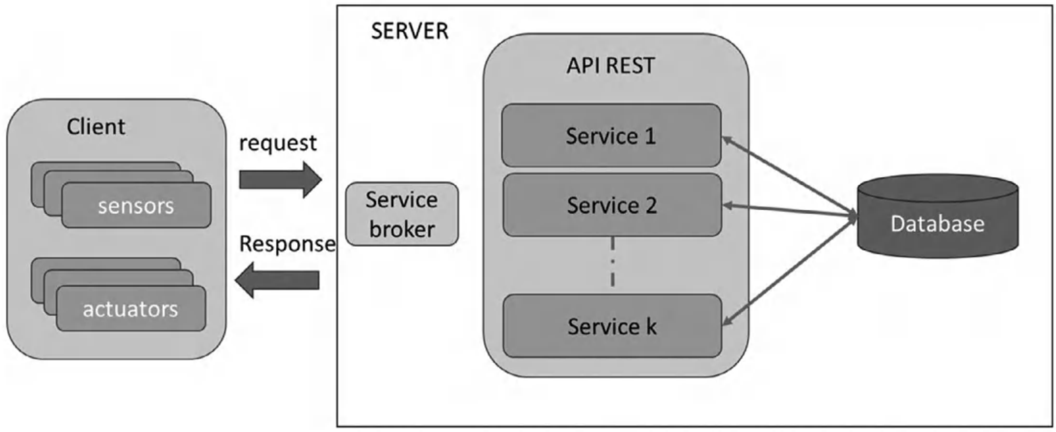

FIGURE 7.2 Request–response architecture model.

Another way to overcome the limitations of request–response models is to use microservices. Microservices are small, independent services that can be easily scaled up or down. This means that if a particular microservice is receiving a lot of requests, it can be scaled up to handle the load.

By combining request–response models with other methods, such as the push–pull method and microservices, it is possible to create efficient and scalable communication systems for IoT applications (Figure 7.2).

7.3.4.4 Cloud Computing

Cloud computing plays a pivotal role in data acquisition and transmission in Smart Agriculture. By leveraging cloud-based platforms and services, farmers can securely store, process, and analyze vast amounts of data from multiple sources. Cloud computing offers scalability, cost-effectiveness, and accessibility, allowing stakeholders to access and collaborate on data from anywhere at any time. Furthermore, it enables integration with advanced analytics and machine learning tools, facilitating data-driven insights and predictive modeling for improved decision-making.

7.3.4.5 Fog Computing

Fog computing is another emerging paradigm in data acquisition and transmission. It aims to bring computational resources closer to the edge devices and sensors, reducing latency and enhancing real-time data processing capabilities. By decentralizing data processing and analysis, fog computing enables faster response times and reduces reliance on cloud-based infrastructure. This is particularly beneficial in scenarios where low-latency decision-making and real-time analytics are critical, such as precision irrigation or pest detection.

By leveraging publish–subscribe, push–pull, pull–push, cloud computing, and fog computing methods, along with standardized data formatting like JSON, Smart Agriculture can efficiently acquire and transmit data. These methods and technologies provide the necessary infrastructure for capturing real-time information and enabling data-driven decision-making. In the subsequent sections of this chapter, strategies and considerations for organizing IoT data in the context of Smart Agriculture will be explored, optimizing the utilization of these data acquisition and transmission methods to enhance the management of agronomic inputs such as water, fertilizers, and energy.

7.4 DATA ORGANIZATION PRINCIPLES IN IOT SYSTEMS

Relational models play a pivotal role in the field of database management systems (DBMS) by providing a structured approach to organizing and managing data. A relational model represents data as a collection of tables, where each table consists of rows and columns. These tables, also known as relations, establish relationships between different entities and define the structure of the data.

The foundation of a relational model lies in the concept of the relational schema, which defines the structure, attributes, and relationships of the entities being modeled. The schema serves as a blueprint for creating the tables and establishing the relationships between them. It outlines the entities, their attributes, and the constraints that govern the data.

The relational model plays a crucial role in organizing and managing data in IoT systems for Smart Agriculture. In this section, various aspects of the relational model and its significance in tracking the entire lifecycle of crops and optimizing agricultural processes are explored.

One of the key aspects that the relational model addresses is the need to track and record essential parameters of plant species throughout their growth cycle. This includes optimal ranges for factors such as moisture, pH levels, nitrogen, phosphorus, potassium, and micronutrients, as well as ambient temperature and humidity. By capturing and storing this data, the system can facilitate informed decision-making and enable precision control over the cultivation environment.

Furthermore, the relational model allows for the georeferencing and tracking of planting sites, which here are referred to as *containers*. It enables the system to manage the layout of the planting sites and accurately locate them within the agricultural infrastructure. This information is critical for optimizing resource allocation, monitoring plant health, and implementing targeted interventions.

To enable comprehensive analytics and gain valuable insights, the system must maintain a historical record of data for each crop species. This includes managing agricultural cycles and tracking the phenological stages specific to each species. By analyzing this historical data, patterns and trends can be identified, helping farmers make informed decisions and optimize agricultural practices.

In conclusion, relational models serve as a fundamental framework for organizing and managing data in DBMS. By defining entities, attributes, relationships, and constraints, stakeholders can create a structured and efficient representation of their data. The relational model's methodology ensures data integrity, reduces redundancy, and enables effective data retrieval and analysis, making it an essential tool in the field of DBMS.

7.4.1 Data Model Methodology

The aim of this volume is not to teach the already established methodologies for database design. The topic can be summarized by outlining a path. The objective is to create a relational model (ER).

To design a relational model, it is essential to follow a specific methodology. The process typically involves the following steps:

1. *Identify Entities*: The first step is to identify the entities that need to be represented in the database. These entities can be tangible objects, such as customers or products, or conceptual entities, such as orders or transactions.
2. *Define Attributes*: Once the entities are identified, the next step is to define the attributes associated with each entity. Attributes represent the characteristics or properties of the entities. For example, a customer entity may have attributes like name, address, and contact information.
3. *Establish Relationships*: Relationships define the associations and dependencies between different entities. They capture the connections and interactions among the entities. Relationships can be one-to-one, one-to-many, or many-to-many, depending on the nature of the entities involved.
4. *Normalize the Data*: Normalization is a crucial step in ensuring data integrity and eliminating redundancies in the database. It involves breaking down the data into smaller, more manageable tables and removing any redundant or duplicated information.

5. *Create Tables*: Based on the identified entities, attributes, and relationships, tables are created to represent the data. Each table corresponds to an entity, with rows representing individual instances of the entity and columns representing the attributes.
6. *Define Primary and Foreign Keys*: Primary keys are unique identifiers assigned to each row in a table, ensuring data integrity and enabling efficient data retrieval. Foreign keys establish the relationships between tables by referencing the primary key of another table.
7. *Establish Constraints*: Constraints enforce rules and restrictions on the data, ensuring data consistency and integrity. Examples of constraints include unique constraints, which ensure the uniqueness of values in a column, and referential integrity constraints, which enforce the relationships between tables.

By following this methodology, a relational model can be designed, providing a solid foundation for managing and systemizing data in a structured and efficient manner. The relational model's flexibility and scalability make it a widely adopted approach in various domains, including Smart Agriculture, where the management of complex and interrelated data is crucial for optimizing farming practices.

Let's consider a simple example in the domain of agriculture to illustrate the concept of a relational model. Suppose that a database to manage crop data for a farm is needed.

1. *Identify Entities:*
   - *Entity 1*: Crop
   - *Entity 2*: Field
   - *Entity 3*: Farmer—represents the farmers responsible for managing the fields and crops.
2. *Define Attributes*:
   - *Crop*: crop_id, crop_name, optimal_humidity, optimal_temperature
   - *Field*: field_id, field_name, location, size
   - *Farmer*: farmer_id, farmer_name, contact_info
3. *Establish Relationships*:
   - One farmer can *manage* multiple fields. One field is managed by a single farmer (one-to-many relationship).
   - One crop can be grown on multiple pieces of land, and similarly, multiple crops can be grown on a single piece of land. **In this case, one crop has fields, and one field has crops. This is a true statement, as a crop can be grown on multiple fields, and a field can have multiple crops grown on it. So, this relationship can be denoted with the name *has*** (many-to-many relationship).
4. *Normalize the Data*:
   - Break down the data into smaller tables to eliminate redundancies and improve data integrity.
5. *Create Tables*:
   - *Table*: CROP
     - crop_id (Primary Key)
     - crop_name
     - optimal_humidity
     - optimal_temperature
   - *Table*: FIELD
     - field_id (Primary Key)
     - field_name
     - location
     - size

- *Table*: FARMER
  - farmer_id (Primary Key)
  - farmer_name
  - contact_info
- *Table*: has
  - crop_id
  - field_id

In this case, the pair (crop_id, filed_id) represents the primary key of this table.

6. *Define Primary and Foreign Keys*:
   - In the *FIELD* table, the *fk_farmer_id* would serve as a foreign key referencing the farmer_id in the FARMER table.
   - In the *has* table, the *fk_crop_id would serve as a* foreign key referencing the crop_id in the CROP table, and the *fk_field_id* would serve as a foreign key referencing the field_id in the FIELD table.

There is a graphical method for drawing an ER model. The method is very simple to apply, but one should not be deceived by the simplicity of the formalism. Real-world application requires a lot of experience. This method involves representing entities as rectangles and relationships as diamond shapes connecting the entities. Attributes are typically represented as ovals connected to their respective entities. Cardinality and participation constraints are indicated using lines and annotations.

Last but not least, the names of entities are always capitalized, while the names of relationships are written in lowercase.

The graphical method (Figure 7.3) helps visualize the structure of the database, including how different entities are related and the attributes associated with each entity. It aids in creating a clear and understandable representation of the data model, making it easier for stakeholders to grasp the relationships and constraints in the system.

By constructing a relational model in this manner, data related to crops, fields, and farmers can be effectively organized and managed. The tables and relationships enable us to track the optimal conditions for each crop, assign fields to specific crops, and associate farmers with their respective fields. This structured approach facilitates efficient data retrieval, analysis, and decision-making in the agricultural context.

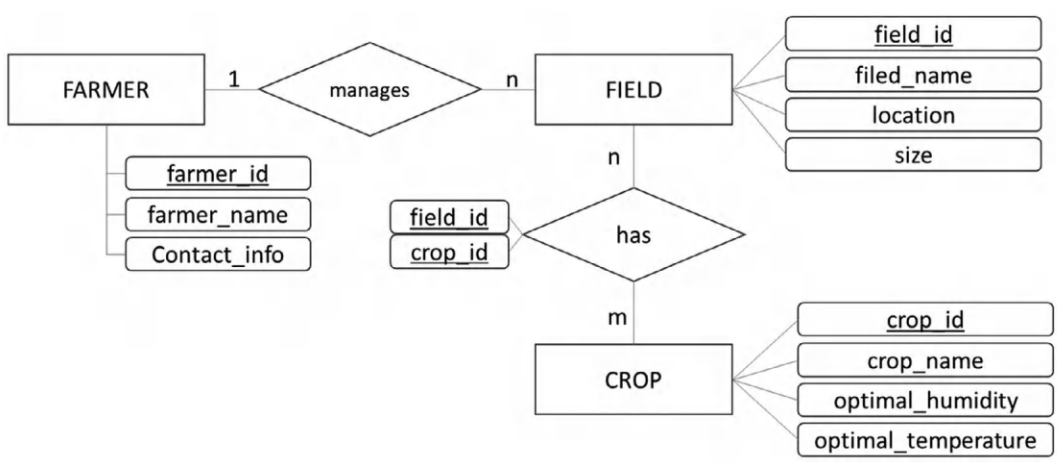

FIGURE 7.3 Entity–relationship data model.

Please note that this is a simplified example for illustrative purposes, and in real-world scenarios, more complex and interconnected data structures would be involved.

One of the key advantages of the relational model is its ability to handle complex data relationships and hierarchies. For example, it allows the organization of data into hierarchies based on crop types, geographical locations, or other relevant criteria. This hierarchical structure enables efficient data retrieval and analysis at different levels, facilitating a more comprehensive understanding of the agricultural system.

Moreover, the relational model provides the foundation for integrating external data sources and APIs into Smart Agriculture systems. This allows the enrichment of data with external information, such as weather forecasts, market prices, or soil composition data. By combining these diverse data sources, stakeholders can gain a holistic view of the agricultural landscape and make data-driven decisions that optimize resource utilization and enhance overall productivity.

The relational model forms the foundation for effective data organization in IoT systems applied to Smart Agriculture. It enables tracking of crop lifecycles, management of planting sites and layouts, storage of historical data, and integration of sensors and actuators for precision control. By harnessing the power of the relational model, agricultural stakeholders can optimize resource utilization, improve crop yields, and drive sustainable and efficient farming practices.

7.4.2 Entity and Relationship Dictionary

To facilitate data organization and retrieval, the use of dictionaries becomes essential within the relational model. An entity dictionary allows for the definition and categorization of various entities involved in the model, such as crops, fields, containers, sensors, and actuators. This dictionary serves as a reference for ensuring consistency and clarity in data representation and querying.

Similarly, a relationship dictionary provides a comprehensive overview of the relationships between different entities within the system. It captures the dependencies, associations, and interactions between crops, containers, sensors, and actuators. The relationship dictionary helps in understanding the complex network of interactions and dependencies, enabling more informed decision-making and analysis.

There are the dictionaries of entities and relationships shown in Table 7.3 and Table 7.4, respectively.

By utilizing the relational model, along with entity and relationship dictionaries, Smart Agriculture systems can effectively manage and organize data for optimized resource utilization, improved decision-making, and enhanced agricultural practices. This approach enables the integration of various data sources, facilitates data analysis, and supports the development of advanced analytics and machine learning algorithms.

TABLE 7.3
Entity Dictionary

Name	Description	Attributes	Attribute Types
CROP	Represents different types of crops grown on the farm	crop_name optimal_humidity optimal_temperature	string(25) integer float
FIELD	Represents the specific fields where crops are planted	field_name location size	string(50) string(32) float
FARMER	Represents the farmer responsible for managing the fields and crops	farmer_name Contact_info	string(50) string(100)

TABLE 7.4
Relationship Dictionary

Name	E1:E2	Attributes	Attribute Types	Cardinality
has	E1: CROP	fk_field_id	long int	n:m
	E2: FIELD	fk_crop_id	long int	
manage	E1: FARMER	no		1:n
	E2: FIELD			

7.4.3 Graph-Based Sensor and Actuator Mapping

Having reached this point, a data model can be built to manage an IoT system that controls parameters (in the ground, on plants, and in the environment) that have the characteristic of being reactive. This last capability is essential because the system will not only have to analyze data but will also have to make decisions and act on them in the field. From the authors' point of view, decision-making models can be considered as black boxes that need input data for working and producing output data. The model that is about to be built will have to contain these data, allowing software modules to use them in decision-making processes, monitoring, and acting.

Within the relational model, IoT nodes are related to each other to define rules for engaging actuators based on the sensor data they receive. This allows for dynamic control and automation in response to specific conditions or triggers. Moreover, the system must keep track of the states of actuators and the measurements captured by sensors. As these entities generate a significant amount of data (big data), periodic migration to NoSQL solutions is necessary, retaining only the most recent data for current operations.

The relational model also supports the need for data management related to the various states of crops throughout their growth cycles. By capturing and storing information about phenological stages, such as germination, vegetative growth, flowering, and fruiting, the system can effectively track and monitor the progress of each crop. This information is vital for determining the optimal timing of specific agronomic practices, such as irrigation, fertilization, and pest control.

In addition to plant-related data, the relational model facilitates the tracking of the states and measurements of actuators and sensors. This includes recording the status of actuators, such as irrigation systems, greenhouse ventilation, and nutrient delivery systems, as well as the data captured by sensors, including temperature, humidity, light intensity, soil moisture, pH, nutrient level, and EC. The ability to store and analyze this data is crucial for evaluating the performance of the system, detecting anomalies, and fine-tuning the control algorithms.

To design a solution for describing the relationship between sensors and actuators, a specific sensor can control many actuators, and a specific actuator can be controlled by many sensors. Moreover, both sensors and actuators can be defined as IoT devices.

Therefore, it is useful to define an entity for representing this concept, and the best name for this entity is IOT_DEVICE.

At this point, it is necessary to find a way to distinguish whether a specific IoT device is a sensor or an actuator. To solve this problem, let's introduce two new entities named SENSOR and ACTUATOR, which will be two specializations of the IOT_DEVICE entity. In graphical form, this concept can be represented as a circled *d* as disjoint, because an IoT device cannot be both a sensor and an actuator at the same time (Figure 7.4).

In terms of database design, there are two main approaches to designing the proper tables:

1. Create a single table named IOT_DEVICE that contains its own attributes and the attribute sets of the two specialized entities ACTUATOR and SENSOR. A further attribute type could be valued as *a* to indicate an actuator IoT device or *s* to indicate a sensor IoT device.

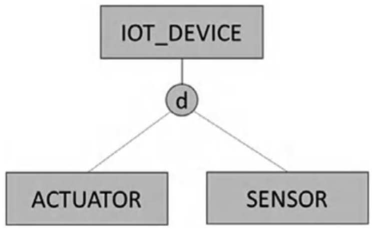

FIGURE 7.4 Template 1—IOT_DEVICE.

2. Design two separate one-to-one relationships that link the IOT_DEVICE entity with the two specialized entities.

Figure 7.5 shows the graphical view in both cases.

Obviously, in the second approach, adding a further *type* attribute to the IOT_DEVICE entity could be useful for reducing query time.

7.4.4 Advanced Entity–Relationship Model Proposal

Now, a relational data model can be built that has the characteristics of generality, extensibility, efficiency, and effectiveness when it is used as a knowledge base for IoT applications in agriculture.

To this end, a set of requirements can be defined, classifying them according to functions that a hypothetical monitoring and implementation application could cover: Localization of crop sites, layout of transplants, placement of sensing and acting IoT nodes, management of measurements, management of states, and management of agricultural cycles.

Here is an example of requirements for each of the previously indicated functions and the data model proposed to satisfy those requirements.

7.4.4.1 Crop Site Localization Requirements

- The data repository shall allow the management of both georeferenced and non-georeferenced sites.
- A crop site may have any shape.
- The repository shall allow the georeferencing of the entire perimeter of a crop site.
- A subject may manage multiple crop sites, geographically distributed, possibly georeferenced.
- A crop site may be divided into sub-sites.
- The division of a site into sub-sites shall track the motivation for the division.
- Each crop site may have multiple divisions with different motivations simultaneously.

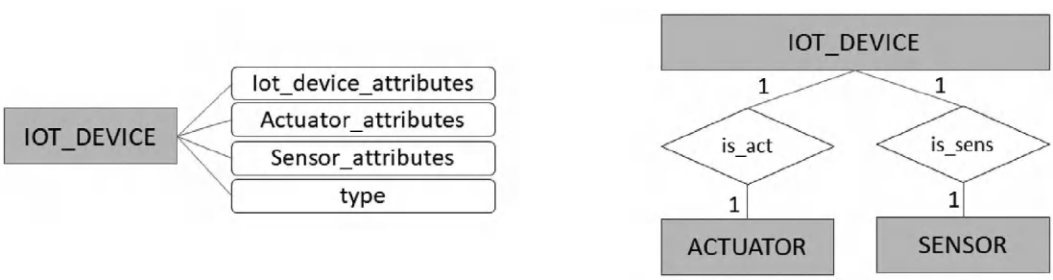

FIGURE 7.5 Template 1 – entity–relationship (ER) model for IoT devices: (a) implementation with a single IOT_DEVICE table and typed attributes; (b) implementation with separate ACTUATOR and SENSOR entities linked to IOT_DEVICE.

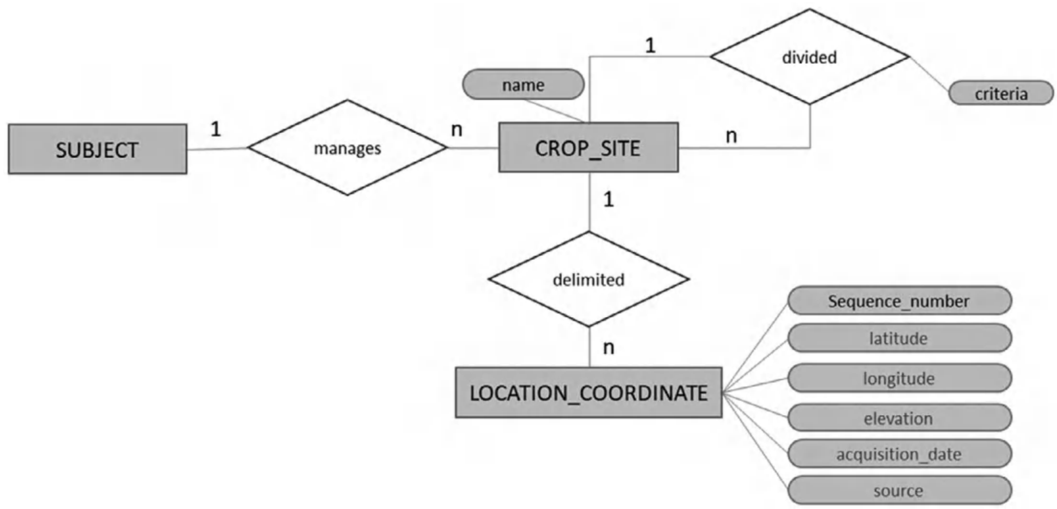

FIGURE 7.6 Template 2—CROP_SITE location and land splitting.

7.4.4.2 Data Model

The proposed data model (Figure 7.6) allows a SUBJECT to manage multiple cultivation sites. The *divided* self-relation generates a tree hierarchy where each child node has a criterion that expresses the reason for the division. The node name is simply the name assigned to the underlying division level and the criterion that led to that division. An example could be that of a land named *name1* (Figure 7.7) being decomposed into subzones, one created with the criterion of exposure and the other with the criterion of soil texture.

7.4.4.3 Transplant Layout

- The repository must allow for the management of the spatial distribution of transplants.
- In order to use the repository in organic farming, it will be possible to manage cultivation sites with a high biodiversity rate (diversification of the species grown on irrigation lines).

These two requirements constrain the data container to define a very fine grain for the representation of transplant positions. In a nutshell, in the phases of planting, transplant lines are taken into consideration. Each transplant line will therefore have a step (i.e., the certified distance between two drippers) and a certain number of drip positions that will depend on the length of the line itself. Figure 7.8 is the proposed data model to cover these requirements.

The diagram shows that the location of each dripper on the line is tracked. This allows precision irrigation applications to target specific areas of the field with water, minimizing water use.

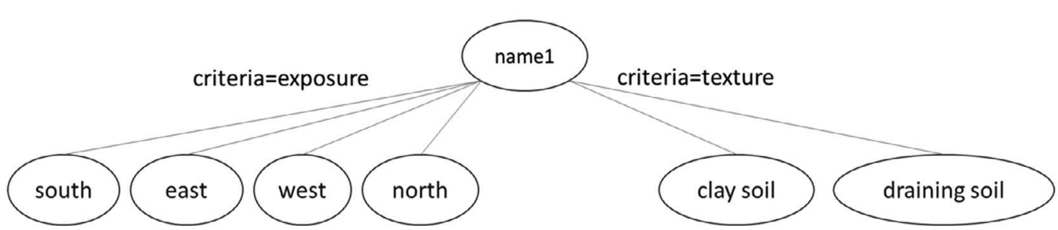

FIGURE 7.7 Example of cultivation site classification tree.

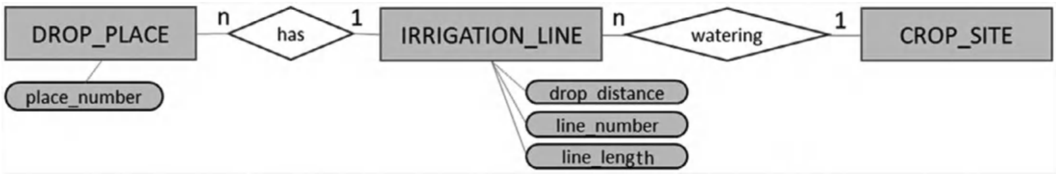

FIGURE 7.8 Template 3—IRRIGATION_LINE configuration.

7.4.4.4 IoT Node Positioning for Sensing and Actuation

- IoT nodes can be positioned in specific locations indicated by coordinates.
- IoT nodes can be positioned in specific locations indicated by irrigation line number.
- IoT nodes can be positioned in specific locations indicated by position number on an irrigation line.
- IoT nodes must refer exclusively to the cultivation sites in which they operate.

These requirements concern the positioning of IoT nodes in the workplace, which can be in a protected site (greenhouse) or in the open field. In general, an IoT node must be positioned appropriately within the system to be effective. Considering that IoT nodes can perform monitoring (sensor nodes) or actuation (irrigation, fertigation, window control, lighting, etc.) functions, the information related to their positioning can be generalized by observing the following:

- Monitoring can concern general and environmental parameters (air humidity, air temperature, lighting levels, etc.).
- Monitoring can be related to individual lines of actuation or at the level of the dripper position.

In the first case, the positioning is relative to the CROP_SITE, while in the second case, it will refer in a targeted way to a particular area of the site served by one or more lines, up to the point of referring to the single dripper point.

Figure 7.9 presents the ER model that can be used to track this information.

There is no direct link between IOT_DEVICE and LINE. This information is superfluous, as the line of actuation/monitoring can be traced indirectly through the DROP_PLACE entity. One instance of DROP_PLACE is linked to one and only one instance of LINE.

7.4.4.5 Relationship Between IoT Nodes

- An actuator node can be controlled by one or more sensor nodes.
- A sensor node can control from zero to n actuator nodes. Therefore, it may not control any actuator node and can be configured as a mere monitoring node.

That requirement set is one of the most important aspects of a system that aims to perform monitoring–decision–action in a smart farming environment. Considering a hypothetical algorithm that has been designed to make a decision on where to irrigate based on real-time data coming from sensors situated on the ground, precisely at the beginning of each irrigation line, it is possible to draw the implementation of that algorithm as a black box (Figure 7.10; e.g., a web REST API) that receives a set of inputs (the sensor measurements and the actual solenoid status) and produces as a result the set of new statuses for the array of IoT nodes that controls the solenoids mounted at the beginning of each irrigation line.

The system configuration previously drawn lacks an important piece of information: How is the relationship between sensors and actuators designed? The requirements require that a sensor node can be used to control many IoT actuators, and an actuator can be controlled by many sensors

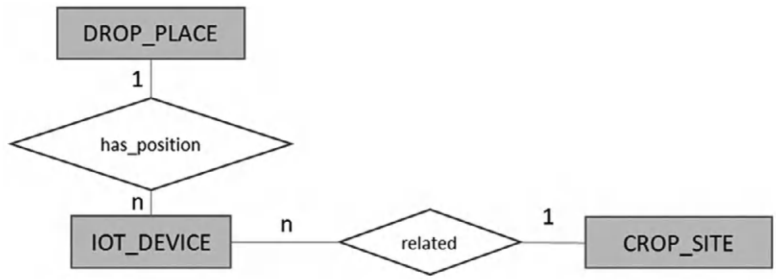

FIGURE 7.9 Template 4—IOT_DEVICE positioning.

(of the same or different types). This means that a many-to-many relationship is essential for the ER template model that will satisfy the relationship requirements.

In the algorithm black-box schema, a further input parameter is required to communicate a variety of information, such as the particular algorithm to use, or any other internal parameters that the algorithm needs to use.

The ER model template proposed is in Figure 7.11. A graphic visualization of that kind of relationship is a multi-graph where many sensors are connected to many actuators with many parameters. It should be noted that the value of k could be zero and that means the absence of parameters.

This template is very effective and general. Any decision-making algorithm can use the input data provided by the schema, which, in a nutshell, creates a map of the relationships between IoT nodes on graph structures for which very efficient queries and calculation models have been studied in the literature and implemented in both modern DBMS and graph-oriented APIs.

7.4.4.6 Measurement Management

- All of the most common ways of expressing a measurement must be considered: Numerical point measurements, spatially resolved measurements, and qualitative measurements referred to as scales (e.g., Likert scale).
- Each measurement must refer to the unit of measurement to which it refers.
- Each measurement must refer to the measurement time (day, month, year, hours, minutes, seconds).

Sensors used in agriculture can measure a wide variety of parameters: Soil moisture, temperature, EC, pH, nutrient content, etc. Each measurement must be referenced to a unit of measurement and a time of acquisition. Sensor measurements can also be complex, for example, a sensor that acquires spatially resolved data such as images in the visible or in different bands. Special sensors are also those defined as multi- or hyper-spectral that report a measurement in specific bands of the electromagnetic spectrum, even very narrow ones.

When a sensor data is digitized, it can always be represented in an n-dimensional vector space. Therefore, the data model that will have to manage it must necessarily contain this type of information for any number of dimensions in which a measurement is made.

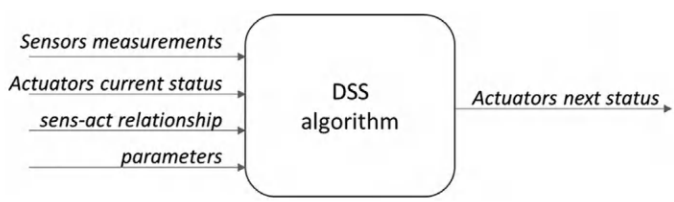

FIGURE 7.10 Decision-making algorithm as a black box.

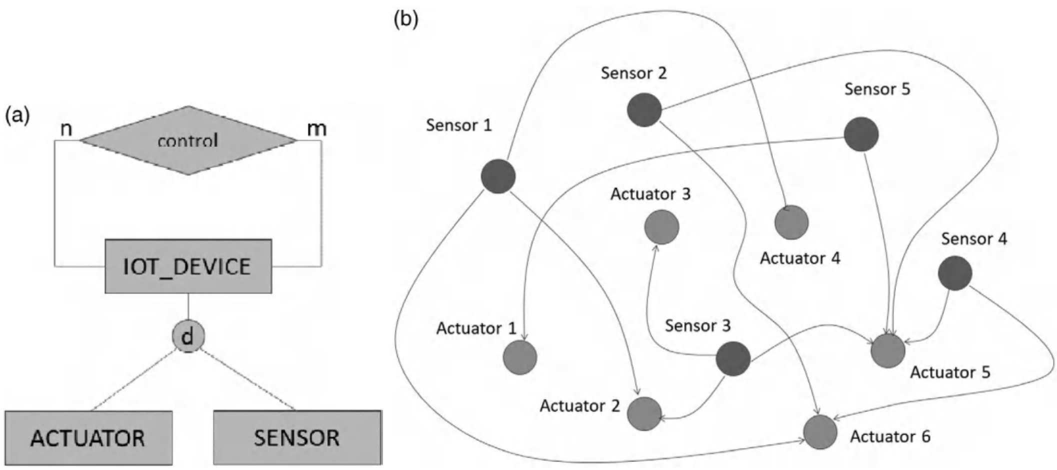

FIGURE 7.11 Template 5 – IOT_DEVICE sensor–actuator control graph management: (a) ER model specifying which sensors control which actuators as a self-relation on IOT_DEVICE; (b) graphical representation of this self-relation as a control graph.

The data model that meets the measurement requirements is shown in the diagram in Figure 7.12.

Each sensor is related to n instances of the MEASURE entity, each of which is characterized by the time of measurement. Each measurement instance is in turn related to the dimensions. Each DIMENSION has a unit of measurement, a value (which can be expressed in numerical or functional form), and a name (temperature, humidity, pH, etc.). The *referred_to* self-relation expresses a functional relationship between different dimensions.

7.4.4.7 State Management

- Each actuator must have a current state.
- Each state must reference the time (day, month, year, hours, minutes, seconds) at which the state came into effect.
- The system must be able to manage any number of states.
- The system must have a history of states.

A relational structure that meets all the requirements is the one in Figure 7.13.

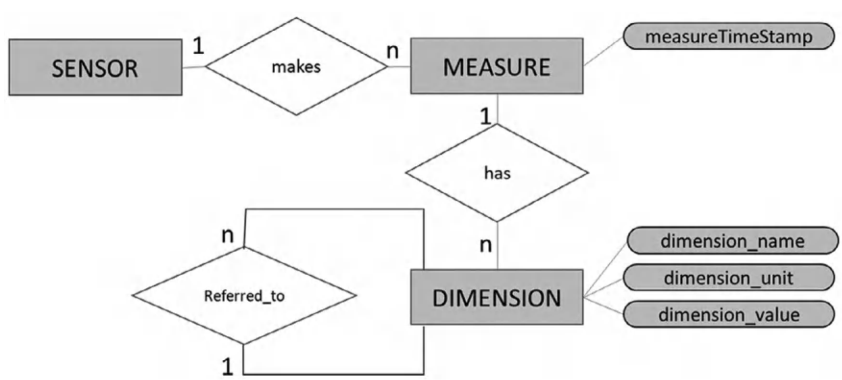

FIGURE 7.12 Template 6—Sensors MEASURE management.

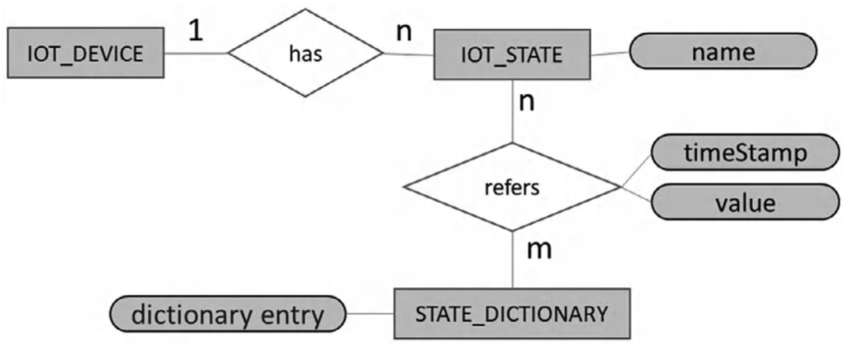

FIGURE 7.13 Template 7—IOT_STATE management.

Each IOT_DEVICE is connected to one or more IOT_STATE instances. To generalize the concept of state, it can be simple (name, value, timestamp) or complex. In the latter case, a dictionary of possible states that includes the simple case may be defined. The structure permits to keep track of the history of states through the timestamp attribute. This means that questions like, *how long has an IOT_DEVICE been in the same state? When did the state change? What is the current state? For how long? What is the total amount of time spent in a state? What is the average time spent in a state over some time?* can be answered. In addition, these queries can be made more specific by filtering the type of IOT_DEVICE that someone may be interested in.

7.4.4.8 Agricultural Cycle Management

- The repository must store all data acquired in the field.
- The system must react in terms of DSS only to the last active agricultural cycle.
- The system must characterize an indefinite number of species.
- Each species must be characterized by the optimal conditions of its main parameters.

The agricultural cycle is defined as the period of time that, for a well-defined set of species, begins with planting in the ground and ends with the harvest of the finished product. In an agricultural cycle, depending on the individual species, the agricultural cycle will have sub-periods referred to as the phenological phases of the species itself.

An example is the tomato plant. The tomato cycle, from planting to harvest, takes about 90–120 days. However, this period can vary depending on the tomato variety, climate, and growing conditions.

In general, the tomato cycle can be divided into four phases:

- *Germination Phase*: This phase takes about 7–10 days. Planting is done in a seedling tray, where the seedlings develop for about 2–3 weeks.
- *Transplanting Phase*: This phase takes about 1–2 weeks. The seedlings are transplanted into the field, where they will grow until harvest.
- *Production Phase*: This phase takes about 40–60 days. During this phase, the tomatoes grow and ripen.
- *Harvesting Phase*: This phase takes about 10–15 days. The tomatoes are harvested when they are ripe.

The production phase is the longest phase of the tomato cycle. The time it takes for tomatoes to ripen varies depending on the variety. Some varieties ripen in about 40 days, while others can take up to 60 days.

The data model responsible for managing agricultural cycles must keep track of this information. In addition, it is of fundamental importance to include in the model structures capable of containing site-specific information, up to the granularity of irrigation lines or even planting points. Why is it necessary to push the data model to be so site-specific?

In conventional or industrial agriculture, monocultures have always been managed for the sake of more agile standardization of production processes and cost management. Unfortunately, some problems have emerged over the years, mainly related to the resilience of monocultural systems, soil impoverishment, and biodiversity loss. This volume will not address these issues, but it should be noted that a data model that enables site-specific actions must also be accurate in managing information. This increases the amount of data available at a very fine spatial and temporal resolution and consequently enables the study and development of decision-making algorithms that were previously unthinkable.

A concrete example could be that which concerns organic agriculture and in particular the practices that fall within the scope of the so-called synergistic agriculture. These practices are based on the observation that if a cropping system has a high degree of spatial biodiversity, it will consequently need fewer treatments and in general less quantities of agronomic inputs (water and fertilizers). In the literature, there are tables of associations between vegetables that aim to highlight which are the positive spatial pairings, the negative ones, and the neutral ones. The optimal combination on a small land surface (a few tens of square meters) is manageable by a human being who will have to identify the best combinations for his or her own garden. Unfortunately, this practice is not applicable to large areas where computational and combinatorial complexity grows exponentially. In this case, an AI algorithm (for example, based on constraint programming models) could converge in acceptable times but needs to be fed with well-structured data and produce planting schemes that in turn could be interpreted by robots responsible for preparing seedbeds.

Having said that, it is easy to see that the relational model template in the management of agricultural cycles will have to include entities, such as species, phenological stage, irrigation lines, and transplanting points. Figure 7.14 shows a possible template that organizes data about the listed entities.

Closely observing the model, it can be noted that each species has one or more phenological stages, but the *has_now* relationship specifies in which of them a species is located during the current agricultural cycle. The *has_now* relationship also includes the set of parameters that characterize a specific phenological stage of a specific species, and the optimal value of the parameter can change from stage to stage. Typical examples of parameters are the minimum and maximum values of nutrients expressed in mg/kg or ppm, or the minimum and maximum pH value, or even the range of soil moisture, etc.

Another aspect of the proposed model template is the absence of a direct relationship between the agricultural cycle and the *has_now* relationship. This choice is due to the fact that the current agricultural cycle can be acquired from the *start_date* and *end_date* attributes. This implies that the model only allows to monitor the current cycle. If there is the need to build a history of agricultural cycle data, it is sufficient to create a link between the latter and the *has_now* relationship with a cardinality of *k*.

7.4.5 Linking Sensor Measurements in a NoSQL Structure

The MEASUREMENT table could grow exponentially over time if measurements are in real time. This is because real-time measurements are collected at a constant rate, regardless of the number of sensors or the amount of data generated by each sensor. For example, if a sensor is collecting temperature measurements every second, then the measurement table will grow by one row every second. If there are many sensors, then the measurement table could grow very quickly.

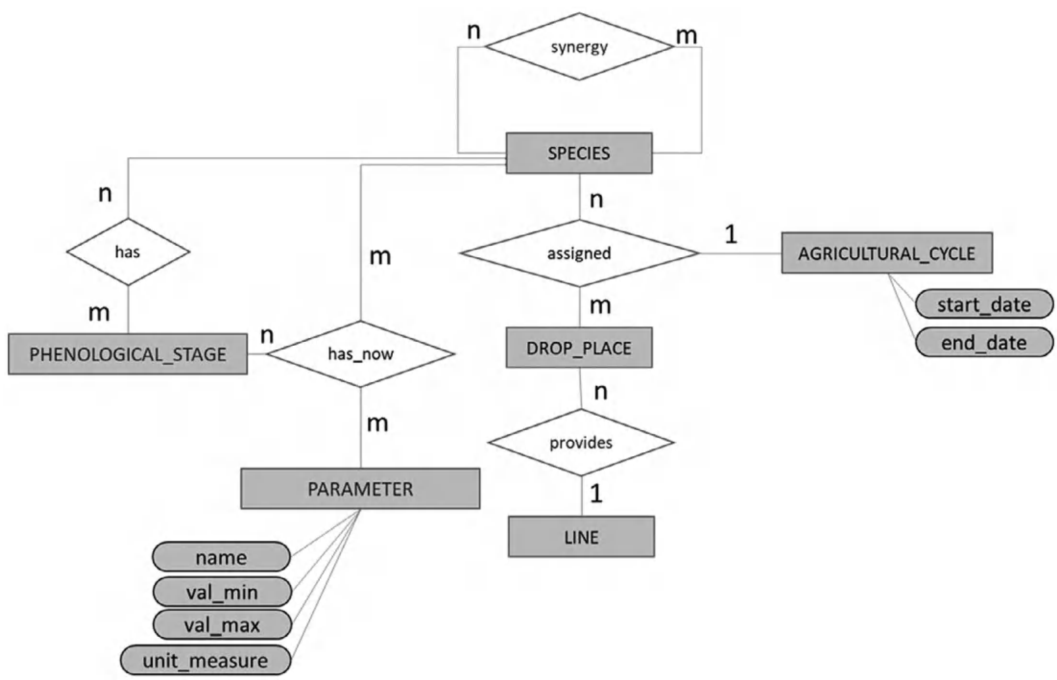

FIGURE 7.14 Template 8—SPECIES and crop management.

For example, if there are 100 sensors collecting temperature measurements every second, then the measurement table will grow by 100 rows every second. The rate at which the measurement table grows will also depend on the amount of data generated by each sensor. For example, if a sensor is collecting a high-resolution image every second, then the measurement table will grow much more quickly than if the sensor is collecting a low-resolution image.

It is possible to migrate the MEASUREMENT table to a NoSQL database. In this case, a NoSQL database that supports the storage of large and high-frequency data can be used. Some examples of NoSQL databases that can be used to migrate the MEASUREMENT table are the following:

- Apache Cassandra
- Amazon DynamoDB
- Google Cloud Spanner
- MongoDB

These NoSQL databases are designed to handle large amounts of data, as well as high-frequency queries.

Here is an example of how to migrate the MEASUREMENT table to a NoSQL database:

1. Use a data export tool to extract the data from the MEASUREMENT table in a format compatible with the NoSQL database.
2. Use a data import tool to import the data into the NoSQL database.
3. Update the applications to use the NoSQL database. For example, SQL queries to use the NoSQL database's APIs can be modified.

Once the MEASUREMENT table is migrated to a NoSQL database, it is possible to take advantage of the benefits offered by NoSQL databases, such as scalability, availability, and performance.

Here are some of the benefits of using a NoSQL database for the MEASUREMENT table in Smart Agriculture:

- *Scalability*: NoSQL databases can scale dynamically to meet the needs of data growth.
- *Availability*: NoSQL databases are designed to be available 24/7.
- *Performance*: NoSQL databases can deliver high performance for high-frequency queries.

However, it is important to note that migrating a relational table to a NoSQL database can be a complex process. It is mandatory to carefully evaluate the application's requirements before performing the migration.

CASE STUDIES: SUCCESSFUL IMPLEMENTATIONS OF DATA ORGANIZATION STRATEGIES

In this section the ER model templates proposed in the previous sections are seen in action in a real case. The experimentation covered several areas in order to test the generality of the data models and their applicability even in unconventional situations.

The experimental site is a greenhouse used to simultaneously grow several horticultural species with different cultivation methodologies, i.e., soil and soilless crops. The selected species are combined according to principles called *strip intercropping* provided by organic and sustainable agricultural practices. These agronomic techniques fall under the so-called *synergistic agriculture*. Specifically, synergistic agriculture involves increasing the number of species per square meter in order to trigger positive interactions between them, increasing biodiversity in the soil, and, consequently, strengthening the resilience of the cropping system.

Six irrigation lines numbered from 1 to 6 (Table 7.5) were installed in the greenhouse. Each irrigation line accommodated a certain number of plants of the same species spaced according to specific transplanting techniques. Table 7.5 shows the transplanting layout.

The layout of species on the lines was calculated by an AI algorithm based on a combinatorial optimization technique called *constraint programming*. The algorithm defines the transplant layout in a way that maximizes synergy among species.

TABLE 7.5
Transplanting Configuration in Greenhouse

#Line	Transplanted Species	Distance on the Line (cm)
1	Tomato on the ground	30
2	Tomato on the ground	30
3	Tomato soilless	25
4	Zucchini on the ground	90
5	Cucumber	60
6	Two-level soilless freckles (80 and 150 cm above the ground)	10

The greenhouse is equipped with a *nervous system* consisting of sensor IoT nodes and actuator nodes. Specifically, each irrigation line is equipped with a solenoid valve controlled by an IoT node whose microcontroller is an Arduino NANO 33 IoT module. A second IoT node, again based on an Arduino NANO 33 IoT, is installed on each irrigation line and is connected to an electrochemical sensor that measures nitrogen (N), phosphorus (P), potassium (K) in mg/kg, electrical conductivity (μS/cm), temperature (°C), pH, and soil moisture (%).

The NPK sensor, in theory, can measure nutrients separately. In fact, the approach used to produce this type of sensor is called ISE (ion selective electrodes). These sensors use the measurement of read EC, to which calibration curves are applied to determine macronutrients. This mode of measurement does not really provide the absolute value of the nutrients, and therefore in experimentation it was decided to use a single mother mix, concentrated 100 times. The fertilizer injection rule was to have at least two macronutrients out of three subthresholds. The macronutrient mixture is distributed in two different containers (A and B) to have maximum solubilization compatibility. Micro- and meso-elements were distributed in the two tanks, A and B. The third mixture contributes nitric acid and is used exclusively to bring the pH of the soil into the optimal ranges (Figure 7.15).

The field system acquires real-time (every minute) sensor measurements and sends them to the back-end component hosted on the cloud. The back-end component has a microservices architecture. The exposed services have specialized tasks and deal with the registration of IoT nodes, registration of sensor measurements, registration of actuator status, and eventually decision-making that affects irrigation and fertigation processes. Specifically, a knowledge-driven AI algorithm has been developed and exposed on the cloud as a REST service. The algorithm asynchronously receives requests for a new state to be assumed by actuators. The algorithm accesses the knowledge base through an intermediary service that acts as a gateway and reads the sensor data. Once computed, the final response is transmitted to the requesting node, which will perform real-time control on the actuator (e.g., open a solenoid valve, start the south window motor, and activate a metering pump).

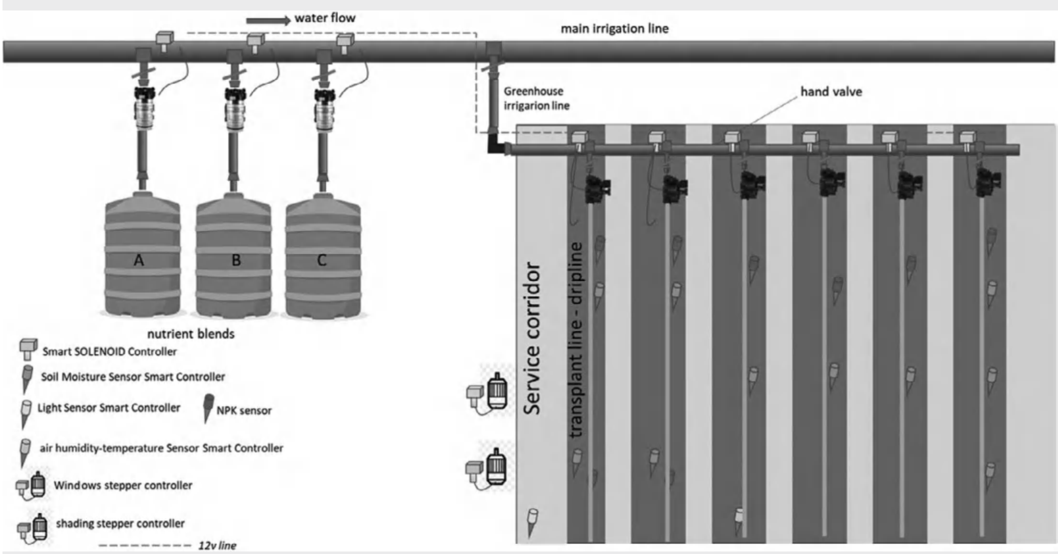

FIGURE 7.15 Smart fertigation system layout.

The database that manages all system data was implemented using the templates previously described in this chapter. Specifically, the ER templates were used according to the following criteria:

- The way IoT nodes of sensor or actuator type are classified is implemented using a single table with a type of field that discriminates sensors from actuators. Depending on the value taken by the type of attribute ("S" = sensor; "A" = actuator), some fields will be considered while others will be ignored (Figure 7.5(a)).
- The greenhouse in question was part of a group of greenhouses located on the same property. The overall plot (main container) was divided into child containers (the greenhouses), all related to the base container. Each greenhouse was referenced on the four edges (Figure 7.6).
- Each irrigation line (transplant line) has a length and pitch. This data is used to generate all instances of the drip points (Figure 7.8).
- Each irrigation line solenoid valve (and its microcontroller) was placed in DROP_PLACE 0 of the line (Figure 7.9).
- Sensor and actuator nodes that do not serve irrigation lines but control environmental parameters such as air temperature and humidity were instantiated with DROP_PLACE null and connected to the container (Figure 7.9).
- For each humidity sensor–solenoid pair arranged on an irrigation line, an instance was inserted in the database controls table that pairs a sensor to an actuator (Figure 7.11).
- For each N/P/K/pH sensor pair and IoT node controlling the related metering pump, an instance was inserted into the *controls* table of the database that couples a sensor to an actuator (Figure 7.11).
- The measurements read by the sensors are all one-dimensional in nature and are characterized by a *value* and a unit of measurement (Figure 7.12).
- The state of the actuators is implemented through a value, a timestamp, and a priority level that can be 0 (the state can be changed by an AI decision-maker) or 1 (the state has been forced for maintenance purposes, e.g., via a mobile app, and cannot be changed by an automatic decision-maker) (Figure 7.13).
- Transplanted species were characterized according to literature data on minimum and maximum thresholds of available soil nutrients, optimum pH, minimum and maximum soil moisture (Figure 7.14).
- The input data to the REST service implementing the field biodiversity maximization algorithm is defined in a synergy matrix whose cell (I, J) represents the compatibility between two species. The value (−1 = not compatible, 0 = neutral compatibility, 1 = positive compatibility) is entered into the database in the table expressing *synergy* self-relation (Figure 7.14).
- The output of the field biodiversity maximization algorithm was stored in the table expressing the *assigned* relationship (Figure 7.14).

The objective of the experimentation was to test the flexibility of the data model. Specifically, the knowledge management of an IoT system that is given the exclusive management of irrigation and fertigation processes, keeping in mind the following requirements:

- Each line can request to be irrigated/fertigated individually and independently of the others.

- The System has to handle multiple species simultaneously, each with its own water and fertilizer requirements.
- The System must be able to handle different agronomic practices, including ground cultivation and above-ground cultivation.
- The System must also manage via IoT the greenhouse home automation, consisting of the independent opening of windows according to weather conditions.
- Soil pH should be adjusted before any other nutrient deficiency.

Below are the greenhouse dimensions and irrigation system parameters:

- *Width*: 8 m
- *Length*: 12 m
- *Height to Ridge*: 5 m
- *Greenhouse Irrigation Pipe*: 1″ (32 cm)
- *Irrigation Lines*: 16 mm diameter dripline, 150 mm pitch, flow rate to dripline 2 L/h

The System, as soon as it was started, immediately acquired data from the sensors and, as expected, started acid channel injection to adjust the pH level where there was a need to do so. At steady state, it was able to handle all possible events because of the data structure built through a specific combination of the templates described in the first part of this chapter.

Figures 7.16–7.20 show the evolution over time of the species grown along the fertigation lines. As can be seen, all plants develop and fruit consistently with their phenological stages, highlighting the canopy whose development is correct with respect to expectations on the specific species.

FIGURE 7.16 Organization of irrigation lines in the greenhouse. (Photograph by the author.)

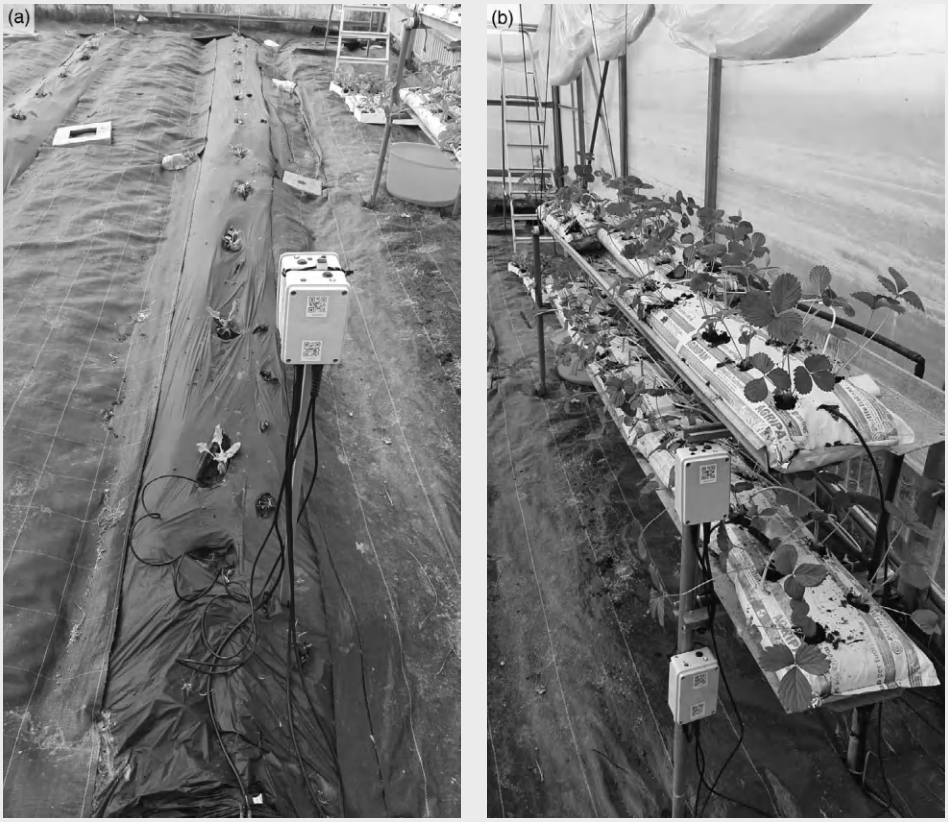

FIGURE 7.17 Installation of IoT nodes and transplanting of seedlings: (a) sensor and actuator nodes mounted together on a stake in a soil-grown line; (b) in the soilless strawberry cultivation, the nodes are mounted directly on the supporting structure holding the substrate bags. Photographs by the author.

FIGURE 7.18 Early stages of growth. (Photograph by the author.)

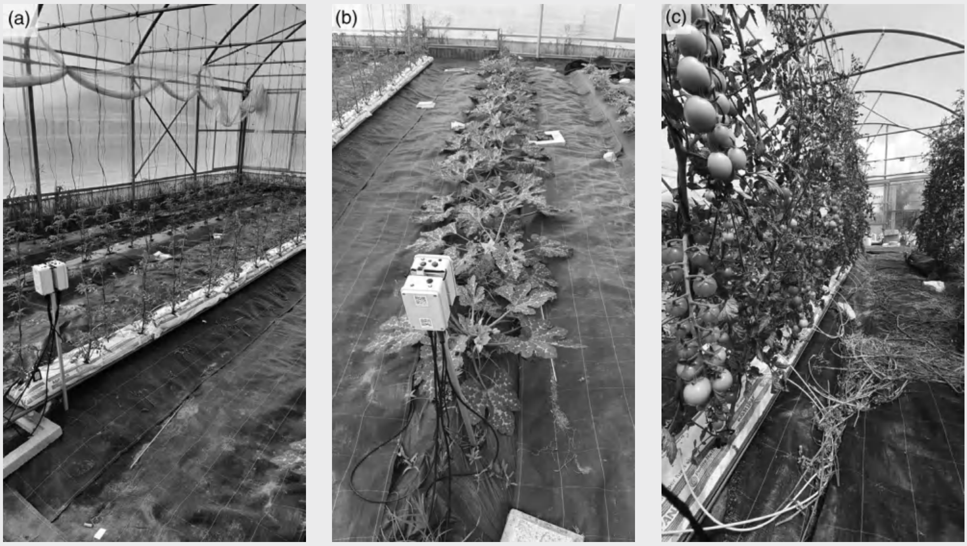

FIGURE 7.19 Close-up views of crop growth in the experimental greenhouse: (a) irrigation lines 1 and 2 with tomatoes grown on soil, and line 3 with the same tomato variety grown soilless; (b) line 4 with zuchini plants; (c) line 3 with soilless tomato plants at the fruiting stage. (Photographs by the author.)

FIGURE 7.20 Close-up views of the experimental greenhouse crops: (a) foreground of irrigation lines 4 and 5 with courgettes and watermelons; (b) foreground of line 6 with soilless strawberry cultivation. (Photographs by the author.)

7.5 CONCLUSION

7.5.1 Summary of Key Points

In this chapter, the fundamental importance of adopting relational template data modeling methodologies in Smart Agriculture has been explored. One of the main conclusions that emerges is the significant reduction in system development time when starting from the base of elementary building blocks instead of a blank sheet of paper. This methodology enables the creation of a robust and flexible digital ecosystem that can meet a wide range of data requirements, resulting in significant advantages in the systems development process.

In particular, this approach demonstrates its importance in the context of Smart Agriculture, where it is critical to configure complex information packages to be used as inputs for AI algorithms. By using predefined elementary building blocks, these blocks of data structures can be quickly combined and adapted to meet the specific needs of the algorithm, greatly accelerating the development process. This is crucial because AI algorithms are often tasked with making real-time decisions that must be promptly implemented in the field to maximize the effectiveness and efficiency of agricultural operations.

The relational template approach, possibly supplemented with NoSQL structures, not only provides a solid framework for organizing data in Smart Agriculture but also proves to be critical in reducing system development time and optimizing integration with AI algorithms, thus helping to improve efficiency, effectiveness of decisions, and/or prescriptions. This all reverberates in optimizing agronomic inputs.

7.5.2 Implications of Effective Data Organization for Smart Agriculture and Future Developments

The effective organization of data in Smart Agriculture offers several tangible benefits, with significant impacts on optimizing agricultural processes and reducing resource waste. Particularly relevant is the crucial role of properly organized data in performing life cycle analysis (LCA) of agricultural processes. The integration of services based on these data enables accurate and detailed assessment of the environmental impacts of agricultural practices, providing valuable information for adopting sustainable strategies and reducing overall environmental impacts.

In addition, such systems contribute significantly to the reduction of wasted water and fertilizer, which are crucial resources in agriculture. Through the use of organized data and advanced algorithms, irrigation and fertigation can be optimized, ensuring precise water and nutrient delivery targeted to plant needs. This not only increases agricultural efficiency and productivity but also reduces the overconsumption of natural resources, contributing to the sustainability of the agricultural sector. In the experimentation conducted, standard fertigation mixtures were used, with implementation only where necessary. However, it is important to note that this approach can still result in some over fertigation, especially when attempting to make up a deficiency of a particular nutrient by also distributing others that are not needed. This limitation could be overcome by separating the macronutrient mixtures and injecting only what is deficient into the irrigation circuit. This development requires the integration of specific sensors and the expansion of data models to provide for the possibility of conceptualizing the injection channel as well. These solutions represent a future prospect, fueled by ever-growing research in this rapidly evolving field.

BIBLIOGRAPHY

Adamo, T., Colizzi, L., Dimauro, G., Guerriero, E., & Pareo, D. (2024). Crop planting layout optimization in sustainable agriculture: A constraint programming approach. *Computers and Electronics in Agriculture*, *224*, 109162.

Colizzi, L., Caivano, D., Ardito, C., Desolda, G., Castrignanò, A., Matera, M., Khosla, R., Moshou, D., Hou, K., Pinet, F., Chanet, J.P., Hui, G. & Shi, H. (2020). Introduction to agricultural IoT. In *Agricultural internet of things and decision support for precision smart farming* (pp. 1–33). Academic Press.

Elbasi, E., Mostafa, N., AlArnaout, Z., Zreikat, A. I., Cina, E., Varghese, G., Shdefat, A., Topcu, A.E., Abdelbaki, W., Mathew, S. & Zaki, C. (2022). Artificial intelligence technology in the agricultural sector: A systematic literature review. *IEEE Access*, *11*, 171–202.

Elmasri, R., Navathe, S. B., Elmasri, R., & Navathe, S. B. (2020). Fundamentals of database systems. In *Advances in databases and information systems: 24th European Conference, ADBIS 2020, Lyon, France, August 25–27, 2020, Proceedings* (Vol. 12245, p. 139). Springer Nature.

Friha, O., Ferrag, M. A., Shu, L., Maglaras, L., & Wang, X. (2021). Internet of things for the future of smart agriculture: A comprehensive survey of emerging technologies. *IEEE/CAA Journal of Automatica Sinica*, *8*(4), 718–752.

Hobbs, J. R., & Israel, D. (1994). Principles of template design. In *Human language technology: Proceedings of a Workshop Held at Plainsboro, New Jersey, March 8–11, 1994*.

Naud, O., Taylor, J., Colizzi, L., Giroudeau, R., Guillaume, S., Bourreau, E., Crestey, T. & Tisseyre, B. (2020). Support to decision-making. In *Agricultural internet of things and decision support for precision smart farming* (pp. 183–224). Academic Press.

Soussi, A., Zero, E., Sacile, R., Trinchero, D., & Fossa, M. (2024). Smart sensors and smart data for precision agriculture: A review. *Sensors*, *24*(8), 2647.

Zhang, Q., Chen, M., & Liu, L. (2017). A review on entity relation extraction. In *2017 second international conference on mechanical, control and computer engineering (ICMCCE)* (pp. 178–183). IEEE.

8 Smart Sensing and Digital Twin Technology for Yield Estimation and Phenomics Prediction in Strawberries

Daeun Choi, Xu Wang, and Omeed Mirbod

8.1 INTRODUCTION

Strawberries are one of the most popular and economically important fruits globally, with a production volume of 9.2 million metric tons in 2021, consumed by millions of people worldwide (FAOSTAT, 2023). In the United States, strawberries are one of the important horticultural crops, with a total value of US$3 billion per year (Adams, 2019). California is the leading producer of fresh strawberries in the United States (90%), followed by Florida (8%), and other contributions from Oregon, and North Carolina (Kramer, 2021). The industry supports tens of thousands of jobs and is vital to the economy of many rural communities. However, strawberry production faces several challenges that affect both the quantity and quality of the harvest. To overcome these challenges and increase productivity, farmers are seeking opportunities in digital and Smart Agriculture technology, which has the potential to transform crop growth, harvesting, and distribution processes.

Smart sensing, phenomics prediction, and digital twin technology are three digital agriculture techniques that offer significant potential to improve strawberry production. Smart sensing involves using sensors to collect data on environmental conditions, plant growth, and fruit development (Amaya Diaz et al., 2020). Phenomics prediction focuses on analyzing plant traits and predicting their impact on yield and quality (Tardieu et al., 2017). Digital twin technology creates virtual models of agricultural fields and simulates crop growth and development, enabling growers and scientists to test different scenarios and optimize their strategies (Nasirahmadi & Hensel, 2022). This book chapter aims to explore the potential of these digital agriculture techniques for strawberry production in plasticulture, a common production system used by strawberry growers in the United States (Tabatabaie & Murthy, 2016). The chapter will provide an overview of each technique and its applications, as well as the steps required to implement them in strawberry production. The chapter will also provide case studies of successful implementations of these techniques and practical considerations for growers who want to adopt them.

Section 8.2 of the chapter will focus on smart sensing applications for yield estimation. This section will describe the types of sensors used in strawberry production, how they are installed and calibrated, and the yield estimation models that can be developed using the sensor data. Section 8.3 will focus on phenomics prediction and how it can enhance crop improvement. The section will describe methods used to collect and analyze phenotypic data and their typical process. Section 8.4 will focus on digital twin technology and its potential to optimize strawberry production. The section will describe how digital twins are created in strawberry production, the use cases for digital twins in crop management, and the integration of digital twins with other digital agriculture tools. Section 8.5 will discuss the challenges and opportunities that come with the adoption of digital and Smart Agriculture technology in strawberry production.

DOI: 10.1201/9781003510598-8

8.2 SMART SENSING APPLICATIONS FOR YIELD ESTIMATION

Smart sensing is a critical digital agriculture technique that can provide field data on environmental conditions, plant growth, and fruit development in strawberry production. By using smart sensing, strawberry growers can optimize their resources, prevent crop damage, and predict yield accurately. In this section, the implementation steps for smart sensing in strawberry production are described, such as sensor selection, installation and calibration, model development, and their successful smart sensing applications for yield estimation.

8.2.1 Sensor Selection

For optimal results in farm operations and location-specific needs, it is important to choose appropriate sensors. Factors such as cost-effectiveness, reliability, and compatibility with existing technologies should be taken into account during this selection process. There are several types of sensors that can be used in strawberry production, each with its specific function and benefits. Some of the most common sensors used in strawberry production include the following:

1. *RGB sensors*: RGB (Red, Green, Blue) sensors capture images in three primary color bands and are useful for monitoring plant health, growth, and development. They provide valuable visual information on the crop's condition, including number and size of plants and fruit (Choi et al., 2021).
2. *Multispectral sensors*: Multispectral sensors capture images in multiple spectral bands, beyond the human-visible range. These sensors provide detailed information about plant health and stress conditions, enabling targeted interventions to improve yield and quality (Liu et al., 2014).
3. *Hyperspectral sensors*: Hyperspectral sensors collect images across a wide range of spectral bands, offering a more detailed view of the crop's condition. They can identify specific plant stressors, such as diseases or nutrient deficiencies, allowing for precise management strategies (Siedliska et al., 2018).
4. *Thermal sensors*: Thermal sensors detect and measure the heat emitted by objects, including plants. In strawberry production, they are useful for monitoring plant temperature, detecting stress from heat or cold, and identifying areas with varying levels of water use, helping growers optimize irrigation and temperature management (Swarup et al., 2020).
5. *LiDAR sensors*: LiDAR (light detection and ranging) sensors use laser pulses to measure distances and create detailed, three-dimensional (3D) maps of the environment. In plasticulture-based strawberry production, LiDAR can assess plant height, canopy structure, and growth patterns, aiding growers in optimizing plant spacing and pruning strategies within the plastic mulch system (Zheng et al., 2021).

8.2.2 Installation and Calibration of Sensors

When installing optical sensors for strawberry farming, several factors are taken into consideration. The sensors should be mounted on an appropriate platform, which could be a fixed structure like a pole or a mobile one such as a drone, depending on the sensor type and application. The sensor should be positioned to ensure a clear line of sight to the strawberry plants within the plasticulture system, avoiding any obstructions. The height and angle of installation need to be optimized for the specific data collection requirements of each sensor type, ensuring accurate and reliable measurements. The sensors should be securely fastened to prevent any movement or misalignment during operation, which could interfere with data collection or potentially damage the sensors. For sensors sensitive to lighting conditions, such as RGB or multispectral sensors, artificial lighting sources can be used to maintain uniform lighting conditions across the monitored area. Calibration is an important step to ensure accurate data collection. Calibration involves comparing the sensor readings to a known standard and adjusting the sensor output accordingly.

1. *RGB sensors*
   - Regularly calibrate the sensor using a color calibration target, such as a color chart, to maintain accurate color representation.
   - Calibrate under similar lighting conditions to those in the field or greenhouse.
2. *Multispectral sensors*
   - Follow the manufacturer's guidelines for calibrating the sensor.
   - Regularly check the sensor's performance using known reference targets to ensure accurate spectral data.
3. *Hyperspectral sensors*
   - Follow the manufacturer's instructions for calibration.
   - Use radiometric calibration targets to maintain sensor accuracy.
   - Perform calibration checks periodically to ensure consistent data collection.
4. *Thermal sensors*
   - Calibrate the thermal sensor according to the manufacturer's guidelines.
   - Periodically check the sensor's performance using reference temperature sources, such as blackbody radiators, to ensure accurate temperature measurements.
5. *LiDAR sensors*
   - Follow the manufacturer's instructions for calibrating the LiDAR sensor.
   - Regularly assess the sensor's performance by comparing its measurements to known reference targets, ensuring accurate distance and elevation data.

8.2.3 Data Acquisition and Model Development for Yield Estimation

Smart sensing offers a significant benefit in strawberry production, primarily through its ability to establish crop monitoring and yield estimation systems. A crucial first step in this process is data acquisition and analysis. By gathering data from diverse sensor types, including RGB, multispectral, hyperspectral, thermal, and LiDAR sensors, users can gain comprehensive insights into plant health, growth, potential stressors, and yield. The typical steps for building yield estimation models are as follows:

1. *Model selection*: Choose an appropriate machine learning technique based on the complexity of the problem and the available data. Common machine learning algorithms include traditional machine learning algorithms (such as decision trees and support vector machines) and more complex deep learning models (such as convolutional neural networks).
2. *Feature extraction and selection*: When using traditional machine learning algorithms, identify and extract relevant features from the sensor data, such as vegetation indices (VIs), canopy temperature, plant height, canopy structure, fruit count, and fruit size. These features can be used as input variables for the yield estimation models, providing a direct link between sensor data and yield predictions. Deep learning has automated this process, eliminating the need for manual feature extraction and selection. Figure 8.1 displays the benefits of an effective feature selection in machine learning models.
3. *Model training and validation*: Use sensor data and corresponding groundtruth (such as yield measurement) to train and validate the selected model. Split the dataset into training and validation sets, ensuring that the model can generalize well to new, unseen data.
4. *Model optimization*: Fine-tune the model's parameters and features to improve its accuracy and predictive performance.

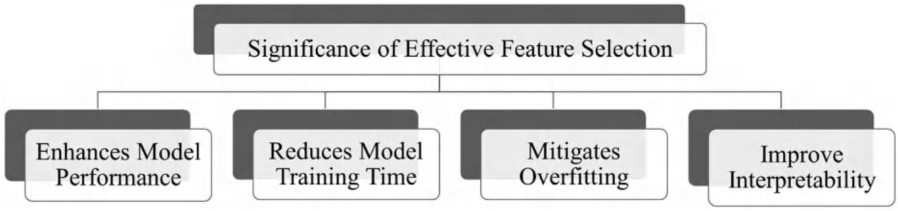

FIGURE 8.1 The impact of effective feature selection. The four key benefits of effective feature selection in machine learning models.

8.2.4 Examples of Successful Applications for Strawberry Production

Smart sensing has been used successfully in strawberry production to optimize resource use, prevent crop damage, and enhance yield and quality. Here are some examples of successful smart sensing applications in strawberry production:

1. VIs *using spectral sensors*: By analyzing data from multispectral sensors, growers can calculate VIs, such as the normalized difference vegetation index (NDVI) and the enhanced vegetation index (EVI) (Nasr et al., 2022). These indices can be correlated with plant biomass (Guan et. al., 2020), growth stage, and overall crop health (Veleva et al., 2022), providing an indirect measure of yield potential.
2. *Fruit counting using RGB images*: Machine learning and artificial intelligence techniques, such as decision trees, support vector machines, and deep learning models, have been employed to develop yield estimation models based on fruit detection and counting (Figure 8.2). Numerous studies have shown that these models can successfully identify and count strawberries in RGB images, even in complex environments with varying lighting conditions, plant densities, and fruit orientations (Yu et al., 2019). The fruit count data, along with other parameters like size and color (Wang et al., 2022), can then be used to predict the total yield (Lamb & Chuah, 2018; Zhang et al., 2022).
3. *Canopy structure and plant height-based estimation*: LiDAR sensors have been used to assess plant height (Figure 8.2), canopy structure, and growth patterns in strawberry production (Saha et al., 2022). By correlating these measurements with historical yield data, growers can develop yield estimation models that help optimize plant spacing, pruning strategies, and other cultivation practices to maximize yield potential.

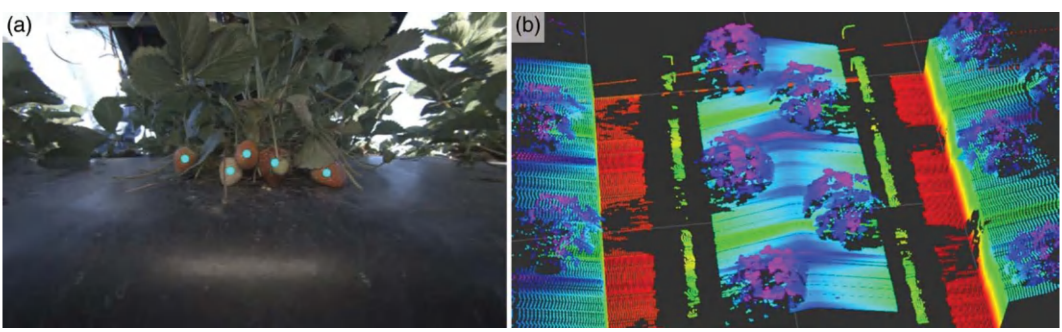

FIGURE 8.2 Two examples of smart sensing applications in strawberry production. (a) Strawberry yield forecasting using RGB images and deep learning algorithm. (b) Strawberry canopy and bed height measurement using LiDAR sensing technology.

4. *Thermal-based stress detection and yield prediction*: Thermal sensor data can be used to identify areas of water stress, heat stress, or cold stress in strawberry production (Li et al, 2010). By addressing these stressors, growers can improve plant health and enhance yield potential. Yield estimation models that incorporate thermal data can help predict the impact of stress on overall yield and guide appropriate interventions.

8.3 PHENOMICS PREDICTION

8.3.1 Introduction to Phenomics and Its Relevance to Crop improvement

Technological advancements in DNA (deoxyribonucleic acid) sequencing have profoundly impacted numerous biological disciplines, including crop improvement through breeding, transforming them from areas with limited genomic resources to information-rich sciences. Although the capacity to generate genomic data has expanded exponentially since the early 2000s, the phenotypic information crucial to unlocking the potential of data-driven breeding has not kept pace. It is only recently that this aspect has begun to evolve into a high-throughput, data-rich endeavor. Phenotypic data on such a scale is essential to establish genotype-to-phenotype relationships, a challenge commonly referred to as the G2P problem (Cooper et al., 2002). The deficit of phenotypic information is often identified as a bottleneck to plant improvement (Richards et al., 2010), as well as genetics and genomics studies, which includes the implementation of genomic selection (GS) (Cobb et al., 2013). Historically, the collection of phenotypic data has been labor-intensive, time-consuming, and costly. Unfortunately, many of these constraints still persist today.

Phenomics, which involves the comprehensive study of phenotypes, has emerged as a promising field to mitigate the slow pace and low throughput associated with phenotyping (Cobb et al., 2013; Furbank & Tester, 2011). Tools in phenomics have been applied in both field and controlled environments, examining multiple levels of plant organization from whole plant canopies to individual leaves. Phenomic prediction is a concept rooted in the field of phenomics. Although a standard definition for phenomic prediction is yet to be established, there is a general consensus that it refers to the process of using extensive phenotypic data (often collected through high-throughput phenotyping (HTP) technologies) along with other information such as genomic data, to predict specific traits or characteristics in plants. Typically, HTP technologies can be characterized by one or several of the following features: the ability to measure plants non-invasively (Reynolds & Langridge, 2016), automation to reduce labor (Cabrera-Bosquet et al., 2012; Cobb et al., 2013), the capacity to measure multiple traits or plots (or both) concurrently (Bai et al., 2016; Barker et al., 2016), and the existence of efficient automated or semi-automated data processing pipelines (Araus & Cairns, 2014; Coppens et al., 2017). By integrating large-scale phenotypic data with genotypic data and environmental information, researchers can develop models to predict phenotypic outcomes. These models can then be applied to breeding programs to guide selections and accelerate the development of new varieties with desired traits.

8.3.2 Phenotypic Measurements in Strawberry

Data from HTP platforms are utilized to illustrate the growth and development of plants (Fahlgren et al., 2015; Fiorani & Schurr, 2013). A variety of physiological traits have been gauged using non-destructive imaging or sensor techniques, including canopy coverage, temperature, disease severities, fruit conditions, and stress indicators (Zheng et al., 2021). These measurements often rely on the use of diverse wavelengths of the electromagnetic spectrum, ranging from color (400–700 nm) for RGB digital imagery, near-infrared radiation for spectral indices (700–1000 nm), to hyperspectral (350–2500 nm) for full-spectrum readings (Fahlgren et al., 2015). Moreover, technologies such LiDAR and infrared thermometers (IRT) for thermal readings also leverage the electromagnetic spectrum (Fahlgren et al., 2015).

By judiciously selecting sensors that align with their specific targets, researchers have achieved success in evaluating plant growth. In the case of strawberries, Zheng et al. (2021) conducted a comprehensive review of a multitude of phenotyping techniques, including but not limited to canopy temperature, spectral reflectance, chlorophyll fluorescence, and direct growth measurements such as plant height and maturity. These measurements were captured using an array of point and image sensors, as detailed in *Overview of phenotypic data collection and processing—Sensors*. This wealth of data on plant growth and development can be utilized to inform decisions regarding breeding selection. For instance, spectral reflectance indices and canopy temperature have proven useful for the indirect selection of fruiting efficiency in strawberries (Li et al., 2010).

Image data derived from RGB cameras and active spectrophotometers have been employed for the measurement of early plant vigor (Dong et al., 2020), leaf area (Guan et al., 2020), and plant biomass (Zheng et al., 2022) in strawberries. Beyond analyzing data at a single point in time, researchers have monitored temporal plant growth using high-resolution RGB and near-infrared imaging. This approach has been successfully used for estimating strawberry biomass (Zheng et al., 2022). By training deep convolutional neural networks (DCNN) with digital images collected throughout the growing season, Zheng et al. (2022) demonstrated a high correlation and minimal disparity between the predicted biomass and manually measured biomass. This finding substantiates the feasibility of biomass estimation using phenomic prediction. As phenotyping methods have improved, researchers have begun to successfully employ imaging technologies to evaluate complex traits in strawberries. These include fruit detection (Yu et al., 2019), flower detection (Lin & Chen, 2018), 3D fruit modeling (He et al., 2017), and plant disease identification (Mahmud et al., 2020). The ability to accurately evaluate these traits provides researchers with opportunities to enhance their understanding of crop performance and make more informed selection decisions.

The range of traits measurable via HTP methods is constrained only by the ability to identify a sensor system that accurately evaluates a desired trait. For instance, over 100 VIs were reviewed by Xue and Su (2017), and the growing interest in hyperspectral imaging is likely to expand the number of VIs used in crop assessment. Any trait without a substantial body of literature supporting its measurement method should be carefully examined to confirm that the protocol indeed measures the trait of interest. For example, significant correlations were observed between unmanned aerial vehicle (UAV) measurements (Zheng et al., 2022) and ground vehicle measurements (Guan et al., 2020) across growth stages from early to late. This provides evidence that the UAV system offers data comparable to that obtained from ground-based sources.

While numerous traits have been suitable for HTP application, advancements in sensor technology and data analysis methods will likely enable the measurement or estimation of an even greater number of traits through non-destructive measures. For research programs implementing HTP methodologies, it's crucial to determine which target traits to measure and how to assess them in order to achieve optimal results. A frequent challenge with HTP is that while data collection is often straightforward—thereby enabling the creation of large datasets—these datasets may not always address the questions posed by researchers. This misalignment can result in the inefficient utilization of resources within research programs.

8.3.3 Phenotypic Data Collection and Processing

8.3.3.1 Data Collection Platforms

Various phenotyping platforms have been implemented in breeding and research programs. Simple, affordable, and portable hand-carried systems have been widely used (Peñuelas et al., 1992). More complex solutions, equipped with stereo cameras and capable of simultaneously measuring multiple plots for spectral reflectance and canopy architecture, offer increased throughput (Guan et al., 2020). Airborne systems, particularly UAVs, carrying color and multispectral cameras, are also employed for field-based phenotyping (Zheng et al., 2022). Gantry systems, such as the LemnaTech

GmbH (Germany) Field Scanalyzer, provide precision movement and incorporate a variety of sensor modules. Numerous commercial smart sensors, like the Smartfield™ FIT System and Agrela Ecosystems™ PheNode, can be deployed in the field and monitor plant traits in real-time. However, despite the detailed data these platforms can offer, they are often limited to small, fixed areas. The current challenge lies in selecting a system that can affordably measure desired traits. Researchers should define the size and scope of their program, identify the traits to be measured, and choose an appropriate measurement device. They also need to consider the time and monetary resources available, as well as any specialized training or licensing required for safe and legal operation of the platform.

8.3.3.2 Sensors

Remote sensing is a pivotal technology in plant phenotyping, with two common types of phenotypic data being point-based sensor observations and multi-dimensional data sets (i.e., images and point cloud data). Low-cost point-based sensors are generally used on ground platforms and provide easily derived trait measurements. For higher throughput and spatial resolution, imaging sensors are becoming more popular. Zhang and Zhang (2018) have reviewed most commonly used imaging technologies for plant HTP. Imaging technologies for plant HTP, such as multi- and hyperspectral cameras, require considerations of the number of spectrum bands, the band width, and the overlap between two consecutive spectral bands. Thermal cameras need evaluations of measurement resolution to accurately reflect dynamic temperature variation. Correct camera settings, like shutter speed, aperture value, and white balance, are crucial for image acquisition, particularly when taken from a moving platform. Camera manuals and photography experts can provide guidance to optimize these settings. Most spectral sensors can be categorized as active or passive. Active sensors have their own light source, making them less susceptible to environmental conditions, whereas passive sensors rely on ambient light and are influenced by changing environmental conditions. Sensor selection should also consider factors like field-of-view (FoV), measurement resolution, and expandability. FoV determines the area that a sensor observes during measurement, and sensor resolution refers to how precisely a trait can be measured. Expandability provides sensors with the ability to offer different measurements based on user needs. Given these considerations, understanding the sensors, their mode of action, and the factors affecting measurements is essential to ensure that the collected data is suitable for downstream analysis.

The advent of advanced technology promises the possibility of achieving super high-resolution and throughput phenotypic data through videos (i.e., 6K videos) and satellite photos (i.e., ground sampling distance <10 cm). As these technologies evolve, they are likely to become more prevalent in field-based HTP. These advancements will facilitate the generation of more high-dimensional phenotypic datasets through sensor fusion techniques (Jiang et al., 2018). For instance, sensor fusion technologies can integrate LiDAR point cloud data with pixel information from cameras (i.e., GeoSLAM Hub and Draw, https://geoslam.com), assisting in differentiating plant tissues. Moreover, more advanced sensing techniques such as radar could be employed to gather phenotypic data from beneath plant canopies. X-ray micro computed tomography has been used to reconstruct wheat grain structure without damaging the wheat spike physically (Hughes et al., 2017). These innovative sensing technologies will undoubtedly contribute to further discoveries in field phenomics research, while concurrently posing more challenges for data processing.

8.3.3.3 Data Acquisition Systems

Data acquisition systems establish the link between various sensors and immediate data storage. For individual sensors, such as the Trimble GreenSeeker, data acquisition happens automatically, allowing users to download a comprehensive file of observations. Some autopilot systems for UAVs perform a similar task by automating image collection at consistent time or space intervals. However, as HTP systems become more complex and integrate more sensors, users will likely need to develop protocols for consolidating sensor data. LabView (National Instruments, Austin, TX, USA) has been utilized on several phenotyping platforms (Barker et al., 2016) due to its ability to interface with sensors outputting different rates and types of signals. Programming languages like Python have also been employed to interact with and record data from multiple sensors (McGahee, 2016). While data acquisition systems may not be the primary concern for users of pre-established HTP systems, those building their own systems should be mindful of potential issues when connecting many, often disparate, sensors. Frequently, the most straightforward solution is to collaborate with engineers or computer programmers who possess the necessary skills to quickly resolve potential problems.

8.3.3.4 Data Processing

Significant progress has been made in the development of HTP platforms, but data management often gets overlooked. Regardless of the data type, the primary goal is to accurately assign data points or images to a specific plot for subsequent statistical analysis or crop modeling. The exact processing steps can vary across platforms, but in general, data should be processed for quality control and trait extraction as early as possible to identify potential errors (White et al., 2012).

All HTP data needs processing to convert raw data observations into values usable in modeling. Point data is often paired with global navigation satellite system (GNSS) information, based on the time of data collection (Barker et al., 2016). Image or multi-dimensional data is more challenging and requires several steps to process raw images into indices or values. Numerous processing pipelines have been presented for image data, with common themes including format conversion, image correction, ortho-mosaicking, radiometric calibration, and subsequent data extraction (Shi et al., 2016).

Regardless of the type of data, the primary goal is the accurate assignment of data points or images to a plot or a plant for subsequent use in statistical analysis or crop models. While GNSS tagging through point data or the generation of ortho-mosaic image data is almost universal, establishing the link between a data point's geographical location and the plot or plant it belongs to is crucial. The use of image-based deep learning for segmentation is gaining popularity, with techniques such as machine vision successfully identifying strawberry plants (Zheng et al., 2022).

Despite the effort devoted to extracting values from data and pairing phenotypic data with plot information for immediate analysis, long-term data storage and utilization have received less attention. The standards for data storage and curation often take a back seat to phenomics goals of QTL (Quantitative Trait Loci) mapping, trait dissection, or enhancing genetic gains in crops. Several resources, like the Phenomics Ontology Driven Data for Australian phenomics work, have been developed for storing phenomic data. However, these databases might not store all intermediary processing steps or raw data, which can impede the reproducibility of analysis. As such, it is recommended that researchers consider the entire data lifecycle, from collection to storage, with an emphasis on potential data reuse. This would entail storing raw data, backups, extracted traits, and the processes used to develop them, along with plot information.

8.4 DIGITAL TWIN TECHNOLOGY

Digital twins in agriculture provide cutting-edge technology for creating virtual replicas of crops and agricultural systems. They are digital copies of physical objects or systems that provide up-to-date representation of themselves as they interact within a simulated environment (VanDerHorn & Mahadevan, 2021). By providing real-time exchange of information between the physical and virtual world, digital twins provide a powerful capability that growers, researchers, and engineers can leverage in different agricultural applications. For example, strawberry growers can optimize their management strategies and enhance their decision-making capabilities. Researchers can monitor the effect of external factors and stresses on plant growth and development. Engineers and innovators can evaluate new agricultural tools and machineries in simulation, detecting potential problems early on, and therefore lessening cost and time spent testing equipment on the farm.

In this section, there is a description of how digital twins are created, their use cases in crop management, and the integration of digital twins with other digital agriculture techniques. The case studies that are provided are of successful digital twin applications in crop management and strawberry production, such as the use of digital twins to simulate different irrigation scenarios and analyze post-harvest quality assessment of strawberry fruit. Finally, an example of how digital twins can be used in strawberry production is given.

8.4.1 Creation and Updating of Digital Twins

Digital twins can be characterized by three core components, the physical object in the real world, the physical object in the virtual world, and the flow of information that connects the physical and digital space together (Grieves, 2014; Nasirahmadi & Hensel, 2022; VanDerHorn & Mahadevan, 2021). Although multiple studies have attempted to create guidelines on how to make digital twins, a widely accepted approach has not yet been established. The outline below summarizes some commonly employed steps in the creation of digital twins (Figure 8.3).

1. *Defining scope*: It is important to first identify the necessary features and levels of abstraction needed for a digital twin in a particular application (VanDerHorn & Mahadevan, 2021). This can help maximize its usability while optimizing for cost and effort to develop it. *Twin* does not necessarily mean *the same* but rather complex enough to solve the required problem (Zhang et al., 2021). This approach will also help plan for the types of data to collect and sensors to use.
2. *Data collection*: A digital twin requires accurate and reliable data so it can coevolve with its physical counterpart throughout its lifecycle (Ariansyaha et al., 2020). These data sources can come from smart sensors, models of physical objects created by computer software, historical data, research literature, or manual measurements collected from human observation.
3. *Model development*: The virtual model is the core of a digital twin, reproducing its geometry, physical and behavioral properties, and rules of the physical object (Segovia & Garcia-Alfaro, 2022). The model should be accurate and validated against field data to ensure its reliability.
4. *Connectivity and information flow*: A link needs to be established between the physical and virtual entity. Here, the issues of speed, latency, and cyber security also need to be addressed depending on the application. The link can be wireless or wired, depending on the physical asset's characteristics, and data should be transformed from raw to a usable format (Ariansyaha et al., 2020). Internet of things (IoT) devices taking measurements of a physical asset and sending the information to the cloud is one example of connectivity and information flow.

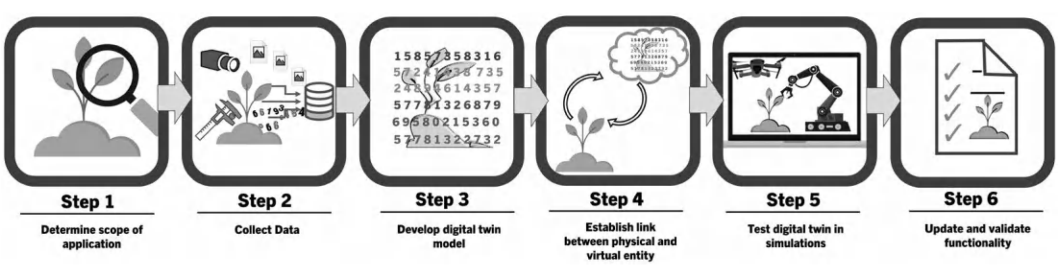

FIGURE 8.3 Sample outline steps for creating a digital twin.

5. *Simulation*: Simulation software is often used to observe the interaction of digital twins in a virtual environment to help optimize a system. This can include simulating crop growth for yield prediction, testing the effects of post-harvest practices, analyzing different irrigation regimes, or testing agricultural equipment and robotics systems.
6. *Update and validate*: The digital twin should be updated regularly to reflect changes in the crop and the environment. The updates can be made using new data collected from sensors or other sources, or by adjusting the model parameters based on field observations and simulation results. These updates should be validated against the original purpose and scope of the digital twin.

CASE STUDIES FOR DIGITAL TWINS IN CROP MANAGEMENT

Digital twin technology offers several use cases for crop management in strawberry production, such as optimization of resource use, prediction of yield and crop quality, and testing of management scenarios. Below are some examples of use cases for digital twins in strawberry production:

1. *Simulation of irrigation scenarios*: Digital twins can be used to simulate different irrigation scenarios and optimize water use efficiency. For example, a digital twin can simulate the growth and development of strawberries under different irrigation regimes, such as drip irrigation, sprinkler irrigation, or subsurface irrigation, and predict the impact on yield and quality.
2. *Growth modeling*: Digital twins can be used to predict plant growth patterns from genomics data as well as simulate the growth and development of strawberries under different fertilizer application rates, planting densities, or cultivars.
3. *Post-harvest packaging*: Retailers demand high-quality fruit from growers that meet certain criteria including packing weight. For automated harvesters, a digital twin replica of strawberry fruit can be created with variable size and shape to determine the most optimized pick and placement of fruit in a packaging container to consistently meet the retailer's criteria.
4. *Robotic systems for harvesting*: Digital twins can be used to support robotic system training for strawberry production tasks. For example, to prevent damage to strawberry plants, robotic harvesters can initially be trained in simulation to interact and receive sensor feedback from the digital twin representation of a strawberry plant and its surrounding environment before being deployed to the field for testing.

INTEGRATION WITH OTHER DIGITAL AGRICULTURE TECHNIQUES

Digital twin technology can be integrated with other digital agriculture techniques, such as decision support systems (DSS) to maximize their benefits and improve decision-making. Below are some examples of integration of digital twin technology with other digital agriculture techniques:

1. *Integration with internet of things*: IoT-based applications were some of the earliest approaches in agriculture to leverage digital twins (Verdouw & Kruize, 2017). Their focus was on basic monitoring capabilities, such as using sensors to send movement of cattle to the cloud, essentially creating digital twin representations of cattle to monitor their health, provide behavior detection, and make predictions on breeding cycles. The digital twins would be updated and tuned from each cattle's movement.

2. *Integration with automation and robotics*: Growers are increasingly turning toward mechanization and robotics to fill the labor shortage in agriculture. Digital twins of robotic systems can be developed to analyze their performance in 3D-simulated agricultural environments. Simulated sensor data streamed in real-time can help develop and test robotic systems algorithms and reduce time-consuming field trials (Linz et al., 2019).
3. *Integration with crop growth models to improve DSS*: Predictive modeling on strawberry plant growth has been studied in both its geometric development on canopy structure (Guan et al., 2022) and crop growth models for yield prediction (Hopf et al., 2022). Digital twins can provide real-time data on the status of agricultural crops with more precise monitoring to enhance DSS capabilities. For example, weather data is a common DSS input which includes temperature, humidity, and precipitation that can affect use of irrigation systems. By incorporating soil moisture sensors for continuous feedback on the status of soil beds, the DSS can make better predictions on needed water usage for irrigation (Alves et al., 2019).
4. *Integration with big data analytics*: Digital twins can be used to generate synthetic data and integrated with big data analytics tasks such as training neural network models for strawberry detection in images (Goondram et al., 2020). Strawberry plants have varying physical attributes depending on the chosen cultivar, including canopy density, fruit shape, or flowering habits. Collecting images for every cultivar is impractical and costly but slight modifications to digital twin parameters can allow for generating desired plant traits with randomized variations for image data collection.

EXAMPLES OF SUCCESSFUL DIGITAL TWIN APPLICATIONS IN STRAWBERRY PRODUCTION

Digital twin technology has been used successfully to optimize resource use, enhance crop quality, and improve decision-making. Below are some examples of successful digital twin applications in strawberry and other crop production systems:

1. *Use of digital twins for post-harvest quality assessment (Figure 8.4a)*: In a study conducted in Switzerland, digital twins were used to determine the effect on fruit quality during cold chain shipment from Spain to Switzerland. The study found that strawberries could be losing considerable fruit quality (up to 70%) from harvest to reaching grocery shelves, emphasizing the importance of shortening shipment time and analyzing the temperature performance of each shipping segment (Shoji et al., 2022).
2. *Use of digital twins for irrigation optimization*: A virtual environment consisting of a digital twin irrigation system was created where different irrigation strategies combined with farm practices could be simulated. The method used an IoT platform where data was sourced from soil probes, weather station, and the irrigation system to calculate water deficiency and send daily irrigation prescriptions to a simulated farm's irrigation system (Alves et al., 2023).
3. *Use of digital twins for crop damage assessment (Figure 8.4b)*: In one study, a "digital potato" was created as a plastic object having the same weight and size as a real potato. It was then equipped with sensors to detect impacts, shocks, and rotations during machine harvest and post-harvest processes. As the digital potato ran through the same procedures of real potatoes during harvest, real-time data was analyzed to adjust machine harvest and conveyor settings to minimize crop damage (Kampker et al., 2019).

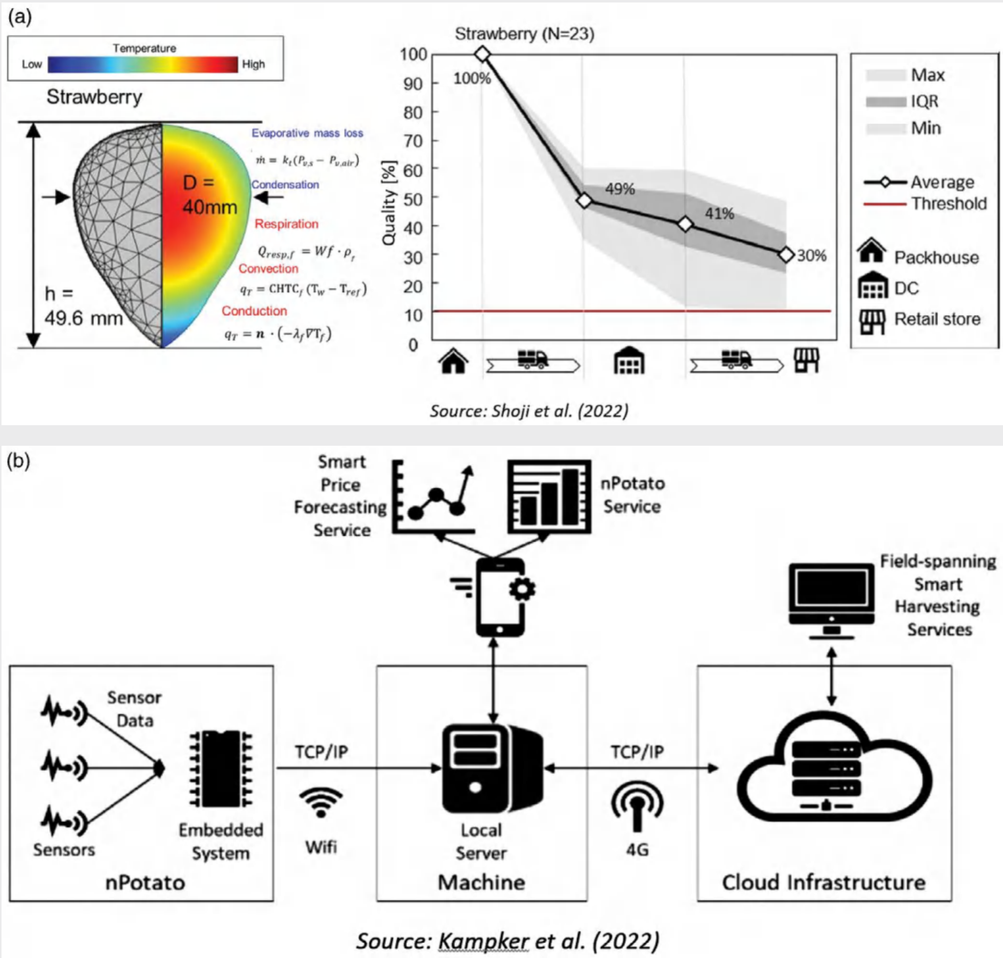

FIGURE 8.4 Two implementations of digital twin technology in agriculture with (a) showing how strawberry fruit is modeled to keep track of fruit quality during shipment, and (b) showing architecture for collecting sensor data from A potato as it passes through harvest and post-harvest stages.

IMPLEMENTATION OF DIGITAL TWIN TECHNOLOGY IN PLASTICULTURE

There are numerous potential applications for digital twin technology in plasticulture strawberry production. Since automation and robotics will play a crucial role in future of strawberry management tasks, one task may be to develop a path-planning mechanism for a ground vehicle to traverse over a strawberry bed. Testing equipment in the field is time-consuming and costly for engineers, and growers risk damage to their fields from equipment malfunction during early trials. A digital twin representation of a strawberry farm environment with a strawberry bed will therefore be useful for reading sensor data, such as a LiDAR, to develop and test the navigation algorithm. Below are some potential steps that could be used to implement this digital twin (Figure 8.5):

1. *Defining scope*: The farm environment will require a replica strawberry bed, a soil surface structure, and strawberry plants. The bed and ground surface will need to be

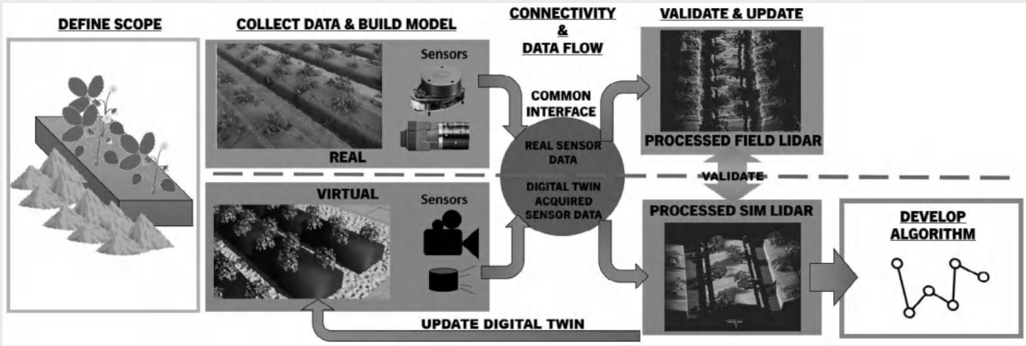

FIGURE 8.5 Sample workflow of creating and updating a digital twin representation of a strawberry field for the application of developing a robotic navigation algorithm using a LiDAR sensor.

representative of the field, but the strawberry plants can be a simplified model since interaction with the plants will be limited.

2. *Data collection*: Data can be measured manually or inquired from an extension agent or farm manager. Example data to collect are bed width, height, and bed surface geometry. Row spacing and row length for testing vehicle clearance will also be important. Plant height and maximum canopy size will be useful to determine the minimum clearance a vehicle needs away from the bed. LiDAR sensor data will also be collected from the strawberry beds for later validation.
3. *Modeling*: Measurements from the bed can be input into a 3D computer-aided design (CAD) software. Strawberry plants can be generated using a procedural modeling software or 3D graphics design software. The virtual model in Figure 8.5 shows the sample strawberry bed, field, and plants in a simulation environment.
4. *Simulation, connectivity, and information flow*: Simulation tools contain sensor replica models that can be imported and run to collect data. Figure 8.5 shows the processed simulated LiDAR data acquired from the digital twin strawberry bed with plants. The LiDAR sensor is simulated, and data is processed by a robotic software plugin tool. The same tool can connect and collect data from a real-world LiDAR sensor, therefore acting as a common interface between the virtual and real domains.
5. *Update and validate*: Sensor data collected from the digital twin is validated against sensor data collected from a field trial. Additional adjustments to the digital twin strawberry farm and the simulated LiDAR sensor can then be made such as reducing the sensor resolution to match the field sensor's output, introducing noise to the data, or adjusting the soil texture for more uneven representation of the ground floor. Once these updates are made, the digital twin can then be used to develop a navigation algorithm.

8.5 CHALLENGES AND OPPORTUNITIES

While smart sensing, phenomics prediction, and digital twin technology offer numerous benefits for strawberry production, it also poses several challenges and opportunities.

1. *Cost*: Smart sensors, phenotyping equipment, and digital twin software can be expensive, and growers may not have the resources to invest in these tools. Moreover, the adoption of these technologies requires specialized knowledge and skills, which may not be readily available in all regions.

2. *Integration with other digital agriculture techniques*: To maximize the benefits and improve decision-making, data collected from smart sensors and phenotyping equipment must be accurate and consistent across different systems. This requires the development of standardized protocols for sensor installation, calibration, and data analysis.
3. *Model accuracy*: The accuracy of digital agriculture models depends on the quality and reliability of the data used to create it. It is important to ensure that the data collection, modeling, and simulation processes are accurate and validated against field data.
4. *Customization*: Digital agriculture technologies should be customized to the specific needs and conditions of each grower and location. The optimal sensor placement, calibration, and yield estimation model will depend on factors such as climate, soil type, and cultivar characteristics.
5. *Training of workforce*: It is necessary to train new workforce on the use of digital agriculture technology and its integration with existing production practices. This will help ensure that everyone is on board and understands the benefits and challenges of the new approach.

Despite these challenges, the integration of smart sensing, phenomics prediction, and digital twin technology offers significant opportunities for the strawberry industry.

1. *Yield optimization*: By integrating data on plant health, growth, and environmental conditions, these technologies could help predict and optimize crop yields, aiding in market planning and reducing waste.
2. *Climate change adaptation*: The integration of these technologies could be used to develop more resilient crops by identifying traits that make them more resistant to changes in weather patterns, pests, and diseases.
3. *Consumer-centric breeding*: Advanced sensing and prediction technologies could help breeders develop new varieties with traits that consumers desire, such as better taste, texture, or nutritional content, potentially creating new markets and increasing profitability.
4. *Scalability*: These technologies could be applied at different scales, from small family farms to large agricultural businesses, making them versatile tools for a variety of contexts.

8.6 CONCLUSION

Smart sensing, phenomics prediction, and digital twin technologies represent a significant opportunity for the strawberry industry. By providing growers with a more comprehensive view of their crops, these technologies can help optimize management practices, increase productivity and profitability, and promote sustainable agriculture.

However, the adoption of these technologies poses several challenges, including high costs and the need for standardized protocols for data collection and analysis. To overcome these challenges, stakeholders in the strawberry industry must work together to develop innovative solutions and promote the adoption of these technologies.

Overall, the integration of smart sensing, phenomics prediction, and digital twin technology has the potential to transform the strawberry industry and pave the way for more sustainable and profitable agriculture. By leveraging these tools, growers can improve their crop management practices, optimize resource use, and reduce the environmental impact of their operations.

To fully realize the benefits of these technologies, however, there is a need for continued research and development. New sensors, phenotyping equipment, and digital twin software must be developed to meet the specific needs of the strawberry industry. Moreover, standardized protocols for data collection and analysis must be established to ensure the accuracy and consistency of the data generated by these tools.

ACKNOWLEDGEMENT

This study was supported by the USDA National Institute of Food and Agriculture Multistate Research under Project #FLA-GCR-006262 and Accession #7003555. AI-assisted technology was used to improve readability and language of the manuscript.

REFERENCES

Adams, R. (2019). *The prospect of American strawberries*. NC State Extension, July 29, 2025. Retrieved May 10, 2023. https://ipm.ces.ncsu.edu/2019/02/the-prospects-of-american-strawberries/

Alves, R. G., Maia, R. F., & Lima, F. (2023). Development of a digital twin for smart farming: Irrigation management system for water saving. *Journal of Cleaner Production*, 388, 135920.

Alves, R. G., Souza, G., Maia, R. F., Tran, A. L. H., Kamienski, C., Soininen, J. P., Plinio, A.J. & Lima, F. (2019). A digital twin for smart farming. In *2019 IEEE global humanitarian technology conference (GHTC)* (pp. 1–4). IEEE.

Amaya Diaz, J.C., Rojas Estrada, L., Cardenas-Ruiz, C. A., Ariza-Colpas, P. P., Piñeres-Melo, M. A., Ramayo González, R. E., Morales-Ortega, R. C., Ovallos-Gazabon, D. A., & Collazos-Morales, C. A. (2020). Monitoring system of environmental variables for a strawberry crop using IoT tools. *Procedia Computer Science*, *170*, 1083–1089.

Araus, J. L., & Cairns, J. E. (2014). Field high-throughput phenotyping: The new crop breeding frontier. *Trends in Plant Science*, *19*(1), 52–61.

Ariansyaha, D., Fernàndez del Amo, I., Erkoyuncu, J. A., Agha, M., Bulka, D., De La Puante, J., Langlois, M., M'khinini, Y., Sibson, J., & Penver, S. (2020). Digital twin development: A step by step guideline. *SSRN Electronic Journal*. https://doi.org/10.2139/ssrn.3717726

Bai, G., Ge, Y., Hussain, W., Baenziger, P. S., & Graef, G. (2016). A multi-sensor system for high throughput field phenotyping in soybean and wheat breeding. *Computers and Electronics in Agriculture*, *128*, 181–192.

Barker, J., III, Zhang, N., Sharon, J., Steeves, R., Wang, X., Wei, Y., & Poland, J. (2016). Development of a field-based high-throughput mobile phenotyping platform. *Computers and Electronics in Agriculture*, *122*, 74–85.

Cabrera-Bosquet, L., Crossa, J., von Zitzewitz, J., Serret, M. D., & Luis Araus, J. (2012). High-throughput phenotyping and genomic selection: The frontiers of crop breeding converge F. *Journal of Integrative Plant Biology*, *54*(5), 312–320.

Choi, J. Y., Seo, K., Cho, J. S., & Moon, K. D. (2021). Applying convolutional neural networks to assess the external quality of strawberries. *Journal of Food Composition and Analysis*, *102*, 104071.

Cobb, J. N., DeClerck, G., Greenberg, A., Clark, R., & McCouch, S. (2013). Next-generation phenotyping: Requirements and strategies for enhancing our understanding of genotype–phenotype relationships and its relevance to crop improvement. *Theoretical and Applied Genetics*, *126*, 867–887.

Cooper, M., Chapman, S. C., Podlich, D. W., & Hammer, G. L. (2002). The GP problem: Quantifying gene-to-phenotype relationships. *In Silico Biology*, *2*(2), 151–164.

Coppens, F., Wuyts, N., Inzé, D., & Dhondt, S. (2017). Unlocking the potential of plant phenotyping data through integration and data-driven approaches. *Current Opinion in Systems Biology*, *4*, 58–63.

Dong, C., Wang, G., Du, M., Niu, C., Zhang, P., Zhang, X., Ma, D., Ma, F. & Bao, Z. (2020). Biostimulants promote plant vigor of tomato and strawberry after transplanting. *Scientia Horticulturae*, *267*, 109355.

Fahlgren, N., Gehan, M. A., & Baxter, I. (2015). Lights, camera, action: High-throughput plant phenotyping is ready for a close-up. *Current Opinion in Plant Biology*, *24*, 93–99.

FAOSTAT. (2023). *Strawberry production in 2021, crop and livestock statistics (pick lists).* Food and Agriculture Organization of the United Nations. Retrieved May 10, 2023.

Fiorani, F. & Schurr, U. (2013). Future scenarios for plant phenotyping. *Annual Review of Plant Biology*, *64*, 267–291. https://doi.org/10.1146/annurev-arplant-050312-120137

Furbank, R. T., & Tester, M. (2011). Phenomics – Technologies to relieve the phenotyping bottleneck. *Trends in Plant Science*, *16*(12), 635–644.

Goondram, S., Cosgun, A., & Kulic, D. (2020). *Strawberry detection using mixed training on simulated and real data*. arXiv preprint arXiv:2008.10236.

Grieves, M., 2014. Digital twin: Manufacturing excellence through virtual factory replication. *White Paper*, *1*, 1–7.

Guan, Z., Abd-Elrahman, A., Fan, Z., Whitaker, V. M., & Wilkinson, B. (2020). Modeling strawberry biomass and leaf area using object-based analysis of high-resolution images. *ISPRS Journal of Photogrammetry and Remote Sensing*, *163*, 171–186.

Guan, Z., Abd-Elrahman, A., Whitaker, V., Agehara, S., Wilkinson, B., Gastellu-Etchegorry, J. P., & Dewitt, B. (2022). Radiative transfer image simulation using L-system modeled strawberry canopies. *Remote Sensing*, *14*(3), 548.

He, J. Q., Harrison, R. J., & Li, B. (2017). A novel 3D imaging system for strawberry phenotyping. *Plant Methods*, *13*(1), 1–8.

Hopf, A., Boote, K. J., Oh, J., Guan, Z., Agehara, S., Shelia, V., Whitaker, V.M., Asseng, S., Zhao, X. & Hoogenboom, G. (2022). Development and improvement of the CROPGRO-Strawberry model. *Scientia Horticulturae*, *291*, 110538.

Hughes, A., Askew, K., Scotson, C. P., Williams, K., Sauze, C., Corke, F., Doonan, J.H. & Nibau, C. (2017). Non-destructive, high-content analysis of wheat grain traits using X-ray micro computed tomography. *Plant Methods*, *13*(1), 1–16.

Jiang, Y., Li, C., Paterson, A. H., Sun, S., Xu, R., & Robertson, J. (2018). Quantitative analysis of cotton canopy size in field conditions using a consumer-grade RGB-D camera. *Frontiers in Plant Science*, *8*, 2233.

Kampker, A., Stich, V., Jussen, P., Moser, B., & Kuntz, J. (2019). Business models for industrial smart services – The example of a digital twin for a product-service-system for potato harvesting. *Procedia Cirp*, *83*, 534–540.

Lamb, N., & Chuah, M. C. (2018). A strawberry detection system using convolutional neural networks. In *2018 IEEE international conference on big data (big data)* (pp. 2515–2520). IEEE.

Li, H., Li, T., Gordon, R. J., Asiedu, S. K., & Hu, K. (2010). Strawberry plant fruiting efficiency and its correlation with solar irradiance, temperature and reflectance water index variation. *Environmental and Experimental Botany*, *68*(2), 165–174.

Lin, P., & Chen, Y. (2018). Detection of strawberry flowers in outdoor field by deep neural network. In *2018 IEEE 3rd international conference on image, vision and computing (ICIVC)* (pp. 482–486). IEEE.

Linz, A., Hertzberg, J., Roters, J., & Ruckelshausen, A. (2019). Digitale Zwillinge als Werkzeug für die Entwicklung von Feldrobotern in landwirtschaftlichen Prozessen. In *39. GIL-Jahrestagung, Digitalisierung für landwirtschaftliche Betriebe in kleinstrukturierten Regionen – ein Widerspruch in sich?*

Liu, C., Liu, W., Lu, X., Ma, F., Chen, W., Yang, J., & Zheng, L. (2014). Application of multispectral imaging to determine quality attributes and ripeness stage in strawberry fruit. *PLoS ONE*, *9*(2), e87818.

Mahmud, M. S., Zaman, Q. U., Esau, T. J., Chang, Y. K., Price, G. W., & Prithiviraj, B. (2020). Real-time detection of strawberry powdery mildew disease using a mobile machine vision system. *Agronomy*, *10*(7), 1027.

McGahee, K. (2016). *Image-based mapping system for transplanted seedlings* [Doctoral dissertation, Kansas State University].

Nasirahmadi, A., & Hensel, O. (2022). Toward the next generation of digitalization in agriculture based on digital twin paradigm. *Sensors*, *22*(2), 498. https://doi.org/10.3390/s22020498

Nasr, I., Nassar, L., & Karray, F. (2022). Enhancing fresh produce yield forecasting using vegetation indices from satellite images. In *2022 IEEE international conference on systems, man, and cybernetics (SMC)* (pp. 2863–2868). IEEE.

Peñuelas, J., Savé, R., Marfà, O., & Serrano, L. (1992). Remotely measured canopy temperature of greenhouse strawberries as indicator of water status and yield under mild and very mild water stress conditions. *Agricultural and Forest Meteorology*, *58*(1–2), 63–77.

Reynolds, M., & Langridge, P. (2016). Physiological breeding. *Current Opinion in Plant Biology*, *31*, 162–171.

Richards, R. A., Rebetzke, G. J., Watt, M., Condon, A. T., Spielmeyer, W., & Dolferus, R. (2010). Breeding for improved water productivity in temperate cereals: Phenotyping, quantitative trait loci, markers and the selection environment. *Functional Plant Biology*, *37*(2), 85–97.

Saha, K. K., Tsoulias, N., Weltzien, C., & Zude-Sasse, M. (2022). Estimation of vegetative growth in strawberry plants using mobile LiDAR laser scanner. *Horticulturae*, *8*(2), 90.

Segovia, M., & Garcia-Alfaro, J. 2022. Design, modeling and implementation of digital twins. *Sensors*, 22(14), 5396. https://doi.org/10.3390/s22145396

Shi, Y., Thomasson, J. A., Murray, S. C., Pugh, N. A., Rooney, W. L., Shafian, S., Rajan, N., Rouze, G., Morgan, C. L. S., Neely, H. L., Rana, A., Bagavathiannan, M. V., Henrickson, J., Bowden, E., Valasek, J., Olsenholler, J., Bishop, M. P., Sheridan, R., Putman, E. B. & Yang, C. (2016). Unmanned aerial vehicles for high-throughput phenotyping and agronomic research. *PLoS ONE*, *11*(7), e0159781.

Shoji, K., Schudel, S., Onwude, D., Shrivastava, C., & Defraeye, T. (2022). Mapping the postharvest life of imported fruits from packhouse to retail stores using physics-based digital twins. *Resources, Conservation and Recycling*, *176*, 105914.
Siedliska, A., Baranowski, P., Zubik, M., Mazurek, W., & Sosnowska, B. (2018). Detection of fungal infections in strawberry fruit by VNIR/SWIR hyperspectral imaging. *Postharvest Biology and Technology*, *139*, 115–126.
Swarup, A., Lee, W. S., Peres, N., & Fraisse, C. (2020). Strawberry plant wetness detection using color and thermal imaging. *Journal of Biosystems Engineering*, *45*, 409–421.
Tabatabaie, S. M. H., & Murthy, G. S. (2016). Cradle to farm gate life cycle assessment of strawberry production in the United States. *Journal of Cleaner Production*, *127*, 548–554.
Tardieu, F., Cabrera-Bosquet, L., Pridmore, T., & Bennett, M. (2017). Plant phenomics, from sensors to knowledge. *Current Biology*, *27*(15), R770–R783.
Kramer, J. (2021). *USDA Economic Research Service Chart Detail – U.S. fresh strawberry production expands with newer varieties*. Charts of Notes 5/19/2021. Retrieved May 10, 2023. https://www.ers.usda.gov/data-products/charts-of-note/chart-detail?chartId=101156
VanDerHorn, E., & Mahadevan, S. (2021). Digital twin: Generalization, characterization and implementation. *Decision Support Systems*, *145*, 113524. https://doi.org/10.1016/j.dss.2021.113524
Veleva, P., Todorova, M., Atanasova, S., Georgieva, T., Yorgov, D., & Atanassova, S. (2022). The relationships between different vegetation indices and chlorophyll content index values (CCI) in strawberry leaves. In 2*022 8th international conference on energy efficiency and agricultural engineering (EE&AE)* (pp. 1–5). IEEE.
Verdouw, C. N., & Kruize, J. W. (2017). Digital twins in farm management: Illustrations from the FIWARE accelerators SmartAgriFood and Fractals. In *Proceedings of the 7th Asian-Australasian conference on precision agriculture digital*, Hamilton, New Zealand (pp. 16–18).
Wang, Y., Yan, G., Meng, Q., Yao, T., Han, J., & Zhang, B. (2022). DSE-YOLO: Detail semantics enhancement YOLO for multi-stage strawberry detection. *Computers and Electronics in Agriculture*, *198*, 107057.
White, J. W., Andrade-Sanchez, P., Gore, M. A., Bronson, K. F., Coffelt, T. A., Conley, M. M., Feldmann, K.A., French, A.N., Heun, J.T., Hunsaker, D.J., Jenks, M.A., Kimball, B.A., Roth, R.L., Strand, R.J., Thorp, K.R., Wall, G.W. & Wang, G. (2012). Field-based phenomics for plant genetics research. *Field Crops Research*, *133*, 101–112.
Xue, J., & Su, B. (2017). Significant remote sensing vegetation indices: A review of developments and applications. *Journal of Sensors*, 2017.
Yu, Y., Zhang, K., Yang, L., & Zhang, D. (2019). Fruit detection for strawberry harvesting robot in non-structural environment based on Mask-RCNN. *Computers and Electronics in Agriculture*, *163*, 104846.
Zhang, L., Zhou, L., & Horn, B. K. P. (2021). Building a right digital twin with model engineering. *Journal of Manufacturing Systems*, *59*, 151–164. https://doi.org/10.1016/j.jmsy.2021.02.009
Zhang, Y., Yu, J., Chen, Y., Yang, W., Zhang, W., & He, Y. (2022). Real-time strawberry detection using deep neural networks on embedded system (rtsd-net): An edge AI application. *Computers and Electronics in Agriculture*, *192*, 106586.
Zhang, Y., & Zhang, N. (2018). Imaging technologies for plant high-throughput phenotyping: A review. *Frontiers of Agricultural Science and Engineering*, *5*(4), 406–419.
Zheng, C., Abd-Elrahman, A., & Whitaker, V. (2021). Remote sensing and machine learning in crop phenotyping and management, with an emphasis on applications in strawberry farming. *Remote Sensing*, *13*(3), 531.
Zheng, C., Abd-Elrahman, A., Whitaker, V., & Dalid, C. (2022a). Prediction of strawberry dry biomass from UAV multispectral imagery using multiple machine learning methods. *Remote Sensing*, *14*(18), 4511.
Zheng, C., Abd-Elrahman, A., Whitaker, V. M., & Dalid, C. (2022b). Deep learning for strawberry canopy delineation and biomass prediction from high-resolution images. *Plant Phenomics*, 2022.

9 Remote Sensing for Automatic Disease Monitoring in Wheat

Orly Enrique Apolo-Apolo, Luis Sánchez-Fernández, Simon Appeltans, Gregorio Egea, and Manuel Perez-Ruiz

9.1 INTRODUCTION

Using remote sensing to detect diseases in crops is a challenging approach that integrates advanced technologies and expert knowledge to enhance agricultural productivity. This process begins with comprehensive crop field and environmental measurements, including critical soil (e.g., soil moisture and soil temperature) and meteorological (e.g., rainfall, wind speed, and relative humidity) variables. Considering their disease susceptibility, the choice of wheat cultivars is also crucial. Technologies such as unmanned aerial vehicles (UAVs), satellites, and ground vehicle sensors collect extensive data, which is then processed using big data and artificial intelligence (AI) algorithms to detect disease patterns and predict outbreaks. Agronomy and plant pathology experts interpret these processed data to develop effective disease management strategies. Decision-making involves selecting appropriate actions based on these insights, such as determining the location, speed, and type of implements used for disease control measures. Implementing innovative applications, including advanced prescription maps, variable rate applications, and auto-spreading technologies, ensures precise and efficient disease management. Environmental factors, such as soil health, nutrient balance, water availability, and climatic conditions, play significant roles in the occurrence of crop diseases and must be considered in monitoring efforts (Figure 9.1). By understanding and monitoring these factors, more accurate and effective disease detection and management strategies can be developed, leading to healthier crops and optimized agricultural productivity.

In this chapter, we will focus on the specific case of diseases in wheat, as it is one of the most widely cultivated crops worldwide, along with maize and rice.

9.2 GLOBAL SIGNIFICANCE OF WHEAT

In many countries (Europe, North Africa, West Asia, and parts of America), wheat (*Triticum aestivum*) is considered a staple food due to its numerous nutrients, properties, and the exceptional quality of its flour. Since ancient times, it has accounted for around 41% of the global cereal calorie uptake from direct consumption and 20% of the total calories consumed by humans (Shiferaw et al., 2013). It is the leading source of vegetable proteins in human food. Currently, global production stands at 781 million tons annually. The cultivated area is 220 million ha, making it the third most-produced cereal in the world (behind maize and rice) and the first in terms of cultivated area. This extensively cultivated area is due, among other factors, to wheat's adaptability to a wide range of climatic conditions, allowing it to be cultivated in almost every region, except tropical and polar areas. It is most extensively cultivated in Europe and Asia (Hyles et al., 2020). Global wheat production has tripled since 1960 and is expected to grow further through this century, driven by the usefulness of gluten to the food industry.

Wheat is a pivotal crop regarding calorie intake, ensuring global food security, and its economic impact. In 2022, it was the world's 49th most traded product, totaling $73.3B and representing 0.31% of global trade. Looking to the future, it is essential to continue increasing wheat production

 DOI: 10.1201/9781003510598-9

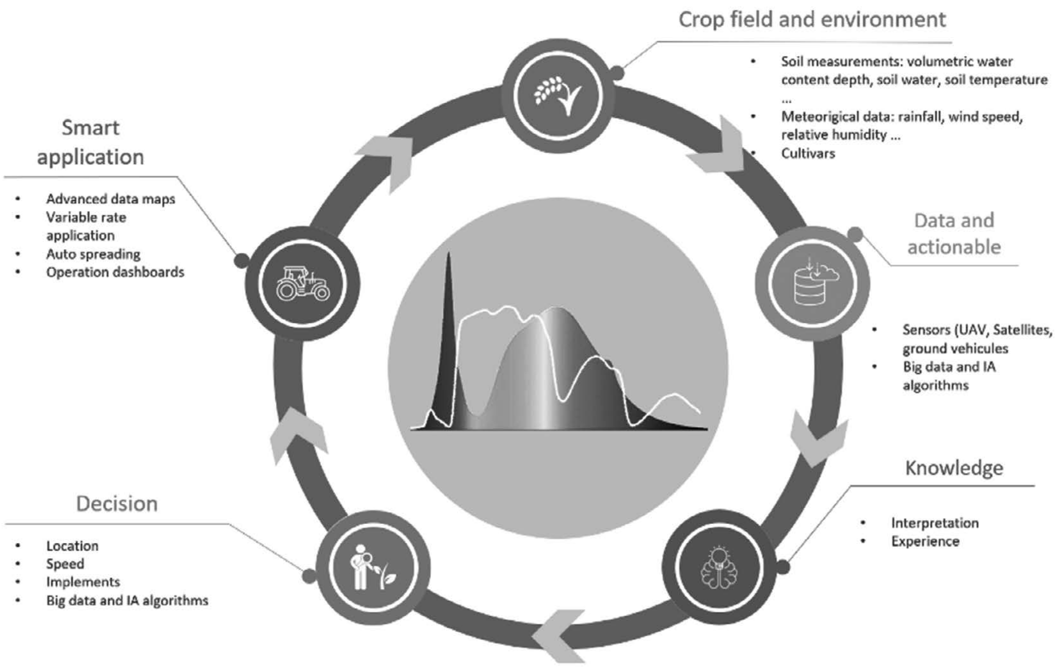

FIGURE 9.1 Integrated approach to crop disease detection and management using remote sensing technologies.

and quality while conserving available resources and minimizing adverse environmental effects. This requires a significant focus on research and increasingly remarkable contributions from agricultural science. Research must integrate advances in molecular sciences, biotechnology, and plant and pest ecology with a deeper understanding of plant production to optimize efficiency and create synergies using soil, water, and nutrients. Effective use of advances in information and communication technology will be necessary to facilitate interactions across this broad spectrum of scientific disciplines, to document and integrate traditional wisdom and knowledge in research planning, and to disseminate research results widely. Several research groups work in this field, but some key references are ETH Zurich (Figure 9.2a), University of Nebraska (Figure 9.2b), or the Smart Biosystems Laboratory research group at the University of Seville (Figure 9.2c and 9.2d), among others.

9.3 DISEASES IN WHEAT

Plant diseases emerge at various times and locations, influenced by inoculum availability, the crop's growth stage, and weather conditions. Wheat is affected by more than 100 diseases caused by various pathogens and pests. Around 21.5% of global wheat production is lost due to these diseases annually. The most economically damaging diseases are leaf rusts, *Fusarium head blight* (FHB), and *Tritici blotch* (Savary et al., 2019).

Asexually produced spores of rust fungi and powdery mildews, typically dry and airborne, are passively released under windy conditions. These spores can be dispersed to altitudes exceeding 10 km and have been documented to travel across continents, spreading pathogens over vast distances. While some species' spores are sensitive to environmental conditions, others are remarkably resilient, tolerating radiation, desiccation, and freezing. This resilience can lead to the widespread distribution of spores, resulting in either localized infection foci or uniform disease patterns, depending on the presence of inoculum. Additionally, some fungal spores and bacteria are associated with ice

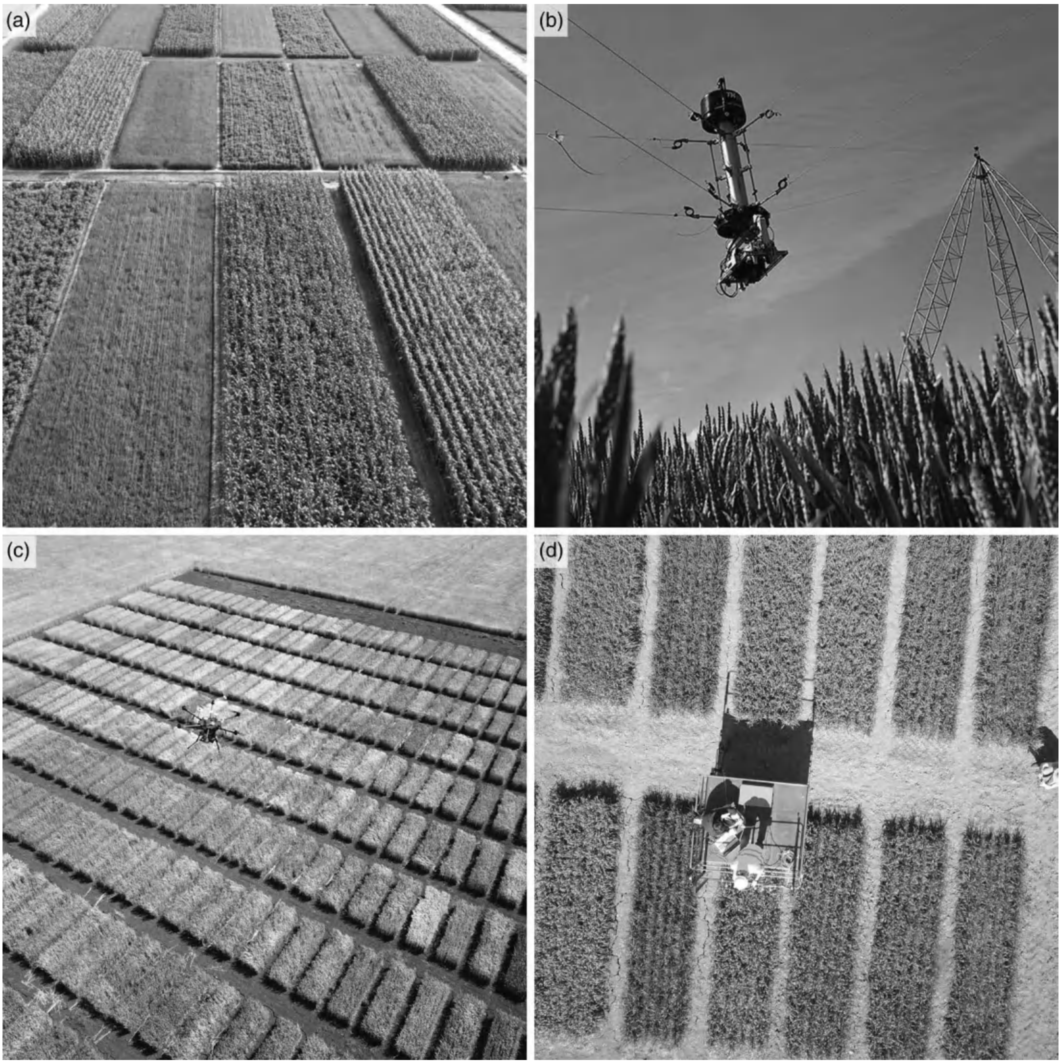

FIGURE 9.2 Advanced wheat-field phenotyping using complementary sensing technologies: (a) proximal measurements with handheld instruments, (b) high-throughput data from the Nebraska cable-driven phenotyping platform, (c) UAV-based multispectral imaging over multi-genotype plots, and (d) detailed canopy characterization from a ground phenotyping cart, all conducted in experimental plots aimed at advancing the understanding of early disease detection in wheat through remote sensing.

nucleation or enhanced water condensation on their surfaces, contributing to snow or rain formation, which returns the spores to the ground from high altitudes (Fröhlich-Nowoisky et al., 2009; Morris et al., 2013).

9.3.1 Factors Influencing Wheat Growth and Disease Appearance

9.3.1.1 The Crop Ecosystem

Traditional agriculture was characterized by a diverse environment with various plants, insects, and other animal species. In contrast, modern intensive monoculture agriculture aims to reduce this variability to meet the needs of a single target crop. Physical, biological, thermal, or chemical methods control unwanted weeds and pests. These artificial environments theoretically create ideal growing conditions for the cultivated crop. However, they can be more susceptible to crop pathogens than natural ecosystems, as they often exclude natural enemies. Therefore, monoculture agriculture requires significant time, effort, and resources to produce high yields.

On the other hand, extensive agriculture employs the opposite technique by using low amounts of inputs within a more "natural" ecosystem. While this may reduce yields, the input/output balance can be more favorable, especially when incorporating environmental costs associated with intensive production. Throughout this chapter, we will distinguish between intensive and extensive crop production.

9.3.1.2 Determinants of Disease Presence in the Crop Canopy

Three main factors determine the presence of disease in the crop canopy:

1. *The presence of inoculum*: The presence of inoculum is the first determining factor for any disease: Without the presence of the pathogen or pest, there simply will not be an infection. Although logical, it is an essential step in the crop protection strategy. First and foremost, farmers must attempt to safeguard their crops by maintaining proper sanitary measures. These include washing tools, clothes, and machinery between fields; using clean, certified planting material (when available); and removing infected plants from the field when possible. Removing infected plants, for example, is more feasible in small-scale banana cultivation than in large-scale, monoculture wheat fields.
2. *The crop microclimate*: The crop microclimate refers to the immediate area surrounding the cultivated plants. Depending on the crop, this zone may extend from the soil to the first few dozen centimeters above it (e.g., wheat) or up to one or two meters above the crop (e.g., for palm or banana trees). Within this microclimate, several factors influence crop growth and disease presence. One of the most critical factors is the relative humidity of the air around the crop. For instance, certain diseases, such as *Phytophthora infestans*, a well-known pathogen affecting potatoes, require high moisture to facilitate infection. As a result, farmers can use humidity data to assess infection risk. Applying fungicides might be economically undesirable during prolonged dry periods due to the low risk of infection. Such information has been increasingly incorporated into disease forecasting models in recent years.
3. *Cultivar characteristics*: An essential part of crop protection is the selection of an appropriate cultivar. Generally, highly productive, specially bred cultivars tend to be more susceptible to diseases. At the same time, older wild varieties may offer excellent disease resistance but often lack the high productivity of cultivated varieties. Genetically modified organisms (GMO) crops with specific resistance genes integrated into modern, high-yield cultivars can provide a solution when available. The selection of a particular cultivar also depends on the availability of other crop protection methods. For example, a disease-resistant variety might be more economically beneficial in rural regions without access to fungicides, even if its maximum yield is lower.

9.3.1.3 Soil: The Cornerstone of Crop Production

A healthy soil is the basis for sustainable agriculture. Despite their uniform appearance, soils are complex ecosystems containing vast amounts of microbes, insects, and other organisms. The bulk of soil consists of a mix of sand, silt, and clay particles, which determine the soil's texture. As a result, this texture influences essential characteristics such as water permeability, compaction potential, and nutrient retention. Key nutrients in the soil that are necessary for plant growth include nitrogen (N), phosphorous (P), potassium (K), calcium (Ca), magnesium (Mg), sulfur (S), and soil organic carbon (SOC) as well as trace amounts of essential heavy metals. The balance of these nutrients throughout the growing season is one of the most critical factors influencing crop growth.

Plants under nutrient stress often show reduced resistance to pathogens. In extreme cases, nutrient deficiencies may cause symptoms similar to those caused by crop pathogens, such as chlorosis, stunted growth, and growth deformation.

Apart from maintaining a good nutrient balance, an essential aspect of the soil ecosystem is the presence of soilborne pathogens. A distinction can be made between pathogens and pests that spend their entire lives in the soil, such as certain nematodes, and those that spend only part of their lifecycle in the soil, like specific fungal pathogens that produce survival spores. In either case, these pathogens pose a risk for farmers. Often, these soilborne pathogens have a historical presence in particular fields, prompting farmers to adjust their crop production strategies by increasing crop rotation. In extreme cases, local governments may implement quarantine policies to restrict the spread of particularly destructive pests and diseases. Such policies can make it illegal for farmers to grow certain crops on fields infected by specific pathogens for a set period. This highlights the importance of understanding one's soil and the pathogens present.

Last, water is a pivotal component of the soil ecosystem. It is the most important factor in crop production in many regions. The amount of water in the soil matrix, measured by soil water potential, directly influences the growth potential of crops. First, water is essential for the photosynthetic reaction. Second, it replaces the water lost through the plant's stomata during photosynthesis, and this process also delivers nutrients from the soil's water solution to the plant. In this way, plants under water stress also experience nutrient stress and reduced growth, making them more vulnerable to biotic stresses from pathogens. It is, therefore, important to provide sufficient irrigation. However, excess water can also hinder crop production in several ways. Many pathogens thrive in high humidity or when free water is on crop surfaces or within the soil matrix. Moreover, prolonged water saturation creates an anaerobic environment around the roots, hindering plant growth and potentially leading to rotting symptoms. Such circumstances might occur during extreme rainfall or in fields suffering from soil compaction.

Farmers must balance soil nutrient and water status and be aware of the presence of soilborne pathogens to ensure a solid base for crop protection.

9.3.1.4 Importance of Effective Disease Management Strategies

Modern agriculture increasingly relies on advanced tools and technologies for effective disease management. Remote sensing techniques, including spectral imaging, LiDAR, and weather data analysis, are becoming essential for monitoring and managing wheat diseases. As farmers become more reliant on mechanized equipment, the demand for automated and user-friendly diagnostic tools grows. Practical, readily available, and cost-effective methods for pathogen detection are crucial to supporting farmers in disease management. Several countries have established disease-forecasting networks for specific pathogens. These networks use various diagnostic methods, including spectral, fluorescence, and image analysis, to detect and identify spores at the microscopic scale.

9.3.1.5 Monitoring Inoculum Presence for Disease Management

Monitoring for inoculum presence to support disease management decisions is not new and has been used for decades in numerous pathosystems. Most of these approaches focus on determining the initial amount of inoculum levels for soilborne diseases. However, several successful efforts have been made to monitor airborne inoculum to enhance disease management systems.

Most disease management strategies of airborne plant pathogens assume that inoculum is always present and often fail to predict the severity of an epidemic because they do not account for the quantity of initial inoculum at a specific location. Perhaps the most common method for monitoring the presence of airborne inoculum is scouting for disease symptoms in a management unit. However, this approach is labor-intensive since it is challenging to accurately assess low levels of disease in large fields, particularly in the early stages of epidemics. Additionally, disease levels may be underestimated due to latency or the absence of visual symptoms. Furthermore, symptom-based assessments only estimate how much inoculum was present before the assessment date, meaning there may be far more infected plant tissue than visible at the evaluation time. This method can lead to control failures depending on past and current weather conditions, the amount of inoculum generated, critical periods of host susceptibility, and the scouting frequency. These challenges drive research into alternative methods for assessing inoculum availability, such as detecting pathogen inoculum in the air.

Currently, the primary wheat diseases are the following:

- Yellow rust (*Puccinia striiformis*)
- Brown rust (*Puccinia triticina*)
- Stem rust (*Puccinia graminis*)
- Septoria leaf blotch (*Zymoseptoria tritici*)
- Powdery mildew (*Blumeria graminis* f. sp. tritici)

Traditionally, diseases are identified by their characteristic visual symptoms; however, this approach has a significant disadvantage: The disease is detected only after it has already caused considerable damage to the crop's physiological processes, which can impact yield. In contrast, spectral detection methods enable early detection of diseases before visual symptoms manifest.

9.4 PRINCIPLES OF SPECTRAL INFORMATION

Remote sensing is a pivotal technology in modern agriculture, providing essential insights into crop development and ecophysiological processes throughout the growth cycle. This technology leverages the principles of electromagnetic radiation and its interactions with crop structures and biochemical processes, such as photosynthesis, which are essential for plant development. By detecting changes in plant physiological processes, the electromagnetic spectrum enables early detection and diagnosis of pathogens or diseases even before visual symptoms appear.

The electromagnetic spectrum encompasses all forms of electromagnetic radiation, categorized by their wavelengths and frequencies. Remote sensing primarily utilizes specific regions of this spectrum to capture detailed crop information. Key regions include the following:

- *Visible light* (*400–700 nm*): The portion of the spectrum perceptible to the human eye, including blue (~450 nm), green (~550 nm), and red light (~650 nm).
- *Near-infrared* (*NIR, 700–1100 nm*): Located just beyond the visible spectrum, NIR is useful due to the strong reflection by healthy plants.
- *Shortwave infrared* (*SWIR, 1100–2500 nm*): Valuable region for analyzing mineral and vegetation moisture content.
- *Thermal infrared* (*TIR, 8–14 μm*): Measures emitted thermal radiation, allowing temperature determination.

When electromagnetic radiation interacts with plant structures, it undergoes several processes:

1. *Absorption*: Specific wavelengths are absorbed by plant pigments, water, or other constituents. For example, chlorophyll absorbs blue and red light while reflecting green, which gives plants their green appearance.
2. *Reflection*: Light that is not absorbed is reflected based on its wavelength.
3. *Transmission*: Some wavelengths, such as NIR and SWIR, can penetrate leaf tissues to a certain extent, providing insights into internal plant structure.

Each crop has a unique spectral signature (Figure 9.3), a specific pattern of reflectance across different wavelengths, which is used to identify crops, assess their developmental status and

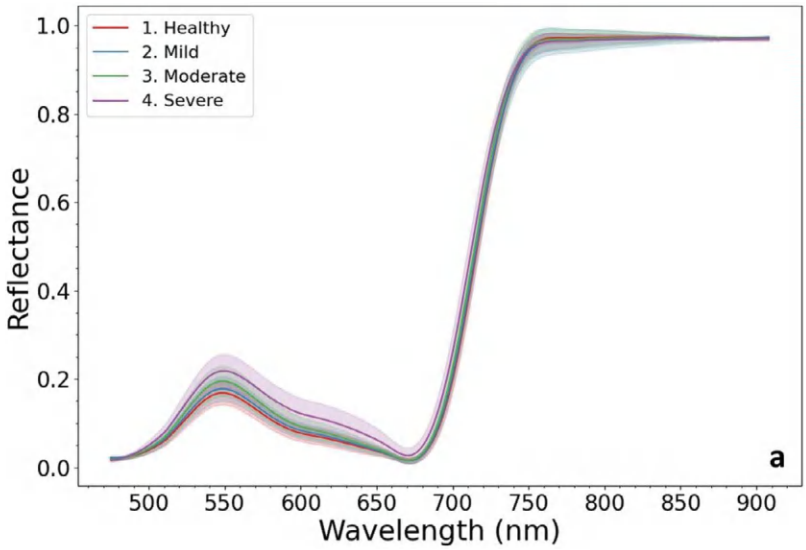

FIGURE 9.3 Average spectral reflectance curves with standard deviations for four plant health classes: Class 1 (healthy), class 2 (mild impairment), class 3 (moderate impairment), and class 4 (severe impairment). Reflectance values were recorded across the 450–900 nm wavelength range. Distinct spectral differences, particularly in the visible (500–700 nm) and red-edge (around 700 nm) regions, indicate progressive physiological degradation with increasing severity. The sharp rise near 700 nm corresponds to the red-edge transition typical of healthy vegetation, while decreasing reflectance in the visible range for impaired classes suggests reduced chlorophyll content. Shaded bands represent the standard deviation for each class, highlighting the variability within each disease severity group.

phenological state, monitor photosynthetic activity, detect pathogens or diseases, and identify various abiotic or biotic stresses.

9.5 TYPES OF SPECTRAL SENSORS

Spectral sensors can be either active or passive. Passive sensors detect radiation, such as sunlight or artificial light reflected off objects, while active sensors emit their radiation and measure the reflection from target objects.

Based on the number of wavelengths they detect, spectral sensors are classified as monospectral, multispectral, or hyperspectral. Multispectral sensors are the most widely used in agriculture, as they enable the calculation of vegetation indices that correlate with plant development and physiological status. Within this category, red–green–blue (RGB) sensors are particularly noteworthy. These sensors collect data from the spectrum's red, green, and blue sections, producing visual images that can be easily interpreted. This capability makes RGB sensors invaluable for monitoring and analyzing crop health and growth in a cost-effective manner.

9.5.1 Sensors

Since the beginning of this century, the application of remote sensing in agriculture has become feasible thanks to the development of new sensors, continuous monitoring systems, data transmission technology, and GNSS. Initially, the use of these technologies was restricted due to the high cost of sensors and the limited processing capacity and automatization in the field. Recently, as these technologies have become more affordable and widely available, it has become easier for growers to adopt them. Miniaturization has enabled the integration of spectral sensors into moving platforms, such as satellites, UAVs, and terrestrial vehicles. Nowadays, multispectral images with a resolution of 10 m are freely accessible; thanks to the Sentinel and LandSat satellite constellations, which provide data every few days. This resolution is often sufficient for monitoring field crops like wheat. However, identifying incipient disease areas in certain crops may require higher spatial resolution.

UAVs offer a potential solution to this challenge by capturing high spatial and temporal resolution spectral data. However, their limited payload and battery life restrict the area that can be monitored. Although UAVs are cost-effective, the need for a pilot and the complexity of data processing can hinder widespread adoption by farmers.

Spectral sensors can also be mounted on terrestrial platforms, allowing for much higher resolution and payload capacity and overcoming the main limitations of UAVs. Their proximity to the crop enables them to capture data at the plant level. While scanning speed is typically slower than that of UAVs, the ability to attach spectral sensors to standard farming machinery offers real-time, high-resolution disease detection during routine tasks.

9.5.1.1 Soil Sensors

Soil sensors map the variability of specific parameters within a field. Classic techniques for measuring soil variability rely on the expensive laboratory analysis of manually collected soil samples, which is time-consuming and costly. This approach typically provides only a few samples per hectare. To address this limitation, scientists have developed rapid, high-resolution methods for measuring soil variability.

Two main types of sensors provide soil information: Ground-based and aerial sensors.

- Ground-based sensors are instruments that physically contact the soil or are mounted on equipment in contact with the soil. Examples include stationary moisture sensors, electromagnetic induction (EMI) sensors, and spectroradiometric sensors.
- Aerial sensors are mounted on drones, airplanes, or satellites. Their main advantage over ground sensors is their ability to collect data on a larger scale. However, this often comes with reduced data resolution (e.g., satellites with a resolution of 10 by 10 m). Moreover, analyzing such data might be challenging, especially when noise caused by atmospheric interference or environmental factors is present.

Combining ground and aerial sensors may balance data quality and resolution well.

9.5.1.2 Crop Spectral Sensors

Crop sensing is an important part of precision agriculture. Six major spectral sensor types are discussed in this chapter:

- RGB sensors
- Multispectral sensors
- Hyperspectral sensors
- Thermal sensors
- Fluorescence sensors
- Lidar sensors

RGB sensors have become commonplace worldwide due to their simplicity, low cost, and integration into commercially available smartphones. Unsurprisingly, their use in precision agriculture has significantly increased over the past few years.

An RGB image contains two key types of information: Spatial and spectral. As the name implies, spectral information is captured for each pixel in three wavebands: Red (625–740 nm), green (520–565 nm), and blue (430–500 nm). This spectral data enables the calculation of vegetation indices, such as the Triangular Green Index (TGI), which can be used in classical statistical models or machine learning algorithms.

The second type of information contained in RGB images is spatial information. This includes the geometry of leaves, patterns from diseased spots, or physical damage caused by machinery. Such spatial details are valuable for identifying crop damage and diseases. Machine learning, particularly deep learning (DL) neural networks, is well-suited for analyzing these spatial patterns and associating them with specific characteristics, such as leaf rust, characterized by orange pustules, or powdery mildew, visible as white, powdery patches.

Since RGB sensors mainly capture information on leaf deformation and color changes due to disease, they cannot detect symptoms earlier than the naked eye. This limitation restricts their usefulness for early disease detection. However, due to their low cost and potential for automated disease detection and mapping, RGB sensors remain valuable for monitoring disease spread across fields.

Multispectral sensors are similar to RGB sensors, with the addition of several extra wavebands (usually less than a dozen). These additional bands generally include wavelengths in the spectrum's NIR region (740–1400 nm), which is associated with structural damage to plant cells. Such damage can result from various factors, including pathogens growing within the plant. In these cases, multispectral sensors can detect plant diseases before they become visible to the human eye. Moreover, multispectral sensors are more affordable than hyperspectral sensors, making them one of the most favored tools for crop sensing. Many important vegetation indices in agricultural research utilize information from the NIR region, including the Normalized Difference Vegetation Index (NDVI), the Red Edge Index (REI), and the Simple Ratio Index (SR), among others, as suggested by Xue and Su (2017).

Like indices derived from RGB cameras, data from multispectral sensors can be analyzed using classical statistical models or ML techniques. Multispectral sensors are available in two formats: Point measurement and snapshot. Point measurements represent an average over a specific scanning area (e.g., 5 by 5 cm). In contrast, snapshot images resemble standard photographs with a defined number of pixels but contain spectral information across up to a dozen bands rather than just red, green, and blue. This expanded spectral range allows a more comprehensive analysis of the target area's spectral properties.

Hyperspectral sensors go one step beyond multispectral sensors by capturing reflectance in several dozen to hundreds of bands, usually visible (VIS) and NIR regions. The advantage of having spectral information in more bands is that it enables data processing methods, such as smoothing algorithms, derivation, and feature selection. For example, feature selection can identify the optimal wavebands for detecting specific pests or diseases. This information can then be used to develop multispectral cameras to measure these precise wavebands.

From a practical applications perspective, developing multispectral cameras based on hyperspectral research is essential, as the high cost of hyperspectral cameras remains prohibitive for many farmers. Additionally, hyperspectral data files are large, with significant processing and storage requirements, making them less feasible than multispectral sensors in practical on-farm use.

Thermal sensors measure emitted radiation in the "thermal" infrared region, which ranges from 3 to 14 μm. However, most thermal sensors typically operate in the so-called atmospheric window, which extends from 8 to 14 μm. This heat can result from an organism's internal heat production or radiation absorbed and re-emitted as thermal energy.

In precision agriculture, thermal cameras are useful for detecting water stress due to insufficient irrigation. In such cases, thermal cameras are mounted on UAVs or satellites and used to generate water stress maps of the field, allowing farmers to adjust their irrigation strategies accordingly.

Apart from water management, thermal cameras have also been used in research for disease detection. Diseases induce stress responses in plants, including stomatal closure, which reduces evapotranspiration and raises the leaf surface temperature. Additionally, thermal cameras have been used to map temperature variations across a field. An increased temperature range can indicate "hot spots" where crop surface temperature is higher, potentially due to disease.

However, the interpretation of thermal signatures is not straightforward. In some cases, the leaf surface temperature might decrease due to symptoms of crop disease. For instance, diseases that cause rotting can release water from plant cells, creating cool, wet lesions that lower the leaf's surface temperature.

Fluorescence sensors (FL) detect physiological changes in plants by measuring chlorophyll fluorescence, which is influenced by pathogens, nutrient deficiencies, and environmental stressors such as drought or heat. Early detection of these issues allows targeted interventions, improving crop yields and quality. These sensors also aid in identifying nutrient deficiencies, enabling precise fertilizer application. When mounted on UAVs, FL sensors support precision agriculture by quickly assessing large fields.

LiDAR sensors are active sensors that emit laser pulses to create 3D reconstructions of plants, allowing measurements of canopy structure. They can detect subtle changes caused by diseases, such as fungal infections or pest infestations, which alter plant geometry and density. Early detection of disease-related changes, such as variations in leaf angles or plant height, enables timely intervention, allowing farmers to target affected areas more effectively. LiDAR is also helpful for estimating vegetation density, which can indicate stress or the presence of disease. Modern multispectral LiDAR systems go a step further than conventional LiDAR by adding spectral information to the plant reconstruction, allowing for the analysis of different wavelengths reflected by the soil or plant tissues. This multispectral data provides additional information regarding plant health by revealing variations in leaf pigmentation, water content, and nutrient status indicative of plant stress or disease. Recent studies, such as the one by Rodríguez-Vázquez et al. (2025), have demonstrated that LiDAR data is suitable for crop characterization and practical for disease detection (Figure 9.4).

9.6 MONITORING DISEASE USING SPECTRAL INFORMATION

9.6.1 Pre-Epidemic Disease Risk Assessment

Disease monitoring begins with assessing the risk of pathogens causing outbreaks in a crop at any given time. An essential aspect of this is monitoring weather conditions. Humidity is one of the main drivers of disease incidence, especially for fungal pathogens that often rely on water for part of their infection cycle. Therefore, farmers sometimes rely on weather-based decision support systems (DSSs) to make decisions regarding informed disease management. These systems provide real-time data on weather conditions, helping farmers anticipate and mitigate disease risks based on environmental factors. A successful example from Italy showed that managing large areas (18,000 ha) of durum wheat is possible using a weather-based DSS for treating FHB (Rossi et al., 2015). However, a downside of these systems is that they are often disease-specific and require substantial experimental data to model. Additionally, they may not always predict the right moments of high infection risk and may not work equally well for every disease. On the other hand, these systems are relatively cheap to operate once the model's training has been completed.

Another possible strategy for preventive disease monitoring and risk assessment is the detection of potential inoculum in the air or soil. Monitoring inoculum presence to aid in disease management decisions is not new and has been used for decades in numerous pathosystems. Most of these approaches focus on determining the amount of initial inoculum for soilborne diseases. However, several successes have been made in monitoring airborne inoculum to aid disease management systems. Crossover technologies from the biomedical and biosecurity sectors are allowing the development of automated on-site detection kits, which help growers rapidly identify plant pathogens, allowing them to implement timely integrated pest control strategies.

Perhaps the most common method for monitoring the presence of airborne pathogens is scouting for disease symptoms within a management unit. However, this method is labor-intensive and challenging, particularly for accurately assessing low levels of disease in large fields during the early stages of an epidemic. This approach does not allow preventive treatment since the disease

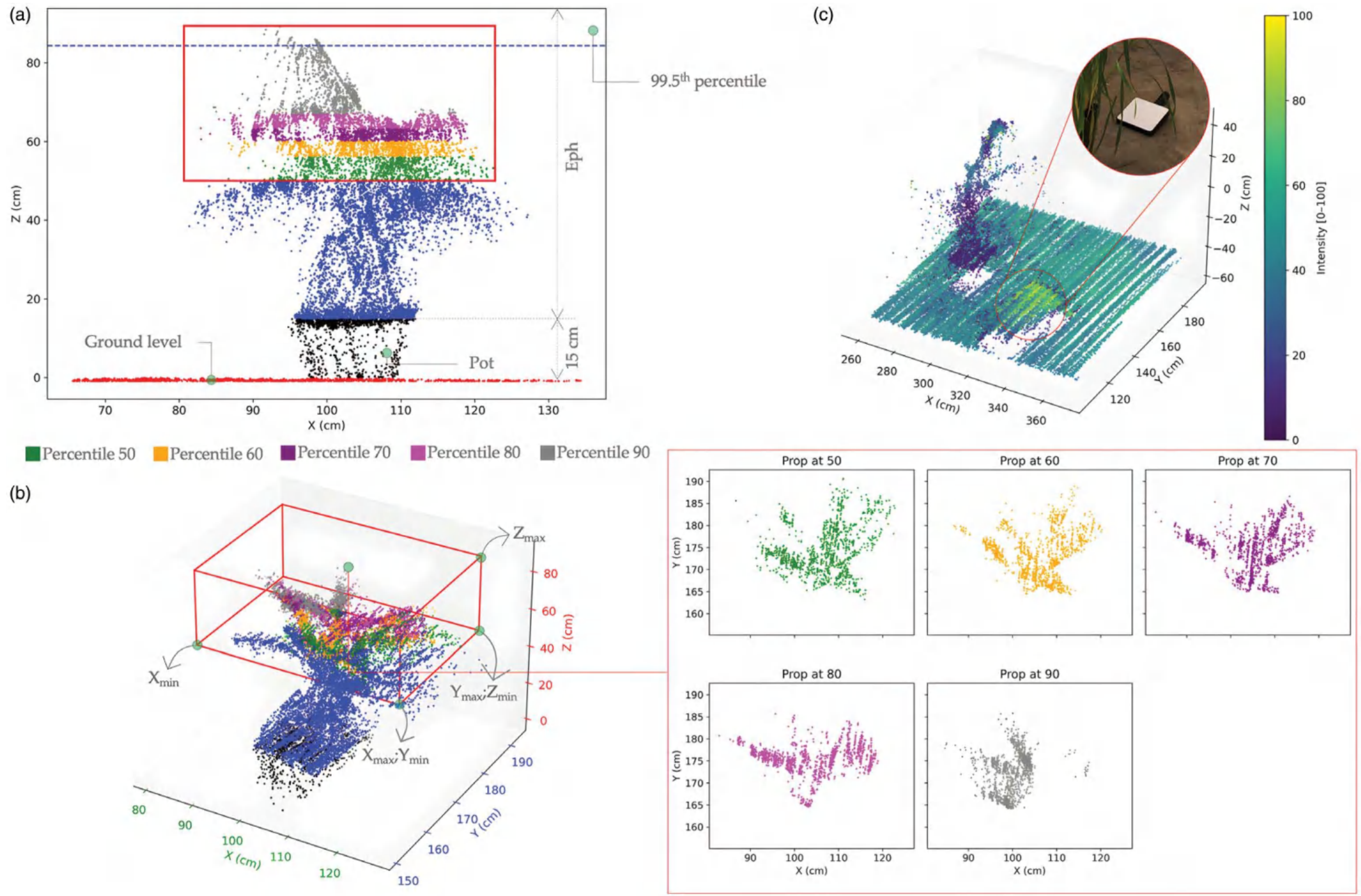

FIGURE 9.4 Analysis of 3D point cloud data for plant structure characterization (From Rodríguez-Vázquez et al., 2025). Side view of the segmented plant point cloud, showing different height percentiles (50th–90th) in distinct colors. The red box represents the extracted region of interest, while the dashed blue line marks the 99.5th percentile. The pot and ground levels are also indicated (a). A 3D perspective view of the plant point cloud with percentile-based segmentation and cross-sections at different height percentiles (50, 60, 70, 80, and 90) demonstrates the plant's spatial distribution in the X–Y plane (b). The top-right visualization of the scanned area, highlighting point cloud intensity values along with the inset image, provides a detailed view of the white reference, showing intensity values of 100% (c).

is already present when symptoms are visible. While most airborne pathogen management strategies assume that inoculum is always present, this method often underestimates disease levels due to latency or the absence of visual symptoms. It may fail to predict the severity of an upcoming epidemic.

Furthermore, assessing disease symptoms only estimates the amount of inoculum present before the assessment date, meaning there is likely much more infected plant tissue in the field than is visible at the assessment time. This approach could lead to control failures depending on the previous and current weather conditions, the amount of inoculum being generated, critical periods of host susceptibility and the frequency of scouting. These challenges drive research into alternative methods for assessing inoculum availability, such as detecting pathogen inoculum in the air.

The future will likely include the real-time quantification of inoculum and disease presence in crops using a combination of molecular identification, olfactory sensing, and spectral imagery collected by autonomous farm equipment as it moves through the fields. These data will be integrated in real-time with modeling systems for crop growth, pathogen dispersion, and disease development to generate spatially explicit disease risk maps, guiding the precision applications of cultural and pesticide management practices.

9.6.2 Sensing of Crop Traits Using Spectral Information

As mentioned in the previous section, it is not always easy to monitor the risk of crop infection preventively. Infection is likely to occur, especially with omnipresent airborne diseases and ordinary soilborne diseases, once suitable conditions are met. To address this, farmers rely on early-stage detection methods.

In the crop sensors section, we discussed several sensing technologies used to monitor different types of disease. The most used methods include RGB, multispectral, hyperspectral, and thermal imaging. After data acquisition, specific preprocessing steps are needed to make the data suitable for modeling. Generally, a reference value is measured to calibrate the sensing device. This is often a gray or white reflectance target that has a known reflectance pattern. This measurement is then used to normalize the data, accounting for variations in lighting conditions. Thermal sensors are usually calibrated using a reference target with a known temperature profile, such as a wet sphere (Meron et al., 2010). It is important to note that each sensor requires optimized settings, including exposure time, ISO value, scanning speed, frequency, and measuring distance. After sensor calibration, the data needs to be preprocessed.

9.6.2.1 RGB

RGB data is commonly used to model visible disease symptoms once they have appeared. These symptoms often relate to plant health indicators, such as leaf color, canopy cover percentage, plant height, and plant density. Typically, these characteristics are derived from remote sensing measurements taken from an aerial perspective, such as UAV images. Preprocessing is necessary to extract useful information for specific parameters (e.g., canopy cover percentage). For instance, we would need to remove the soil background from the image to measure the proportion of canopy versus soil area. This process is known as image segmentation or, more specifically, in this context, background removal. In cases where the spatial resolution of an image is relatively low, as is often the case with aerial imagery, techniques tend to focus on pixel-level information. This approach is essential because low-resolution images make it challenging to identify individual objects using detection models. However, object detection becomes more feasible with close-up images where individual plants or plant parts are visible.

Kior et al. (2024) provide a recent review of various RGB imaging techniques to derive crop traits. As mentioned earlier, background removal in RGB images for remote sensing applications often relies on the spectral information in each pixel, particularly the red, green, and blue bands. We can differentiate between soil and crop areas by selecting threshold values for these bands. For instance, if the soil has low reflectance in the green band while the crop has a high reflectance due to chlorophyll, we can classify pixels with reflectance above a certain threshold as crop and the rest as soil. While individual color bands have been successfully used for segmentation in this manner, thresholding alone is sometimes not enough. In cases where there is limited contrast between the soil and the crop, it may be challenging to segment an image using only these methods. This is particularly true when dark-colored fruits are present, soils have high reflectance (e.g., white sand or shiny, moist areas), or shadows cause parts of the crop to appear dark with low reflectance.

Color vegetation indices, which are ratios of different wavebands included in the RGB spectral range, are commonly used for segmentation and analysis (Meyer & Neto, 2008). By combining information from multiple visible bands, these indices provide reliable indicators to distinguish plant material from soil or other objects in the image. Examples include the Excess Green Index (EGI), the Excess Red Index (ERI) and the Normalized Green Red Difference Index (NGRDI). Once an index is calculated for each pixel, thresholding can be applied using several methods. Researchers may select a threshold by visually inspecting pixel values and iteratively adjusting, consult established thresholds from the literature, or employ data-driven thresholds. Examples of such techniques include Otsu-based methods, Ridler-based methods, the triangle method, and histogram-based methods (Geipel et al., 2014; Hague et al., 2006; Kataoka et al., 2003; Liu & Pattey, 2010; Searcy & Reid, 1986; Roth & Streit, 2018). Additional preprocessing steps for acquisition methods, such as drone-based photography, may be necessary. For instance, images might need to be stitched together to create a unified RGB image of the entire field.

After separating the background from the crop pixels, we can analyze the specific crop parameters under study. A key aspect of RGB imaging is that the resulting data can reflect various underlying processes, depending on the measurement conditions. For instance, if a particular area of the crop shows reduced canopy cover, lighter coloration (indicating less pigment), or dark spots, these could be signs of disease. However, similar symptoms could also result from nutrient deficiencies, drought, or mechanical damage. To ensure that RGB imaging data is valuable, it is essential to supplement it with additional information from the field. This might involve visually inspecting the crop or integrating the data with other information sources, such as risk prediction systems. For example, if there is no risk of drought or non-pathogen-related damage, but a significant reduction in canopy cover appears in certain regions on an RGB image, this could potentially suggest a disease outbreak.

A case study by Francesconi et al. (2021) demonstrated the use of RGB imaging for phenotyping wheat against FHB using vegetation indices, such as the Green Leaf Index (GLI). Their results revealed correlations between vegetation indices in RGB images and disease symptoms. Similarly, Hong et al. (2022) used RGB images to detect FHB, employing machine vision models like YOLOv4 to identify the disease on wheat ears in very high-resolution images, where the details of the ears were visible. In another example, Qiu et al. (2019) successfully combined DL models with RGB images on a wheeled phenotyping platform to detect FHB. For yellow rust, Zhou et al. (2015) reported a strong correlation between RGB-derived vegetation indices (e.g., Green Fraction and Greener Fraction) and the presence of the disease.

Dehkordi et al. (2020) demonstrated that UAV-based RGB imagery was sufficient to treat winter wheat affected by stripe and leaf rust during critical growth stages (stem elongation and booting), achieving correlation coefficients over 0.9 for both diseases. These case studies underscore RGB's potential for monitoring existing crop infestations. However, they also highlight significant limitations. Due to the limited spectral range of RGB imagery (only three bands), distinguishing between different types of crop stress or various diseases can be challenging and often impossible.

RGB imaging offers a cost-effective, relatively low-tech solution that can aid in managing certain wheat diseases when combined with robust preprocessing, data analysis pipelines, and DL techniques. However, exploring other technologies, such as multispectral, hyperspectral, or thermal imaging, may be convenient for more advanced applications.

9.6.2.2 Multispectral/Hyperspectral

The complexity of datasets generated by multispectral, especially hyperspectral, sensors makes AI greatly helpful for data analysis. Even as early as 2007, researchers were using basic machine learning techniques, such as decision trees with NDVI data derived from satellite images, to classify powdery mildew and leaf rust diseases in winter wheat (Franke & Menz, 2007), achieving varying levels of success.

More recently, Gongora-Canul et al. (2020) measured wheat canopies using a UAV equipped with a multispectral camera at an altitude of 15 m to study symptoms of wheat leaf blast and wheat spike blast. Although detecting leaf symptoms before spike emergence proved challenging, they achieved reasonable accuracy depending on disease intensity, the vegetation indices used, and whether the model focused on disease incidence or severity. They concluded that wheat spike blasts could be detected at moderate or high levels of visual infection.

Su et al. (2019) studied the spatio-temporal spread of rust disease in winter wheat throughout an entire growing season using five-band (VIS–NIR) multispectral imaging (Figure 9.5). They concluded that combining multiple vegetation indices was most effective for classifying the disease, noting that the optimal combination may vary for detecting early versus late disease stages.

Numerous studies have used multispectral imaging for disease monitoring in wheat. In the following section, we will discuss techniques for analyzing multispectral and hyperspectral data, highlighting the differences between these workflows and providing examples of hyperspectral imaging used in wheat disease monitoring.

To begin, we examine a recent review by Kumar and Kukreja (2022), which summarizes DL techniques for analyzing multispectral images of wheat crops. Their review indicates discrepancies in the effectiveness of DL techniques for different pests and diseases when applied to spectral data (Figure 9.6). Most of the studies they reviewed focus on RGB images captured by UAVs, with some exploring multispectral and hyperspectral imaging. This was expected, as RGB data are generally more accessible and less expensive to analyze than hyperspectral and multispectral data to a lesser extent.

However, as discussed earlier, there is a growing trend in wheat disease monitoring studies that emphasizes the added value of the NIR region in both multispectral and hyperspectral imaging, suggesting its importance for accurate disease detection.

The question arises: What advantages does hyperspectral imaging offer over multispectral imaging? To answer this, we must first explore their differences. Hyperspectral data includes information across hundreds of bands, which can lead to extremely large datasets. This brings challenges

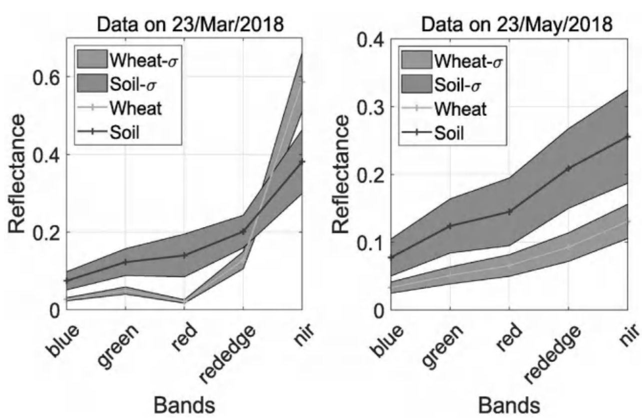

FIGURE 9.5 Reflectance spectra of soil and wheat on two different measurement days illustrate variation in the reflectance pattern for wheat, with comparatively less variation in the soil reflectance. (From Su et al. 2019.)

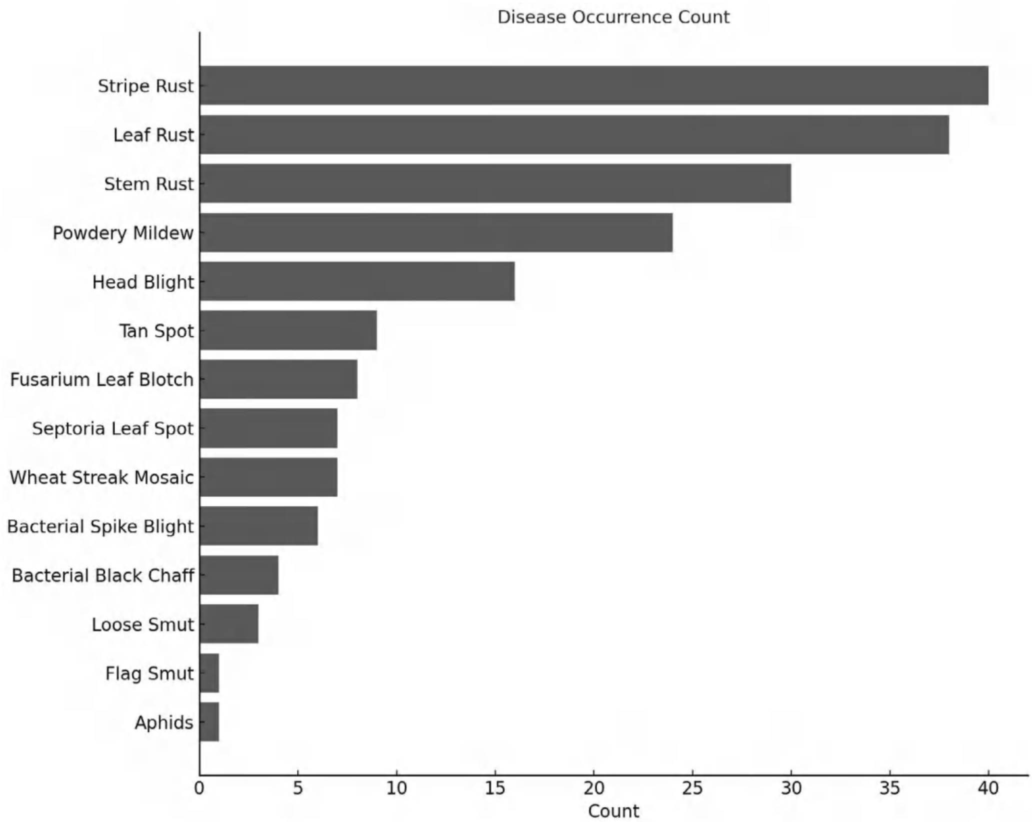

FIGURE 9.6 Literature review regarding deep learning algorithms used to classify diseases in wheat crops. The x-axis depicts the number of publications. (Adapted from Kumar and Kukreja 2022.)

regarding data acquisition, as fast storage disks, ideally solid-state drives (SSD), are required for high-speed acquisition modes (e.g., high framerates). Additionally, storing, accessing and processing this large amount of data can be complex. One standard solution in the literature is dimensionality reduction (Kumar & Kukreja, 2022; Ruiz Hidalgo et al., 2021). Ruiz Hidalgo et al. (2021) discuss supervised and unsupervised dimensionality reduction methods. Supervised methods, such as linear discriminant analysis or nonparametric weighted feature extraction, use labeled hyperspectral data to define a feature subspace that maximizes the separability of different classes. Another widely used approach involves supervised band selection, which can use selection algorithms on labeled data or rely on band choices informed by previous research.

The challenge with supervised dimensionality reduction methods in disease monitoring is that a priori information (class labels) is often unavailable at the beginning of the modeling process. As a result, scientists are increasingly turning to unsupervised dimensionality reduction methods (Table 9.1). These methods aim to represent the data in a lower-dimensional space, making it easier to use this information for modeling.

In addition to dimensionality reduction, hyperspectral data analysis requires various preprocessing steps, such as white and dark reference correction, smoothing, normalization, and noise reduction (Figure 9.7) (Li et al., 2021; Paulus & Mahlein, 2020). When images are acquired from a satellite, atmospheric corrections are also necessary. As previously discussed, specific processing steps depend on the type of hyperspectral sensor used. For example, images from a snapshot hyperspectral camera may need to be stitched together, while line scan sensors require correlating line scans to spatial reference points to create a 2D image (Fu et al., 2020).

TABLE 9.1
Unsupervised Methods for Dimensionality Reduction

Unsupervised Dimensionality Reduction	
Unsupervised Methods	**Algorithm**
Based on the information content	Theoretical knowledge
	Band variance
	Entropy
Projection-based	PCA (principal component analysis)
	ICA (independent component analysis)
Similarity measures	Bands correlation
	Graphs lambda () vs lambda ()
	Spectral derivative analysis
Frequency analysis	Wavelet decomposition

Source: Inspired by Hidalgo et al. (2021).

Various modeling techniques can be applied to hyperspectral data after preprocessing, calibration, dimensionality reduction, and feature selection (Paulus & Mahlein, 2020). Like the dimensionality reduction step, these techniques include supervised and unsupervised methods. Unsupervised machine learning methods, such as the K-means algorithm, aim to cluster data, such as specific pixels, based on the spectral information of each pixel. However, supervised methods are more commonly used and require labeled data.

The labeling step is often incorporated into the experimental design. For example, by scanning healthy and diseased plants in separate plots, researchers can define specific areas that contain only diseased pixels. As shown in Figure 9.8, the researchers manually selected regions that they visually confirmed to include different stages of disease symptoms, extracted pixel information from these areas and derived the average spectral signatures. Note in Figure 9.7 how the reflectance in the green-to-red region of the visible spectrum and the NIR region varies significantly across the five different disease stages. This variation is expected, as rust disease produces orange-red pustules and degrades chlorophyll, turning green leaves orange.

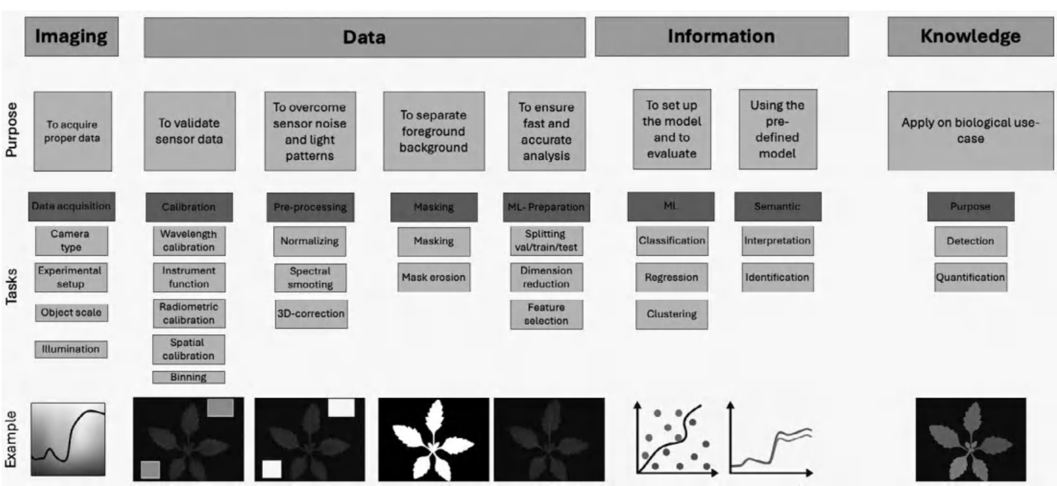

FIGURE 9.7 Workflow for hyperspectral images, from camera selection to disease detection. (Adapted from Paulus and Mahlein 2020.)

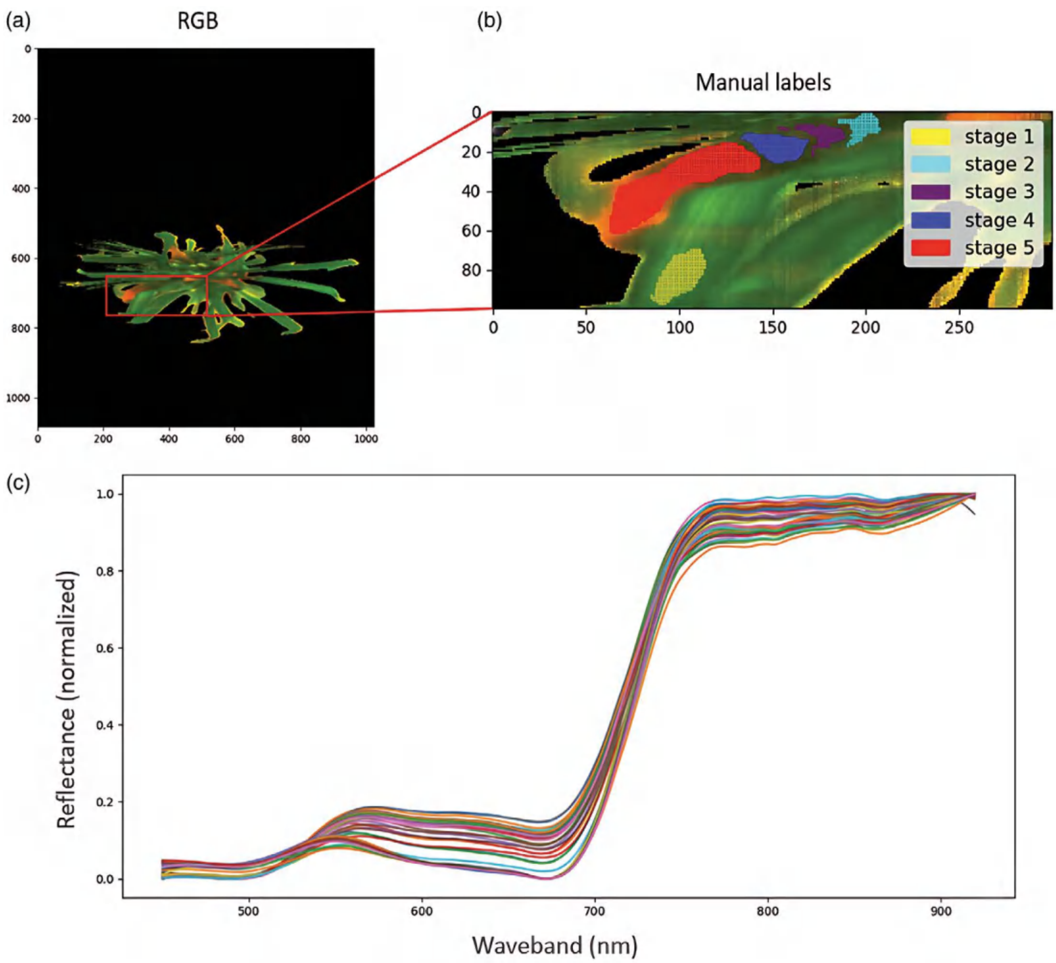

FIGURE 9.8 A representation (a) of a hyperspectral image displaying only the RGB bands for visualization purposes with labels indicating five different stages of leaf rust infection in wheat plants (b), manually labeled using Python. (From Appeltans et al., 2021.) (c) The corresponding spectral signatures are shown, following normalization and smoothing.

After labeling, the choice of model depends on whether the experiment aims for classification or regression. Regression is used when the model's output is a numeric value, such as the percentage of crop cover, moisture content, NDVI, or photosynthetic efficiency. In contrast, classification is used when modeling provides categorical variables like disease status, drought stress level, or crop type. Typical examples of machine learning models for supervised classification include decision trees, support vector machines (SVMs), and neural networks. Logistic regression is also worth mentioning, as it can be used for classification tasks. For regression tasks, support vector regression is a commonly used model.

9.7 INTEGRATING DATA FUSION FOR ENHANCED DISEASE MONITORING

9.7.1 Definition and Importance

Although each of the technologies and sensors mentioned above has achieved considerable progress in disease detection, relying on a single data source often lacks the precision required to reflect real field conditions accurately. Data fusion offers a methodological approach combining multiple data sources, resulting in more precise, reliable, and actionable insights than any single source alone (Pantazi et al., 2016). Some researchers, including Barbedo (2022), Liang et al. (2023), and Ouhami et al. (2021), propose an expanded definition of data fusion. Their definition goes beyond combining data sources and emphasizes the importance of considering probability-based, evidence-based, and knowledge-based approaches. Additionally, they highlight the importance of considering data at multiple scales and applying various techniques for feature extraction, which enhance the accuracy and depth of analysis.

In this section, we explore data fusion within the context of wheat disease management. In this context, data fusion involves combining information from different types of sensors, each capturing unique aspects of the wheat crop's health and applying multiple analytical techniques. This integrated approach improves our ability to detect early signs of disease, monitor its progression, and implement targeted interventions, leading to more effective disease management strategies. The advantages of data fusion extend beyond disease management to other areas of agriculture. By enhancing accuracy, enabling early detection, optimizing resources, and supporting informed decision-making, data fusion ultimately contributes to more sustainable and productive farming practices.

9.7.1.1 Enhanced Accuracy

By merging data from multiple sources, farmers can obtain a more accurate and reliable understanding of wheat crop conditions. This is particularly important for detecting diseases that might not be visible through a single data type. For example, spectral data can reveal changes in leaf pigments that suggest fungal infections (Moshou et al., 2005), while LiDAR data provides information on structural changes, such as plant height and canopy density, which may also suggest the presence of diseases (Mao et al., 2010). Combining these data types enables the detection of diseases like FHB and *Septoria Tritici* blotch, which might go unnoticed with only one data source. Enhanced accuracy in disease detection leads to better-targeted treatments, minimizing crop loss and increasing overall yield.

9.7.1.2 Early Detection

Integrated data can help in the early detection of diseases, allowing for timely interventions. Early detection is critical in managing wheat diseases, as many can spread rapidly and cause extensive damage before visible symptoms appear. Combining data from various sources makes it possible to detect subtle changes in crop health that indicate the early stages of disease. For example, thermal imaging can identify stressed areas in a wheat field due to disease before visual symptoms appear (Liu et al., 2024; Mahlein et al., 2019; Singh et al., 2023; Zhu et al., 2018). Spectral imaging can reveal changes in chlorophyll content and photosynthetic activity, while LiDAR can detect slight structural anomalies. Combining these early indicators facilitates prompt intervention, significantly reducing crop losses and improving yield quality (Mahlein et al., 2019).

9.7.1.3 Resource Optimization

Improved disease monitoring leads to more efficient use of resources such as water, fertilizers, and pesticides, reducing both costs and environmental impact. Precision agriculture focuses on applying the right inputs at the right time and place. Data fusion enhances this capability by providing accurate, detailed information about where and when interventions are needed. For example, rather than applying pesticides uniformly across an entire field, farmers can target specific areas where disease is detected, minimizing chemical use (Appeltans et al., 2021; Whetton et al., 2018). Similarly, irrigation can be optimized by combining soil moisture data with weather forecasts and crop health information, ensuring water is applied only where and when needed. This reduces costs and minimizes the environmental footprint of agricultural practices by reducing the runoff and leaching of chemicals into the environment.

9.7.1.4 Informed Decision-Making

Comprehensive data supports better decision-making in crop management, enabling more precise and targeted interventions. With data fusion, farmers have access to a wealth of information that can be used to make informed decisions regarding optimal timing for planting, irrigation, fertilization, and harvesting. It can also help select the best wheat varieties and farming practices suited to specific field conditions. DSSs that integrate data from multiple sources can provide recommendations and alerts, helping farmers take proactive measures. By relying on comprehensive and accurate data, farmers can optimize their practices, improve crop yield and quality, and reduce disease risk. Data fusion enhances crop health monitoring and promotes sustainable agriculture, ensuring long-term productivity and environmental stewardship.

9.7.2 Overview of Data Fusion in Wheat Disease

The concept of data fusion is not new; it was initially proposed by Hackett and Shah (1990) and Schistad Solberg et al. (1994). However, its application for monitoring wheat diseases is relatively recent, emerging in the 2000s (Moshou et al., 2005). This development is likely attributed to the broader adoption of sensors for data collection, combined with advancements in computing technology that facilitated complex mathematical analyses (Barbedo, 2022).

Table 9.2 presents the most representative studies on data fusion techniques identified in the literature review. As shown, most methods proposed fall within the scope of AI. The most compelling cases use machine learning techniques such as SVM. In recent years, there has been a noticeable increase in the use of DL techniques, particularly those focused on spectral or multispectral imaging.

TABLE 9.2
Applications of Data Fusion Techniques in Different Fields

Ref.	Method	Source Data	Application
Huang et al. (2020)	PSO-SVM Model using Fusion of Image and Spectral Features	Hyperspectral images (400–1000 nm), RGB color model, texture, and color features	Accurate early diagnosis of wheat Fusarium head blight (FHB) severity; enhancement of disease monitoring and precise pesticide application in wheat production
Liang et al. (2023)	Mid-Level Data Fusion Combined with Fingerprint Region	NIR and FT-MIR spectra	Classification of DON levels in Fusarium head blight (FHB) wheat
Feng et al. (2022)	Multi-Source Data Fusion for Disease Monitoring	Hyperspectral data (VI), thermal infrared images (TP), RGB images (TF)	Prediction and monitoring of wheat powdery mildew disease using RFR, PLS, and SVR models; improvement of remote sensing accuracy for crop disease status
Wójtowicz et al. (2021)	Spectral Analysis and Random Forest Modeling	Pure spectra from FieldSpec 3 spectrometer, vegetation indices (CRI, PRI, GNDVI, etc.)	Identification and classification of leaf rust symptoms in wheat and rye; enhancement of plant disease detection accuracy at leaf scale using spectral data and vegetation indices

(*Continued*)

TABLE 9.2 (*Continued*)
Applications of Data Fusion Techniques in Different Fields

Ref.	Method	Source Data	Application
Singh et al. (2023)	Machine Learning Modeling for Disease Severity Prediction	RGB and thermal images of wheat, image indices (IN), PLS scores, disease severity (DS), Yeo–Johnson (YJ) transformed values	Prediction of wheat yellow rust (WYR) severity using machine learning models; assessment of different dataset combinations for optimal WYR severity prediction accuracy in the field
Gu et al. (2021)	Feature Fusion using Deep Convolution and Shallow Features	High-resolution RGB images of wheat FHB at different severity levels	Recognition and classification of wheat Fusarium head blight (FHB) severity levels using a robust feature fusion model; improvement in fungicide application decisions and cost reduction in wheat production
Mustafa et al. (2023)	Machine Learning Sequential Floating Forward Selection (ML-SFFS) algorithm to classify the severity of FHB infection into nine levels based on multimodal data fused with HSI, CFI, and HT	Hyperspectral reflectance (HR), chlorophyll fluorescence imaging (CFI), high-throughput phenotyping (HTP)	Real-time nondestructive detection of Fusarium head blight (FHB) in wheat; improvement in early disease monitoring and targeted fungicide application through feature fusion and machine learning
Mustafa et al. (2024)	Development of Wheat Fusarium Spectral and Texture Indices, Classifier Evaluation	Near-infrared hyperspectral imaging and non-imaging data, wavelet features (WFs), and texture features (TFs)	Early monitoring and classification of Fusarium head blight (FHB) severity in wheat using developed spectral and texture indices; application in precision agriculture for improved disease management
Mahlein et al. (2019)	Sensor Comparison and SVM Classification	Infrared thermography (IRT), chlorophyll fluorescence imaging (CFI), hyperspectral imaging (HSI)	Early detection and differentiation of Fusarium head blight (FHB) in wheat; improved accuracy in disease monitoring using combined sensor data and support vector machine (SVM) classification
Zhang et al. (2022)	Image Processing, Handcrafted Features (HFs), and Deep Features (DFs), Parallel Feature Fusion images, deep learning models (e.g., ResNet101, AlexNet, VGG16)	Paired color and color-infrared (CIR)	Automatic and objective diagnosis of wheat diseases (leaf rust and tan spot); improvement in detection accuracy using parallel feature fusion and deep learning models, with applications in the greenhouse and potential field settings
Ma et al. (2021)	UAV-Based Hyperspectral Imaging, Spectral Feature Combination, SVM Model	UAV hyperspectral images, spectral bands (SBs), vegetation indices (VIs), wavelet features (WFs)	Field-scale detection of wheat Fusarium head blight (FHB) using a combination of spectral features; improvement in detection accuracy through feature fusion and UAV technology

(*Continued*)

TABLE 9.2 (*Continued*)
Applications of Data Fusion Techniques in Different Fields

Ref.	Method	Source Data	Application
Song et al. (2022)	Multi-angle Canopy Spectra Analysis using CARS-ELM Model	Multi-angle canopy spectra, disease severity indices (DIs), wavelength variable-selected algorithms (SPA, CARS, Relief-F, GA)	Timely diagnosis and prediction of wheat powdery mildew severity; enhancement of disease monitoring accuracy across multiple viewing angles, particularly at extreme angles (± 60°); application in large-scale, rapid monitoring of wheat powdery mildew
Azadbakht et al. (2019)	Hyperspectral Signature Analysis and Machine Learning (ν-SVR, BRT, RFR, GPR)	Spectral data (350-2500 nm), Leaf Area Index (LAI) levels, spectral vegetation indices (SVIs)	Accurate diagnosis and severity estimation of wheat leaf rust at canopy scale under varying LAI levels; ν-SVR model demonstrated superior performance with R^2 around 0.99 across all LAI levels; application in precision farming for reliable identification of wheat leaf rust, with improved performance of ML methods over SVIs, especially at low LAI levels
Su et al. (2021)	Mask Region Convolutional Neural Network (Mask-RCNN) with Feature Pyramid Network (FPN) based on ResNet-101	Color images of wheat spikes, labeled and segmented sub-images of diseased areas	Rapid and accurate identification of Fusarium head blight (FHB) severity in wheat spikes; facilitates high-throughput phenotyping in wheat breeding programs by automating the detection and quantification of disease severity; prediction accuracy of 77.19%, with detection rates of 77.76% for spikes and 98.81% for diseased areas

9.8 RESEARCH GAPS AND CHALLENGES

As discussed above, most data fusion techniques rely on state-of-the-art AI models. Although researchers have access to various data sources, numerous technical challenges remain to be addressed.

1. *Data alignment*: Ensuring that data from different sources is temporally and spatially aligned is crucial. This may involve time-stamping data points and georeferencing spatial data to ensure consistency and accuracy. Several methods have been suggested to address this challenge:
   - *Statistical methods:* Statistical algorithms can correlate and combine data from different sources. For example, regression models may integrate weather data with spectral indices to predict disease risk.
   - *Machine learning:* Techniques such as neural networks and random forests can identify patterns and relationships between data types. These models can be trained to predict disease outbreaks by combining LiDAR, spectral, and weather data (Pantazi et al., 2017).

- *Geospatial analysis:* GIS (Geographic Information Systems) tools allow for overlaying and analyzing spatial data, facilitating visualization of disease spread and identification of high-risk areas.

2. *Data Quality and consistency:* Data quality and consistency from different sources can be challenging due to differences in resolutions, format, and accuracy. Data preprocessing steps, such as normalization and calibration, are often required to address these issues.
3. *Complexity in integration:* Integrating diverse data types requires sophisticated algorithms and significant computational resources. Handling large datasets and ensuring real-time processing can be particularly challenging.
4. *Scalability*: Developing scalable data fusion solutions that can process large volumes of data in real-time is critical. This requires robust infrastructure and efficient algorithms.
5. *Interoperability:* Different systems and technologies must work together seamlessly to enable effective data fusion. This often involves developing standard protocols and data formats.

9.9 FUTURE DIRECTIONS

Numerous studies demonstrate that sensor applications, particularly hyperspectral cameras, hold significant potential for addressing various agronomic challenges and plant diseases. However, specific requirements related to the measurement system and data processing currently limit the transfer of these techniques from fundamental research to practical application. For example, leaf geometry can significantly affect data quality (Behmann et al., 2016). Depending on leaf shape and recording angle (e.g., leaf curling in maize), the spectrum may become distorted, and this factor must be considered in data evaluation.

New approaches in data science and increased use of machine learning for feature extraction will help discover previously unknown predictors for the early detection of cereal diseases.

In the future, agricultural disease management will likely involve real-time quantification of inoculum and disease presence using a combination of molecular identification, olfactory sensing, and spectral imagery with autonomous farm equipment operating in the fields. This data will be integrated in real-time with models for crop growth, pathogen spread, and disease progression to create detailed disease risk maps. These maps will then guide the precise application of cultural and pesticide management practices. Early detection of low disease levels and accurate diagnosis require high spatial resolution, achievable only from proximal sensing systems.

In conventional farming, the spatial variability of disease symptoms complicates the decision-making for disease control. Crops must be surveyed multiple times through the growing season, often requiring complex sampling schemes to provide representative results for uniform fungicide application across a field. Automatable detection, identification, and quantification of diseases at a plant level are essential for site-specific fungicide application that aligns with disease incidence and is both spatially and temporally precise.

Application maps can be generated using data from sensors and GIS, or sensors can be connected directly to actuators and more sophisticated online systems.

9.10 CONCLUSIONS

Effective disease management in wheat cultivation involves understanding and addressing multiple factors, including inoculum presence, crop microclimate, cultivar characteristics, and soil health. Advanced technologies such as remote sensing and automated pathogen detection are becoming crucial in modern agriculture. As these technologies evolve, they offer the potential to enhance disease prediction and control, ultimately improving crop yields and reducing environmental impacts. Maintaining balanced soil nutrients and water levels and implementing proper monitoring and management strategies are essential for sustainable wheat production and effective disease control.

Finally, in the advanced plant monitoring community, there is a risk of technology-driven rather than application-driven research. This exchange should be bidirectional: We urge plant scientists to guide remote sensing specialists and the breeding community toward research that supports more sustainable agricultural practices.

REFERENCES

Appeltans, S., Pieters, J. G., & Mouazen, A. M. (2021). Detection of leek white tip disease under field conditions using hyperspectral proximal sensing and supervised machine learning. *Computers and Electronics in Agriculture*, *190*. https://doi.org/10.1016/j.compag.2021.106453

Azadbakht, M., Ashourloo, D., Aghighi, H., Radiom, S., & Alimohammadi, A. (2019). Wheat leaf rust detection at canopy scale under different LAI levels using machine learning techniques. *Computers and Electronics in Agriculture*, *156*, 119–128. https://doi.org/10.1016/j.compag.2018.11.016

Barbedo, J. G. A. (2022). Data fusion in agriculture: Resolving ambiguities and closing data gaps. *Sensors*, *22*(6). MDPI. https://doi.org/10.3390/s22062285

Behmann, J., Mahlein, AK., Paulus, S. et al. Generation and application of hyperspectral 3D plant models: methods and challenges. *Machine Vision and Applications 27*, 611–624 (2016). https://doi.org/10.1007/s00138-015-0716-8.

Dehkordi, R. H., EL JARROUDI, M., Kouadio, L., Meersmans, J., & Beyer, M. (2020). Monitoring wheat leaf rust and stripe rust in winter wheat using high-resolution UAV-based red-green-blue imagery. *Remote Sensing*, *12*(22), 1–21. https://doi.org/10.3390/rs12223696

Feng, Z., Song, L., Duan, J., He, L., Zhang, Y., Wei, Y., & Feng, W. (2022). Monitoring Wheat Powdery Mildew Based on Hyperspectral, Thermal Infrared, and RGB Image Data Fusion. *Sensors*, *22(1),* 31. https://doi.org/10.3390/s22010031

Francesconi, S., Harfouche, A., Maesano, M., & Balestra, G. M. (2021). UAV-based thermal, RGB imaging and gene expression analysis allowed detection of Fusarium head blight and gave new insights into the physiological responses to the disease in durum wheat. *Frontiers in Plant Science*, *12:628575*. https://doi.org/10.3389/fpls.2021.628575

Franke, J., & Menz, G. (2007). Multi-temporal wheat disease detection by multi-spectral remote sensing. *Precision Agriculture*, *8*(3), 161–172. https://doi.org/10.1007/s11119-007-9036-y

Fröhlich-Nowoisky, J., Pickersgill, D. A., Després, V. R., & Pöschl, U. (2009). High diversity of fungi in air particulate matter. *Proceedings of the National Academy of Sciences of the United States of America*, *106*(31), 12814–12819. https://doi.org/10.1073/pnas.0811003106. Epub 2009 Jul 17. PMID: 19617562; PMCID: PMC2722276.

Fu, Y., Yang, G., Li, Z., Li, H., Li, Z., Xu, X., Song, X., Zhang, Y., Duan, D., Zhao, C., & Chen, L. (2020). Progress of hyperspectral data processing and modelling for cereal crop nitrogen monitoring. In *Computers and electronics in agriculture* (Vol. 172). Elsevier B.V. https://doi.org/10.1016/j.compag.2020.105321

Geipel, J., Link, J., & Claupein, W. (2014). Combined spectral and spatial modeling of corn yield based on aerial images and crop surface models acquired with an unmanned aircraft system. *Remote Sensing*, *6*(11), 10335–10355. https://doi.org/10.3390/rs61110335

Gongora-Canul, C., Salgado, J. D., Singh, D., Cruz, A. P., Cotrozzi, L., Couture, J., Rivadeneira, M. G., Cruppe, G., Valent, B., Todd, T., Poland, J., & Cruz, C. D. (2020). Temporal dynamics of wheat blast epidemics and disease measurements using multispectral imagery. *Phytopathology*, *110*(2), 393–405. https://doi.org/10.1094/PHYTO-08-19-0297-R

Gu, C., Wang, D., Zhang, H., Zhang, J., Zhang, D., & Liang, D. (2021). Fusion of deep convolution and shallow features to recognize the severity of wheat Fusarium head blight. *Frontiers in Plant Science*, *11*. https://doi.org/10.3389/fpls.2020.599886

Hackett, J. K., & Shah, M. (1990, May). Multi-sensor fusion: a perspective. In *Proceedings, IEEE International Conference on Robotics and Automation* (pp. 1324–1330). IEEE.

Hague, T., Tillett, N. D., & Wheeler, H. (2006). Automated crop and weed monitoring in widely spaced cereals. *Precision Agriculture*, *7*(1), 21–32. https://doi.org/10.1007/s11119-005-6787-1

Hong, Q., Jiang, L., Zhang, Z., Ji, S., Gu, C., Mao, W., Li, W., Liu, T., Li, B., & Tan, C. (2022). A lightweight model for wheat ear Fusarium head blight detection based on RGB images. *Remote Sensing*, *14*(14). https://doi.org/10.3390/rs14143481

Huang, L., Li, T., Ding, C., Zhao, J., Zhang, D., & Yang, G. (2020). Diagnosis of the severity of Fusarium head blight of wheat ears on the basis of image and spectral feature fusion. *Sensors (Switzerland)*, *20*(10). https://doi.org/10.3390/s20102887

Hyles, J., Bloomfield, M. T., Hunt, J. R., Trethowan, R. M., & Trevaskis, B. (2020). Phenology and related traits for wheat adaptation. *Heredity*, *125*(6), 417–430.

Kataoka, T., Kaneko, T., Okamoto, H., & Hata, S.-I. (2003). *Crop growth estimation system using machine vision*. *Proceedings 2003 IEEE/ASME International Conference on Advanced Intelligent Mechatronics (AIM 2003)*, Kobe, Japan, 2003, pp. b1079–b1083, vol.2. https://doi.org/10.1109/AIM.2003.1225492.

Kior, A., Yudina, L., Zolin, Y., Sukhov, V., & Sukhova, E. (2024). RGB imaging as a tool for remote sensing of characteristics of terrestrial plants: A review. *Plants*, *13*(9). Multidisciplinary Digital Publishing Institute (MDPI). https://doi.org/10.3390/plants13091262

Kumar, D., & Kukreja, V. (2022). Deep learning in wheat diseases classification: A systematic review. *Multimedia Tools and Applications*, *81*(7), 10143–10187. https://doi.org/10.1007/s11042-022-12160-3

Li, Y. H., Tan, X., Zhang, W., Jiao, Q. B., Xu, Y. X., Li, H., Zou, Y. B., Yang, L., & Fang, Y. P. (2021). Research and application of several key techniques in hyperspectral image preprocessing. *Frontiers in Plant Science*, *12*. https://doi.org/10.3389/fpls.2021.627865

Liang, K., Song, J., Yuan, R., & Ren, Z. (2023). Mid-level data fusion combined with the fingerprint region for classification DON levels defect of Fusarium head blight wheat. *Sensors*, *23*(14). https://doi.org/10.3390/s23146600

Liu, J., & Pattey, E. (2010). Retrieval of leaf area index from top-of-canopy digital photography over agricultural crops. *Agricultural and Forest Meteorology*, *150*(11), 1485–1490. https://doi.org/10.1016/j.agrformet.2010.08.002

Liu, Y., Liu, G., Sun, H., An, L., Zhao, R., Liu, M., Tang, W., Li, M., Yan, X., Ma, Y., & Zhao, F. (2024). Exploring multi-features in UAV based optical and thermal infrared images to estimate disease severity of wheat powdery mildew. *Computers and Electronics in Agriculture*, *225*. https://doi.org/10.1016/j.compag.2024.109285

Ma, H., Huang, W., Dong, Y., Liu, L., & Guo, A. (2021). Using UAV-based hyperspectral imagery to detect winter wheat Fusarium head blight. *Remote Sensing*, *13*(15). https://doi.org/10.3390/rs13153024

Mahlein, A. K., Alisaac, E., Al Masri, A., Behmann, J., Dehne, H. W., & Oerke, E. C. (2019). Comparison and combination of thermal, fluorescence, and hyperspectral imaging for monitoring Fusarium head blight of wheat on spikelet scale. *Sensors (Switzerland)*, *19*(10). https://doi.org/10.3390/s19102281

Mao, S. L., Wei, Y. M., Cao, W., Lan, X. J., Yu, M., Chen, Z. M., Chen, G. Y., & Zheng, Y. L. (2010). Confirmation of the relationship between plant height and Fusarium head blight resistance in wheat (*Triticum aestivum* L.) by QTL meta-analysis. *Euphytica*, *174*(3), 343–356. https://doi.org/10.1007/s10681-010-0128-9

Meron, M., Tsipris, J., Orlov, V., Alchanatis, V., & Cohen, Y. (2010). Crop water stress mapping for site-specific irrigation by thermal imagery and artificial reference surfaces. *Precision Agriculture*, *11*(2), 148–162. https://doi.org/10.1007/s11119-009-9153-x

Meyer, G. E., & Neto, J. C. (2008). Verification of colour vegetation indices for automated crop imaging applications. *Computers and Electronics in Agriculture*, *63*(2), 282–293. https://doi.org/10.1016/j.compag.2008.03.009

Morris, C. E., Sands, D. C., Glaux, C., Samsatly, J., Asaad, S., Moukahel, A. R., Gonçalves, F. L. T., and Bigg, E. K. Urediospores of rust fungi are ice nucleation active at > -10 °C and harbor ice nucleation active bacteria, *Atmos. Chem. Phys.*, *13*, 4223–4233, https://doi.org/10.5194/acp-13-4223-2013, 2013.

Moshou, D., Bravo, C., Oberti, R., West, J., Bodria, L., McCartney, A., & Ramon, H. (2005). Plant disease detection based on data fusion of hyper-spectral and multi-spectral fluorescence imaging using Kohonen maps. *Real-Time Imaging*, *11*(2), 75–83. https://doi.org/10.1016/j.rti.2005.03.003

Mustafa, G., Zheng, H., Khan, I. H., Zhu, J., Yang, T., Wang, A., Xue, B., He, C., Jia, H., Li, G., Cheng, T., Cao, W., Zhu, Y., & Yao, X. (2024). Enhancing Fusarium head blight detection in wheat crops using hyperspectral indices and machine learning classifiers. *Computers and Electronics in Agriculture*, *218*. https://doi.org/10.1016/j.compag.2024.108663

Mustafa, G., Zheng, H., Li, W., Yin, Y., Wang, Y., Zhou, M., Liu, P., Bilal, M., Jia, H., Li, G., Cheng, T., Tian, Y., Cao, W., Zhu, Y., & Yao, X. (2023). Fusarium head blight monitoring in wheat ears using machine learning and multimodal data from asymptomatic to symptomatic periods. *Frontiers in Plant Science*, *13*. https://doi.org/10.3389/fpls.2022.1102341

Ouhami, M., Hafiane, A., Es-Saady, Y., El Hajji, M., & Canals, R. (2021). Computer vision, IoT and data fusion for crop disease detection using machine learning: A survey and ongoing research. *Remote Sensing*, *13*(13). MDPI AG. https://doi.org/10.3390/rs13132486

Pantazi, X. E., Moshou, D., Alexandridis, T., Whetton, R. L., & Mouazen, A. M. (2016). Wheat yield prediction using machine learning and advanced sensing techniques. *Computers and Electronics in Agriculture*, *121*, 57–65. https://doi.org/10.1016/j.compag.2015.11.018

Paulus, S., & Mahlein, A. K. (2020). Technical workflows for hyperspectral plant image assessment and processing on the greenhouse and laboratory scale. *GigaScience*, *9*(8). https://doi.org/10.1093/gigascience/giaa090

Qiu, R., Yang, C., Moghimi, A., Zhang, M., Steffenson, B. J., & Hirsch, C. D. (2019). Detection of Fusarium head blight in wheat using a deep neural network and colour imaging. *Remote Sensing*, *11*(22). https://doi.org/10.3390/rs11222658

Searcy, S. W., & Reid, J. F. (1986). Vision-based guidance of an agricultural tractor. In 1986 American Control Conference (pp. 931–937). IEEE.

Rodríguez-Vázquez, J. N., Apolo-Apolo, O. E., Martínez-Moreno, F., Sánchez-Fernández, L., & Pérez-Ruiz, M. (2025). Monitoring leaf rust and yellow rust in wheat with 3D LiDAR sensing. *Remote Sensing*, *17*, 1005. https://doi.org/10.3390/rs17061005

Rossi, V., Manstretta, V., & Ruggeri, M. (2015). A multicomponent decision support system to manage Fusarium head blight and mycotoxins in durum wheat. *World Mycotoxin Journal*, *8*(5), 629–640. https://doi.org/10.3920/WMJ2015.1881

Roth, L., & Streit, B. (2018). Predicting cover crop biomass by lightweight UAS-based RGB and NIR photography: An applied photogrammetric approach. *Precision Agriculture*, *19*(1), 93–114. https://doi.org/10.1007/s11119-017-9501-1

Ruiz Hidalgo, D., Bacca Cortés, B., & Caicedo Bravo, E. (2021). Dimensionality reduction of hyperspectral images of vegetation and crops based on self-organized maps. *Information Processing in Agriculture*, 8(2), 310–327. https://doi.org/10.1016/j.inpa.2020.07.002

Savary, S., Willocquet, L., Pethybridge, S. J., Esker, P., McRoberts, N., & Nelson, A. (2019). The global burden of pathogens and pests on major food crops. *Nature Ecology and Evolution*, 3, 430–439. https://doi.org/10.1038/s41559-018-0793-y

Schistad Solberg, A. H., Jain, A. K., & Taxt, T. (1994). Multisource classification of remotely sensed data: Fusion of Landsat TM and SAR images. *IEEE Transactions on Geoscience and Remote Sensing*, *32*(4).

Shiferaw, B., Smale, M., Braun, H. J. et al. (2013). Crops that feed the world 10. Past successes and future challenges to the role played by wheat in global food security. *Food Security*, *5*, 291–317. https://doi.org/10.1007/s12571-013-0263-y

Singh, R. N., Krishnan, P., Singh, V. K., & Das, B. (2023). Estimation of yellow rust severity in wheat using visible and thermal imaging coupled with machine learning models. *Geocarto International*, *38*(1). https://doi.org/10.1080/10106049.2022.2160831

Song, L., Wang, L., Yang, Z., He, L., Feng, Z., Duan, J., Feng, W., & Guo, T. (2022). Comparison of algorithms for monitoring wheat powdery mildew using multi-angular remote sensing data. *Crop Journal*, *10*(5), 1312–1322. https://doi.org/10.1016/j.cj.2022.07.003

Su, J., Liu, C., Hu, X., Xu, X., Guo, L., & Chen, W. H. (2019). Spatio-temporal monitoring of wheat yellow rust using UAV multispectral imagery. *Computers and Electronics in Agriculture*, *167*. https://doi.org/10.1016/j.compag.2019.105035

Su, W. H., Zhang, J., Yang, C., Page, R., Szinyei, T., Hirsch, C. D., & Steffenson, B. J. (2021). Automatic evaluation of wheat resistance to Fusarium head blight using dual mask-rcnn deep learning frameworks in computer vision. *Remote Sensing*, *13*(1), 1–20. https://doi.org/10.3390/rs13010026

Whetton, R. L., Waine, T. W., & Mouazen, A. M. (2018). Evaluating management zone maps for variable rate fungicide application and selective harvest. *Computers and Electronics in Agriculture*, *153*, 202–212. https://doi.org/10.1016/j.compag.2018.08.004

Xue, J., & Su, B. (2017). Significant remote sensing vegetation indices: A review of developments and applications. *Journal of Sensors*, 2017(1), 1353691.

Zhang, Z., Flores, P., Friskop, A., Liu, Z., Igathinathane, C., Han, X., Kim, H. J., Jahan, N., Mathew, J., & Shreya, S. (2022). Enhancing wheat disease diagnosis in a greenhouse using image deep features and parallel feature fusion. *Frontiers in Plant Science*, *13*. https://doi.org/10.3389/fpls.2022.834447

Zhou, B., Elazab, A., Bort, J., Vergara, O., Serret, M. D., & Araus, J. L. (2015). Low-cost assessment of wheat resistance to yellow rust through conventional RGB images. *Computers and Electronics in Agriculture*, *116*, 20–29. https://doi.org/10.1016/j.compag.2015.05.017

Zhu, W., Chen, H., Ciechanowska, I., & Spaner, D. (2018). Application of infrared thermal imaging for the rapid diagnosis of crop disease. *IFAC-PapersOnLine*, *51*(17), 424–430. https://doi.org/10.1016/j.ifacol.2018.08.184

10 Deep Learning Object Detection for Robotic Harvesters in Rice

Jiajun Zhu, Yang Li, and Michihisa Iida

10.1 INTRODUCTION

Globally, the problem of labor shortage in agriculture is getting more serious (Ma et al., 2019; Zahniser et al., 2018). To solve this problem, manually driven agricultural machinery was commonly used for food production, getting larger and more powerful machinery over time. However, manually driven agricultural machinery has some disadvantages. For example, their driving is tough and dangerous (Caffaro et al., 2018), and the operator needs experience and high skill. Therefore, robotic agricultural machinery is being developed globally.

Robotic combine harvesters which can work automatically under human operator's surveillance have been developed and commercialized to harvest rice and wheat. However, they are unequipped with any object detection sensors for safety. Thus, the next important issue to be solved for a robotic combine harvester is how to detect objects in real farmland for safe and efficient work. Particularly, a robotic combine harvester should detect harvested and unharvested rice areas because it should run along the boundary line between those areas to prevent leaving uncut rice. Moreover, it should also detect rice lodging to efficiently harvest crops without jamming and clogging. Then, humans and field ridges should also be detected for avoiding collisions and automatic stopping, respectively.

The traditional methods to detect the different areas and humans involve individually detecting each object using various algorithms and sensors. Zhang et al. (2020) and Cho et al. (2014a) used the machine vision method with a camera to detect the edge between uncut and cut crops. Teng et al. (2016) and Cho et al. (2014b) utilized a laser range finder (LRF) to measure the height of the crops and detect the edge between harvested and unharvested rice areas. Masuda et al. (2013) used the wavelet transform with a low-cost USB camera to detect rice lodging. Morimoto et al. (2020a, 2020b) reported about the detection of rice lodging existence based on Histogram of Oriented Gradient (HOG) and the detection of rice lodging degree based on deep learning (DL), and both utilized the sensor RGB camera. Yang and Noguchi (2012) used the sum of squared differences (SSDs) method with omni-directional stereo vision to locate humans, while Asada et al. (2019) used DL and point cloud data with stereo cameras to detect humans. Li, Hong, et al. (2020) proposed an image segmentation algorithm based on support vector machine to detect the paddy field boundary line with an RGB camera, and He et al. (2022) applied the MobileV2-UNet and RANSAC with an RGB camera to detect the boundary line. Sun et al. (2023) reported about the semantic segmentation (RL-DeepLabv3+) to detect only the lodging rice area for the unmanned combine harvester.

The deployment of multiple algorithms to individually detect various objects makes the detection system complex and requires different sensors, which increases the system cost. Moreover, implementing multiple algorithms simultaneously would significantly increase the computational cost, making real-time detection difficult. One approach to solving these problems is to construct a semantic segmentation (SS) model based on DL using a regular RGB camera to detect all objects.

DOI: 10.1201/9781003510598-10

The DL-based SS method is a recent image processing method that can achieve pixel-wise prediction of images. Compared with the traditional method, the DL-based SS method is more suitable for multiple object detection. Recently, the DL-based SS methods have commonly been used and shown excellent performances in agriculture field. They have been employed for tasks such as apples detection in an orchard (Kang & Chen, 2020), grapes detection (Santos et al., 2020), crop, weed, and background separation in real time (Milioto et al., 2018), disease and pest identification for coffee leave (Tassis et al., 2021), fish body extraction (Fernandes et al., 2020), and crop areas mapping based on satellite images (Du et al., 2019). By using DL-based SS methods, all significant objects in the paddy field can be detected simultaneously. This will help the robotic combine harvester to quickly and accurately identify their surrounding environment.

10.2 APPLICATION

10.2.1 Application of Full Convolutional Network for Detecting Paddy Field Objects

Convolutional neural networks (CNNs) (Krizhevsky et al., 2012) are DL models designed for image processing and pattern recognition. They employ convolutional layers to automatically extract features from images and reduce dimensionality. When an input image is provided to the CNN model, it can output a classification result. For instance, if a dog image and a cat image are fed into a trained CNN model, it can correctly classify which image is of a dog and which is of a cat.

The fully convolutional network (FCN) (Long et al., 2015) is based on CNNs but transforms fully connected layers into convolutional layers (Long et al., 2015), enabling the FCN to output SS results. For example, as shown in Figure 10.1, when an image is inserted into an FCN model, it can output a prediction where pixels are painted differently. In this prediction, the left part is painted in yellow, indicating unharvested areas, while the right part is painted in gray, representing harvested areas.

Li, Iida, Suguri, et al. (2020) were the first to apply the DL-based SS method for detecting paddy field objects, such as harvested and unharvested areas, as well as ridges. In this study, an upgraded version of the FCN was used. The structure of the upgraded FCN is shown in Figure 10.1, where H is the height of an image in pixels, and W is the width of the image in pixels. The resolution of the images (H × W) was 640 × 480 Megapixels. The fractions 1/8, 1/16, and 1/32 denote the ratios of the convolution layer size to the original image size, and this size changes during the convolution step. *Pool* refers to the pooling layer, a commonly used component in CNNs that downsamples feature maps, manages computational complexity, and retains essential information during image processing.

Both VGG (Simonyan & Zisserman, 2014) and ResNet (He et al., 2016) are high-performance CNN models, which has a much stronger ability to extract features from images than the convolution structure in original FCN model. Therefore, in this study, the convolution layers before the pool

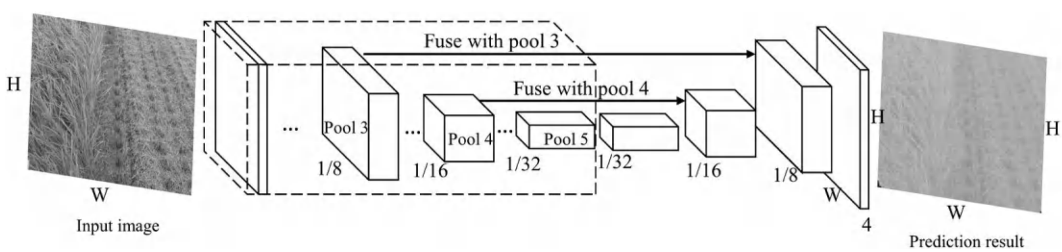

FIGURE 10.1 FCN-8s structure for image segmentation. pool 3, pool 4, pool 5 are pooling layers; H and W are height and width, respectively; Networks in dotted lines will be replaced by corresponding VGG and ResNet networks, respectively.

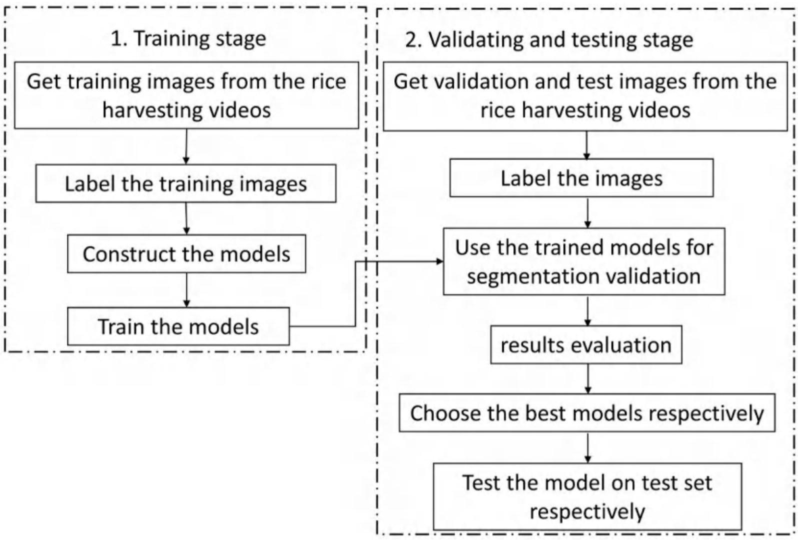

FIGURE 10.2 Flowchart of image segmentation based on fully convolutional networks.

5 layer (including the pool 5 layer) in FCN were replaced with VGG11, VGG13, VGG16, VGG19 (Simonyan & Zisserman, 2014), ResNet18, ResNet34 and ResNet50 (He et al., 2016), respectively. In this study, only convolution layers of VGG and ResNet were used, whereby all fully connected layers in both the VGG and ResNet were removed.

All FCN-8s models were trained to distinguish various areas in paddy field images (e.g., harvested rice area, unharvested rice area, lodging rice area…) by feeding with training images. Then, they were validated, this is, to find the best-trained models during the training process, and then, images were tested, which consist of giving the program different images from the ones in the training phase and evaluate the performance of the prediction results. Figure 10.2 shows the sequence of actions from the training stage to the testing stage.

In this study, Python 3 and the DL computing framework PyTorch 0.3 were used to train, validate, and test the field image segmentation models. The initial learning rate was 0.02, the decay coefficient of the learning rate was 0.5, the decay frequency was 20 epochs, and the regularization parameter λ was 0.00001.

Some examples of paddy field images, prediction result, and its ground truth are shown in Figure 10.3. Images in column A are the original photos retrieved from the camera. For example, image 1A is showing unharvested area on the left, and harvested area on the right. After the normalization stage, which consists of standardizing the brightness of all photos to mitigate the adverse effects of uneven brightness, original images appear as shown in the images of column B. The predicted image is shown in column C. The predicted image 2C is showing a mistake in the upper right zone, as well as some little area in the upper left zone. Column D is showing the proper segmentation (classification) of areas in the image. For example, image 2D has just two different zones according to the original photo (2A).

By comparing the prediction results with the ground truth in Figure 10.3, it can be inferred that the harvested area, unharvested area, and ridge area were mostly successfully segmented. Table 10.1 presents the segmentation accuracy, and the computational speed of each model tested on a desktop PC with a GeForce Dual-GTX1070-08G GPU.

In this study, the FCN model was applied to segment paddy field images, and the results demonstrated that the constructed networks effectively segmented the harvested areas, unharvested areas, and ridge areas in the field. However, two issues still remain. First, since the paddy field environment is complex, there are other objects such as humans and lodged rice that need to

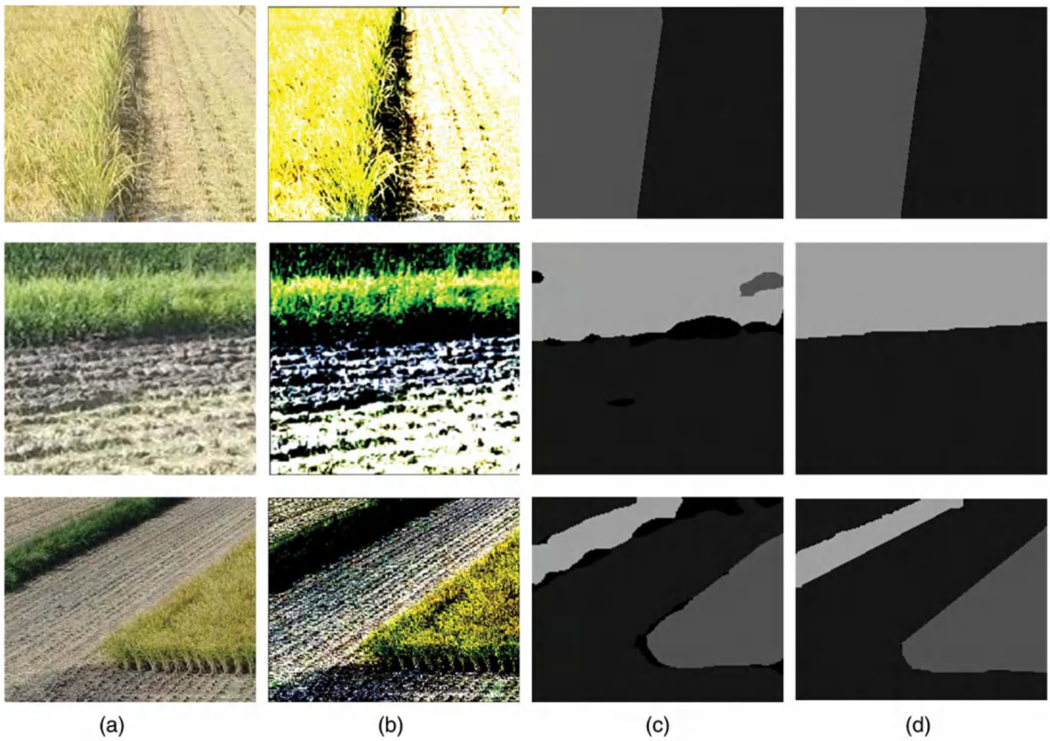

FIGURE 10.3 Examples of semantic segmentation results with different scenes: Column (a) images are the original photos taken with the camera, images in column (b) are photos after normalization, images in column (c) are the predicted images while column (d) images show the proper classification (ground truth).

be detected in addition to the harvested area, unharvested area, and ridge area. Unfortunately, the networks constructed in this study were unable to segment these other objects. Second, the networks constructed in this study are heavy and slow SS models that can only run on desktop PC with high-quality GPU. Given the limitations of space and energy consumption, a compact embedded processor would be more suitable for a robotic combine harvester than a desktop PC. Therefore, a light and fast SS model is needed to run on the embedded processor for the robotic combine harvester.

TABLE 10.1
Segmentation Accuracy and Segmentation Speed of Each FCN-8s Model

Models	Pixel Accuracy	Mean Accuracy	Mean IoU (Intersection Over Union)	Forward Time (ms)	Size of Model Parameter File (MByte)
FCN-8s-ResNet50	0.9517	0.8608	0.8007	29	89.9
FCN-8s-ResNet34	0.9476	0.8320	0.8063	25	81.3
FCN-8s-ResNet18	0.9423	0.8274	0.7920	21	42.7
FCN-8s-VGG19	0.9475	0.8677	0.8151	37	76.5
FCN-8s-VGG16	0.9362	0.8899	0.8334	34	56.2
FCN-8s-VGG13	0.9432	0.8670	0.8215	30	35.9
FCN-8s-VGG11	0.9434	0.8591	0.8058	27	35.2

10.2.2 Real-Time Semantic Segmentation of Human Detection for Robotic Combine Harvesters

In order to prevent collisions with humans while working in the paddy field, it is necessary to detect human for the robotic combine harvester. Additionally, since the robotic combine harvester needs to adjust its direction and speed based on real-time paddy field detection results, a real-time SS model is required. Because most of the robotic combine harvesters use embedded terminals, they do not have a powerful computational ability, so a lighter model with faster speed is needed. However, the FCN models mentioned in Section 10.2.1 are too heavy, which makes they could not achieve real-time detection in embedded terminals. The image cascade network (ICNet) (Zhao et al., 2018) is a lighter model and easily achieves real-time detection in embedded terminals.

Li, Iida, Suyama, et al. (2020) upgraded the algorithm to the ICNet to achieve real-time detection of paddy field objects, including the harvested area, unharvested area, ridge, and humans. The structure of ICNet is shown in Figure 10.4. The ICNet takes cascade image inputs (i.e., medium- and high-resolution images), and it adopts a pyramid pooling module (PPM) to extract the context information and a cascade feature fusion (CFF) unit to fuse the feature maps with different resolution. The structures of PPM and CFF unit are shown in Figure 10.5. And then it was trained with cascade label guidance. Different-scale (e.g., 1/16, 1/8, and 1/4) ground truth labels were utilized to guide the learning stage of low-, medium- (320 × 240) and high-resolution input.

The constructed ICNet model was then trained and validated using some paddy field images. To improve the segmentation speed, a pruning algorithm is required to eliminate the unnecessary portions of the trained model. In this section, the Network Slimming method (Liu et al., 2017) was employed to remove less important connections with small weights in each convolution layer. The compaction ratio refers to the percentage of weight in the trained model that is removed after the pruning process. The fine-tuned pruned models were tested on Jetson Xavier (one of the embedded terminals developed by Nvidia) using various compaction ratios, and the segmentation accuracy was plotted in Figure 10.6. This figure is plotting mean Intersection over Union (mIoU) (it evaluates the segmentation accuracy of trained model) versus compaction ratios in percentage. The blue curve shows the variation of training mIoU versus compaction ratios in percentage. The orange curve shows the variation of validation mIoU versus compaction ratios in percentage. The gray curve shows the variation of test mIoU versus compaction ratios in percentage. As the compaction ratio continues to increase, there is a small loss in the accuracy of the model. However,

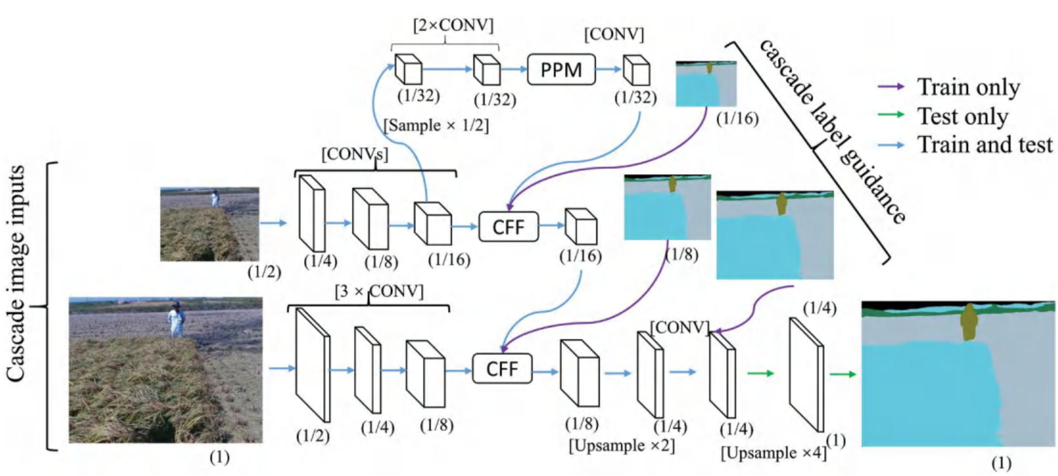

FIGURE 10.4 ICNet structure for image segmentation.

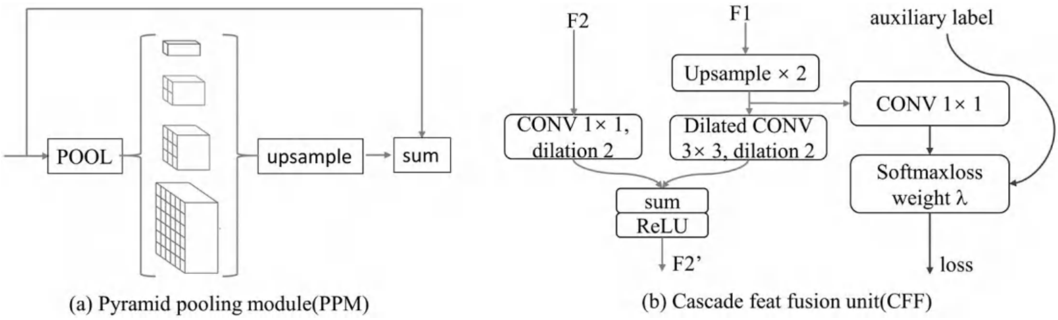

FIGURE 10.5 Pyramid pooling module (PPM) (a) and cascade feat fusion (CFF) unit in ICNet (b).

when the compaction ratio is greater than 80%, the accuracy of the model seriously degrades. When the compaction ratio is less than 80%, compelling results are achieved in comparison to the original counterpart.

The prediction speed of pruned models with different compaction ratio is shown in Table 10.2. As the accuracy of the model drops sharply when the compaction ratio is greater than 80%, only models with a compaction ratio of less than 80% were measured. Table 10.2 shows that as the compaction ratio increases, the size of the model volume decreases and the speed of the model increases. With 80% of the channel been pruned, the model has a 97.4% reduction of model volume size and ran 1.33 times faster with comparable detection accuracy to the original model. Segmentation performance and the inference run-time performance reveal that when the compaction ratio is less than 80%, the Network Slimming method could be used for decreasing the computational cost of the ICNet for field image segmentation.

Finally, a field test was conducted to measure the accuracy of human detection. Out of 60 instances where humans appeared in front of the combine harvester, the human was successfully detected in 58 instances, resulting in an average success rate of collision avoidance of 96.6%. Some segmentation results are presented in Figure 10.7.

In this study, ICNet and the Network Slimming method were used to create a real-time SS model capable of segmenting harvested areas, unharvested areas, ridges, and humans in paddy field images. The model achieved a frames per second (FPS) of 32.2 on the Jetson Xavier, sufficient for real-time detection. However, the model does not include the detection of rice lodging.

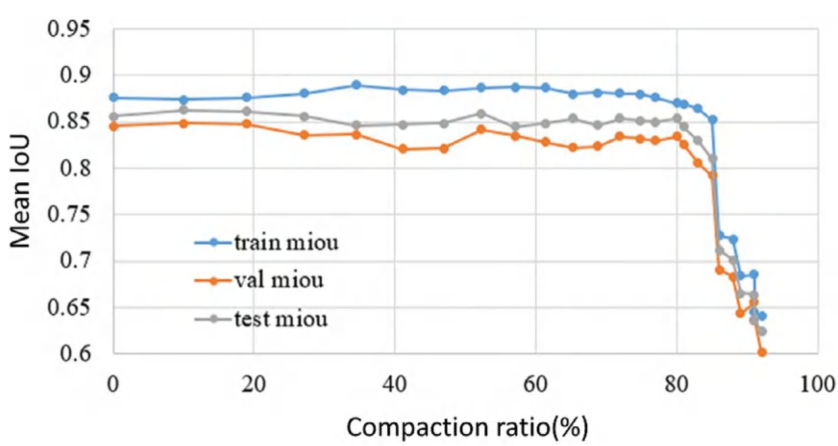

FIGURE 10.6 The mean IoU at different compaction ratio.

TABLE 10.2
The Frames per Second (FPS) on the Jetson Xavier and Model Volume of Different Pruned Models

Compaction Ratio (%)	FPS on Xavier	Inference Time (ms)	Volume Size of Model Parameter file (MB)
0	24.2	41.3	30.8
10.0	26.2	38.2	26.7
19.0	28.4	35.2	21.8
27.1	29.0	34.4	17.5
34.4	29.4	34.0	13.8
41.0	29.5	33.9	10.8
46.9	30.5	32.8	8.5
52.3	30.6	32.7	6.6
57.1	30.5	32.8	5.1
61.4	30.5	32.8	4.1
65.3	30.7	32.6	3.1
68.8	30.8	32.5	2.4
71.9	32.0	31.3	1.8
74.7	31.3	31.9	1.4
77.0	32.0	31.3	1.0
80.0	32.2	31.1	0.8

10.2.3 Semantic Segmentation Model for Rice Lodging Detection

The detection of rice lodging existence is crucial for the robotic combine harvester. When harvesting lodging rice, the robotic combine harvester should lower its header and slow down to gently harvest the lodging rice; otherwise, the rice plant may get jammed in the header, feeder, or thresher.

Zhu, Iida, Li, et al. (2022) upgraded ICNet to detect all significant objects in the paddy field, including the harvester's header, harvested area, unharvested area, lodging area, human, and ridge. The upgraded ICNet's structure is shown in Figure 10.8, and the basic architecture remains the same as the ICNet mentioned in Section 10.2. However, the backbone of ICNet, shown in the dotted rectangle in Figure 10.8, is replaced with Residual Network (ResNet) (He et al., 2016) or VGG (Simonyan & Zisserman, 2014). Six different ICNet models and one FCN model were constructed for comparison, which are listed in Table 10.3.

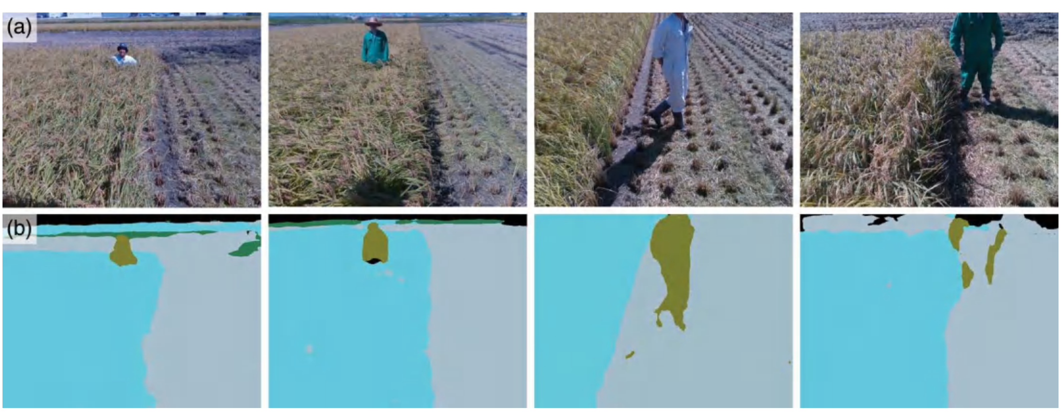

FIGURE 10.7 Examples of images where humans appear (a) and segmentation results (b) of the model.

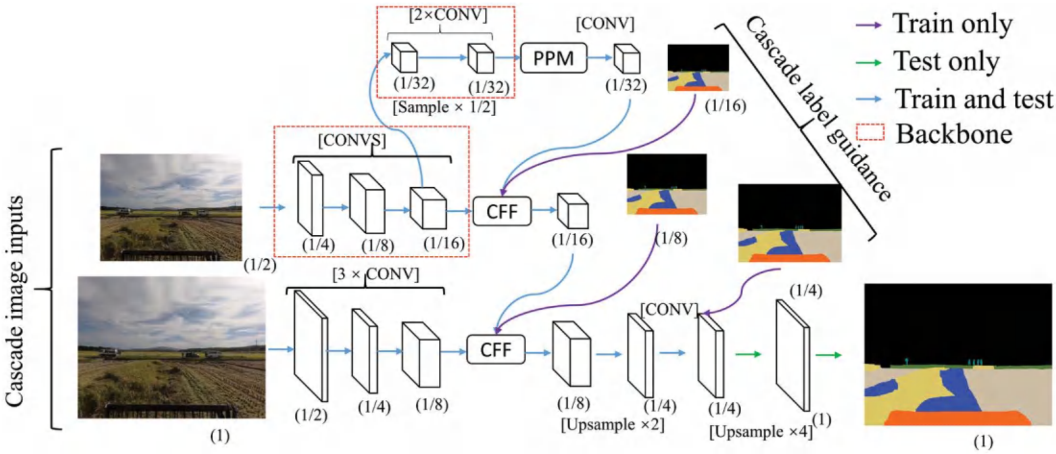

FIGURE 10.8 Network architecture of upgraded ICNet.

Then, all ICNet models were trained, validated, and tested with some paddy field images. The model training and validation were carried out on a desktop PC, while the testing was done on a cheaper embedded processor, Jetson TX2, in contrast to the Jetson Xavier used in Section 10.2. Based on the type of camera, camera installation heights, depression angles, and rice cultivars, all images were divided into three datasets (Dataset 1, Dataset 2, Dataset 3). The test results are shown in Table 10.4, and some examples of paddy field images, prediction results, and ground truth are shown in Figure 10.9.

The mean IoUs of all models are above 0.81, indicating that all classes were successfully segmented. Comparing the FPS and mean IoUs in the ICNet-based models, the best model was ICNet-VGG11, with FPS and mean IoU reaching 14.04 and 0.8449, respectively. Since the maximum speed of the robotic combine harvester during harvesting is approximately 1.5 m/s, this prediction speed could almost satisfy real-time detection. Furthermore, compared to FCN-8S-VGG16, the accuracy of ICNet-VGG11 was slightly lower, but the speed was much faster.

When comparing the IoUs of different classes, it was found that the classes of background, harvested area, human, and header had higher IoUs than the remaining classes, indicating that those classes could be successfully segmented. However, the ridge class had a relatively lower IoU because it could only be detected when the combine was near it, resulting in relatively lower accuracy.

TABLE 10.3
List of Six Different ICNet Models and FCN Model

Basic Architecture	Backbone	Model
ICNet	ResNet50	ICNet-ResNet50
	ResNet34	ICNet-ResNet34
	ResNet18	ICNet-ResNet18
	VGG16	ICNet-VGG16
	VGG13	ICNet-VGG13
	VGG11	ICNet-VGG11
FCN	VGG16	FCN-8S-VGG16 (Same model proposed by Long et al., 2015)

TABLE 10.4
Segmentation Accuracy and Prediction Speed of Each Model Tested on Jetson TX2

Model	ICNet-ResNet50	ICNet-ResNet34	ICNet-ResNet18	ICNet-VGG16	ICNet-VGG13	ICNet-VGG11	FCN-8S-VGG16
Pixel accuracy	0.9702	0.9703	0.9687	0.9721	0.9710	0.9719	0.9717
Mean accuracy	0.8804	0.8792	0.8745	0.8914	0.8808	0.8801	0.8929
Mean IoU	0.8214	0.8213	0.8186	0.8477	0.8410	0.8449	0.8519
IoU of background	0.9630	0.9628	0.9616	0.9648	0.9629	0.9633	0.9617
IoU of harvested area	0.7979	0.8065	0.8141	0.8624	0.8500	0.8461	0.8697
IoU of unharvested area	0.7948	0.7878	0.7767	0.8129	0.8097	0.8123	0.8191
IoU of lodging area	0.6517	0.6639	0.6574	0.6523	0.6590	0.6933	0.6937
IoU of ridge	0.7931	0.7692	0.7568	0.8253	0.8066	0.8022	0.8056
IoU of human	0.7979	0.8065	0.8141	0.8624	0.8500	0.8461	0.8697
IoU of header	0.9517	0.9524	0.9493	0.9538	0.9486	0.9501	0.9437
FPS	4.81	9.13	13.29	8.84	10.37	14.04	2.62

Another issue is that the IoU of unharvested area was relatively lower and the IoU of lodging area was not very high. There were two reasons for this. First, the boundary between lodging area and unharvested area was difficult to segment. For example, in Dataset 1 (a) and Dataset 2 (b) shown in Figure 10.9, some parts of the lodging area were mistakenly segmented as unharvested area, which decreased the IoUs of both areas. Second, sometimes lodging areas were segmented while the lodging area actually did not exist. The red circle in Figure 10.9 mistook a detection of a lodging area showing this problem, despite this error was small.

Finally, the detection accuracy of lodging existence was also tested. A threshold value was set to determine whether the rice lodging existed or not to reduce the influence of mistakes like the red circle in Figure 10.9. Only if the number of pixels belonging to class *lodging area* in one segmented picture was over the threshold value, the rice lodging would be determined to exist in this segmented picture. In this test, the threshold value was set to be 1000 pixels.

Table 10.5 shows the result of the detection accuracy of lodging existence. The detection accuracy of all seven models could reach over 0.92, which means the lodging existence could be successfully detected by all the SS models.

In this study, ICNet was applied to detect all objects in a paddy field in real time and the rice lodging existence could be detected with a high accuracy. The models were tested on a cheaper embedded processor, Jetson TX2. However, the segmentation accuracy and prediction speed were not high enough to fully satisfy real-time detection requirements. Additionally, since the embedded

TABLE 10.5
The Result of the Detection Accuracy of Lodging Existence

Model	TP	FP	TN	FN	Detection Accuracy of Lodging Existence
ICNet-ResNet50	259	12	41	358	0.9209
ICNet-ResNet34	267	13	33	357	0.9313
ICNet-ResNet18	274	9	26	361	0.9478
ICNet-VGG16	274	13	26	357	0.9418
ICNet-VGG13	271	13	29	357	0.9373
ICNet-VGG11	275	12	25	358	0.9448
FCN-8S-VGG16	273	18	27	352	0.9328

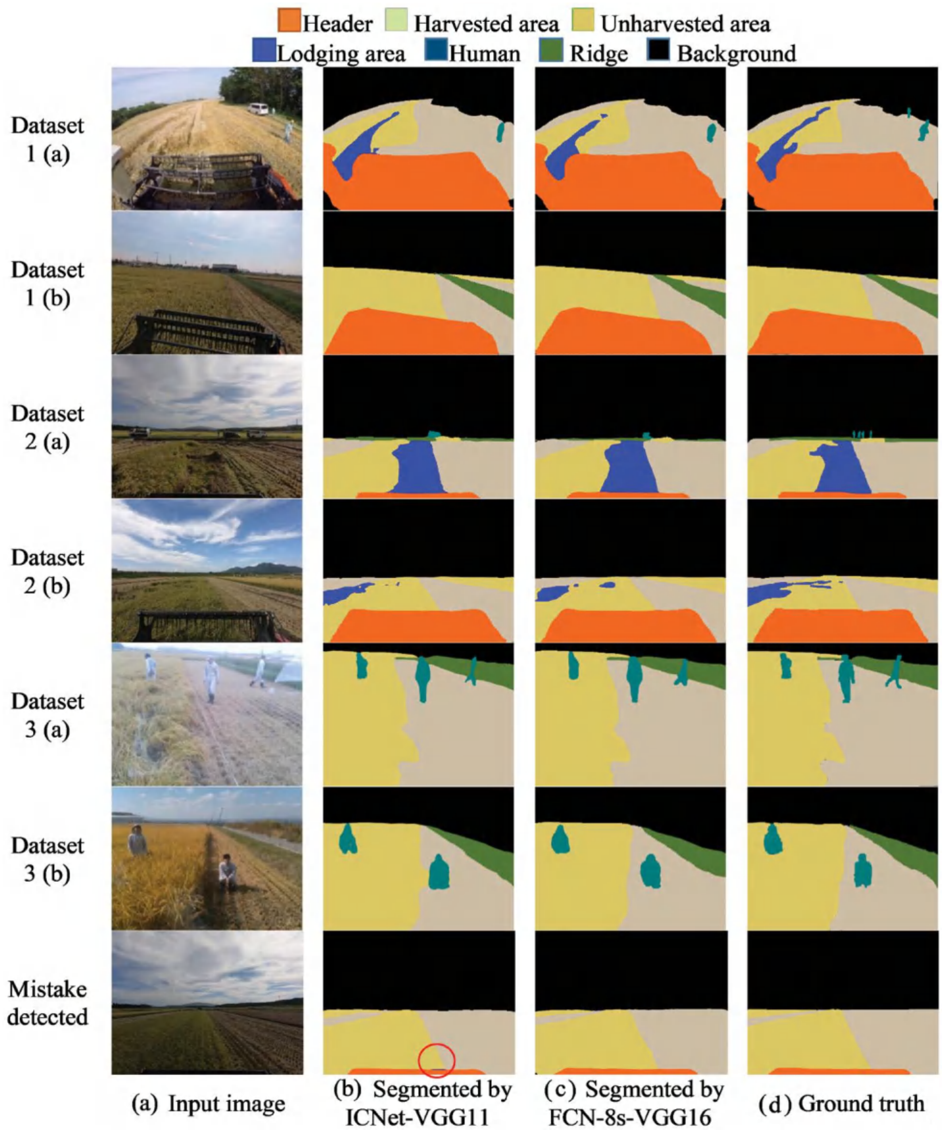

FIGURE 10.9 Examples of input images (original photo in (a)), segmentation results with ICNet-VGG11 (b), and FCN-8s-VGG16 (c), and ground truth of each dataset (d).

processor also needs to run the control program for the robotic combine harvester, a faster and more accurate SS model is needed.

10.2.4 Real-Time Semantic Segmentation Model for All Objects in Paddy Field

To improve the segmentation accuracy and prediction speed of the SS model, Zhu, Iida, Suguri, et al. (2022) utilized the deep dual-resolution networks (DDRNets) (Hong et al., 2021). The structure of DDRNets is shown in Figure 10.10. Among all DDRNets, the fastest one, DDRNet-23-slim, was applied in this study. DDRNet-23-slim consisted of two branches: A high-resolution branch (green block) to obtain spatial information, and a low-resolution branch (pink block) to obtain semantic information. Both branches used the ResNets backbone (He et al., 2016).

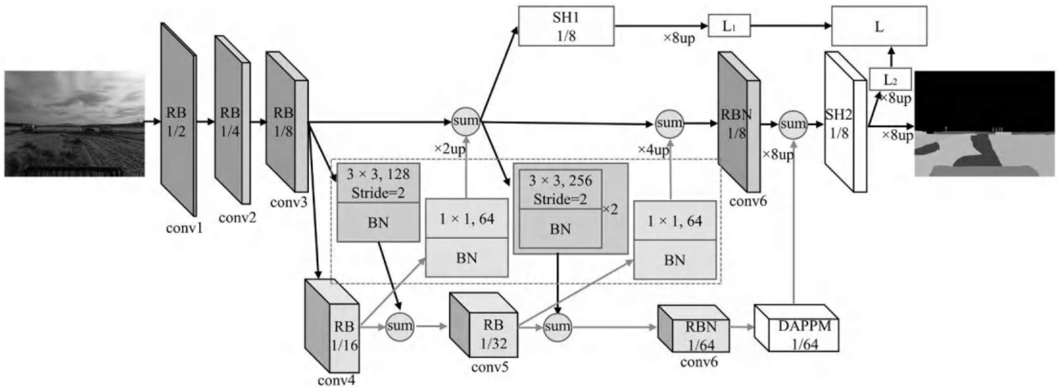

FIGURE 10.10 Structure of DDRNets.

Feature fusion (Jiang et al., 2020) is a technique commonly used in machine learning to merge features at various stages within the model, allowing for a more flexible integration of information. Feature fusion can enhance model robustness, improve accuracy, and enrich object representation. As one of the feature fusion techniques, bilateral fusion (Hong et al., 2021) is a module used to fuse the feature maps between two branches to prevent loss of information during downsampling, shown by a blue dotted rectangle in Figure 10.10. In Figure 10.10, RB stands for residual basic block (He et al., 2016); RBN denotes the residual bottleneck block (He et al., 2016); SH means segmentation head (one convolution layer that output segmentation results); BN denotes batch normalization. L refers to the final loss. At the end of the low-resolution branch, a Deep Aggregation Pyramid Pooling Module (DAPPM) (Hong et al., 2021) was added to extract contextual information.

Finally, two segmentation heads SH1 and SH2 were used to get a prediction result. Losses L_1 and L_2 were calculated by the difference between prediction result and ground truth.

The final loss can be calculated as the following:

$$L = 0.4 \times L_1 + L_2 \tag{10.1}$$

where L is the final loss, L_1 is the auxiliary loss and L_2 is the normal loss.

Additionally, ICNet-VGG11 and FCN-8s were also constructed for comparison.

In this study, NVIDIA TensorRT was used as speed acceleration method to further enhance the prediction speed of the SS model. Unlike the Network Slimming method mentioned in Section 10.2, TensorRT can improve the inference speed without sacrificing accuracy. The TensorRT can rebuild and optimize the trained network mainly by three steps as Figure 10.11 revealed (Vanholder, 2016), where CBR are … (explain abbreviations that were not explained before):

1. Delete the unused convolution layer in the network to reduce computation.
2. Vertical fuse the convolution layer, batch normalization (BN) layer, and ReLU layer to one convolution, BN, and ReLU (CBR) layer.
3. Horizontal fuse multiple 1 × 1 CBR layers to one 1 × 1 CBR layer.

Additionally, it should be highlighted that TensorRT can improve the inference speed without sacrificing accuracy.

Then, all models were trained on a desktop PC and tested on the Jetson TX2, and the results are shown in Table 10.6. From the table, it is obvious that the FPS of all models significantly increased after acceleration by the TensorRT. DDRNet-23-slim had the highest FPS of 23.08 after

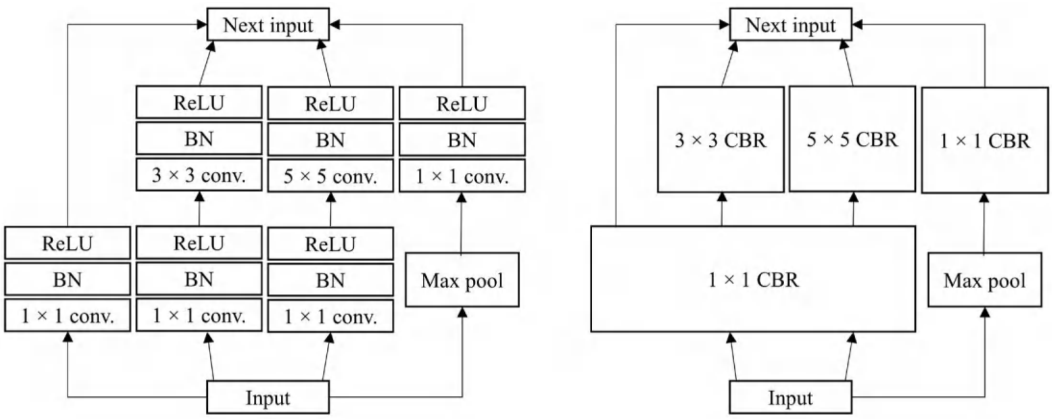

FIGURE 10.11 (a) Un-optimized network. (b) TensorRT-optimized network.

acceleration, which is totally sufficient for the real-time detection. Additionally, DDRNet-23-slim had a mean IoU of 0.844, which was significantly higher than other models. In terms of segmentation accuracy and prediction speed, DDRNet-23-slim is the best model, and its accuracy and speed are both significantly better than other models.

When comparing the IoUs of different classes in Table 10.6, all classes had high IoUs, indicating that all classes can be successfully segmented. Among all classes, the classes of background, harvested area, ridge, human, and header had higher IoUs than the classes of unharvested area and lodging.

There are two reasons that decreased the IoUs of lodging area and unharvested area. The first reason is that the boundary between lodging area and unharvested area was difficult to segment. Second, misdetection may occur, as shown in Figure 10.12(c). The lodging area would be segmented even though it did not actually exist. However, the misdetection part of the lodging area was always small and could be removed by setting a threshold value. In this case, if the pixel amount of the lodging area was less than 1000, the lodging area would not be considered to exist.

In this study, DDRNet-23-slim was applied to detect all objects in paddy field, including the harvester's header, harvested area, unharvested area, lodging area, human, and ridge. And the TensorRT was utilized to accelerate the pruned model. Then, the model was tested on the cheaper embedded processor, Jetson TX2. Results show that all objects could be successfully segmented, and the segmentation accuracy and prediction speed of DDRNet-23-slim are both significantly

TABLE 10.6
Segmentation Accuracy and Speed of Each Model Tested on Jetson TX2

Model	FCN-8s	ICNet-VGG11	DDRNet-23-slim
FPS (before acceleration)	1.57	10.38	16.44
FPS (after acceleration)	3.57	17.32	23.08
Mean IoU	0.824	0.820	0.844
IoU of background	0.926	0.929	0.926
IoU of harvested area	0.820	0.805	0.844
IoU of unharvested area	0.728	0.736	0.761
IoU of ridge	0.787	0.765	0.809
IoU of human	0.820	0.805	0.844
IoU of lodge	0.738	0.732	0.752
IoU of header	0.950	0.970	0.972

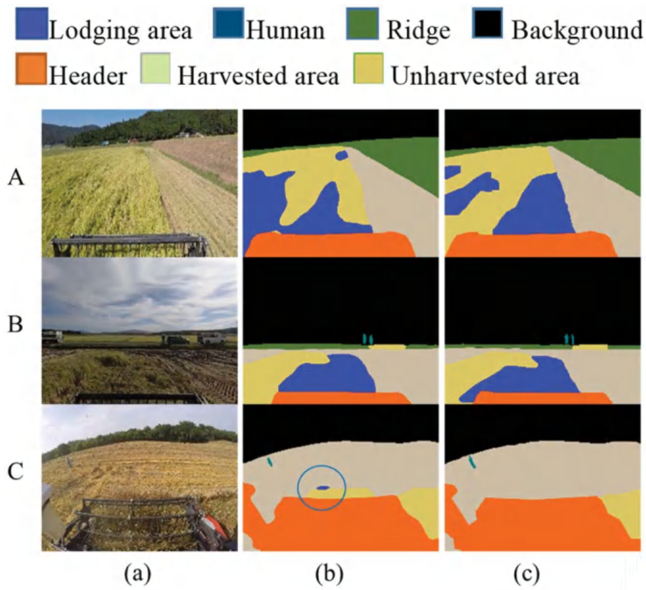

FIGURE 10.12 (a) Input image, (b) DDRNet-23-slim, (c) ground truth.

better than ICNet and FCN. The FPS of DDRNet-23-slim after acceleration reaches 23.08, which is totally sufficient for the real-time detection.

10.3 CONCLUSION

This chapter introduced several studies on paddy field object detection for robotic combine harvesters, utilizing DL-based SS method. In comparison to traditional methods, which require individual detection of objects using various algorithms and sensors, the SS method can detect all objects simultaneously using only one algorithm and one sensor. This greatly reduces the complexity of the detection system and enables real-time detection. Additionally, the use of fewer sensors decreases the cost of the detection system.

In Section 10.2.1, the FCN model was used to segment paddy field images, effectively identifying harvested areas, unharvested areas, and ridge areas in the field. However, two issues remain. First, the complex paddy field environment contains additional objects such as humans and lodging rice that also require detection, but the networks constructed in this study are unable to segment these objects. Second, the networks constructed in this study are heavy and slow SS models that can only run on desktop PC with high-quality GPU. Given the limitations of space and energy consumption, a compact embedded processor would be more suitable for a robotic combine harvester than a desktop PC. Therefore, a light and fast SS model is needed to run on the embedded processor for the robotic combine harvester.

In Section 10.2.2, ICNet and the Network Slimming method were used to create a real-time SS model that can segment harvested areas, unharvested areas, ridges, and humans in paddy field images. The model achieved an FPS of 32.2 on the Jetson Xavier, sufficient for real-time detection. However, it does not detect rice lodging, and the embedded processor used is costly.

In Section 10.2.3, ICNet was used to detect all objects in a paddy field, with high accuracy in rice lodging detection. The models were tested on a cheaper embedded processor, Jetson TX2. However, the segmentation accuracy and prediction speed were not sufficient for real-time detection requirements, and the embedded processor used also needed to run the control program for the robotic combine harvester, being this a big drawback.

In Section 10.2.4, to improve the segmentation accuracy and prediction speed, DDRNet-23-slim was used to detect all objects in the paddy field, including the harvester's header, harvested area, unharvested area, lodging area, human, and ridge. The TensorRT was utilized to accelerate the pruned model, and the pruned model was tested on the cheaper embedded processor Jetson TX2. Results show that all objects were successfully segmented, with significantly higher segmentation accuracy and prediction speed than ICNet and FCN. The FPS of DDRNet-23-slim after acceleration reaches 23.08, sufficient for real-time detection.

In the future, a controlling system will be developed to ensure safe and efficient operation of the robotic combine harvester based on the object detection results provided by the constructed SS models.

REFERENCES

Asada, R., Iida, M., Suguri, M., & Masuda, R. (2019). Object detection and collision avoidance for a robotic combine using stereo camera. *Journal of the Japanese Society of Agricultural Machinery and Food Engineers*, *81*(6), 392–402.

Caffaro, F., Roccato, M., Cremasco, M. M., & Cavallo, E. (2018). Falls from agricultural machinery: Risk factors related to work experience, worked hours, and operators' behavior. *Human Factors*, *60*(1), 20–30.

Cho, W., Iida, M., Suguri, M., Masuda, R., & Kurita, H. (2014a). Vision-based uncut crop edge detection for automated guidance of head-feeding combine. *Engineering in Agriculture, Environment and Food*, *7*(2), 97–102.

Cho, W., Iida, M., Suguri, M., Masuda, R., & Kurita, H. (2014b). Using multiple sensors to detect uncut crop edges for autonomous guidance systems of head-feeding combine harvesters. *Engineering in Agriculture, Environment and Food*, *7*(3), 115–121.

Du, Z., Yang, J., Ou, C., & Zhang, T. (2019). Smallholder crop area mapped with a semantic segmentation deep learning method. *Remote Sensing*, *11*(7), 888.

Fernandes, A. F., Turra, E. M., de Alvarenga, ÉR., Passafaro, T. L., Lopes, F. B., Alves, G. F., & Rosa, G. J. (2020). Deep learning image segmentation for extraction of fish body measurements and prediction of body weight and carcass traits in Nile tilapia. *Computers and Electronics in Agriculture*, *170*, 105274.

He, K., Zhang, X., Ren, S., & Sun, J. (2016). Deep residual learning for image recognition. In P*roceedings of the IEEE conference on computer vision and pattern recognition* (pp. 770–778).

He, Y., Zhang, X., Zhang, Z., & Fang, H. (2022). Automated detection of boundary line in paddy field using mobilev2-unet and RANSAC. *Computers and Electronics in Agriculture*, *194*, 106697.

Hong, Y., Pan, H., Sun, W., & Jia, Y. (2021). *Deep dual-resolution networks for real-time and accurate semantic segmentation of road scenes*. arXiv preprint arXiv:2101.06085.

Jiang, D., Sun, B., Su, S., & Zuo, Z. (2020). Feature fusion methods in deep-learning generic object detection: A survey. In *IEEE 9th joint international information technology and artificial intelligence conference (ITAIC)* (pp. 431–437), Chongqing, China.

Kang, H., & Chen, C. (2020). Fruit detection, segmentation and 3D visualisation of environments in apple orchards. *Computers and Electronics in Agriculture*, *171*, 105302.

Krizhevsky, A., Sutskever, I., & Hinton, G. E. (2012). Imagenet classification with deep convolutional neural networks. *Advances in Neural Information Processing Systems*, *25*.

Li, Y., Hong, Z., Cai, D., Huang, Y., Gong, L., & Liu, C. (2020). A SVM and SLIC based detection method for paddy field boundary line. *Sensors*, *20*(9), 2610.

Li, Y., Iida, M., Suguri, M., & Masuda, R. (2020). Regional segmentation of field image based on convolutional neural network for rice combine harvester. *Journal of the Japanese Society of Agricultural Machinery and Food Engineers*, *82*(1), 47–56.

Li, Y., Iida, M., Suyama, T., Suguri, M., & Masuda, R. (2020). Implementation of deep-learning algorithm for obstacle detection and collision avoidance for robotic harvester. *Computers and Electronics in Agriculture*, *174*, 105499.

Liu, Z., Li, J., Shen, Z., Huang, G., Yan, S., & Zhang, C. (2017). *Learning efficient convolutional networks through network slimming*. arXiv:1708.06519.

Long, J., Shelhamer, E., & Darrell, T. (2015). Fully convolutional networks for semantic segmentation. In *Proceedings of the IEEE conference on computer vision and pattern recognition* (pp. 3431–3440).

Ma, L., Long, H., Zhang, Y., Tu, S., Ge, D., & Tu, X. (2019). Agricultural labor changes and agricultural economic development in china and their implications for rural vitalization. *Journal of Geographical Sciences*, *29*(2), 163–179.

Masuda, R., Fujimoto, S., Iida, M., & Suguri, M. (2013). A method to detect the occurrence of rice plant lodging using wavelet transform. *IFAC Proceedings Volumes*, *46*(18), 75–80.

Milioto, A., Lottes, P., & Stachniss, C. (2018). Real-time semantic segmentation of crop and weed for precision agriculture robots leveraging background knowledge in CNNs. In *2018 IEEE international conference on robotics and automation (ICRA)* (pp. 2229–2235).

Morimoto, E., Inagaki, N., Ueta, D., Takahashi, K., & Nonami, K. (2020a). Estimate of rice lodging based on image processing (Part 1) – Effect verification of histogram of oriented gradient (in Japanese). *Journal of the Japanese Society of Agricultural Machinery and Food Engineers*, *82*(2), 150–155.

Morimoto, E., Inagaki, N., Ueta, D., Takahashi, K., & Nonami, K. (2020b). Estimate of rice lodging based on image processing (Part 2) – Effect verification of convolutional neural network and learning to rank (in Japanese). *Journal of the Japanese Society of Agricultural Machinery and Food Engineers*, *82*(2), 156–161.

Santos, T. T., de Souza, L. L., dos Santos, A. A., & Avila, S. (2020). Grape detection, segmentation, and tracking using deep neural networks and three-dimensional association. *Computers and Electronics in Agriculture*, *170*, 105247.

Simonyan, K., & Zisserman, A. (2014). *Very deep convolutional networks for large-scale image recognition*. arXiv preprint arXiv:1409.1556.

Sun, J., Zhou, J., He, Y., Jia, H., & Liang, Z. (2023). RL-DeepLabv3+: A lightweight rice lodging semantic segmentation model for unmanned rice harvester. *Computers and Electronics in Agriculture*, *209*, 107823.

Tassis, L. M., de Souza, J. E. T., & Krohling, R. A. (2021). A deep learning approach combining instance and semantic segmentation to identify diseases and pests of coffee leaves from in-field images. *Computers and Electronics in Agriculture*, *186*, 106191.

Teng, Z., Noguchi, N., Liangliang, Y., Ishii, K., & Jun, C. (2016). Development of uncut crop edge detection system based on laser rangefinder for combine harvesters. *International Journal of Agricultural and Biological Engineering*, *9*(2), 21–28.

Vanholder, H. (2016). Efficient inference with tensorrt. In *GPU technology conference* (Vol. 1, p. 2).

Yang, L., & Noguchi, N. (2012). Human detection for a robot tractor using omni-directional stereo vision. *Computers and Electronics in Agriculture*, *89*, 116–125.

Zahniser, S., Taylor, J. E., Hertz, T., & Charlton, D. (2018). *Farm labor markets in the United States and Mexico pose challenges for U.S. agriculture*. https://www.ers.usda.gov/webdocs/publications/90832/eib201_summary.pdf?v=334. Accessed July 27, 2021

Zhang, Z., Cao, R., Peng, C., Liu, R., Sun, Y., Zhang, M., & Li, H. (2020). Cut-edge detection method for rice harvesting based on machine vision. *Agronomy*, *10*(4), 590. https://doi.org/10.3390/agronomy10040590

Zhao, H., Qi, X., Shen, X., Shi, J., & Jia, J. (2018). *ICNet for real-time semantic segmentation on high-resolution images*. https://arXiv.org, arXiv:1704.08545v2.

Zhu, J., Iida, M., Li, Y., Chen, S., Cheng, S., Suguri, M., & Masuda, R. (2022). Real-time object detection in rice field images by semantic segmentation for robotic combine harvester-pixel-wise level detection of rice lodging existence. *Journal of the Japanese Society of Agricultural Machinery and Food Engineers*, *84*(3), 145–154.

Zhu, J., Iida, M., Suguri, M., Masuda, R., Chen, S., & Cheng, S. (2022). Real-time field recognition based on semantic segmentation for robotic combine. In *The XX CIGR world congress 2022 (CIGR)* (pp. 96).

11 IoT Middleware Solutions for Arable Crops and Livestock Farming

Eleni Symeonaki, Konstantinos G. Arvanitis, Chrysanthos Maraveas, Dimitrios Loukatos, and Spyros Fountas

11.1 INTRODUCTION

Agricultural production systems, as illustrated in Figure 11.1, differ from other production systems since they require a significant share of natural capital (air, soil, water resources, biodiversity) as inputs to production (Zepeda & FAO, 2001). Moreover, they are characterized by uncontrollable inputs, such as meteorological and climatic conditions, which equally affect their performance.

Based on this evidence, the potential yield of any agricultural production system is a function of its physical and capital and the uncontrolled inputs to it. For a given ideal combination of the above parameters, there is a maximum potential yield based on the optimal uncontrolled inputs (e.g., weather conditions). In real-world conditions, however, performance is a function of:

- the maximum potential return (physical capital),
- uncertainty factors, such as weather and climate conditions,

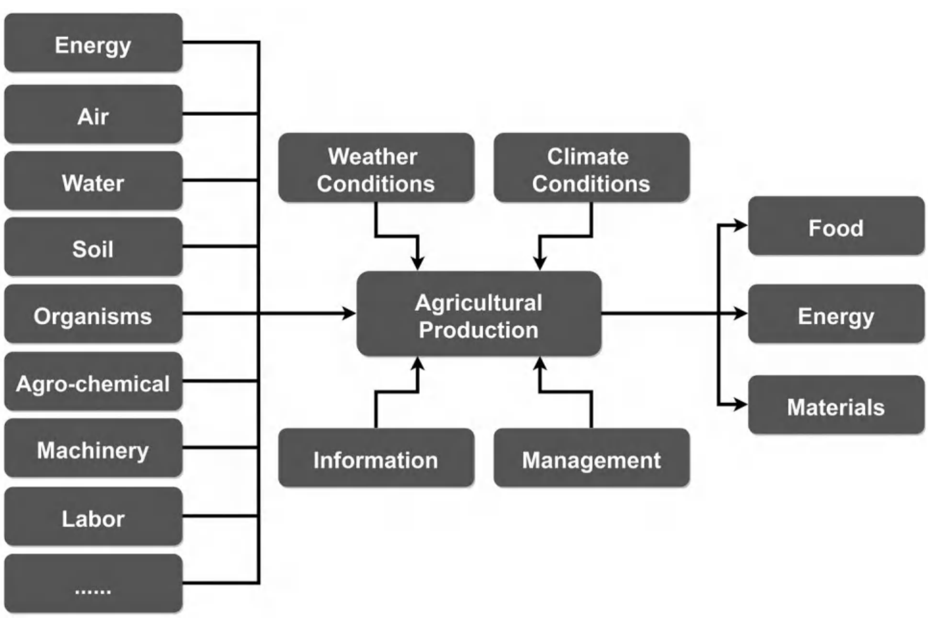

FIGURE 11.1 Inputs and outputs of the agricultural production system.

DOI: 10.1201/9781003510598-11

- the materialized physical capital (labor and machinery), and
- the use of this capital (management),

resulting in the fact that the actual yield of an agricultural production system is consistently reduced compared to the maximum potential yield. As derived, the scope of operation of agricultural production systems is highly variable, and therefore they have to act and react dynamically not only to uncontrolled inputs but also to the different characteristics of their physical capital, such as the operating environment (i.e., agricultural facilities and livestock farms), variations in the physiology of the objects (i.e., crops and types of farm animals), and changing conditions depending on time (seasons or hours of the day).

The automation of agricultural production systems (Puranik et al., 2019) both improves the execution of tasks and enhances the decision-making process (through automated monitoring, data analysis and computational intelligence), contributing therefore to a better use of natural capital. The various automated functions in autonomous harvesters, for example, can help to complete the work faster and more cost-effectively and thus indirectly improve production by reducing harvesting losses and completion time, both quantitatively and qualitatively. Also, in the case of fruit or vegetable harvesting, the quality of the product is increased due to selective harvesting. Both of the above-mentioned improvements (efficiency and effectiveness) inherent in automated agricultural production reduce the gap between the actual and the maximum potential yield of the system (with the same physical capital and external conditions).

According to the guidelines for the operational implementation of Industry 4.0 and correspondingly of Agriculture 4.0 (Liu, Ma, et al., 2021), a production system is considered dynamic when its capabilities can be grouped into four intelligent interconnected stages, including monitoring, control, optimization, and autonomy, following in this way an integrated agricultural management approach (Porter & Heppelmann, 2014). To this end, each stage is structured based on the previous one, as illustrated in Figure 11.2 and discussed below:

- *Monitoring*: Sensors and external data sources allow for comprehensive monitoring of both the status, operation, and use of the system and the external environment. Monitoring also allows for warnings and alerts of any changes.
- *Control*: The software built into the system allows you to control the functions and personalize the end-user experience.
- *Optimization*: Monitoring and control capabilities enable algorithms that optimize the operation and use of the system to improve its performance and allow for proactive diagnosis, maintenance, and repair.
- *Autonomy*: Through a combination of monitoring, control, and optimization, autonomous system operation, improvement and customization, self-coordination of operation with other products and systems, and finally, self-diagnosis and service provision are possible.

FIGURE 11.2 Stages of integrated farm management.

Considering that by 2050, it is imperative that the agricultural sector increase its production by 70% to meet global food needs, while agricultural production systems must be carbon neutral and resilient to climate change-induced extreme weather conditions while remaining profitable (Fraser & Campbell, 2019), a new strategic framework is needed.

This challenge can be addressed through the transition from Agriculture 4.0 to Agriculture 5.0 (Ragazou et al., 2022), which indicates the trend that the agricultural sector will follow in the coming years in the context of the new industrial revolution, in the sense of Industry 5.0, as officially assigned by the European Union in 2021 (Publications Office of the European Union, 2021). The Agriculture 5.0 approach focuses on integrating emerging technologies into agricultural production systems, such as the Internet of Things (IoT), artificial intelligence (AI), machine learning (ML), and the use of big data, to enhance their efficiency through production automation while making them environmentally sustainable (Fraser & Campbell, 2019).

Through the integration of the IoT technologies, it is possible to automatically collect data from various sources (e.g., sensors on agricultural machinery, cameras, and sensors on the ground or in livestock farms) and transfer them to cloud computing, where, with the use of ML algorithms, they can be analyzed and exploited to optimize efficiency and effectiveness through customized solutions, while achieving improved product quality and reduced resource consumption as well as production costs. Cloud computing also enables on-demand services, such as automatic production verification, data analysis to enhance agricultural management, and providing data to search for alternatives in case of problems.

Overall, the development of agricultural production systems that incorporate IoT technologies is essential for the sustainability of the agricultural industry in the future (Puranik et al., 2019). The combined use of these new technologies can lead to smarter, more sustainable, and more efficient agriculture, enhancing the quality production of agri-food products while ensuring both food sufficiency and sustainability of production systems through reduced resource consumption.

Taking into account the requirements mentioned above, it is considered that the proposal of an integrated cloud-based context-aware middleware solution, as part of a flexible system integrated with the IoT, could be beneficial for the automation of agricultural production systems, in particular with a view to intensifying sustainability in the context of Agriculture 5.0.

11.2 STRUCTURE OF THE IoT SYSTEM

The flexibility of agricultural production systems incorporating the IoT technologies refers, among others, to their ability of using cloud computing to automate their operations.

The typical structure of an agricultural production system integrated into the IoT, as illustrated in Figure 11.3, includes a farm facility at the physical level and three components in the cyberspace that exploit the properties of cloud computing:

- the context-aware middleware cloud,
- the services cloud, and
- the social network cloud.

According to this structure, all individual functional components communicate remotely with the context-aware distributed middleware that benefits from the properties of cloud computing and constitutes the core of the system. Hence, this structure can be applied to more than one agricultural facility with different exploitations.

In particular, the parameters collected from the sensing devices of a wireless sensor and actuator network (WSAN) deployed in an agricultural facility are transmitted through wireless gateways as raw data to the middleware cloud, where they are processed to be transformed into context, managed accordingly, and stored. This context data, as well as the incoming rules from the service cloud, are converted into context information while using data fusion (Gong et al., 2022) and ML (Bhanu et al.,

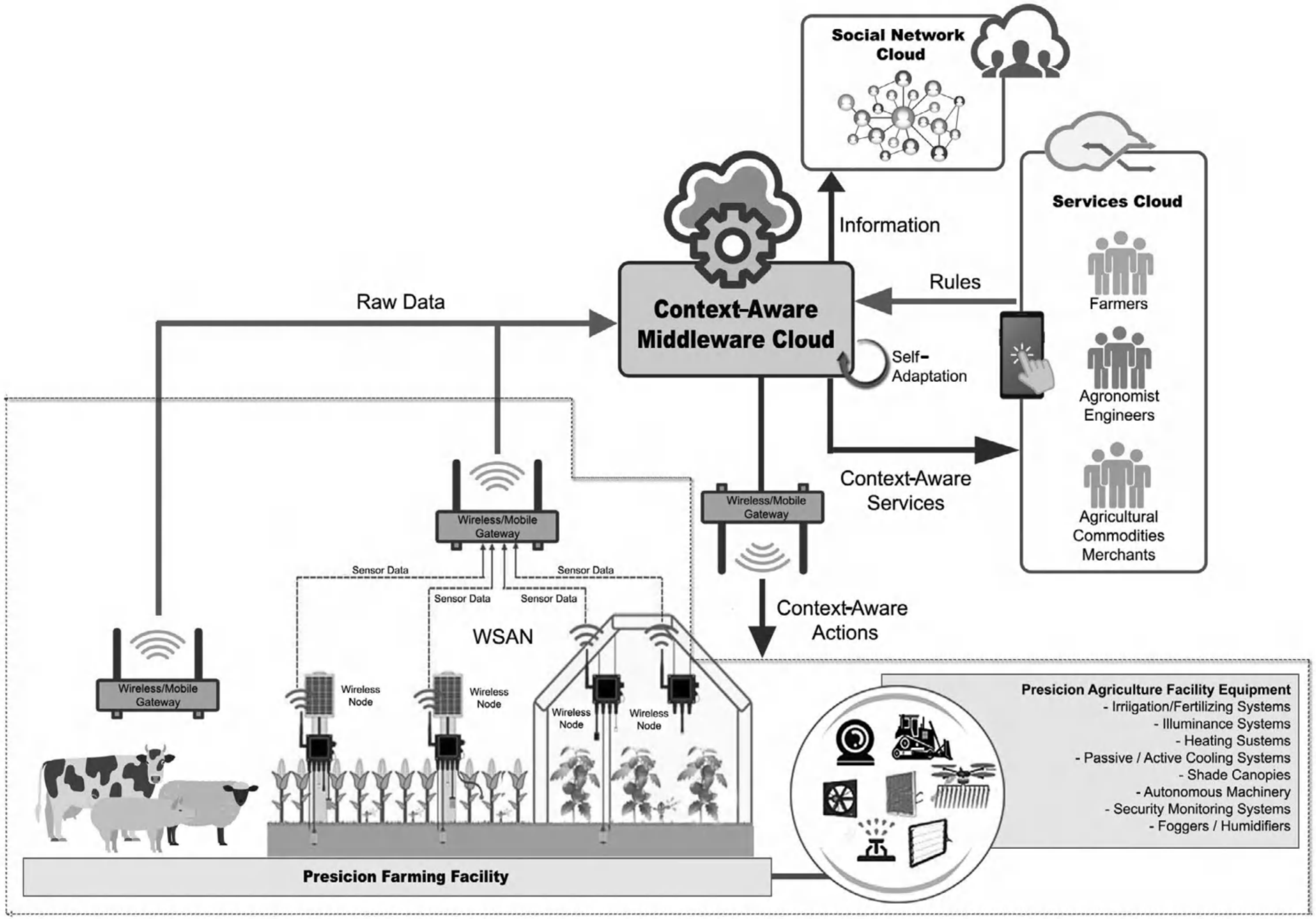

FIGURE 11.3 IoT-integrated agricultural production system.

2020) techniques to achieve higher reliability and lower probability of errors. The middleware then responds with control actions on the actuators of the agricultural facility equipment (e.g., irrigation valves, fertilization sprayers, lighting and heating/cooling systems, autonomous machines, and humidifiers) to carry out the required agricultural operations (e.g., sowing, harvesting, irrigation, and fertilization) and to the end-users (farmers, livestock farmers, agricultural engineers, and agricultural products traders), providing them with information and monitoring services. End-users can also intervene at any time in the system's operations with corrective or supportive actions.

It should be noted that all cloud services (infrastructure as a service (IaaS), platform as a service (PaaS), and software as a service (SaaS)) (Mohammed & Zeebaree, 2021) should preferably be offered through a public or hybrid cloud (Linthicum, 2016) for use by all stakeholders. Due to the fact that a large percentage of agricultural facilities are small to medium scale, hosting the proposed system in a public cloud is considered the most appropriate option, as it will use the hardware infrastructure and computing power of the cloud service provider.

11.3 SYSTEM ARCHITECTURE

As mentioned above, IoT technologies can effectively contribute to achieving integrated agricultural management, ensuring maximum production of optimal quality and increased profitability, in line with sustainable development policies. After reviewing the many different architectures that have been proposed in the literature for the IoT (Burhan et al., 2018; Kassab & Darabkh, 2020; Samizadeh Nikoui et al., 2021; Sethi & Sarangi, 2017), this research chooses to adopt a version of a layered architecture, as depicted in Figure 11.4.

This version of the architecture is an approach based on the distinction of the system into three main layers, the perception layer, the middleware layer (platform layer), and the application layer, each of which represents different functions and capabilities. In particular, the perception layer consists of the physical objects included in an agricultural facility, while the middleware layer provides the ability to store, process, and analyze the data collected in the environment of the agricultural facility and to manage the interaction with it. Finally, at the application layer, the data is exploited to achieve optimal management of agricultural production.

In terms of connectivity, the computing power and management capacity of an intelligent agricultural production system depend on the network communication protocol, making it an extremely important factor for its integration into the IoT. Therefore, it is of paramount importance to ensure that the network communication protocol chosen in this architecture will have the capability to support the transmission of all the heterogeneous data collected at the perception layer in order to ensure the reliable operation of the system.

11.3.1 Perception Level

The lower layer of the proposed architecture represents the perception layer that includes the physical objects of the agricultural installation (Kim et al., 2020; Navarro et al., 2020), such as sensors, actuators, devices, and equipment. The main task of the perception layer is to identify and control the properties of the agricultural facility through the physical objects contained in it.

To this end, a WSAN, consisting of a group of self-powered nodes, is deployed in the agricultural facility. These nodes incorporate sensors that collect data on various parameters related to the agricultural facility in real time and actuators that interact with equipment and devices, enabling the corresponding physical actions. The sensor and actuator nodes are usually equipped with certain data processing and wireless communication capabilities, as well as a power supply. The nodes of the WSAN should be deployed in an appropriate topology (Singh et al., 2018) such that they have sufficient communication range with an appropriate data rate and sufficient power consumption to cover a wide area (Ojha et al., 2015). During operation, new nodes may be added, the state of a node may be switched from a standby to an operational state by the power management mechanism, and

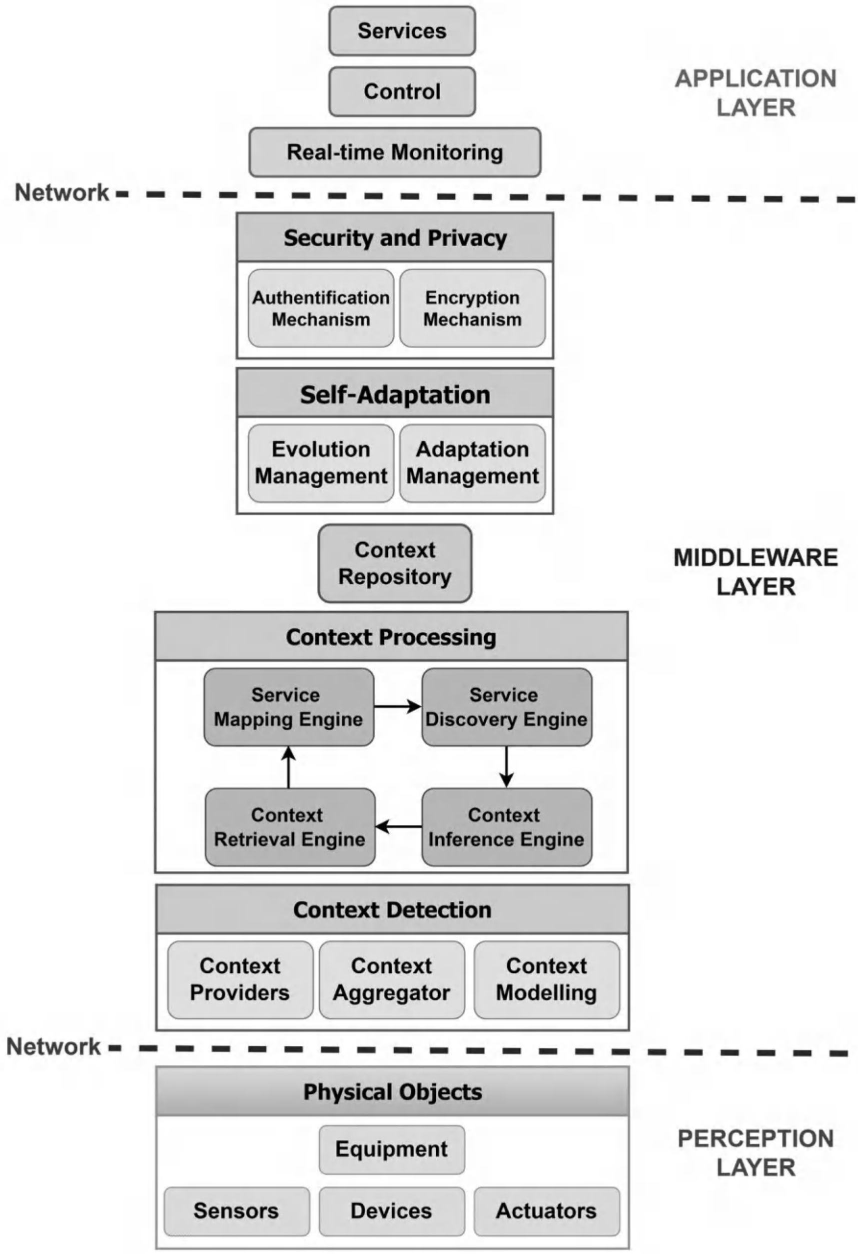

FIGURE 11.4 Architecture of an IoT-integrated agricultural production system.

some nodes may even become inoperative due to battery power depletion. All these factors can cause dynamic changes in the topology of the network; thus, it needs to be adaptive and flexible with respect to changes in available nodes. For example, when an intermediate node is taken out of service, the network should still be able to guarantee reliable real-time communication by exploiting appropriate protocols and algorithms.

Regarding the hardware architecture of wireless sensors, various solutions are reported in literature (Li et al., 2011; Ojha et al., 2015; Piromalis & Arvanitis, 2016), specifically designed for the requirements of operation in rural areas, as they must be robust to the harsh conditions of the rural environment and serve the requirements of the applications that will use the collected data. Since each agricultural facility may include different needs and challenges regarding data collection and processing, the appropriate hardware architecture solution depends on many factors, such as topography and weather conditions, as well as the physiology of both soil, plants, and animals. Therefore, the selection of the appropriate hardware architecture solution is critical for successful data collection and processing in agriculture to develop smart agricultural production systems.

The integration of sensors into the wireless network must, as can be seen from the relevant literature, meet certain functional requirements for applications in both arable (Li et al., 2011; Ojha et al., 2015; van Evert et al., 2017) and livestock farming (Gameil & Gaber, 2020; Hussain et al., 2020; Popović et al., 2017; Vidic et al., 2017), as indicated:

- monitoring of meteorological data;
- monitoring and control of environmental parameters such as temperature, humidity, pressure, gas emissions, and lighting;
- monitoring and control of parameters related to (a) the physiology of the crop and soil, such as temperature (e.g., leaves, root zone, nutrient solution), humidity, oxygen (O_2), carbon dioxide (CO_2), acidity (pH level), nutrient concentration (PPM, EC), etc.; (b) the physiology and behavior of the animals, such as temperature, heart rate, kinesiology, and position;
- prediction and control of imminent diseases and pests;
- surveillance and security control of agri-food establishments.

In order to meet this extensive variety of functional requirements, it is necessary to include a large number of heterogeneous sensors in the wireless network, which can be classified into three general categories based on their properties (Fraden, 2010): (a) physical, (b) mechanical, and (c) chemical, while further breakdown can be obtained depending on the type of measurement they perform. More specifically, physical sensors detect properties, such as temperature, humidity, brightness, and radiation, and help in evaluating the performance of agricultural production. Mechanical sensors can detect motion, weight, pressure, and other mechanical properties and can also measure the presence or absence of objects in the field and allow for automatic data collection. Finally, chemical sensors detect chemical elements and components and can also detect the presence of harmful substances, such as harmful insects and fungi, and alert to the need to prevent and address these problems.

Regardless of the specifications or requirements that exist at the perception layer, a unique framework must be created to represent the context depending on the types of physical objects and services available to be performed during the full implementation of the system. To this end, each physical object shall have a unique identifier in the system so that it can be distinguished in the overall cloud architecture.

11.3.2 Middleware Layer

The middleware layer, i.e., the platform layer, acts as an interface between the perception and the application layers, providing collective functions and services, including, among others, device and data management, access control, and service discovery. In particular, depending on the requirements of the system, the middleware is responsible for generating the information required to implement and simultaneously process various monitoring and control functions (Cope et al., 2017) for the automation needs of the agricultural production system through the integration into the IoT.

The middleware layer of the proposed system refers to the context-aware middleware cloud, which acts as a decision support system (DSS) for the entire model, providing the required context-aware services and actions for its operation. Adopting the IaaS properties of cloud computing consists of a number of tiers for acquiring, processing, managing, and storing context data. Great importance is also given to the aspects of self-adaptation as well as security and privacy. A thorough description of the design and development of the IoT middleware is provided in a following section of this chapter.

11.3.3 Application Layer

The top layer of the proposed architecture represents the application layer that consists of three cloud tiers that perform (a) real-time monitoring, (b) facilities control, and (c) services. This layer adopts the properties of SaaS and is responsible for providing all the important applications for end-user interaction with the integrated agricultural production system. By registering and authenticating on the cloud platform, end-users can not only receive context services but also provide rules for control actions using simple query mechanisms. All rules stored in the context repository of the middleware cloud can be retrieved using appropriate provisioning techniques (Aslam et al., 2012). Once a service rule is retrieved, it can be easily described by control actions based on the ontology of the proposed context model, which is described in detail later in the chapter. In this sense, the application layer is enhanced with logic that contributes significantly to the self-adaptation of the middleware, since it can at any time retrieve high-level context information and make corresponding decisions for equivalent actions. Indicative examples of such services include automated services, symptom detection services, emergency services, advisory services, and software services.

Considering that the services implemented are numerous, as they may address different stakeholders and vary between different agricultural production systems, it is almost impossible to deploy them in a central computing unit. By integrating all services into cloud computing, the issue of resources can be resolved, and by describing them with a single model, the task of mapping services can be simplified.

Although all actions are performed based on the events generated by the context-aware middleware cloud, there are some cases in which manual management is required. Therefore, a variety of web interfaces are provided to manage the middleware cloud in order to store and retrieve context. Complementary interfaces for data visualization analyze the context and present it in the form of a visual representation, which can be posted on a social network of agricultural actors in order to provide real-time monitoring of agricultural production systems. It is believed that such monitoring services can be easily adopted by the proposed model.

11.3.4 Wireless Communication Technologies and Protocols

The design of systems for the IoT is affected by the type of wireless communication network technologies chosen. In order to find the optimal connectivity solutions, it is necessary to understand the requirements of each application.

Currently, a wide variety of wireless communication technologies and protocols with distinct advantages are used for IoT applications to meet requirements in specific areas (Atmaja et al., 2021). Bluetooth, Wi-Fi, ZigBee, and cellular networks (3G/4G/5G) are among the most commonly used options for wireless communication. Wi-Fi and ZigBee, in particular, are ideal solutions for applications where the communication distance does not exceed 100 m, while cellular networks allow a long communication distance but are energy-intensive and costly.

The new generation of low-power wide-area networks (LPWANs) offers long-range (up to 40 km) wireless connectivity and transmission with low power consumption (Mekki et al., 2019) and reduced data rate (Chaudhari et al., 2020). As derived from the comparison of their characteristics, LPWAN technologies are the most suitable for the requirements of the agricultural industry sector (Liya & Arjun, 2020). The most popular LPWAN technologies are Sigfox, LoRa, and NB-IoT. Sigfox technology provides sufficient coverage in urban areas, while LoRa technology makes it possible to perform trade-offs between the volume of data to be transmitted, range, and energy autonomy. Finally, NB-IoT technology is based on cellular networks. This technology offers superior quality of service (QoS) with better penetration inside buildings or underground compared to 2G/3G/4G coverage. As can be seen from the literature, there are several comparative studies (Ayoub et al., 2019; Jawad et al., 2017) on LPWAN technologies in terms of their technical characteristics and properties, such as QoS, coverage, range, latency, energy autonomy, scalability, payload length, deployment, and cost, with respect to the requirements for the IoT (Mekki et al., 2019).

Among the LPWAN technologies, the LoRa technology is the most suitable for the deployment of agricultural applications for the IoT in rural areas, as it offers comparatively the optimal combination of technical features, is secure and easy to maintain, and at the same time has a lower cost (Loukatos et al., 2022). In particular, LoRaWAN, which is an open-source communication protocol that adopts LoRa LPWAN technology, can meet the different requirements of a wide range of IoT applications to create customized solutions for the needs of Agriculture 5.0 (Miles et al., 2020), making it more suitable as a communication option in the proposed architecture, as it can enhance access to more accurate and complete data, resulting in improved performance of agricultural production systems.

11.4 DESIGN OF THE IoT MIDDLEWARE

The functions required by the proposed IoT middleware are mainly determined by the need to process and manage the massive and heterogeneous amounts of data generated in the complex environments of agricultural production systems in order to achieve the efficient interconnection of the smart devices involved in them. Context awareness, which refers to the ability of a system to be continuously aware of its current state in both the physical and virtual environments, has been shown to be an essential advantage of IoT (Dhumane et al., 2018; Pradeep et al., 2021), enabling the collection and extraction of meaningful information from raw data to support decision-making aimed at automation. Furthermore, by properly integrating a semantic ontology model (Huertas Celdran et al., 2016) into the context-aware middleware, it is expected that the efficiency, flexibility, and scalability of the whole system will be ensured. Finally, the proposed IoT middleware aims to enhance the robustness of the system by integrating the IaaS properties of cloud computing to commit the required computing power and storage capacity. Considering that context awareness is integrated into the IoT system to provide intelligent services, the middleware is required to contain corresponding context management functions that correspond to its lifecycle (Zhang et al., 2021). Following, the IoT middleware tiers are described with a particular focus on that of modeling structure.

11.4.1 Context Detection

The tier of the context detection involves the identification and extraction of relevant context information from various context providers, followed by the aggregation and modeling of this information to create a unified and consistent view of the context for providing a comprehensive understanding of the current agricultural environment. This phase is crucial in the IoT middleware, as it forms the foundation for subsequent context processing and adaptation.

11.4.1.1 Context Providers

Context providers are the sources of context data, such as sensors, external services, user input, and system events. The context aggregator is responsible for collecting and integrating the data from these providers to form a cohesive context representation. Context providers are responsible for collecting and supplying context data to the middleware. These providers include the following:

- *Sensors*: Sensor networks play a crucial role in collecting real-time data about various factors related to agricultural production systems, such as soil moisture, temperature, humidity, light intensity, and air quality, as well as animal physiology and behavior. Sensors deployed throughout agricultural facilities provide continuous measurements, generating data that is relevant to the farming context and making it available to the middleware for further processing.

- *IoT devices*: IoT devices, such as weather stations, automated irrigation systems, or smart farm equipment, act as context providers by collecting and transmitting data related to specific agricultural operations. These devices can provide information on weather conditions, water usage, plant growth parameters, or machine performance.
- *Satellite imagery*: Satellite imagery is increasingly utilized in agricultural production systems to monitor crop health, assess vegetation indices, detect anomalies, or identify pest infestations. Satellite imagery providers offer context data in the form of high-resolution images or derived vegetation indices, which can be used to infer the farming context.
- *External data sources*: The IoT middleware may integrate with external data sources, such as weather APIs (application programming interface), agricultural databases, or market data providers. These sources provide additional context information, such as weather forecasts, historical agricultural data, or market prices, which can impact farming decisions and practices.
- *User inputs*: User input providers capture explicit context information provided by users. This can include preferences, settings, profiles, or explicit rules given through various input modalities, such as text input or voice commands.
- *System events*: System event providers notify the middleware about relevant events occurring within the agricultural production system or the applications running on specific devices. Examples include programmed events, incoming notifications, device state changes, or user interactions.

The context providers are responsible for collecting and delivering the context data to the context aggregator in a standardized format or through specific interfaces, ensuring compatibility and interoperability.

11.4.1.2 Context Aggregator

The context aggregator is a key component of the middleware that receives the context data from various providers, performing the following tasks:

- *Data collection*: The aggregator collects the context data from various providers, often through standardized interfaces or APIs. It receives the data in its raw form, which can vary in format and structure.
- *Context fusion*: It involves combining and reconciling data from multiple various sources to create a consistent view of the context. The aggregator resolves conflicts, handles uncertainties, and applies fusion algorithms to aggregate and integrate the data. For example, if different sensors provide conflicting information, the aggregator may employ fusion techniques to determine the most accurate one.
- *Context enrichment*: The aggregator can enrich the acquired context by integrating and correlating data from various providers. This may involve accessing external data sources or performing contextual inference to derive implicit context from the available data. For example, it can combine soil moisture measurements from sensors with weather data from external sources to estimate irrigation needs. By incorporating additional information, the aggregator enhances the completeness and accuracy of the farming context.
- *Context update*: The aggregator continuously updates context as new data becomes available by the relevant components, applications, or services within the system, enabling them to adapt their behavior based on the current context. This ensures that the agricultural operations can dynamically adapt to changes in the context and make informed decisions.

11.4.1.3 Context Modeling

Context modeling is a crucial process in order for the context-aware middleware to meet the end-use needs of the system. As a product of the modeling process, a context model is defined by a set of entities that have defined attributes with specific characteristics, providing a detailed representation of the physical world in which users and devices interact (Alegre et al., 2016). The context model used by a given context-aware application is usually explicitly specified at system design time but may evolve over time (Perera et al., 2014). Therefore, a context model provides a systematic way of specifying and representing knowledge about entities and their interrelationships, which is essential in the development of an architecture and, by extension, in the design of context-aware systems.

Over the last few years, a significant number of context-aware systems based on different context models have been developed for a wide range of applications. This experience has influenced the set of requirements defined for context modeling in order to be able to support reasoning about the context to have sufficient computational efficiency. As can be seen from the literature (Bettini et al., 2010; Perera et al., 2014), the requirements that have been established for context modeling, independent of the application domain of each system, are identified as follows:

- *Heterogeneity and portability:* Context models need to address a wide variety of heterogeneous context data sources that vary in their update rate and semantic level. Especially in the case of agricultural production systems, while sensory devices collect raw data in near real-time that needs to be interpreted before it can be used by applications (dynamic data), user-provided information, such as user profiles, is updated less frequently and generally does not need additional interpretation (static data). Contextual data can also be derived from existing information such as that contained in databases or digital libraries (such as geographic map data). In addition, many applications may be portable, i.e., run on mobile devices or depend on portable sources of context information such as handheld sensors, exacerbating the problem of heterogeneity, as the context model must be able to adapt to this changing environment. Finally, the location and spatial layout of the data play an equally important role in the context modeling. A context model should be able to express all these different types of context data.
- *Correlations and dependencies:* Among the types of context data, there are several correlations that must be recorded to ensure the proper functioning of applications. One such association is dependency, whereby entities in the context model may depend on other entities. For example, a change in the value of one property, such as network bandwidth, may affect the values of one or more other properties, such as the remaining battery power of a wireless node.
- *Awareness:* In the operation of a context-aware system, access to past and future states (forecasting) may be required. Therefore, the awareness of the context history is an attribute that needs to be captured by context models. Managing the context history is difficult if the number of updates is too large, as it may not be possible to store every value for future access. Hence, aggregation techniques should be applied, such as, for example, aggregating the position updates into one function using interpolation techniques.
- *Accuracy:* Due to their dynamic and heterogeneous nature, contextual data can be of varying quality or even incorrect. For example, most sensors have an inherent inaccuracy, and the values collected may further vary as the environment changes, with the result that this inaccuracy increases over time. In addition, context data may be incomplete or in conflict with other context data. Therefore, a good context modeling approach should include modeling the quality of context data to support reasoning about context.
- *Reasoning:* Context-aware systems use data to assess whether there is a change in the context of the user or the computing environment. Making decisions about whether any adaptation to that change is necessary often requires reasoning skills. Therefore, it is important

that context modeling techniques are able to support both model consistency verification and context reasoning techniques. The latter can be used to extract new events from existing ones and/or to draw conclusions about high-level context abstractions that model states of the physical world. The reasoning techniques should be computationally efficient.

- *Usability of modeling schemes:* Context models are created during the design of context-aware systems and are used to manipulate context data. Therefore, one of the important features of modeling schemes is the ease with which physical world concepts can be translated into context models at the design stage and the ease with which applications can, at runtime, use and manipulate context data.
- *Effective context dissemination:* Efficient access to context data can be difficult to achieve in the case of large models and numerous data objects. For the selection of relevant objects, the properties of appropriate access paths must be represented in the context modeling. Access paths, usually supported by pointers, represent dimensions along which applications select context data. These dimensions are often referred to as the primary context, as opposed to the secondary context, which is accessed using the primary context. Common attributes of the primary context are object identity, location, object type, time, etc. Since the choice of primary context properties depends on the particular system and its application domain, a specific set of primary context attributes is used to create competent access paths (e.g., location indexes if the primary context is the location).

Based on the experience gained from the various approaches to context modeling, ranging from very simple early models (Augusto et al., 2018; Koç et al., 2014) to the most recent context models (Chen et al., 2022; Guermah et al., 2021), the context modeling process can generally be divided into two stages:

- *1st stage – development of the context model:* In this stage, the new information about the context is identified in terms of its properties and attributes, its relationships with the already defined context, the quality of its properties, and the queries for synchronized context requests.
- *2nd stage – organization of the context based on the model:* In this stage, the result obtained from the development of the context model needs to be validated. The new context data is then consolidated and included in the existing context repository, which is embedded in the system, from where it becomes available for use when required.

These key stages of context modeling include, as shown in the flowchart in Figure 11.5, defining the scope and purpose of the model, collecting, and analyzing the verbal concepts of the scope, defining the key concepts and relationships to be included in the model, designing and developing the model, evaluating and verifying it, and finally its ongoing evolution. The factors and parameters taken into account for the development of the context model are subjective, as they vary between different solutions, and currently, there is no standard that specifies the type of information that should be taken into account.

Several techniques have been developed for context modeling (Knappmeyer et al., 2013; Maran et al., 2018; Strang & Linnhoff-Popien, 2004), which all have respective advantages and disadvantages. In order to select the most suitable technique for representing the context according to the requirements of the specific middleware system, a comparison of the most popular existing modeling techniques was made, such as key value, markup, graphical, object-oriented, logic-based, and finally ontology-based. Among the modeling techniques reviewed, the ontology-based approach is the most effective, focusing on the broader design of a model that can support context-aware service synthesis for the automation of agricultural production systems with integration into the IoT. In light of this technique, the context is organized into ontologies using semantic technologies, which provide an expressive language for representing relationships and context for modeling purposes.

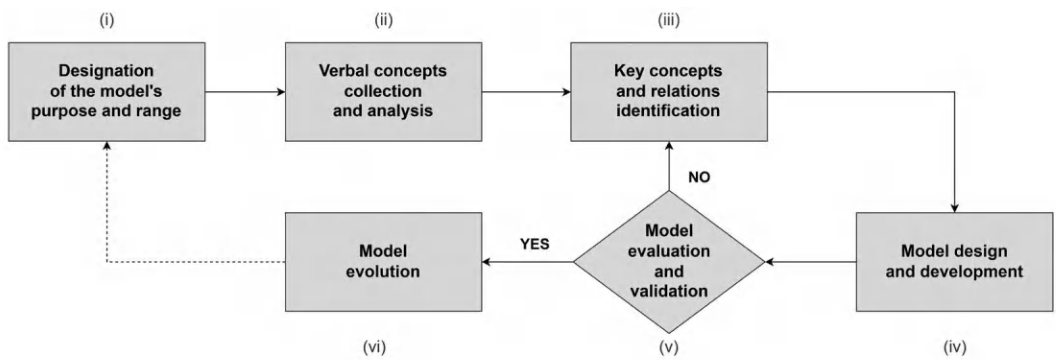

FIGURE 11.5 Flowchart of the context-modeling stages.

There are several reasons for developing and using ontologies as opposed to other modeling techniques. The most common of these are (Rao et al., 2022) the sharing of information structure between users or software agents in a mutually understandable way, the analysis of domain knowledge, the separation of domain knowledge from functional knowledge, the possibility of reusing knowledge, the extraction of high-level knowledge inferences, and the explicit formulation of domain assumptions. Some of the requirements and objectives for the design of an ontology are scope, simplicity, flexibility and scalability, universality and expressiveness, practical accessibility, efficiency, and ease of inference (Hameed et al., 2022; Lee et al., 2007). Due to their dynamic nature, middleware solutions for the IoT should support applications that may not even be known at the time of their design and development. The use of ontologies allows knowledge to be integrated into different application domains when necessary. In addition to providing a distinct way of modeling the representation of complex context data, ontologies are suitable for knowledge sharing, as they provide a formal specification of the semantics of context data. It must be noted that this feature is particularly important in mobile and distributed environments, in which different heterogeneous and distributed entities need to interact to exchange information.

Considering that the modeling structure should represent, in the best possible way, the conceptual association of data with a situation in the light of their collection conditions and their variability, the present research applies the ontology-based context representation technique, in combination with the *5Ws and H* approach (Zhang & Huang, 2013) to define the concepts in different datasets, as well as a functional scheme for ontology synthesis (Lupiana, 2017), adapted to the needs of the field of agriculture and in particular the field of automation of agricultural production systems. Specifically, the *5Ws and H* (What, Who, Where, When, Why, and How) approach is chosen to define the entities (Zhang & Huang, 2013), according to which each concept representing an element of the context can be classified into 5Ws and one H data dimensions.

Reducing this approach to the needs of the scope under consideration, the context includes one or more sensing devices *(What)* located at a particular place *(Where)* and performing context data collection events *(How)* at a given time *(When)*. Observation of changes in the context data parameters (e.g., change in temperature and/or humidity parameters) may signal events according to specific registered rules *(Why)*, activating the appropriate equipment *(What)*. In addition, events may be triggered by one or more users *(Who)*. Based on this, it can be assumed at the initial stage that the context represents some concept describing an event that occurs at a defined location and time, involving an object (thing), which may be a device, equipment, user, or object of interest. The event is observed or triggered by one or more rules. Each of these concepts has specific characteristics describing their basic properties and is associated with one or more of the other concepts. In this case, the context is described by five main entities that have generalized properties and make up five main classes for *thing*, *location*, *time*, *event*, and *rule*.

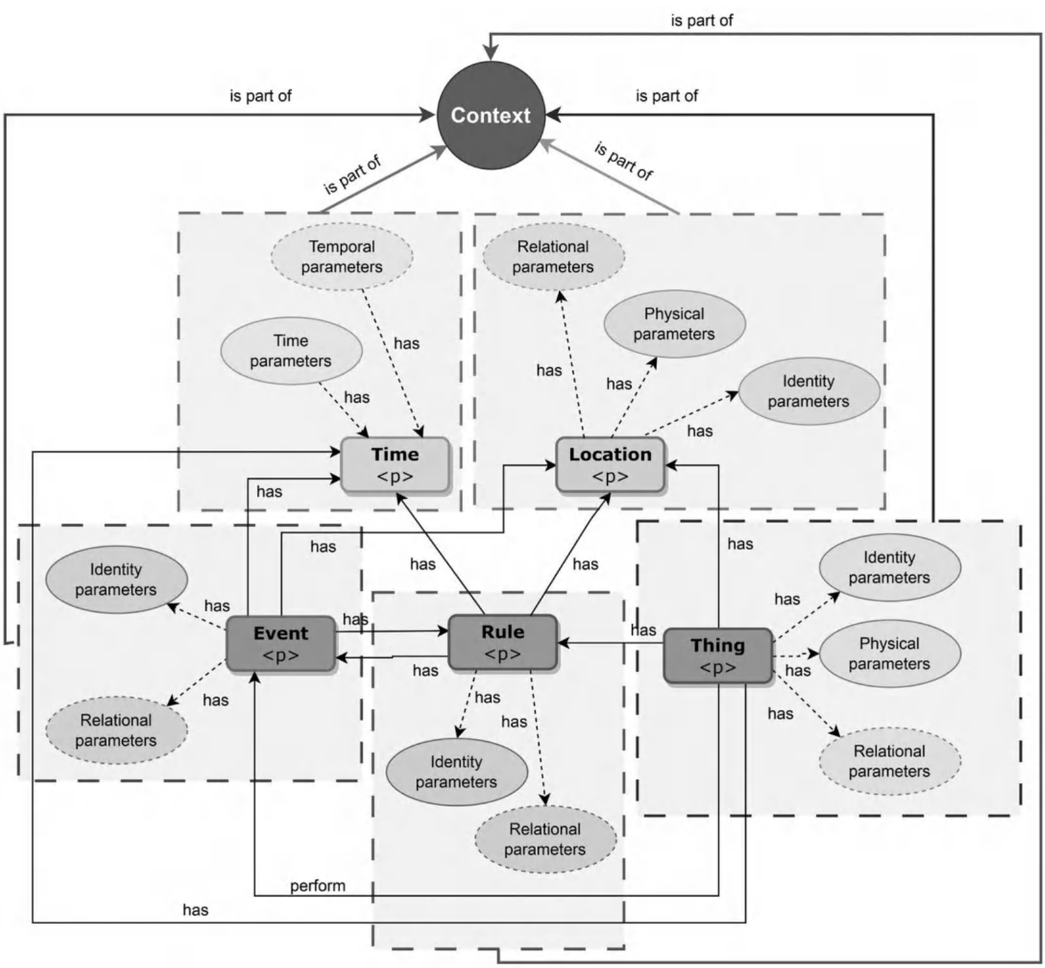

FIGURE 11.6 Basic conceptual representation of the context.

Figure 11.6 provides a conceptual representation of the context as described above, where the main entities are represented by rectangular shapes, the generalized properties by oval shapes, and the classes by dotted outlines of different colors. In order to make the differentiation of properties involving primary and secondary parameters apparent, solid and dotted oval shapes are used, respectively. With regard to the links, these are represented by arcs, of which those relating to relationships between entities or classes have solid lines and those relating to associations between properties and entities have dotted lines. No classification of entities is defined in the model so far, and therefore only assertive links are used. Finally, a context model is intended to cover any uncertainties and therefore each entity is assigned a level of certainty, represented by the <p> symbol. The certainty level is defined as a value indicating the degree of reliability of the data collected by the WSAN. This value may be obtained from training data, application domain experts or manufacturers' specifications, and user actions are also taken into account. Further developing the basic conceptual representation shown in Figure 11.6, the five main classes for objects, place, time, events, and rules are then individually defined, and finally the ontology for the whole prototype model of the context is structured.

The overall structure of the ontology of the context model has been derived by synthesizing the five classes (*thing*), (*location*), (*time*), (*event*), and (*rule*), which include both the entities and properties (static and dynamic) that define their internal characteristics, as well as their corresponding associations. For ease of understanding the model, each class and its elements are represented in a different color in the representation of the overall ontology of the model context model, as shown in Figure 11.7.

This ontology is a generic conceptual model, which has been developed taking into account the needs of agri-farm operations and supports a flexible and semantically expressive representation of the context that can be used for various application scenarios. According to the proposed ontology structure, the number and range of individual entities, and especially their properties, depend on the application domain as well as on the level of automation required in each case. In this way it becomes possible at any time to add new context elements and to define new behavioral patterns for them, resulting in a flexible and adaptable solution. Additional flexibility is considered to be provided by the possibility to use object references as context values instead of simple base values. The proposed ontology structure is believed to contribute to the understanding and representation of the context for automation of agricultural production systems, providing a simple and understandable basis for creating a common model for different applications.

11.4.2 Context Processing

Context processing, involving service mapping, service discovery, context retrieval, and context inference, plays a crucial role in enabling intelligent decision-making and automation in agricultural production systems. In more detail:

- *Context retrieval engine* is responsible for initiating regular requests to retrieve context information and distributing it to the relevant components within the IoT system. Additionally, all system components can easily initiate context requests by utilizing a web service hosted on a cloud server, providing an ID and specifying the desired context attribute. To elaborate further, system components requiring specific context information can subscribe to the IoT middleware cloud, receiving notifications whenever updates relevant to their interests occur. They can also make active queries for critical context information whenever needed. The retrieval engine filters out further duplicate and inappropriate context data, ensuring that the returned information is the most pertinent and accurate response for the respective system component. In this way, the context retrieval engine ensures that the middleware has accurate and timely information about the farming environment.
- *Context inference engine* entails deriving higher level knowledge or insights from the acquired context that is particularly important for decision-making and automation. The context inference engine primarily focuses on reasoning operations such as validating and representing context values in a more complex manner, addressing uncertainties that may arise from context inconsistencies or missing contextual data, and ensuring computational performance is maintained to extract high-quality and high-level contextual information. To achieve these objectives, the context inference engine employs specific reasoning techniques tailored to address each of the aforementioned challenges effectively.
- *Service mapping engine* involves associating context information with specific agricultural services or functionalities. For example, based on context such as soil moisture levels, temperature, and crop type, the middleware can map the context to services like automated irrigation, fertilization, or pest control. Service mapping helps determine which services are appropriate and relevant for the current agricultural conditions.
- *Service discovery engine* focuses on identifying and locating the available services and resources within the agricultural facility ecosystem. This can include services provided by IoT devices, sensors, machinery, or external data sources. The middleware can also employ service discovery mechanisms to identify the available services for monitoring environmental conditions, collecting sensor data, analyzing crop and animal health, or controlling the agricultural facility equipment.

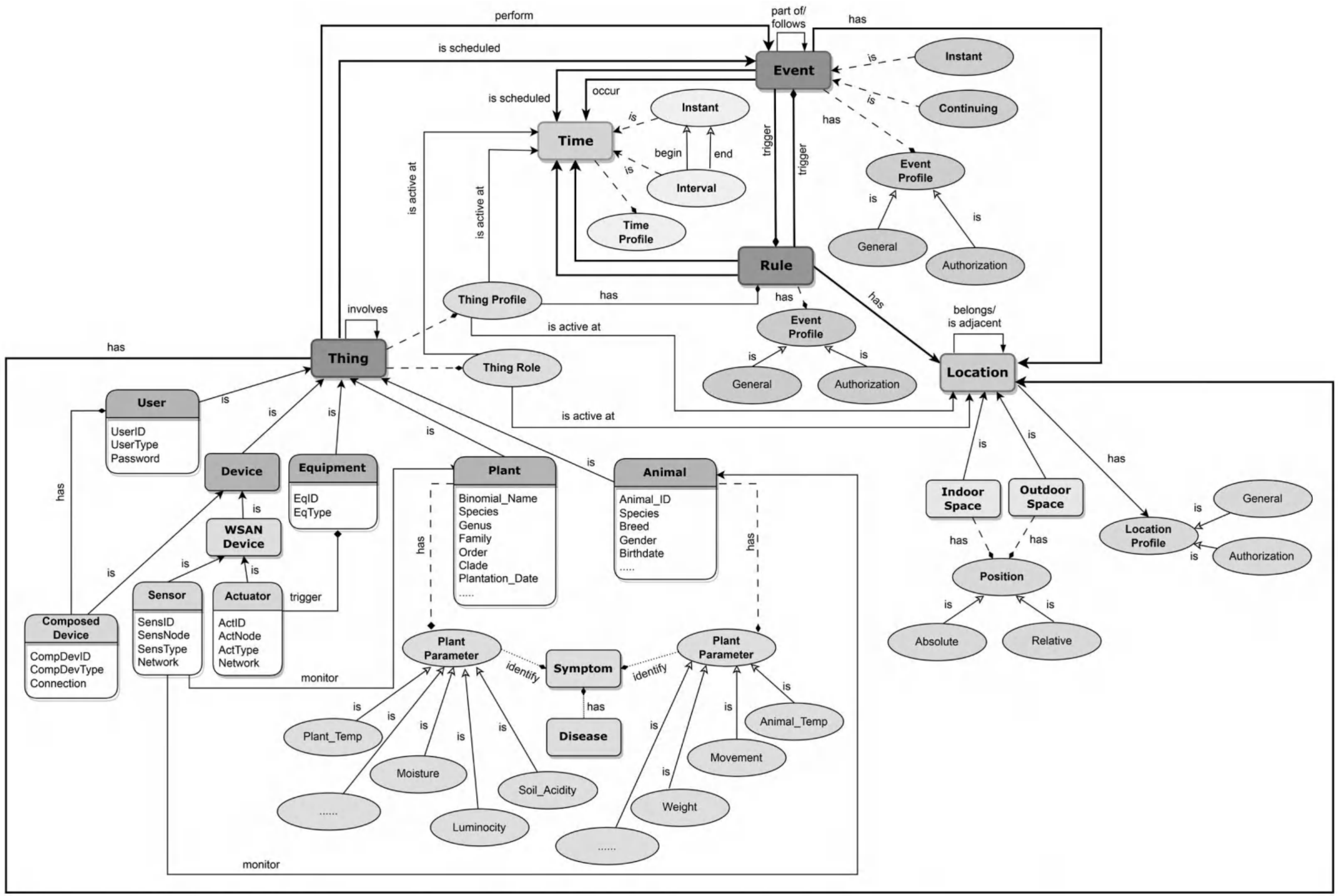

FIGURE 11.7 Ontology of the context model.

By performing service mapping, service discovery, context retrieval, and context inference, the IoT middleware can orchestrate and coordinate various agricultural services, data sources, and control mechanisms. It enables the integration of disparate systems, facilitates data-driven decision-making, and supports automation for improved efficiency, productivity, and sustainability in farming operations.

11.4.3 Context Repository

Given the substantial volume of data generated and processed, it is essential to incorporate a distributed cloud repository into the system to ensure the preservation of contextual information. This repository serves as an expandable knowledge base of ontologies, storing progressive data, and their respective contexts. Additionally, attributes are stored as key-value pairs across multiple ontology repositories, simplifying query operations. Each system component and device is assigned a unique ID to differentiate incoming contextual data within the context repository. The points that have been taken into consideration are in more detail as follows:

- *Data volume and scalability*: Since agricultural environment generates a large volume of data, including real-time sensor readings, environmental parameters, user preferences, and historical context, it is essential to store and manage this vast amount of data into a scalable and distributed cloud repository that can handle the increasing data load efficiently. The distributed nature of the repository allows for horizontal scaling, enabling seamless expansion as the system grows and more data is generated.
- *Context conservation*: Contextual information is highly valuable as it serves as a knowledge base for decision-making, process planning, and inference processes. By conserving contextual information in a distributed cloud repository, system components can access and leverage historical context for analysis, learning, and prediction purposes. The repository acts as a centralized storehouse for context data, ensuring its availability to all relevant system components and services.
- *Ontology-based knowledge representation*: The storage of ontologies in the cloud repository facilitates semantic representation and organization of contextual data. Storing context as an expandable knowledge base of ontologies allows for efficient querying and reasoning, enabling the system to extract meaningful insights and support intelligent decision-making.
- *Unique identifiers*: Assigning unique IDs to system components and devices when interacting with the context repository helps distinguish and manage the incoming contextual data. Each data entry can be associated with the corresponding component or device, allowing for easy retrieval, updating, and tracking of context information. Unique identifiers ensure proper data association and help maintain data integrity within the repository.
- *Historical context and knowledge mining*: The storage of context history in the distributed cloud repository enables knowledge mining and analysis. Historical context data can be leveraged to identify patterns, trends, and correlations that aid in process optimization, predictive analytics, and proactive decision-making. By mining the stored context data, the system can derive valuable insights, discover hidden relationships, and improve its understanding of the environment and user behaviors.

11.4.4 Self-Adaptation

The capability for self-adaptation is a fundamental requirement in context-aware middleware, where context information is used to generate appropriate services and control actions. This process involves self-adaptation and taking charge of diagnosing, detecting, and rectifying potential errors within the middleware workflow. Specifically, through self-adaptation, the context-aware middleware can reduce the development cycle of the system whenever similar context patterns are identified. It accomplishes this by recognizing sets of actions, storing this information, and enhancing its knowledge base. Additionally, the middleware ensures that processing requirements are met and accurate results are obtained while adhering to real-time constraints during the analysis.

Further elaborating, self-adaptation enables the context-aware middleware to dynamically adjust its behavior based on the detected context. By continuously monitoring and analyzing the context information, the middleware can identify patterns or recurring situations. When such patterns are recognized, the middleware can leverage its self-adaptation capabilities to streamline the system's development process by reusing previously stored action sets. This reduces the need for extensive development efforts and promotes agility in adapting to similar context scenarios.

Moreover, the self-adaptation mechanism within the context-aware middleware plays a crucial role in ensuring the accuracy and reliability of the generated results. It considers the real-time constraints of the system and employs efficient processing techniques to obtain accurate outcomes. This involves balancing the need for real-time responsiveness with the necessity of precise analysis and decision-making based on the available context.

By incorporating self-adaptation, the context-aware middleware can enhance its overall performance, reduce development cycles, and improve the quality of its responses. It effectively leverages context information to provide tailored services and control actions, optimizing the system's behavior based on the ever-changing context conditions.

11.4.5 Security and Privacy

Security and privacy are critical issues in IoT middleware systems (Chanal & Kakkasageri, 2020), including context-aware middleware. The key aspects regarding security and privacy that were taken into consideration during the design of this IoT middleware solution are as follows:

- *Authentication and authorization*: The IoT middleware provides mechanisms for authenticating and authorizing users, devices, and services. This ensures that only authorized entities can access and interact with the system. Authentication verifies the identity of users or devices, while authorization determines the permissions and privileges granted to them.
- *Data encryption*: The IoT middleware supports data encryption techniques to protect sensitive information during transmission and storage. Encryption ensures that data remains confidential and cannot be accessed or intercepted by unauthorized entities. Secure communication protocols, such as SSL (Secure Sockets Layer)/TLS (Transport Layer Security) (Liu, Alqazzaz, et al., 2021), have been employed to establish secure connections between middleware components and external services.
- *Access control*: Access control mechanisms have been implemented to regulate and manage access to resources within the middleware. This includes defining user roles, permissions, and access policies. Access control ensures that only authorized users or services can access specific resources and perform permitted actions.
- *Secure communication*: Secure communication protocols have been implemented to protect data exchanged between components, devices, and external services. Secure protocols, such as HTTPS (Mrabet et al., 2020) or MQTT with TLS (Su et al., 2019), encrypt data during transit, preventing eavesdropping or tampering. Additionally, message integrity and authentication mechanisms have been implemented to verify the integrity and origin of messages.

- *Auditing and logging*: The middleware has auditing and logging capabilities to track and record system activities, user interactions, and security-related events. Auditing and logging enable system administrators to monitor and analyze security events, detect potential threats or breaches, and aid in post-incident analysis and forensic investigations.
- *Privacy protection*: Privacy-enhancing measures have been incorporated to protect sensitive personal data. This includes adhering to privacy regulations and best practices, implementing data anonymization or pseudonymization techniques (Ren et al., 2021), and obtaining user consent for data collection and processing.
- *Secure configuration and management*: This involves regularly applying security patches and updates, securing administrative interfaces, and employing secure configuration practices to minimize vulnerabilities and protect against known security threats.
- *Threat detection and intrusion prevention*: The middleware incorporates intrusion detection and prevention mechanisms to identify and mitigate potential security threats. This may include anomaly detection algorithms, intrusion detection systems, or network monitoring tools that can detect suspicious activities and take appropriate action to prevent unauthorized access or attacks.
- *Compliance with security standards*: Established security standards and frameworks (Taherdoost, 2022), such as ISO 27001, NIST Cybersecurity Framework, or GDPR, should be adhered to depending on the applicable regulations and practices. Compliance with these standards ensures that security controls and practices are in place to protect the system and its users' data.

By addressing security and privacy concerns in middleware, sensitive information can be protected, risks can be mitigated and trust with users, and stakeholders can be built. Implementing robust security measures ensures the integrity, confidentiality, and availability of data and services within the middleware system.

11.4.6 Validation Results of the IoT Middleware in Two Case Studies

The IoT middleware was developed using the dynamic programming language Python, including its related libraries and packages (Stancin & Jovic, 2019), such as *NumPy* for performing scientific calculations, *Pandas* for performing data analysis functions, SciKit *Learn* for ML purposes featuring, among others, several regressions, classification, and clustering algorithms and *Scapy* for decoding and managing packets of various protocols. For computational and storage resources, the IaaS, PaaS, and SaaS services of a cloud platform were incorporated.

The proposed ontology-based modeling structure was developed using Web Ontology Language (OWL) 2.0 (Eberhart et al., 2021) and can also be implemented in Extensible Markup Language (XML), which is a platform-independent and robust tool suitable for use in various phases of information representation (Haw et al., 2023), as well as for Simple Object Access Protocol (SOAP)-based communication (Tightiz & Yang, 2020). In terms of context representation and reasoning, the proposed modeling structure has been successfully verified by running the Pellet incremental reasoner, available in *Protégé*, which is a free, open-source ontology framework for building intelligent systems (Rubin et al., 2005). The reasoning process results, as shown in Figure 11.8, indicate that the ontology is running with no inferences.

In order to validate the performance of the proposed IoT middleware, with emphasis on its modeling structure and reasoning techniques, two case studies were performed. The first case study concerned the monitoring of important parameters (air temperature and humidity, soil moisture, and pH) in an arable maize cultivation, while the second case study concerned the smart control of the thermal environment in a medium-sized pig farming facility. Simulation tests regarding the performance and scalability of the IoT middleware have also been performed involving a considerable

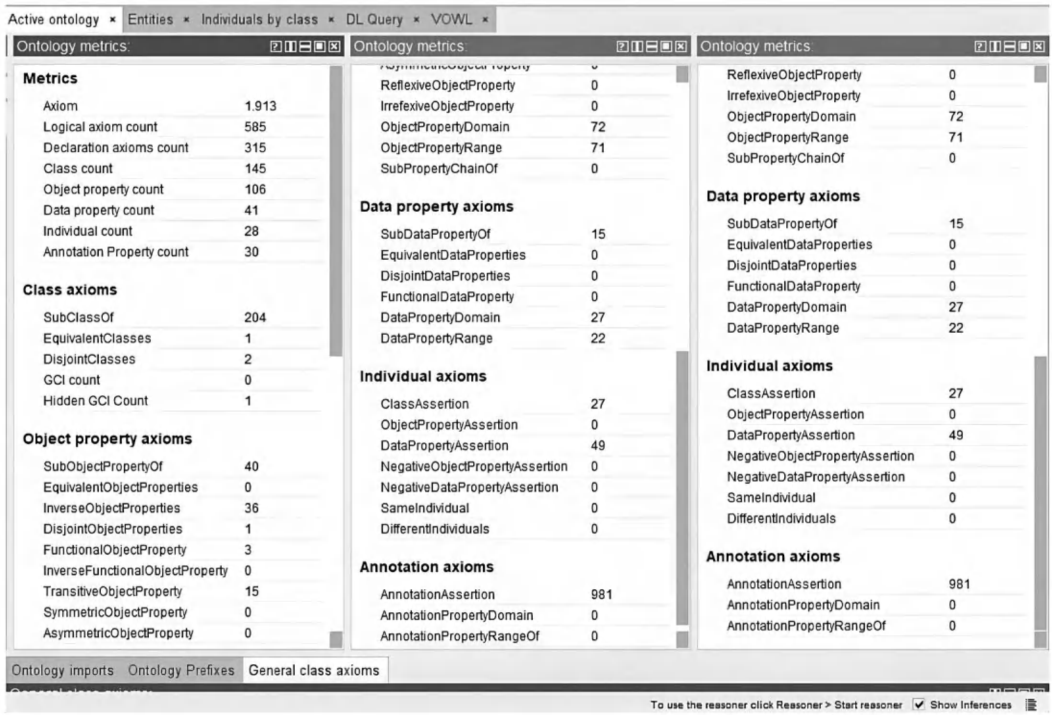

FIGURE 11.8 Verification of modeling structure clarity.

amount of data derived by simulated devices for both the arable cultivation and the livestock farming facility.

The original validation of computational performance initially included approximately 60 deployed devices, incorporating sensors, actuators, and mobile smart devices in each of the two case studies for purposes of consistency. In both the experiments, the IoT middleware demonstrated no bottlenecks, as expected, given the limited amount of context data and rules to be processed. Subsequently, the number of deployed devices was gradually increased to 300, incorporating additional devices, resulting in a higher volume of context data and rules. Aiming to assess the computational performance under conditions of data overload, in the final stage of the validation, the number of devices has been doubled to 600 by adding 300 simulated devices in each of the two case studies. To validate the system's computational performance, metrics such as the average inference cycle time and average response time were analyzed. The inference cycle time refers to the average duration required by the IoT middleware to process a set of corresponding rules, while the response time denotes the average duration from the arrival of a request in the IoT middleware until the dissemination of the processed contextual information to the relevant applications. The results of the computational performance validation are shown in Figures 11.9–11.12.

According to Figures 11.9–11.12, it appears that both the inference cycle time and the response time are linearly correlated to the number of the added devices and rules to be processed, indicating that the IoT middleware responds efficiently even to greater volumes of context data. The slight difference observed between the results concerning the arable cultivation and the livestock facility is attributed to the fact that in the first case the measured parameters of interest are more than those in the second case study.

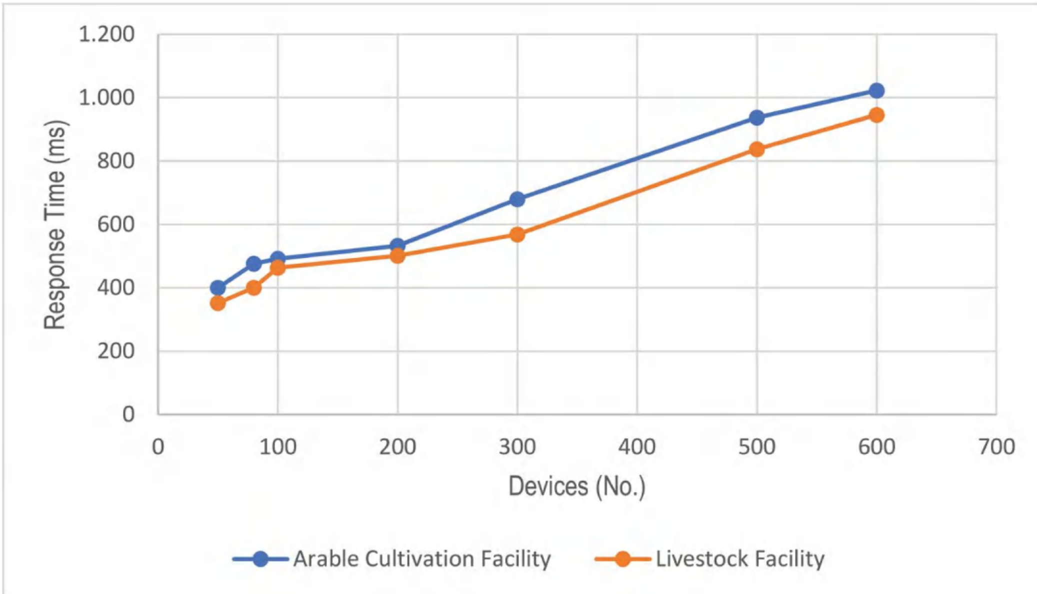

FIGURE 11.9 Correlation between number of devices and response time.

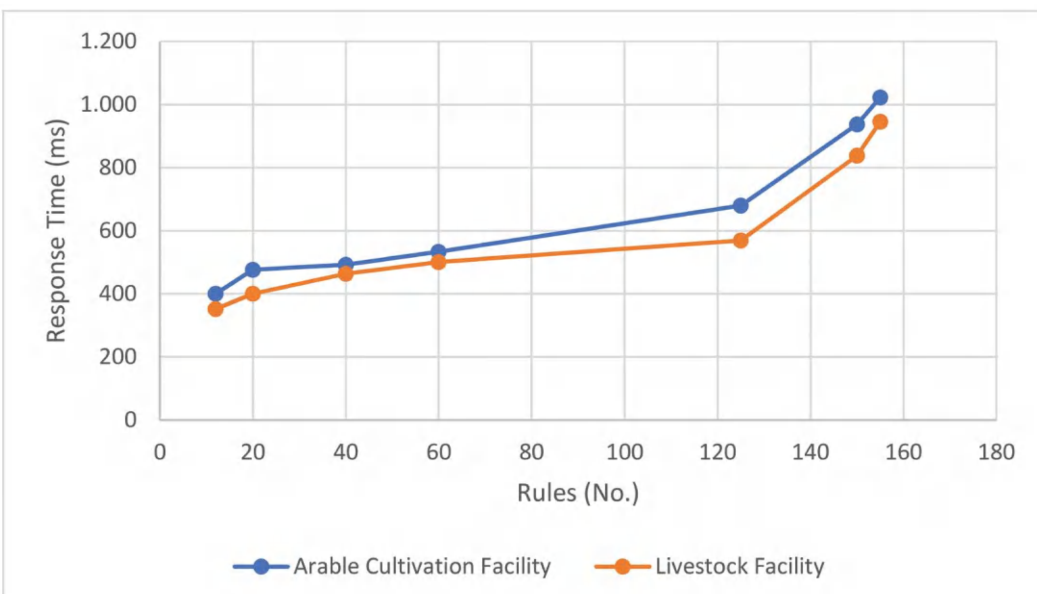

FIGURE 11.10 Correlation between number of rules and response time.

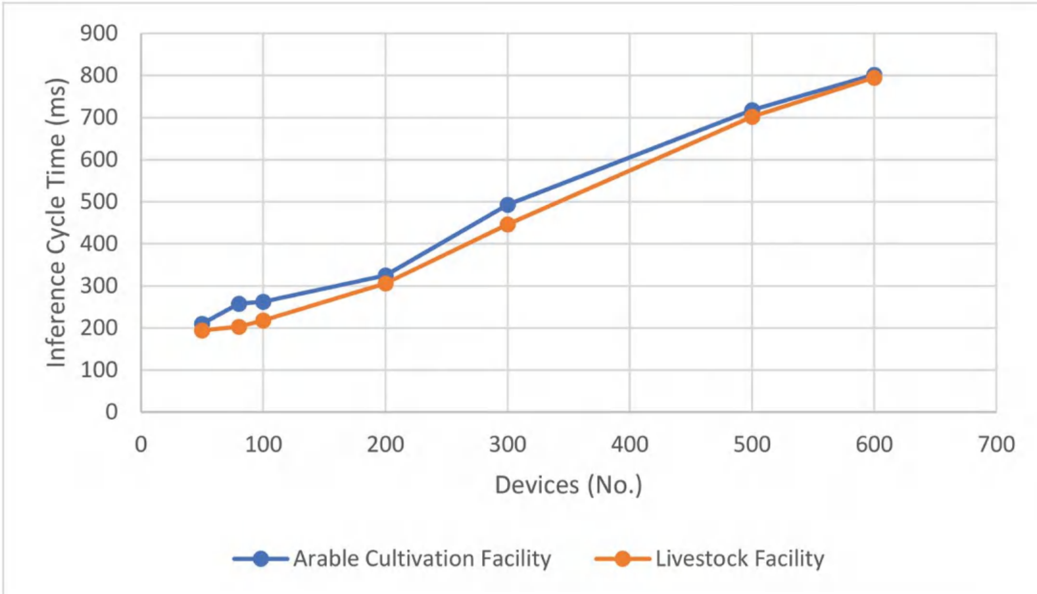

FIGURE 11.11 Correlation between number of devices and inference cycle time.

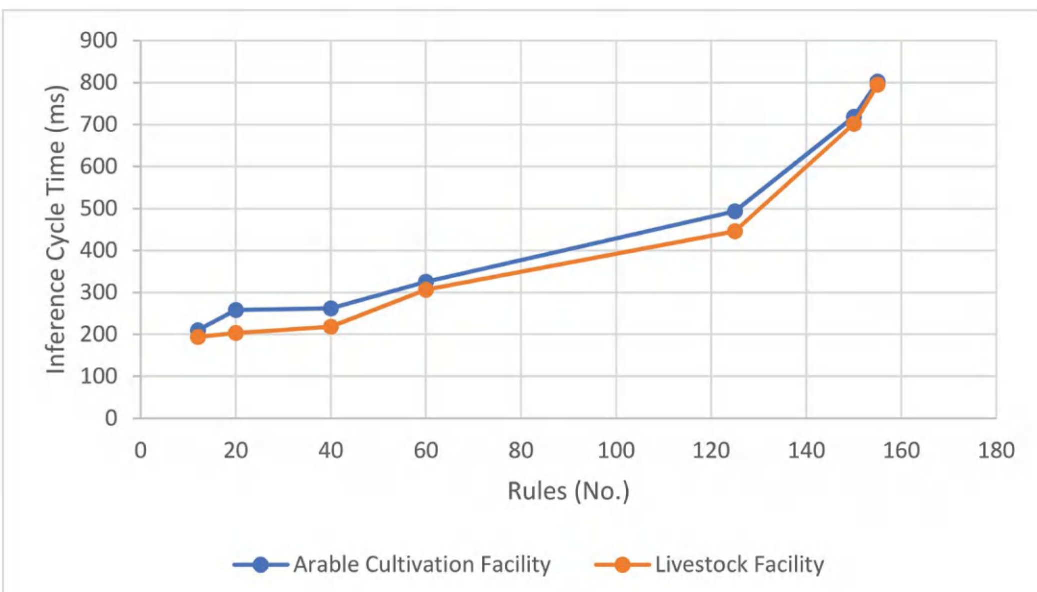

FIGURE 11.12 Correlation between number of rules and inference cycle time.

11.4.7 Conclusion and Future Perspectives

In this chapter, we presented a cloud-based middleware solution for the advanced automation of agricultural production systems toward the trend of Agriculture 5.0. The proposed solution demonstrated the potential of integrating IoT technologies and cloud computing resources to enable interconnectivity, scalability, flexibility, and interoperability in agricultural operations. The chapter focused on the context aware middleware layer of the presented system's architecture while primary emphasis was placed around the modeling of the contextual data.

Through the evaluation of the system in two case studies, one on arable cultivation and the other on livestock farming, we observed promising results. The computational performance of the system was found to be satisfactory, allowing for real-time data processing and decision-making. The coherence, consistency, and effectiveness of the system were validated through the successful implementation and execution of various automation tasks.

The context awareness function played a crucial role in enhancing the system's capabilities. By acquiring, processing, and utilizing contextual information from diverse sources, the middleware facilitated intelligent decision-making, resource optimization, and adaptive control within the agricultural production systems.

Future research directions should aim to enhance context detection, incorporate edge computing, address security and privacy concerns, promote interoperability, and optimize resource management. These advancements will contribute to the further development and adoption of IoT-integrated systems in agriculture, paving the way for increased efficiency, productivity, and sustainability in the agricultural sector.

REFERENCES

Alegre, U., Augusto, J. C., & Clark, T. (2016). Engineering context-aware systems and applications: A survey. *Journal of Systems and Software*, *117*, 55–83. https://doi.org/10.1016/J.JSS.2016.02.010

Aslam, M. S., Rea, S., & Pesch, D. (2012). Service provisioning for the WSN cloud. *Proceedings – 2012 IEEE 5th International Conference on Cloud Computing, CLOUD 2012*, 962–969. https://doi.org/10.1109/CLOUD.2012.132

Atmaja, A. P., Hakim, A. E., Wibowo, A. P. A., & Pratama, L. A. (2021). Communication systems of smart agriculture based on wireless sensor networks in IoT. *Journal of Robotics and Control (JRC)*, *2*(4), 297–301. https://doi.org/10.18196/JRC.2495

Augusto, J., Aztiria, A., Kramer, D., & Alegre, U. (2018). A survey on the evolution of the notion of context-awareness. *Applied Artificial Intelligence*, *31*(7–8), 613–642. https://doi.org/10.1080/08839514.2018.1428490

Ayoub, W., Samhat, A. E., Nouvel, F., Mroue, M., & Prévotet, J. C. (2019). Internet of mobile things: Overview of LoRaWAN, DASH7, and NB-IoT in LPWANs standards and supported mobility. *IEEE Communications Surveys and Tutorials*, *21*(2), 1561–1581. https://doi.org/10.1109/COMST.2018.2877382

Bettini, C., Brdiczka, O., Henricksen, K., Indulska, J., Nicklas, D., Ranganathan, A., & Riboni, D. (2010). A survey of context modelling and reasoning techniques. *Pervasive and Mobile Computing*, *6*(2), 161–180. https://doi.org/10.1016/J.PMCJ.2009.06.002

Bhanu, K. N., Jasmine, H. J., & Mahadevaswamy, H. S. (2020). Machine learning implementation in IoT based intelligent system for agriculture. *2020 International Conference for Emerging Technology, INCET 2020*. https://doi.org/10.1109/INCET49848.2020.9153978

Burhan, M., Rehman, R. A., Khan, B., & Kim, B. S. (2018). IoT elements, layered architectures and security issues: A comprehensive survey. *Sensors*, *18*(9), 2796. https://doi.org/10.3390/S18092796

Chanal, P. M., & Kakkasageri, M. S. (2020). Security and privacy in IoT: A survey. *Wireless Personal Communications*, *115*(2), 1667–1693. https://doi.org/10.1007/S11277-020-07649-9

Chaudhari, B. S., Zennaro, M., & Borkar, S. (2020). LPWAN technologies: Emerging application characteristics, requirements, and design considerations. *Future Internet*, *12*(3), 46. https://doi.org/10.3390/FI12030046

Chen, Y., Yu, P., Zheng, Z., Shen, J., & Guo, M. (2022). Modeling feature interactions for context-aware QoS prediction of IoT services. *Future Generation Computer Systems*, *137*, 173–185. https://doi.org/10.1016/J.FUTURE.2022.07.017

Cope, M., Mikhailova, E., Post, C., Schlautman, M., & McMillan, P. (2017). Developing an integrated cloud-based spatial-temporal system for monitoring phenology. *Ecological Informatics*, *39*, 123–129. https://doi.org/10.1016/J.ECOINF.2017.04.007

Dhumane, A., Guja, S., Deo, S., & Prasad, R. (2018). Context awareness in IoT routing. *Proceedings – 2018 4th International Conference on Computing, Communication Control and Automation, ICCUBEA 2018*. https://doi.org/10.1109/ICCUBEA.2018.8697685

Eberhart, A., Shimizu, C., Chowdhury, S., Sarker, M. K., & Hitzler, P. (2021). Expressibility of OWL axioms with patterns. *Lecture Notes in Computer Science (Including Subseries Lecture Notes in Artificial Intelligence and Lecture Notes in Bioinformatics), 12731 LNCS*, 230–245. https://doi.org/10.1007/978-3-030-77385-4_14

Fraden, J. 2010. Handbook of modern sensors. *Handbook of modern sensors*. https://doi.org/10.1007/978-1-4419-6466-3

Fraser, E. D. G., & Campbell, M. (2019). Agriculture 5.0: Reconciling production with planetary health. *One Earth*, *1*(3), 278–280. https://doi.org/10.1016/J.ONEEAR.2019.10.022

Gameil, M., & Gaber, T. (2020). Wireless sensor networks-based solutions for cattle health monitoring: A survey. In: Hassanien, A., Shaalan, K., Tolba, M. (eds), *Proceedings of the International Conference on Advanced Intelligent Systems and Informatics 2019. AISI 2019*. Advances in Intelligent Systems and Computing, vol 1058. Springer, Cham. https://link.springer.com/chapter/10.1007/978-3-030-31129-2_71

Gong, L., Yan, J., Chen, Y., An, J., He, L., Zheng, L., & Zou, Z. (2022). An IoT-based intelligent irrigation system with data fusion and a self-powered wide-area network. *Journal of Industrial Information Integration*, *29*, 100367. https://doi.org/10.1016/J.JII.2022.100367

Guermah, H., Guermah, B., Fissaa, T., Hafiddi, H., & Nassar, M. (2021). Dealing with context awareness for service-oriented systems: An ontology-based approach. *International Journal of Service Science, Management, Engineering, and Technology (IJSSMET)*, *12*(4), 110–131. https://doi.org/10.4018/IJSSMET.2021070107

Hameed, K., Garg, S., Amin, M. B., Kang, B., & Khan, A. (2022). A context-aware information-based clone node attack detection scheme in internet of things. *Journal of Network and Computer Applications*, *197*, 103271. https://doi.org/10.1016/J.JNCA.2021.103271

Haw, S.-C., Chew, L.-J., Sulistyo Kusumo, D., Naveen, P., & Ng, K.-W. (2023). Mapping of extensible markup language-to-ontology representation for effective data integration. *IAES International Journal of Artificial Intelligence (IJ-AI)*, *12*(1), 432–442. https://doi.org/10.11591/ijai.v12.i1.pp432-442

Huertas Celdran, A., Garcia Clemente, F. J., Gil Perez, M., & Martinez Perez, G. (2016). SeCoMan: A semantic-aware policy framework for developing privacy-preserving and context-aware smart applications. *IEEE Systems Journal*, *10*(3), 1111–1124. https://doi.org/10.1109/JSYST.2013.2297707

Hussain, S. J., Khan, S., Hasan, R., & Hussain, S. A. (2020). Design and implementation of animal activity monitoring system using TI sensor tag. In *Advances in intelligent systems and computing* (Vol. 1040, pp. 167–175). Springer. https://doi.org/10.1007/978-981-15-1451-7_18

Jawad, H. M., Nordin, R., Gharghan, S. K., Jawad, A. M., & Ismail, M. (2017). Energy-efficient wireless sensor networks for precision agriculture: A review. *Sensors 2017*, *17*(8), 1781. https://doi.org/10.3390/S17081781

Kassab, W., & Darabkh, K. A. (2020). A–Z survey of internet of things: Architectures, protocols, applications, recent advances, future directions and recommendations. *Journal of Network and Computer Applications*, *163*, 102663. https://doi.org/10.1016/J.JNCA.2020.102663

Kim, W. S., Lee, W. S., & Kim, Y. J. (2020). A review of the applications of the internet of things (IoT) for agricultural automation. *Journal of Biosystems Engineering*, *45*(4), 385–400. https://doi.org/10.1007/S42853-020-00078-3

Knappmeyer, M., Kiani, S. L., Reetz, E. S., Baker, N., & Tonjes, R. (2013). Survey of context provisioning middleware. *IEEE Communications Surveys and Tutorials*, *15*(3), 1492–1519. https://doi.org/10.1109/SURV.2013.010413.00207

Koç, H., Hennig, E., Jastram, S., & Starke, C. (2014). State of the art in context modelling – A systematic literature review. *Lecture Notes in Business Information Processing, 178 LNBIP*, 53–64. https://doi.org/10.1007/978-3-319-07869-4_5

Lee, K. C., Kim, J. H., Lee, J. H., & Lee, K. M. (2007). Implementation of ontology based context-awareness framework for ubiquitous environment. *Proceedings – 2007 International Conference on Multimedia and Ubiquitous Engineering, MUE 2007*, 278–282. https://doi.org/10.1109/MUE.2007.136

Li, S., Cui, J., & Li, Z. (2011). Wireless sensor network for precise agriculture monitoring. *Proceedings – 4th International Conference on Intelligent Computation Technology and Automation, ICICTA 2011*, *1*, 307–310. https://doi.org/10.1109/ICICTA.2011.87

Linthicum, D. S. (2016). Emerging hybrid cloud patterns. *IEEE Cloud Computing*, *3*(1), 88–91. https://doi.org/10.1109/MCC.2016.22

Liu, A., Alqazzaz, A., Ming, H., & Dharmalingam, B. (2021). Iotverif: Automatic verification of SSL/TLS certificate for IoT applications. *IEEE Access*, *9*, 27038–27050. https://doi.org/10.1109/ACCESS.2019.2961918

Liu, Y., Ma, X., Shu, L., Hancke, G. P., & Abu-Mahfouz, A. M. (2021). From Industry 4.0 to Agriculture 4.0: Current status, enabling technologies, and research challenges. *IEEE Transactions on Industrial Informatics*, *17*(6), 4322–4334. https://doi.org/10.1109/TII.2020.3003910

Liya, M. L., & Arjun, D. (2020). A survey of LPWAN technology in agricultural field. *Proceedings of the 4th International Conference on IoT in Social, Mobile, Analytics and Cloud, ISMAC 2020*, 313–317. https://doi.org/10.1109/I-SMAC49090.2020.9243410

Loukatos, D., Fragkos, A., & Arvanitis, K. G. (2022). Experimental performance evaluation techniques of LoRa radio modules and exploitation for agricultural use. *Springer Optimization and Its Applications*, *182*, 101–120. https://doi.org/10.1007/978-3-030-84144-7_4

Lupiana, D. (2017). Context modeling for context-aware systems. *International Journal of Intelligent Computing Research*, *8*(1), 807–816. https://doi.org/10.20533/IJICR.2042.4655.2017.0099

Maran, V., Machado, G. M., Machado, A., Augustin, I., & de Oliveira, J. P. M. (2018). UPCaD: A methodology of integration between ontology-based context-awareness modeling and relational domain data. *Information*, *9*(2), 30. https://doi.org/10.3390/INFO9020030

Mekki, K., Bajic, E., Chaxel, F., & Meyer, F. (2019). A comparative study of LPWAN technologies for large-scale IoT deployment. *ICT Express*, *5*(1), 1–7. https://doi.org/10.1016/J.ICTE.2017.12.005

Miles, B., Bourennane, E. B., Boucherkha, S., & Chikhi, S. (2020). A study of LoRaWAN protocol performance for IoT applications in smart agriculture. *Computer Communications*, *164*, 148–157. https://doi.org/10.1016/J.COMCOM.2020.10.009

Mohammed, C. M., & Zeebaree, S. R. (2021). Sufficient comparison among cloud computing services: IaaS, PaaS, and SaaS: A review. *International Journal of Science and Business*, *5*(2), 17–30. https://ideas.repec.org/a/aif/journl/v5y2021i2p17-30.html

Mrabet, H., Belguith, S., Alhomoud, A., & Jemai, A. (2020). A survey of IoT security based on a layered architecture of sensing and data analysis. *Sensors*, *20*(13), 3625. https://doi.org/10.3390/S20133625

Navarro, E., Costa, N., & Pereira, A. (2020). A systematic review of IoT solutions for smart farming. *Sensors*, *20*(15), 4231. https://doi.org/10.3390/S20154231

Ojha, T., Misra, S., & Raghuwanshi, N. S. (2015). Wireless sensor networks for agriculture: The state-of-the-art in practice and future challenges. *Computers and Electronics in Agriculture*, *118*, 66–84. https://doi.org/10.1016/J.COMPAG.2015.08.011

Perera, C., Zaslavsky, A., Christen, P., & Georgakopoulos, D. (2014). Context aware computing for the internet of things: A survey. *IEEE Communications Surveys and Tutorials*, *16*(1), 414–454. https://doi.org/10.1109/SURV.2013.042313.00197

Piromalis, D., & Arvanitis, K. (2016). SensoTube: A scalable hardware design architecture for wireless sensors and actuators networks nodes in the agricultural domain. *Sensors*, *16*(8). https://doi.org/10.3390/s16081227

Popović, T., Latinović, N., Pešić, A., Zečević, Ž., Krstajić, B., & Djukanović, S. (2017). Architecting an IoT-enabled platform for precision agriculture and ecological monitoring: A case study. *Computers and Electronics in Agriculture*, *140*, 255–265. https://doi.org/10.1016/J.COMPAG.2017.06.008

Porter, M. E., & Heppelmann, J. E. (2014). *HBR.ORG Spotlight on managing the internet of things how smart, connected products are transforming competition*.

Pradeep, P., Krishnamoorthy, S., Pathinarupothi, R. K., & Vasilakos, A. V. (2021). Leveraging context-awareness for internet of things ecosystem: Representation, organization, and management of context. *Computer Communications*, *177*, 33–50. https://doi.org/10.1016/J.COMCOM.2021.06.004

Publications Office of the European Union. (2021). *Industry 5.0 : Towards a sustainable, human-centric and resilient European industry*. Publications Office of the European Union. https://doi.org/10.2777/308407

Puranik, V., Sharmila, Ranjan, A., & Kumari, A. (2019). Automation in agriculture and IoT. Proceedings – 2019 4th International Conference on Internet of Things: Smart Innovation and Usages, IoT-SIU 2019. https://doi.org/10.1109/IOT-SIU.2019.8777619

Ragazou, K., Garefalakis, A., Zafeiriou, E., & Passas, I. (2022). Agriculture 5.0: A new strategic management mode for a cut cost and an energy efficient agriculture sector. *Energies*, *15*(9), 3113. https://doi.org/10.3390/EN15093113

Rao, M. V., Reddy, D. A., Ampavathi, A., & Munawar, S. (2022). Data mining for cyberphysical systems. In R. Raja, K. Kumar, N. S. Kumar, & K. R. Laxmi (Eds.), *Data mining and machine learning applications* (pp. 235–280). John Wiley & Sons, Ltd. https://doi.org/10.1002/9781119792529.CH10

Ren, W., Tong, X., Du, J., Wang, N., Li, S., Min, G., & Zhao, Z. (2021). Privacy enhancing techniques in the internet of things using data anonymisation. *Information Systems Frontiers*, 1–12. https://doi.org/10.1007/S10796-021-10116

Rubin, D. L., Knublauch, H., Fergerson, R. W., Dameron, O., & Musen, M. A. 2005. Protégé-OWL: Creating ontology-driven reasoning applicationswith the web ontology language. *AMIA Annual Symposium Proceedings*, 2005, 1179. http://pmc/articles/PMC1560433/

Samizadeh Nikoui, T., Rahmani, A. M., Balador, A., & Haj Seyyed Javadi, H. (2021). Internet of things architecture challenges: A systematic review. *International Journal of Communication Systems*, *34*(4), e4678. https://doi.org/10.1002/DAC.4678

Sethi, P., & Sarangi, S. R. (2017). Internet of things: Architectures, protocols, and applications. *Journal of Electrical and Computer Engineering*, *2017*. https://doi.org/10.1155/2017/9324035

Singh, M. K., Amin, S. I., Imam, S. A., Sachan, V. K., & Choudhary, A. (2018). A survey of wireless sensor network and its types. *Proceedings – IEEE 2018 International Conference on Advances in Computing, Communication Control and Networking, ICACCCN 2018*, 326–330. https://doi.org/10.1109/ICACCCN.2018.8748710

Stancin, I., & Jovic, A. (2019). An overview and comparison of free Python libraries for data mining and big data analysis. *2019 42nd International Convention on Information and Communication Technology, Electronics and Microelectronics, MIPRO 2019 – Proceedings*, 977–982. https://doi.org/10.23919/MIPRO.2019.8757088

Strang, T., & Linnhoff-Popien, C. (2004). A context modeling survey. *Workshop Proceedings. First International Workshop on Advanced Context Modelling, Reasoning and Management at UbiComp,* 2004. http://citeseer.ist.psu.edu/strang04context.html

Su, W. T., Chen, W. C., & Chen, C. C. (2019). An extensible and transparent thing-to-thing security enhancement for MQTT protocol in IoT environment. *Global IoT Summit, GIoTS 2019 – Proceedings*. https://doi.org/10.1109/GIOTS.2019.8766412

Taherdoost, H. (2022). Understanding cybersecurity frameworks and information security standards—A review and comprehensive overview. *Electronics*, *11*(14), 2181. https://doi.org/10.3390/ELECTRONICS11142181

Tightiz, L., & Yang, H. (2020). A comprehensive review on IoT protocols' features in smart grid communication. *Energies*, *13*(11), 2762. https://doi.org/10.3390/EN13112762

van Evert, F. K., Fountas, S., Jakovetic, D., Crnojevic, V., Travlos, I., & Kempenaar, C. (2017). Big data for weed control and crop protection. *Weed Research*, *57*(4), 218–233. https://doi.org/10.1111/WRE.12255

Vidic, J., Manzano, M., Chang, C. M., & Jaffrezic-Renault, N. (2017). Advanced biosensors for detection of pathogens related to livestock and poultry. *Veterinary Research*, *48*(1), 1–22. https://doi.org/10.1186/S13567-017-0418-5

Zepeda, L. (2001). *Agricultural investment and productivity in developing countries. FAO* (05)/E21/no.148. *Edited by Lydia Zepeda*. Rome: Food and Agriculture Organization of the United Nations, 2001 https://digitallibrary.un.org/record/456996

Zhang, J., & Huang, M. L. (2013). 5Ws model for big data analysis and visualization. *Proceedings – 16th IEEE International Conference on Computational Science and Engineering, CSE 2013*, 1021–1028. https://doi.org/10.1109/CSE.2013.149

Zhang, J., Ma, M., Wang, P., & Sun, X. dong. (2021). Middleware for the internet of things: A survey on requirements, enabling technologies, and solutions. *Journal of Systems Architecture*, *117*, 102098. https://doi.org/10.1016/J.SYSARC.2021.102098

Index

Note: **Bold** and *italic* page numbers refer to tables and figures, respectively.

Q

R

S

T

U

V